

Diss. ETH No. 13184

**LIGAND BINDING AND SIGNAL TRANSDUCTION  
OF VERTEBRATE  
SOMATOSTATIN RECEPTORS  
RECOMBINANTLY EXPRESSED IN CCL39 CELLS**

A dissertation submitted to the  
SWISS FEDERAL INSTITUTE OF TECHNOLOGY ZÜRICH

for the degree of  
Doctor of Natural Science

Presented by

SANDRA SIEHLER

Dipl. Biol., University of Karlsruhe (TH)  
born January 4, 1971  
Germany

Accepted on the recommendation of

Prof. Dr. Gerd Folkers, Examiner  
Prof. Dr. Vladimir Pliska, Co-examiner  
Dr. Daniel Hoyer, Co-examiner

Zürich, 1999

## Acknowledgements

I deeply thank Dr. Daniel Hoyer, the supervisor of my thesis, for accepting me in his laboratory in the Nervous System Research Department of NOVARTIS Pharma Inc. in Basel, for his great support, advice and encouragement during the three years in his laboratory.

I would like to thank Prof. Dr. Gerd Folkers, head of the Department of Pharmacy (ETH Zurich), for examining this work and for his personal support, confidence and encouragement.

I am grateful to Prof. Dr. Vladimir Pliska (ETH Zurich), for being the coexaminer of my thesis and for his kindly advice.

I am thankful to NOVARTIS Pharma Inc. for financial support, Dr. Klaus Seuwen (NOVARTIS, Basel), who stably transfected CCL39 cells with the human somatostatin  $sst_2$ ,  $sst_3$  and  $sst_4$  receptors, to Prof. Dr. Günther K. H. Zupanc (Manchester, England), who provided me with the fish somatostatin  $sst_3$  receptor plasmid DNA and who prepared the various fish tissues, and to Karl-Heinz Wiederhold (NOVARTIS, Basel), who performed the photographic work of the slides for all my presentations.

I would like to express my special thanks to all the people, who gave me their friendship and the nice atmosphere, and to those, who gave me technical advice and material support for the performance of all my experiments: Dr. Klaus Seuwen, Sarah Limonta, Dr. Dominik Feuerbach, Dr. Raphaela Hiltcher, Dominique Fehlmann, Lucien Gazi, Dr. Nouciba Gourmala, Angelika Mann, Katrin Moser, Dr. Erika Lötscher, Edi Schüpbach, Daniel Langenegger, Jürg Kummer, Caroline Nunn, Dr. Philippe Schoeffter, Dr. Johannes Mosbacher, Dr. Friedrich Raulf, Inge Meigel, Prof. Dr. Hendrikus Boddeke, Dr. Barbara Stolz, Dr. Peter Flor, Dr. Rainer Kuhn, Dr. Rochdi Bouhelal.

Finally, I would like to give me deepest thanks to Mark and my parents, for their endless support of my activities.

# Table of Contents

	page
<b>Abbreviations</b>	1
<b>Summary</b>	5
<b>Kurzfassung</b>	7
<b>Chapter 1: Introduction</b>	
1.1. The Somatostatin peptide family	11
1.1.1. Mammalian somatostatin peptides	11
1.1.2. Non-mammalian somatostatin peptides	13
1.1.3. Synthetic somatostatin analogues	15
1.1.4. Physiological relevance	16
1.2. Somatostatin receptors	17
1.2.1. Receptor subtypes	17
1.2.2. Tissue distribution of receptor subtypes	20
1.2.3. Receptor subtype-specific functions	21
1.3. Signal Transduction	22
1.3.1. Coupling to G-proteins	22
1.3.2. Modulation of adenylate cyclase	23
1.3.3. Modulation of phospholipase C	24
1.3.4. Modulation of further signalling proteins	25
1.4. Outline of the thesis	27

## **Chapter 2: Methods**

2.1.	Cell Culture	29
2.2.	Transient transfection	29
2.3.	Stable transfection	30
2.4.	Radioligand binding assay	30
2.5.	[ <sup>35</sup> S]GTPγS binding assay	32
2.6.	Adenylate cyclase activity (cAMP accumulation) measurement	33
2.7.	Measurement of phosphoinositide turnover (total [ <sup>3</sup> H]-IP <sub>x</sub> accumulation)	35
2.8.	Measurement of intracellular Ca <sup>2+</sup>	36
2.9.	Ligands	36
2.10.	Northern blot analysis	38
2.11.	Reverse transcriptase-polymerase chain reaction (RT-PCR)	39

## **Chapter 3: [<sup>125</sup>I]Tyr<sup>10</sup>-cortistatin<sub>14</sub> labels all five somatostatin receptors**

3.1.	Abstract	43
3.2.	Results	44
3.3.	Discussion	47

## **Chapter 4: [<sup>125</sup>I][Tyr<sup>3</sup>]octreotide labels human sst<sub>2</sub> and sst<sub>5</sub> receptors**

4.1.	Abstract	53
4.2.	Results	54
4.3.	Discussion	58

**Chapter 5: Characterisation of human recombinant somatostatin receptors:**

**1) radioligand binding studies**

5.1. Abstract	67
5.2. Results	68
5.3. Discussion	73

**Chapter 6: Characterisation of human recombinant somatostatin receptors:**

**2) modulation of GTP $\gamma$ S binding**

6.1. Abstract	89
6.2. Results	90
6.3. Discussion	99

**Chapter 7: Characterisation of human recombinant somatostatin receptors:**

**3) modulation of adenylate cyclase activity**

7.1. Abstract	109
7.2. Results	110
7.3. Discussion	115

**Chapter 8: Characterisation of human recombinant somatostatin receptors:**

**4) modulation of phospholipase C activity**

8.1. Abstract	127
8.2. Results	128
8.3. Discussion	134

**Chapter 9: Molecular cloning and pharmacological characterization of a fish-specific somatostatin receptor subtype**

9.1.	Abstract	147
9.2.	Methods	148
	9.2.1. Cloning of <i>A. albifrons</i> sst <sub>3</sub> receptor	148
	9.2.2. Fish tissues	149
9.3.	Results	150
9.4.	Discussion	155

**Chapter 10: Characterization of the fish sst<sub>3</sub> receptor, a member of the SRIF<sub>1</sub> receptor family: atypical pharmacological features**

10.1.	Abstract	163
10.2.	Results	164
10.3.	Discussion	172

**Chapter 11: Fish somatostatin sst<sub>3</sub> receptor: comparison of radioligand and GTP $\gamma$ S binding, adenylate cyclase and phospholipase C activities reveals agonist-dependent pharmacological differences**

11.1.	Abstract	183
11.2.	Results	185
11.3.	Discussion	197

<b>Conclusions</b>	207
<b>References</b>	213

## Abbreviations

A. albifrons	Apteronotus albifrons (gymnotiform fish)
AC	adenylate cyclase
ADP	adenosine-5'-diphosphate
AIDS	acquired immunodeficiency syndrome
ATP	adenosine-5'-triphosphate
B <sub>max</sub>	receptor density
bp	basepairs
BSA	bovine serum albumin
[Ca <sup>2+</sup> ] <sub>i</sub>	intracellular calcium concentration
cAMP	cyclic adenosine monophosphate
CCL39 cells	Chinese hamster lung fibroblast cells
cDNA	copy DNA
°C	Celcius degree(s)
cGMP	cyclic guanosine monophosphate
CHO cells	Chinese hamster ovary cells
Ci	Curie = 3.7 x 10 <sup>10</sup> Bequerel (Bq)
CMV	Cytomegalie virus (promotor)
CNS	central nervous system
COS cells	CV1 Origin SV40 cells (derived from monkey kidney)
cpm	counts per minute
CST	cortistatin
DAG	1,2-diacylglycerol
dATP	desoxy ATP
dCTP	desoxy cytosine-5'-triphosphate
DEAE	diethylaminoethyl-dextran
dGTP	desoxy GTP
DMSO	dimethyl sulfoxide
DNA	desoxyribonucleic acid

dpm	decreases per minute
DTT	dithiothreitol
dTTP	desoxy thymidine-5'-triphosphate
EC <sub>50</sub>	concentration of half-maximal effect
EDTA	ethylene diaminetetraacetic acid
e.g.	for example
E <sub>max</sub>	maximal effect
FBS	foetal bovine serum
f.c.	final concentration
FLIPR	Fluorometric Imaging Plate Reader
FSAC	forskolin-stimulated adenylate cyclase activity
fsst <sub>3</sub>	fish somatostatin receptor subtype 3
g	acceleration due to gravity
G418	geneticin sulphate
GDP	guanosine-5'-diphosphate
GEP	gastroenteropancreatic
GppNHp	5'-guanylyl-imidodiphosphate
G-protein, G	guanyl-nucleotide binding protein
GTP	guanosine-5'-triphosphate
GTP $\gamma$ S	guanosine-5'-O-3'-thio-triphosphate
h	hour(s)
HBS	HEPES-buffered saline
HBSS	Hank's balanced salt solution
HEK293 cells	human embryonic kidney cells
HEPES	N-[2-Hydroxyethyl]piperazine-N'[2-ethanesulfonic acid]
hsst <sub>1-5</sub>	human somatostatin receptor subtypes 1-5
5-HT	5-hydroxytryptamin, serotonin
Hz	Hertz
iev	intracerebroventral
IP <sub>1</sub>	inositol monophosphate
IP <sub>2</sub>	inositol diphosphate
IP <sub>3</sub>	inositol triphosphate



IP <sub>x</sub>	inositol x-phosphate
kb	kilo basepairs
K <sub>d</sub>	equilibrium dissociation constant
M	mol/l
MAPK	mitogen-activated protein kinase
MBq	Mega-Bequerel
MEM	minimal essential medium
μF	μ-Farad
min	minute(s)
mJ	m-Joule
mM	mmol/l
μM	μmol/l
mol wt	molecular weight
MOPS	3-[N-morpholino]-propanesulphonic acid
mRNA	messenger RNA
NK	neurokinin
nM	nmol/l
P	probability
PACAP	pituitary adenylate cyclase activating polypeptide
PBS	phosphate-buffered saline
PCR	polymerase chain reaction
pEC <sub>50</sub>	potency, negative logarithm of the EC <sub>50</sub>
P <sub>i</sub>	inorganic phosphate (PO <sub>3</sub> <sup>2-</sup> )
pK <sub>B</sub>	potency of an antagonist
pK <sub>d</sub>	negative logarithm of the equilibrium dissociation constant
PLC	phospholipase C
pM	pmol/ l
PTX	pertussis toxin
r	correlation coefficient
RGS	regulators of G-protein signalling
RNA	ribonucleic acid
RSV	Rous Sarcoma virus (promotor)

RT	reverse transcriptase
s	second(s)
SDS	sodium dodecyl sulphate
SEM	standard error of the mean
SPA	scintillation proximity assay
SRIF	somatotropin-release-inhibiting factor = somatostatin
SSC	standard saline citrate
sst <sub>1-5</sub>	somatostatin receptor subtypes 1-5
TM	transmembrane domain
Tris	tris(hydroxymethyl)-aminomethane
UV	ultraviolett
V	Volt
WGA	wheatgerm agglutinin

amino acids

Ala	A	alanine	Leu	L	leucine
Arg	R	arginine	Lys	K	lysine
Asn	N	asparagine	Met	M	methionine
Asp	D	aspartic acid	Phe	F	phenylalanine
Cys	C	cysteine	Pro	P	proline
Glu	E	glutamic acid	Ser	S	serine
Gln	Q	glutamine	Thr	T	threonine
Gly	G	glycine	Trp	W	tryptophan
His	H	histidine	Tyr	Y	tyrosine
Ile	I	isoleucine	Val	V	valine

## Summary

Somatostatin (SRIF = somatotropin release inhibiting factor) is a hormone/neuropeptide with multiple endocrine and exocrine effects, effects on inhibition of hormone release, cognitive functions, behaviour, sleep activity and inhibition of tumour growth. The SRIF analogue octreotide is used to treat acromegaly, hormone-secreting tumours, and AIDS-related diarrhoea. In mammals, the SRIF family includes SRIF<sub>14</sub>, SRIF<sub>28</sub>, and the recently identified and putative neuropeptide cortistatin (CST); non-mammalian vertebrates possess SRIF<sub>14</sub> and a second SRIF variant.

A class of G-protein-coupled receptors, the somatostatin receptors, mediate the actions of SRIF, and five mammalian subtypes (sst<sub>1-5</sub>) have been cloned; SRIF receptors are specifically expressed in brain, periphery, and many tumours. The third cytoplasmic loop of G-protein-coupled receptors is suggested to link the receptors to G-proteins, which couple the receptors to specific intracellular signalling cascades. Many cellular effector proteins such as phospholipase C (PLC), phospholipase A<sub>2</sub>, calcium channels, potassium channels, Na<sup>+</sup>/H<sup>+</sup> exchanger, adenylate cyclase (AC), protein tyrosine phosphatases, mitogen-activated protein kinase (MAPK) or p53 are reported to be specifically modulated by SRIF receptor subtypes.

In this study, the five human SRIF receptor subtypes, and the first cloned non-mammalian SRIF receptor, fish sst<sub>3</sub> receptor (of *Apteronotus albifrons*), were characterised by analysing their binding and transductional features under the same environment, i.e. by stable receptor expression in CCL39 hamster lung fibroblast cells.

CST<sub>14/17</sub> and the iodinated analogue [<sup>125</sup>I][Tyr<sup>10</sup>]CST<sub>14</sub>, bound with similar high affinity to all five human SRIF receptors, and thus the pharmacological profiles of the iodinated peptide was established with a number of SRIF/ CST analogues; the affinity profiles were comparable to those established using [<sup>125</sup>I]LTT-SRIF<sub>28</sub>. This underlines the close relation of CST and SRIF peptides, although specific CST receptors may also exist.

Very marked differences in peptide affinities for SRIF receptors have been described in the literature; therefore additional synthetic radioligands ([<sup>125</sup>I]CGP 23996, [<sup>125</sup>I][Tyr<sup>3</sup>]octreotide) were used to establish affinity profiles. Surprisingly, [<sup>125</sup>I][Tyr<sup>3</sup>]octreotide labelled beside human sst<sub>2</sub> also sst<sub>5</sub> receptor sites with high affinity, and some other classically sst<sub>2</sub>-selective compounds (octreotide, seglitide etc.) showed high affinity to sst<sub>5</sub> receptors; hence, sst<sub>5</sub> receptors may mediate physiological effects of octreotide, which previously were attributed to the sst<sub>2</sub> subtype solely.

Ligand affinities and receptor densities were radioligand-dependent at human sst<sub>5</sub>, but not at sst<sub>1-4</sub> receptors: e.g. [<sup>125</sup>I]LTT-SRIF<sub>28</sub> labelled seven times more sst<sub>5</sub> receptor sites than [<sup>125</sup>I][Tyr<sup>3</sup>]octreotide, and the affinity of e.g. octreotide defined with [<sup>125</sup>I]LTT-SRIF<sub>28</sub> was 100-fold lower compared to that defined with [<sup>125</sup>I][Tyr<sup>3</sup>]octreotide.

Although the non-iodinated analogues of the four radioligands are full agonists in functional studies, their binding to sst<sub>5</sub> receptors was differently modulated by the GTP-analogue guanylylimidodiphosphate (GppNHp): e.g. [<sup>125</sup>I][Tyr<sup>3</sup>]octreotide binding was highly affected suggesting selective labelling of G-protein-coupled sst<sub>5</sub> receptors, whereas [<sup>125</sup>I]LTT-SRIF<sub>28</sub> and [<sup>125</sup>I][Tyr<sup>10</sup>]CST<sub>14</sub> seem to label rather uncoupled receptors and hence a higher density; radioligand binding at sst<sub>2</sub>/sst<sub>3</sub> receptors was markedly inhibited, and rather unaffected at sst<sub>1</sub>/sst<sub>4</sub> receptors.

The data do not fit the ternary complex model, instead the existence of multiple G-protein-coupled/ -uncoupled agonist-specific receptor states may be proposed.

In functional studies, all five SRIF receptors inhibited forskolin-stimulated adenylate cyclase (FSAC) activity, *hsst*<sub>2-5</sub> receptors stimulated [<sup>35</sup>S]GTPγS binding (G-protein activation), and *sst*<sub>3/5</sub> activated PLC activity (measured by IP<sub>x</sub> accumulation, intracellular Ca<sup>2+</sup> increase), the latter effect being only partially pertussis toxin (PTX) sensitive (i.e. partly mediated by G<sub>i/o</sub>).

Pharmacological profiles of human SRIF receptors established in these three functional assays correlated significantly, but to various extents even at the same receptor with the different radioligand binding profiles; functional data of *sst*<sub>1/2</sub> receptors correlated only modestly with the affinity profiles suggesting other effector pathways to be more important. In addition, the potency rank orders of SRIF/ CST ligands examined at each human SRIF receptor subtype was distinct from one functional assay to the other, and compared to the affinity profiles. These findings support the hypothesis of receptor induced effector trafficking by presumably different agonist-specific receptor states.

In the brain, fish *sst*<sub>3</sub> receptor transcripts, as detected by RT-PCR, and fish *sst*<sub>3</sub> protein seem to be present, since the profile of *fsst*<sub>3</sub> receptors expressed in CCL39 cells correlated highly with that of native brain receptors [<sup>125</sup>I]LTT-SRIF<sub>28</sub> binding; however, biphasic curves in brain and low correlation with liver sites suggest additional fish SRIF receptors. At recombinant *fsst*<sub>3</sub> receptors radioligand-dependency of receptor densities, affinities, and GppNHp-sensitivity was documented using [<sup>125</sup>I]LTT-SRIF<sub>28</sub>, [<sup>125</sup>I][Tyr<sup>10</sup>]CST<sub>14</sub>, [<sup>125</sup>I]CGP 23996, [<sup>125</sup>I][Tyr<sup>3</sup>]octreotide, similar to the human *sst*<sub>5</sub> receptor. Coupling to signalling pathways seems to be highly conserved between fish and mammalian SRIF receptors: *fsst*<sub>3</sub> receptors mediate stimulation of [<sup>35</sup>S]GTPγS binding, inhibition of FSAC via G<sub>i</sub>/G<sub>o</sub>, and PLC activation partly via G<sub>i</sub>/G<sub>o</sub>. Pharmacological profiles of radioligand binding and functional tests correlated with each other with variations, supporting again a model of specific agonist-induced receptor conformations; species differences on pharmacology: *fsst*<sub>3</sub> profiles fitted best with the *hsst*<sub>5</sub> receptor profiles, in spite of the highest sequence homology with the *hsst*<sub>3</sub> subtype.

**Keywords:** somatostatin (SRIF), cortistatin (CST), octreotide, human recombinant somatostatin receptors (*hsst*<sub>1-5</sub>), fish somatostatin receptor 3; (*fsst*<sub>3</sub>), CCL39 Chinese hamster lung fibroblast cells, guanylylimidodiphosphate (GppNHp), guanosine-5'-O-(3-thio)-triphosphate (GTPγS), adenylate cyclase (AC), phospholipase C (PLC), inositol phosphate (IP<sub>x</sub>), intracellular calcium, pertussis toxin (PTX).

## Kurzfassung

Somatostatin (SRIF = Somatotropin-Freisetzung-inhibierender Faktor) ist ein Hormon/Neuropeptid mit zahlreichen endokrinen und exokrinen Wirkungen, Wirkungen auf Inhibition von Hormon-Freisetzungen, kognitive Funktionen, Verhalten, Schlafaktivität, und auf Hemmung von Tumorwachstum. Das SRIF-Analog Octreotide wird zur Behandlung von Akromegalie, Hormon-sekretierenden Tumoren, und von AIDS-abhängiger Diarrhoea verwendet. Bei Säugern umfasst die SRIF-Familie SRIF<sub>14</sub>, SRIF<sub>28</sub>, sowie das kürzlich identifizierte und vermutlich existente Neuropeptid Cortistatin (CST); Wirbeltiere, die nicht der Klasse der Säuger angehören, besitzen SRIF<sub>14</sub> und eine zweite SRIF-Variante.

Eine Klasse von G-Protein-gekoppelten Rezeptoren, die Somatostatin-Rezeptoren, vermitteln die Wirkungen von SRIF, und fünf Subtypen (sst<sub>1-5</sub>) sind bei Säugern kloniert worden; SRIF-Rezeptoren sind im Gehirn, in der Peripherie, und in vielen Tumoren spezifisch exprimiert. Die dritte cytoplasmatische Schleife von G-Protein-gekoppelten Rezeptoren verbindet vermutlich die Rezeptoren mit G-Proteinen, welche die Rezeptoren an spezifische intrazelluläre Signalkaskaden koppeln. Es wird berichtet, dass viele zelluläre Effektorproteine, wie z. B. Phospholipase C (PLC), Phospholipase A<sub>2</sub>, Calciumkanäle, Kaliumkanäle, Na<sup>+</sup>/H<sup>+</sup>-Austauschpumpen, Adenylat-Cyclase (AC), Proteintyrosin-Phosphatasen, Mitogen-aktivierte Proteinkinase (MAPK) oder p53 von SRIF-Rezeptorsubtypen spezifisch moduliert werden.

In dieser Studie wurden die fünf humanen SRIF-Rezeptorsubtypen, und der erste von einem Nichtsäuger klonierte SRIF-Rezeptor, der Fish sst<sub>3</sub> Rezeptor (von *Apterionotus albifrons*), durch Analyse von Bindungs- und Transduktionseigenschaften im gleichen System charakterisiert, d. h. durch stabile Rezeptorexpression in CCL39 Hamster-Lungenfibroblastenzellen.

CST<sub>14/17</sub> und das iodierter Analog [<sup>125</sup>I][Tyr<sup>10</sup>]CST<sub>14</sub>, banden mit ähnlich hoher Affinität an alle fünf menschlichen SRIF-Rezeptoren, und somit wurden die pharmakologischen Profile des iodierten Peptids mit einer Anzahl an SRIF/ CST Analogas erstellt; die Affinitätsprofile waren vergleichbar mit den unter Verwendung von [<sup>125</sup>I]LTT-SRIF<sub>28</sub> erstellten Profilen. Dies unterstreicht die enge Verwandtschaft von CST- und SRIF-Peptiden, obgleich auch spezifische CST-Rezeptoren existieren könnten.

Für SRIF-Rezeptoren wurden grosse Unterschiede von Peptidaffinitäten in der Literatur beschrieben; deshalb wurden zusätzliche, synthetische Radioliganden ([<sup>125</sup>I]CGP 23996, [<sup>125</sup>I][Tyr<sup>3</sup>]Octreotide) verwendet, um Affinitätsprofile zu erstellen. Überraschenderweise markierte [<sup>125</sup>I][Tyr<sup>3</sup>]Octreotide neben humanen sst<sub>2</sub> auch humane sst<sub>5</sub> Rezeptorstellen mit hoher Affinität, und einige andere klassisch sst<sub>2</sub>-selektiven Verbindungen (Octreotide, Seglitide etc.) zeigten hohe Affinität für sst<sub>5</sub> Rezeptoren; folglich vermitteln sst<sub>5</sub> Rezeptoren möglicherweise physiologische Wirkungen von Octreotide, welche zuvor einzig dem sst<sub>2</sub>-Subtyp zugeordnet wurden.

Ligandenaffinitäten und Rezeptordichte waren bei menschlichen sst<sub>5</sub> Rezeptoren Radioliganden-abhängig, nicht aber bei sst<sub>1-4</sub> Rezeptoren: z. B. markierte [<sup>125</sup>I]LTT-SRIF<sub>28</sub> siebenmal mehr sst<sub>5</sub> Rezeptorstellen als [<sup>125</sup>I][Tyr<sup>3</sup>]Octreotide, und die von z. B. Octreotide ermittelte Affinität war mit [<sup>125</sup>I]LTT-SRIF<sub>28</sub> 100-mal niedriger als mit [<sup>125</sup>I][Tyr<sup>3</sup>]Octreotide.

Obwohl die nicht-iodierten Analoga der vier Radioliganden in funktionellen Studien volle Agonisten sind, war deren Bindung an  $ss_5$  Rezeptoren durch das GTP-Analog Guanylylimidodiphosphat (GppNHp) unterschiedlich moduliert: die Bindung von z. B. [ $^{125}$ I][Tyr<sup>3</sup>]Ostreotide war stark inhibiert, was auf ein selektives Markieren von G-Protein-gekoppelten  $ss_5$  Rezeptoren hinweist, während [ $^{125}$ I]LTT-SRIF<sub>28</sub> und [ $^{125}$ I][Tyr<sup>10</sup>]CST<sub>14</sub> eher ungekoppelte Rezeptoren und daher eine höhere Dichte zu markieren scheinen; die Radioligandenbindung von  $ss_2$ / $ss_3$  Rezeptoren war deutlich inhibiert, und eher unbeeinträchtigt bei  $ss_1$ / $ss_4$  Rezeptoren. Diese Daten passen nicht in das ternäre Komplex-Modell, stattdessen kann die Existenz von multiplen G-Protein-gekoppelten/ -ungekoppelten Agonist-spezifischen Rezeptorzuständen vermutet werden.

In funktionellen Studien inhibierten alle fünf SRIF-Rezeptoren Forskolin-stimulierte Adenylat-Cyclase (FSAC)-Aktivität,  $hsst_{2,5}$  Rezeptoren stimulierten [ $^{35}$ S]GTP $\gamma$ S-Bindung (G-Protein-Aktivierung), und  $ss_3$ / $ss_5$  Rezeptoren aktivierten PLC-Aktivität (gemessen durch IP<sub>x</sub>-Akkumulation, intrazellulären Ca<sup>2+</sup>-Anstieg), wobei der letztere Effekt nur teilweise Pertussis-Toxin (PTX)-sensitiv (d. h. nur teils durch G<sub>i/o</sub> vermittelt) war.

Die in diesen drei funktionellen Versuchsmethoden an menschlichen SRIF-Rezeptoren erstellten pharmakologischen Profile korrelierten signifikant, aber selbst am gleichen Rezeptor zu einem unterschiedlichem Grad mit den verschiedenen Radioliganden-Bindungsprofilen; funktionelle Daten von  $ss_1$ / $ss_2$  Rezeptoren korrelierten nur mässig mit den Affinitätsprofilen, was darauf hinweist, dass andere Effektor-Signalwege bedeutsamer sind. Ausserdem war bei jedem SRIF-Rezeptorsubtypen die untersuchten Reihenfolgen der Potenzen von SRIF/ CST- Liganden von einem funktionellen Assay zum anderen verschieden, sowie verglichen zu den Affinitätsprofilen. Diese Ergebnisse unterstützen die Hypothese von Rezeptor-induziertem Effektor-“Trafficking” durch vermutlich verschiedene Agonist-spezifische Rezeptorzustände.

Im Gehirn scheinen Fisch  $ss_3$  Rezeptor-Transkripte, welche durch RT-PCR nachgewiesen wurden, und Fisch  $ss_3$  Protein vorhanden zu sein, da das [ $^{125}$ I]LTT-SRIF<sub>28</sub>-Bindungsprofil von in CCL39-Zellen exprimierten  $fsst_3$  Rezeptoren stark mit dem von natürlich vorkommenden Gehirnrezeptoren korreliert; jedoch lassen biphasische Kurven im Gehirn und die schwache Korrelation mit Leber-Bindungsstellen zusätzliche Fisch-SRIF-Rezeptoren vermuten. Beim rekombinanten  $fsst_3$  Rezeptor wurde unter Verwendung von [ $^{125}$ I]LTT-SRIF<sub>28</sub>, [ $^{125}$ I][Tyr<sup>10</sup>]CST<sub>14</sub>, [ $^{125}$ I]CGP 23996, und [ $^{125}$ I][Tyr<sup>3</sup>]Ostreotide Radioliganden-Abhängigkeit der Rezeptordichte, der Affinitäten, und der GppNHp-Sensitivität gemessen - ähnlich wie beim menschlichen  $ss_5$  Rezeptor. Das Koppeln an Signalwege scheint bei Fisch- und Säuger-SRIF-Rezeptoren hoch konserviert zu sein: Fisch  $ss_3$  Rezeptoren vermitteln Stimulation von [ $^{35}$ S]GTP $\gamma$ S-Bindung, Inhibition von FSAC über G<sub>i</sub>/G<sub>o</sub>, und PLC-Aktivierung teilweise über G<sub>i</sub>/G<sub>o</sub>. Die pharmakologischen Profile von Radioligandenbindung und funktionellen Tests korrelierten unterschiedlich stark miteinander, was erneut das Modell der spezifischen Agonist-induzierten Rezeptorkonformationen unterstützt; pharmakologische Arten-Unterschiede: die  $fsst_3$  Profile stimmten am besten mit den  $hsst_5$  Profilen überein, trotz der grössten Sequenzhomologie mit dem  $hsst_3$  Subtyp.

**Stichworte:** Somatostatin (SRIF), Cortistatin (CST), Octreotide, menschliche rekombinante Somatostatin-Rezeptoren (hsst<sub>1-5</sub>), Fisch-Somatostatin-Rezeptor 3; (fsst<sub>3</sub>), CCL39 Hamster-Lungenfibroblastenzellen, Guanylylimidodiphosphat (GppNHp), Guanosine-5`O-(3-thio)-Triphosphat (GTP $\gamma$ S), Adenylat-Cyclase (AC), Phospholipase C (PLC), Inositolphosphat (IP<sub>x</sub>), intrazelluläres Calcium, Pertussis-Toxin (PTX).

# Chapter 1

---

## Introduction

---



## 1.1. The Somatostatin peptide family

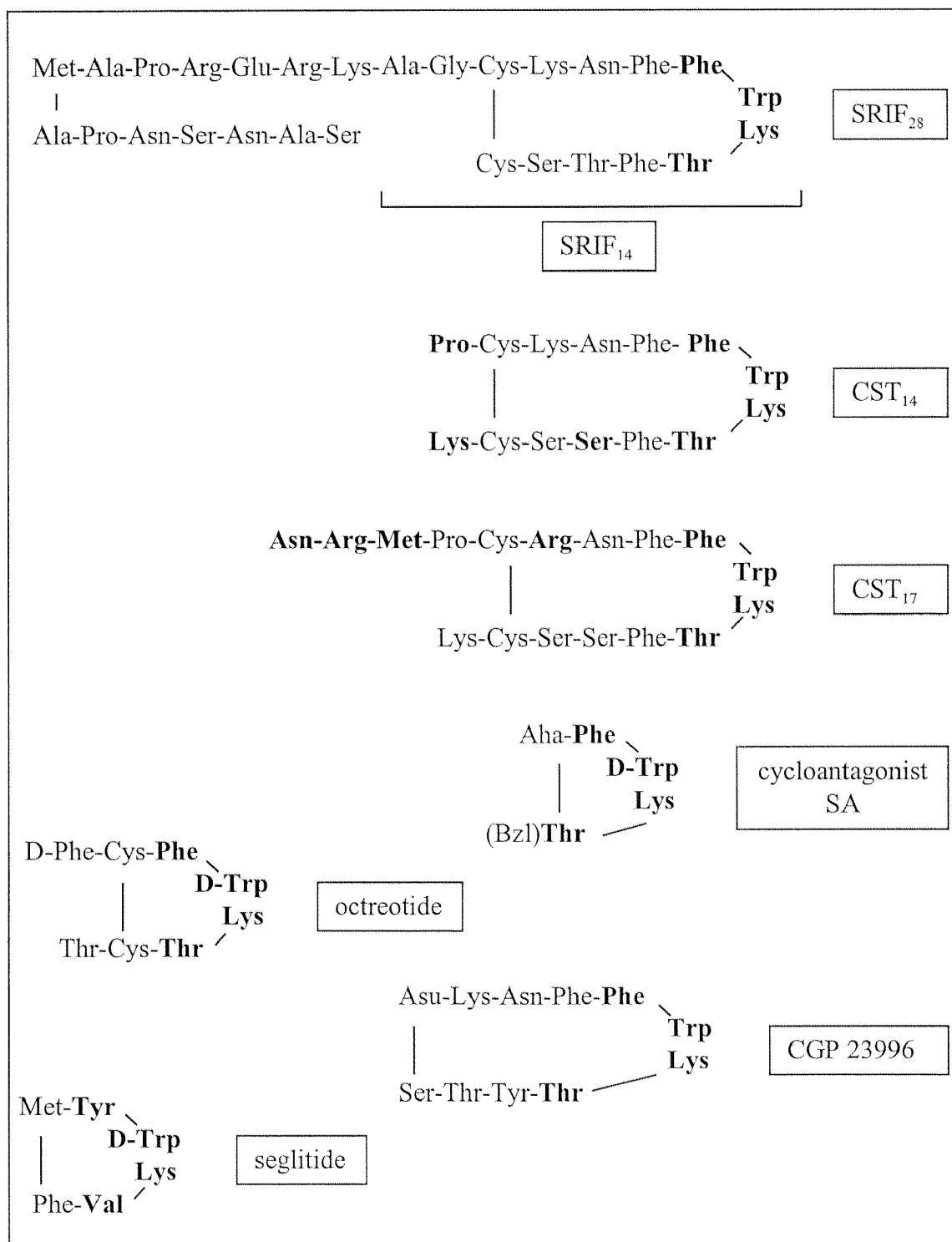
### 1.1.1. Mammalian somatostatin peptides

In mammals, the two physiologically active forms of somatostatin are the tetradecapeptide SRIF<sub>14</sub> (SRIF = somatotropin release inhibiting factor) (Brazeau et al., 1973), which was originally discovered from bovine hypothalamic extracts and found to inhibit somatotropin secretion (Krulich et al., 1968), and the N-terminally extended SRIF<sub>28</sub>, which was originally isolated from porcine duodenum (figure 1) (Pradayrol et al., 1980). The "cyclic" peptides SRIF<sub>14</sub> and SRIF<sub>28</sub> are the products of a common gene, and they are released from their prepropeptide by enzymatic processing; other cleavage products of the precursor molecule reveal no biological activity (figure 2) (Patel et al., 1985; Robbins and Reichlin, 1983; Shen et al., 1982; Zingg and Patel, 1982).

The more recently cloned cortistatin (CST) is the (putative) product of a second gene, and the corresponding precortistatin shows especially in the carboxy terminus high structural similarity to preprosomatostatin; therefore, it may be proteolysed at analogous endonuclease restriction sites to CST<sub>14</sub> in rodents, and to CST<sub>17</sub> in human (figure 2) (De Lecea et al., 1996; 1997b; Fukusumi et al., 1997). The primary sequence of CST is very similar to that of mature SRIF: e.g. CST<sub>14</sub> shares 11 of 14 amino acid residues with SRIF<sub>14</sub> (figure 1) (De Lecea et al., 1996).

The neuropeptide SRIF is widely expressed in the mammalian organism both in the central nervous system (CNS), and also in peripheral tissues: SRIF transcripts were found in the submandibular glands, in the thyroid, in gut, pancreas, kidney, adrenals, prostate, and in placenta (Aguila et al., 1991; Finley et al., 1981; Johansson et al., 1984; Reichlin, 1983; Vincent et al., 1985). SRIF<sub>14</sub> is the predominant form found in neurones, whereas SRIF<sub>28</sub> is the predominant peptide found in some peripheral organs like e.g. stomach and intestine (Patel et al., 1981; 1985). In contrast to SRIF, the prepro-CST mRNA has been located solely to the CNS: in cortex, hippocampus and spinal cord (De Lecea et al., 1996; 1997b; Fukusumi et al., 1997). There is currently no final proof for the existence of mature CST, since CST-selective antibodies have not yet become available, although it is clear that synthetic CST is biologically active.

**Figure 1:** Primary structure of somatostatin, cortistatin and some widely used analogues.



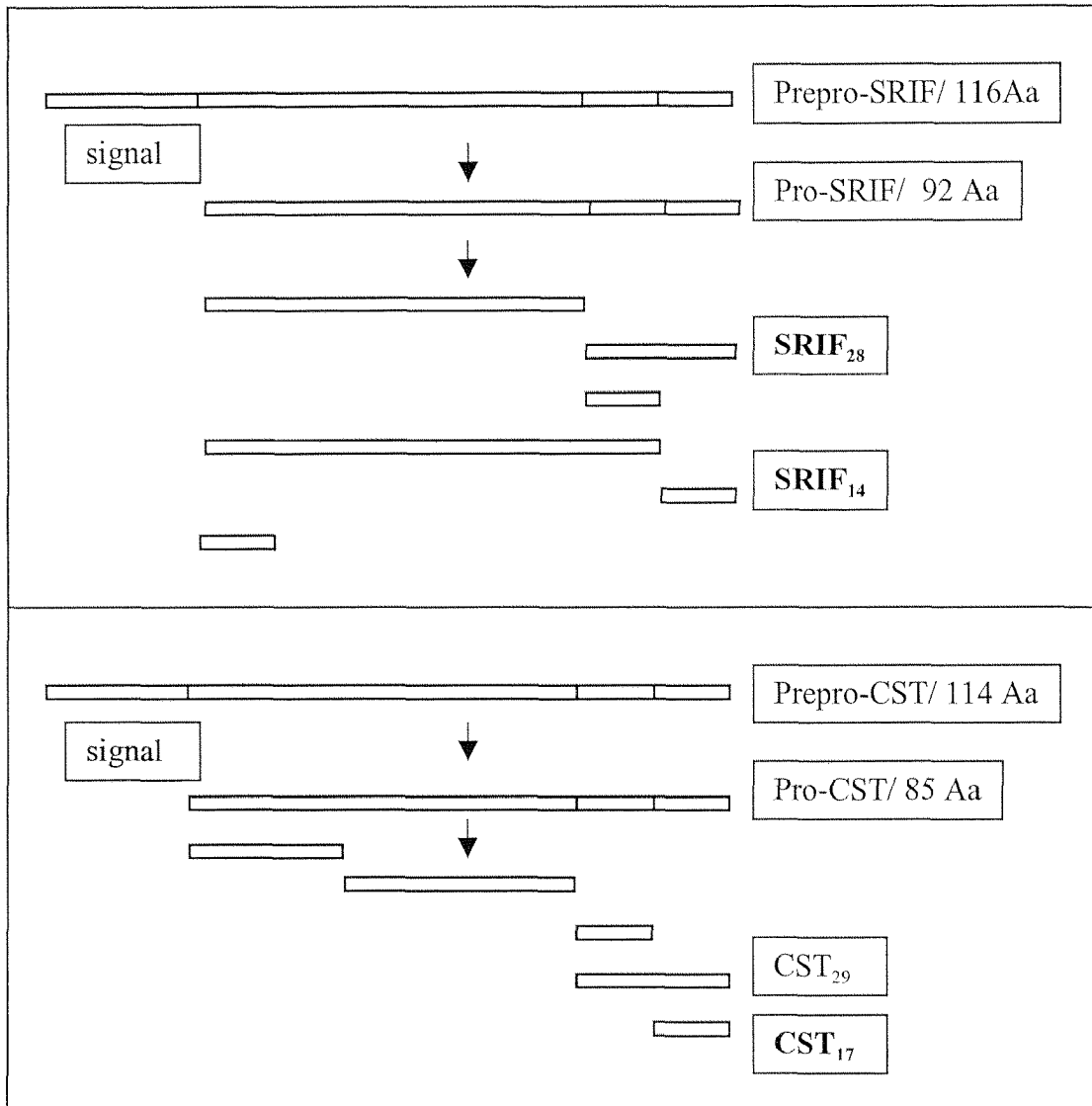
The four amino acids which appear to be crucial for activity in the  $\beta$ -turn (SRIF<sub>14</sub>: Phe<sup>7</sup>-Trp<sup>8</sup>-Lys<sup>9</sup>-Thr<sup>10</sup>) are marked in bold; in CST<sub>14</sub> three further amino acids, which underline the differences to SRIF<sub>14</sub>, are indicated in bold, in CST<sub>17</sub> the four further amino acids in bold emphasise the differences to CST<sub>14</sub>. Abbreviations: Asu = amino suberic acid; Aha = amino heptanoic acid; Bzl = Benzyl-substituent.

### 1.1.2. Non-mammalian somatostatin peptides

SRIF<sub>14</sub> has been found not only in every mammalian species examined thus far, but also in representatives of other vertebrate classes, like birds (Conlon and Hicks, 1990; Spiess et al., 1979), reptiles (Wang and Conlon, 1993), amphibia (Vaudry et al., 1992), and fish (Andrews and Dixon, 1981; Conlon et al., 1985; 1988a; 1988b; 1995; Noe et al., 1979; Plisetskaya et al., 1986; Taylor et al., 1981); therefore, SRIF<sub>14</sub> seems to be highly conserved among vertebrates. Variants of SRIF<sub>14</sub>, like [Pro<sup>2</sup>]SRIF<sub>14</sub>, [Pro<sup>2</sup>, Met<sup>13</sup>]SRIF<sub>14</sub>, [Ser<sup>5</sup>]SRIF<sub>14</sub>, [Ser<sup>12</sup>]SRIF<sub>14</sub>, appear to be rather rare and could be isolated in a few species only (Andrews et al., 1988; Conlon, 1990; Nishii et al., 1995; Vaudry et al., 1992).

Two somatostatin genes are known from various fish species: one encodes the prepropeptide of SRIF<sub>14</sub>, whereas the second gene encodes a precursor molecule which is processed to a SRIF peptide varying with the systematic group (Eilertson et al., 1993; Goodmann et al., 1980; Hobart et al., 1980); this SRIF variant molecule comprises 22-37 amino acids and its primary structure is much less conserved in the course of evolution, particularly in the N-terminal region: e.g. SRIF<sub>22</sub> in catfish, SRIF<sub>25</sub> in salmon and eel (Andrews et al., 1984; Conlon et al., 1988b; Eilertson et al., 1993; Fletcher et al., 1983; Hobart et al., 1980; Magazin et al., 1982; Plisetskaya et al., 1986; Uesaka et al., 1995).

SRIF mRNA has been identified in fish tissue of various organs. In the fish CNS, SRIF is expressed throughout the neuraxis in specific areas (Sas and Maler, 1991; Zupanc et al., 1991; 1994), and possesses multiple physiological functions such as regulation of postnatal development (Stroh and Zupanc, 1993; 1995; 1996; Zupanc, 1996, 1999; Zupanc and Maler, 1997).

**Figure 2:** Prepropeptide processing of mammalian somatostatin and human cortistatin.

Proteolytic processing of mammalian preprosomatostatin at monobasic (Arg) and dibasic (Arg-Lys) cleavage sites (Robbins and Reichlin, 1983; Shen et al., 1982; Zingg and Patel, 1982), and putative cleavage of human precortistatin (Fukusumi et al., 1997). The preprohormones contain a N-terminal signal sequence; the mature products, which are indicated in bold, are released from the carboxy terminus, in which the highest sequence homology of preprohormones is found. Abbreviation: Aa = amino acids.

### 1.1.3. Synthetic somatostatin analogues

SRIF binding sites were initially studied with [<sup>3</sup>H] ligands (Whitford et al., 1985, 1986, 1987), however iodinated ligands offer a number of advantages. Their theoretical specific activity (2175 Ci/ mmol = 1 iodine/ molecule) is much higher than that of tritiated ligands (20- 60 Ci/ mmol), which allows the use of very low amounts of receptors to perform studies. In addition, when autoradiographic studies are to be performed, high specific activity shortens dramatically the exposure time for the autoradiography film. Finally, if needed, the Chloramine T method for iodination offers clearly some economic advantages.

Since SRIF and CST cannot be iodinated, synthetic analogues with tyrosine residues for iodination were created to allow radioligand binding studies to their respective binding sites. Structure-activity studies have shown that analogues containing the Phe<sup>7</sup>-Trp<sup>8</sup>-Lys<sup>9</sup>-Thr<sup>10</sup> residues of SRIF<sub>14</sub> in an appropriate cyclic conformation are sufficient to function as highly potent agonists. The presence of Trp<sup>8</sup>-Lys<sup>9</sup> in the peptide is essential, whereas Phe<sup>7</sup> and Thr<sup>10</sup> can undergo minor substitutions (Brazeau et al., 1972; Epelbaum, 1986; Freidinger et al., 1984; Veber et al., 1981).

To increase the half-life, the peptides were metabolically stabilised by the introduction of D-amino acids. An example of such a metabolically stable peptide which is important for clinical use is the short synthetic SRIF analogue octreotide (figure 1) (SMS 201-995, Sandostatin<sup>®</sup>, Bauer et al., 1982). Octreotide inhibits, like SRIF, the release of GH (growth hormone, somatotropin), and hence is used to treat acromegaly, which is caused by hypersecretion of somatotropin from the anterior pituitary; acromegaly is primarily associated with a pituitary adenoma, and leads to abnormal skeletal and tissue enlargement (Lancranjan et al., 1996). In addition, octreotide has antiproliferative properties *in vitro* in a number of tumour cell lines and *in vivo* in a variety of neuroendocrine and gastroenteropancreatic (GEP) tumours; therefore, octreotide inhibits tumour growth, or even induces tumour shrinkage (Cheung et al., 1995; Kubota et al., 1994; Lamberts et al., 1987; 1991; 1995; Srikant, 1995; Weckbecker et al., 1993) and is currently indicated for the treatment of a number of GEP tumours.

Similar to SRIF, octreotide stimulates water and electrolyte absorption and inhibits epithelial transport and intestinal motility, and the release of gut hormones (Edwards et al., 1986; Efendic and Mattson, 1978; Kraenzlin et al., 1985). Thus, it is used in the control of refractory diarrhoea associated with acquired immunodeficiency syndrome (AIDS) (Cello et al., 1991; Monte et al., 1989). The radionuclide-coupled peptide [<sup>125</sup>In]octreoscan (Pentetreotide®) is used to visualise tumours positive for SRIF binding sites by scintigraphy, whereas [<sup>90</sup>Y]SMZ 487 is currently undergoing clinical trials for tumour radiotherapy (Krenning et al., 1994; 1995).

#### **1.1.4. Physiological relevance**

SRIF (and CST) possesses multiple physiological functions including regulation of endocrine and exocrine secretion, neurotransmission, neuromodulation, cognitive functions, behaviour, regulation of embryonic and postnatal development of neurones, inhibition of tumour growth and modulation of sleep activity (Brazeau et al., 1972; Brown et al., 1977; Buscail et al., 1993; 1994; De Lecea et al., 1996; 1997a; 1997b; Epelbaum, 1986; 1994; Feniuk et al., 1993; Fujii et al., 1994; Fukusumi et al. 1997; Krulich et al., 1968; Mandarino et al., 1981; for review, Patel, 1997; Raynor and Reisine, 1992; Reichlin, 1983; Schally et al., 1988).

SRIF expression is known to be altered in numerous diseases: decreased SRIF production was observed in the brain and/or CSF (cerebro spinal fluid) of patients suffering from Alzheimer's disease, schizophrenia, and epilepsy (Beal et al., 1985; Davies et al., 1980; Nemeroff et al., 1983; Riekkinen et al., 1990), whereas an increased SRIF expression could be determined in the brain of patients with Huntington's chorea, Parkinson's disease, and AIDS (Aronin et al., 1983; Chesselet and Reisine, 1983; Da Cunha et al., 1995; Nemeroff et al., 1983).

## 1.2. Somatostatin receptors

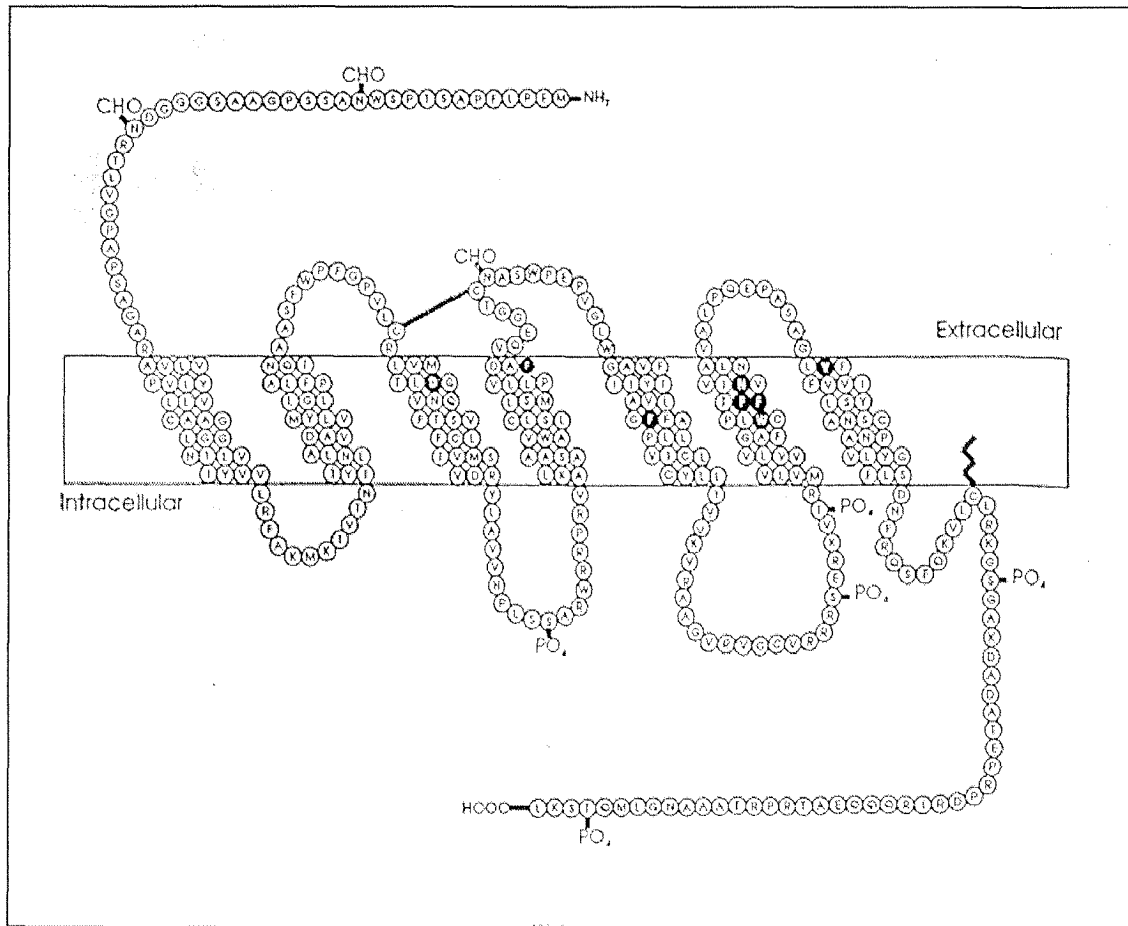
### 1.2.1. Receptor subtypes

SRIF and CST exert their biological effects via membrane-bound receptors - the so-called somatostatin receptors-, which have seven transmembrane-spanning helices and belong to the superfamily of G-protein coupled receptors (Bell and Reisine, 1993); they contain the consensus sequence Asp-Arg-Tyr (= DRY) at the boundary of their third transmembrane domain and their second cytoplasmatic loop, which is characteristic for a subfamily of G-protein-coupled receptors (figure 3) (Reisine and Bell, 1995).

Five mammalian receptor subtypes – designated as  $sst_{1,5}$  (Hoyer et al., 1995a) - have been cloned from human, rat and mouse (Bell and Reisine, 1993; Bruno et al., 1992; Demchyshyn et al., 1993; Kluxen et al., 1992; Li et al., 1992; Lublin et al., 1997; Meyerhof et al., 1992; O'Carroll et al., 1992; 1994; Panetta et al., 1994; Rohrer et al., 1993; Vanetti et al., 1992; Xu et al., 1993; Yamada et al., 1992a; 1992b; 1993; Yasuda et al., 1992); additionally, the porcine and bovine homologues of the  $sst_2$  receptor were cloned (Matsumoto et al., 1994; Xin et al., 1992). Based on structural and operational features, two classes of SRIF receptors can be distinguished: the SRIF<sub>1</sub>-family comprising  $sst_2$ ,  $sst_3$  and  $sst_5$ , and the SRIF<sub>2</sub>-family including  $sst_1$  and  $sst_4$  receptors (Hoyer et al., 1995a).

All cloned receptor subtypes are intron-less in their protein-coding region with the exception of the rodent  $sst_2$  receptor: in addition to the unspliced  $sst_{2A}$  receptor, the  $sst_{2B}$  receptor splice variant, which differs only by a shorter carboxy tail from the unspliced form, was identified in mouse and rat (Schindler et al., 1998b; Vanetti et al., 1992; 1993). Two differentially sized transcripts were detected for the human  $sst_2$  receptor, suggesting alternative splicing to take place also in man (Yamada et al., 1992a), although the existence of the spliced form has not been confirmed so far by cloning.

**Figure 3:** Transmembrane model of the human somatostatin  $sst_5$  receptor.



CHO = putative N-linked glycosylation site, PO<sub>4</sub> = putative phosphorylation site, Σ = putative palmitoyl membrane anchor site (Leu-rich), C-C = disulfide bond between cysteine residues. Black amino acids indicate the proposed ligand binding pocket of SRIF<sub>14</sub> within the transmembrane domains 3- 7. The model was taken from Patel et al. (1995).

The genes of the different SRIF receptor subtypes are localised on separate chromosomes; the human  $sst_{1,5}$  receptors were localised on chromosome 14, 17, 22, 20 and 16, and their protein consists of 391, 369, 356, 418, 388 and 364 amino acids, respectively (Corness et al., 1993; Demchyshyn et al., 1993; Yamada et al., 1993; Yasuda et al., 1993; Panetta et al., 1994; Patel, 1997).



The primary structure of SRIF receptors suggests the presence of seven transmembrane spanning  $\alpha$ -helices, in which highest sequence similarities are found when comparing the different receptor subtypes; in addition, there is suggested to be a disulfide bond between two cysteine residues of the second and the third extracellular loop, as well as several subtype- and species-specific glycosylation and phosphorylation sites (figure 3) (Bell et al., 1995; Dournaud et al., 1996; Nehring et al., 1995; Meyerhof et al., 1992).

The ligand binding pocket of SRIF receptors is species-, subtype- and ligand-specific, but the responsible amino acids are predominantly located within the transmembrane domains 3- 7, and partially in the second and/ or third extracellular loop, as suggested from studies performed with numerous deletion mutants and by site-directed mutagenesis (Fitzpatrick and Vandlen, 1994; Liapakis et al., 1996; Kaupmann et al., 1995; Ozenberger and Hadcock, 1995). The agonist binding of SRIF<sub>1</sub> receptors, but not of SRIF<sub>2</sub> receptors, is negatively modulated by sodium ions (Reubi and Maurer, 1986; Raynor et al., 1993a, 1993b), for which a conserved aspartate residue in the second the transmembrane domain is responsible (Kong et al., 1993).

All SRIF receptor subtypes bind the endogenous peptides SRIF<sub>14</sub>, SRIF<sub>28</sub> and CST with similar high affinity and only little or no selectivity (Fukusumi et al. 1997; Hoyer et al., 1994). In contrast, the short cyclic analogues octreotide and seglitide (MK678) (figure 1) bind selectively to members of the SRIF<sub>1</sub>-receptor family with preferential affinity for sst<sub>2</sub> and sst<sub>5</sub> receptors compared to sst<sub>3</sub> receptors, whereas their affinity to SRIF<sub>2</sub> receptors is very low (Hoyer et al., 1994b; Martin et al., 1991; Patel and Srikant, 1994; Raynor et al., 1993a; Reisine and Bell, 1995; Reubi, 1984; Tran et al., 1985). The iodinated forms of octreotide and seglitide, [<sup>125</sup>I][Tyr<sup>3</sup>]octreotide and [<sup>125</sup>I]MK 678, were suggested to label exclusively sst<sub>2</sub> receptors *in situ*, e.g. in native brain membranes or slices (Hoyer et al., 1994b; Piwko et al., 1997; Schoeffter et al., 1995). The SRIF<sub>2</sub>-family - sst<sub>1</sub> and sst<sub>4</sub> receptors - can be selectively labelled *in situ* with radioligands in the presence of high sodium concentrations, e.g. with [<sup>125</sup>I][Tyr<sup>11</sup>]SRIF<sub>14</sub> or [<sup>125</sup>I]CGP 23996 (Hoyer et al., 1994b; 1995b; Reubi and Maurer, 1986; Thoss et al, 1997).

### 1.2.2. Tissue distribution of receptor subtypes

In mammals, SRIF receptor subtypes were found to be specifically expressed in brain and many peripheral tissues (Bell and Reisine, 1993; Breder et al., 1992; Kaupmann et al., 1993; Raulf et al., 1994; Thoss et al. 1996; 1997), as well as in a number of tumours (Reubi et al., 1984; 1987; 1990a; 1990b); their expression undergoes changes in a spatial and temporal manner during ontogenesis (Wulfsen et al., 1993; Hartmann et al., 1995; Thoss et al., 1995; 1996).

In brain, the transcripts of  $sst_{1-4}$  receptors are widely distributed and high levels were found in cortex, hippocampus and hypothalamus; however,  $sst_5$  receptor mRNA was detected primarily in the preoptic area and hypothalamus (Bito et al., 1994; Bruno et al., 1993; Meyerhof et al., 1992; Perez and Hoyer, 1995; Raulf et al., 1994; Thoss et al., 1996; 1997). Among the two  $sst_2$  receptor splice variants, the  $sst_{2A}$  receptor form is preferentially expressed over the  $sst_{2B}$  variant in brain and pituitary of rat, but not of mouse (Sarret et al., 1998; Vanetti et al., 1992). Also cellular coexpression of different receptor subtypes has been reported, e.g. of  $sst_3$  and  $sst_4$  (Perez and Hoyer, 1995).

In the periphery, expression of human  $sst_{1-5}$  receptors ( $hsst_{1-5}$ ) was observed in pituitary, stomach and various tumours. In addition, the expression of the  $hsst_1$  receptor was detected in liver and ovary, of the  $hsst_2$  receptor in kidney, adrenals and pancreas, of the  $hsst_3$  receptor in spleen, liver, pancreas, lymph nodes and smooth muscle, of the  $hsst_4$  receptor in lung, and of the  $hsst_5$  receptor in liver, adrenals, pancreas and heart (Kubota et al., 1994a; Le Romancier et al., 1996; O'Carroll et al., 1994; Panetta et al., 1994; Raulf et al., 1994; Reubi et al., 1998; Vikić-Topić et al., 1995; Yamada et al., 1992a).

Receptor-specific antibodies are being used to localise the corresponding receptor proteins. Human  $sst_{1,3}$  receptors were immunolocalised in tumour tissues (Reubi et al., 1998; Schulz et al., 1998b), and  $hsst_2$  receptors in the cerebral cortex, hippocampus and cerebellum of brain (Schindler et al., 1998a), as well as in the peripheral nervous system, in lymphatic tissue and in the gastrointestinal smooth muscle (Reubi et al., 1999).

In rat, the sst<sub>2</sub> receptor protein was similarly found in brain and spinal cord, and also in pancreas (Dournaud et al., 1996; Hunyady et al., 1997; Schindler et al., 1997; Schulz et al., 1998a); the sst<sub>1</sub> receptor protein was widely distributed in brain (Helboe et al., 1998; Hervieu et al., 1998), and the sst<sub>3</sub> receptor was immunolocalised in neuronal cilia (Händel et al., 1999); preliminary reports suggest sst<sub>5</sub> receptors to be present in the rat brain, but with very low abundance, and they seem to be limited to the more rostral regions of the brain (Stroh et al., 1998).

### **1.2.3. Receptor subtype-specific functions**

The sst<sub>1</sub> receptor subtype is suggested to regulate intrahypothalamic pulsatility of somatotropin (Lanneau et al., 1999). Mainly responsible for the inhibition of somatotropin release from anterior pituitary is the sst<sub>2</sub> receptor subtype (Raynor et al., 1993b); the sst<sub>2</sub> receptor additionally plays a major role in the inhibition of glucagon release from the pancreas, of histamine release from the antrum, of gastrin release from the mucosa, of acid and ion secretion in the colon, of cell firing in the locus coeruleus, and mediates inhibition of neurotransmission in the ileum (Coy and Taylor, 1996; Feniuk et al., 1995; Prinz et al., 1994; Rossowski and Coy, 1994; Warhurst et al., 1996; Zaki et al., 1996). Sst<sub>2</sub> receptor knockout mice were devoid of severe defects, but were refractory to the somatotropin-mediated negative feedback, and revealed an increased gastric acid secretion (Zheng et al., 1997; Martinez et al., 1998). The sst<sub>3</sub> receptor is suggested to mediate inhibition of gastric smooth muscle contraction, and partially functions in inhibition of insulin release (Coy et al., 1998; Gu et al., 1995). No functional effects have been attributed to sst<sub>4</sub> receptors so far. The sst<sub>5</sub> receptor subtype is suggested to be involved in inhibition of amylase release, of insulin release from the pancreas, as well as of mitogen-induced regeneration of aortic vascular smooth muscle cells (Coy and Taylor, 1996; Coy et al., 1998; Lauder et al., 1997; Rossowski et al., 1994).

### 1.3. Signal transduction

#### 1.3.1. Coupling to G-proteins

Mammalian SRIF receptors are specifically coupled to intracellular signal transduction cascades via various pertussis toxin (PTX)-sensitive ( $G_i$  and  $G_o$ ) and PTX-insensitive G-proteins (e.g.  $G_q$ ,  $G_{14}$ ,  $G_{16}$ ) (Bell and Reisine, 1993; Kagimoto et al., 1994; Kleuss et al., 1991; Komatsuzaki et al., 1997; Kubota et al., 1994b; Law et al., 1991; 1994; Murthy et al., 1996; Patel et al., 1994; Reisine et al., 1995; Yatani et al., 1987). The third cytoplasmatic loop of agonist-activated G-protein-coupled receptors binds to the C-terminus of  $G\alpha$ -subunits, which forms heterotrimeric complexes with  $G\beta\gamma$  subunits (for review, Hamm et al., 1998; Kobilka et al., 1988; Reisine et al., 1994).

The activated receptor bound to the inactive G-protein catalyses the exchange of GDP to GTP on the  $G\alpha$  subunit, which activates the G-protein; it is assumed that the  $G\alpha$ -subunit dissociates from the  $G\beta\gamma$ -subunit upon G-protein activation, although dissociation may not be the rule under physiological conditions (Rebois et al., 1997). The GTP-bound G-protein modulates the activity of downstream effector molecules, and is deactivated by  $G\alpha$ -catalysed hydrolysis of GTP to GDP and  $P_i$  (Birnbaumer and Birnbaumer, 1995; Gilman, 1987; Hamm et al., 1998). In addition, GTPase-activating proteins, the so-called regulators of G-protein-signalling (RGS), modulate G-protein-signalling, especially of  $G_i$ -proteins (Roush et al., 1996).

The binding rate of GTP and thereby the ability of a receptor to activate G-proteins can be measured using the non-hydrolysable GTP-analogue guanosine-5'-O-(3-[ $^{35}$ S]thio)-triphosphate ( $[^{35}\text{S}]\text{GTP}\gamma\text{S}$ ). The agonist-induced receptor/ G-protein/  $[^{35}\text{S}]\text{GTP}\gamma\text{S}$  complexes can be determined quantitatively by measuring the bound radioactivity, which is a reflection of the capacity of agonists to trigger intracellular signalling events (Lorenzen et al., 1993). In addition, binding of GTP or analogues to the G-protein induces dissociation of the agonist from the receptor/ G-protein complex, and therefore inhibits ligand binding (Brown and Schonbrunn, 1993; Hjorth et al., 1996; Koch and Schonbrunn, 1984; Rens-Domiano et al., 1992).

Multiple subunits isoforms of heterotrimeric G-proteins couple SRIF receptor subtypes specifically to the different intracellular targets (for review, Birnbaumer and Birnbaumer, 1995; Gutkind, 1998). Thus, SRIF receptors mediate inhibition of adenylate cyclase activity via  $G\alpha_{i1}$ ,  $G\alpha_{i2}$ ,  $G\alpha_{i3}$  and  $G\alpha_o$  depending on the receptor subtype and the cell system, but they also activate phospholipase C via  $G\alpha_{i1}$ ,  $G\alpha_o$ ,  $G\alpha_{i4}$  and  $G\alpha_{i6}$  (Patel, 1997); for instance,  $ssr_2$  receptors are coupled via  $G\alpha_{i1}$  to inhibition of adenylate cyclase (Kagimoto et al., 1994), via  $G\alpha_{i3}$  to stimulation of  $K^+$ -channels (Yatani et al., 1987), and via  $G\alpha_o(\beta_1/\gamma_2)$  to stimulation of  $Ca^{2+}$ -channels (Kleuss et al., 1991).

### 1.3.2. Modulation of adenylate cyclase

Each of the five mammalian SRIF receptors has been shown to couple to inhibition of adenylate cyclase (AC) activity as suggested from earlier work performed in tissue and cell preparations (Chneiweiss et al. 1987; Jakobs et al., 1983; Kaupmann et al., 1993; Koch and Schonbrunn, 1984; Patel et al., 1994; Raynor and Reisine 1992; Reisine et al., 1995); the inhibition of AC by somatostatin is blocked by pertussis toxin, which ADP-ribosylates and thereby inactivates the  $\alpha$  subunits of  $G_i$  and  $G_o$  (Reisine et al., 1985). Nine distinct mammalian AC variants, which are membrane-spanning, are known.  $G_i$  and  $G_o$ -proteins effectively inhibit the activity of the  $Ca^{2+}$ -calmodulin-stimulated AC type I;  $G_i$  additionally inhibits AC's type V and VI (for review, Sunahara et al., 1996; Taussig et al., 1993; 1994). AC type I is primarily expressed in neurones, while type V and VI are ubiquitously expressed (for review, Birnbaumer and Birnbaumer, 1995). The  $G\alpha$  subunit of  $G_i$  and  $G_o$  is myristoylated, which is required for membrane anchoring and interaction with the AC enzyme (Jones et al., 1990; Mumby et al., 1990; Taussig et al., 1993). SRIF receptors have been reported to couple to inhibition of AC via  $G_{i1}$ ,  $G_{i2}$ , and  $G_{i3}$ , depending on the receptor subtype and the cell line (Kagimoto et al., 1994; Kubota et al., 1994b; Law et al., 1993a; 1993b; Liu et al., 1994; Senogles, 1994; Tallent and Reisine, 1992; Yajima et al., 1993).

SRIF-induced inhibition of AC activity, and thereby decreased cAMP levels, cause inhibition of protein kinase A activation, and subsequently inhibition of phosphorylation and therefore activation of the cAMP response element-binding protein - CREB - (Tentler et al., 1997).

In mammals, AC inhibition by somatostatin was measured in various tissues/ organs such as brain (Chneiweiss et al., 1984), pituitary (Epelbaum et al., 1987), pancreas (Rodriguez et al., 1997; Viguierie et al., 1988), retina (Colas et al., 1992), enteric cells (Barber et al., 1987), intestinal smooth muscle cells (Murthy et al., 1996), kidney-derived cells (Roy, 1984), and astrocytes, in which somatostatin inhibits interleukin 6 release (Grimaldi et al., 1997).

In fish, SRIF has been reported to inhibit AC activity in the pituitary (Helms et al., 1991); the nature of the AC isozymes has not yet been characterised in fish, but adenylate cyclases are present in many tissues like in pituitary, heart, liver, ovary, and gill (Fabbri et al., 1992; Guibbolini et al., 1992; Helms et al., 1991; Srivastava et al., 1994; Vornanen, 1998).

### 1.3.3. Modulation of phospholipase C

All five human SRIF receptor subtypes have been described to couple to activation of phospholipase C (PLC), when expressed in COS-7 cells (Akbar et al., 1994). In F<sub>4</sub>C<sub>1</sub> rat pituitary cells, mouse sst<sub>2</sub> receptors mediated activation of PLC, but not rat sst<sub>1</sub> receptors (Chen et al., 1997). In intestinal smooth muscle cells, endogenously expressed sst<sub>3</sub> receptors induced activation of PLC<sub>β3</sub> and Ca<sup>2+</sup>-release via Gβγ-subunits of G<sub>i1</sub>/G<sub>o</sub> (Murthy et al., 1996). The activation of PLC by human sst<sub>1-5</sub>, mouse sst<sub>2</sub>, and guinea pig sst<sub>3</sub> receptors was only partially pertussis toxin (PTX)-sensitive (Akbar et al., 1994; Chen et al., 1997; Murthy et al., 1996). PTX ADP-ribosylates G<sub>v0</sub>α at a specific cysteine residue at -4 position, and G<sub>o</sub>α additionally at -3 position from the carboxy terminus, which inactivates these G-proteins by preventing their interaction with receptors (Avigan et al., 1992; West et al.; 1985).

The PLC enzyme family comprises at least 9 different isoforms, which all require  $\text{Ca}^{2+}$  for activity; G-protein-coupled receptors primarily stimulate the activity of the 4  $\beta$ -isoforms,  $\text{PLC}_{\beta 1-4}$ , via direct interaction of activated G-proteins. The  $\alpha$  subunits of  $G_{i/o}$  do not directly activate  $\text{PLC}_{\beta}$ , but as a result of activation of  $G_{i/o}\alpha\beta\gamma$ , the  $\beta\gamma$ -complex will activate  $\text{PLC}_{\beta 2/3}$ .  $G_q\alpha$  and  $G_{11}\alpha$  are primarily responsible for coupling of receptors to  $\text{PLC}_{\beta 1}$  and  $\text{PLC}_{\beta 3}$ ; in addition,  $G_q\alpha$  activates  $\text{PLC}_{\beta 4}$  (Berridge, 1993; for review: Exton, 1996; Simon et al., 1991; Sternweiss et al., 1992). Receptor-mediated stimulation of membrane-associated PLC activity acts on phosphatidylinositol 4,5-biphosphate hydrolysis, which leads to generation of the second messengers inositol 1,4,5-triphosphate ( $\text{IP}_3$ ) and 1,2-diacylglycerol (DAG).  $\text{IP}_3$  molecules bind to their respective receptors at the membranes of the intracellular  $\text{Ca}^{2+}$ -stores, the Endoplasmic Reticulum and the Golgi apparatus, which results in an increase of cytoplasmatic  $\text{Ca}^{2+}$  levels.  $\text{Ca}^{2+}$  and DAG activate the protein kinase C enzyme, that regulates cell growth and cell differentiation.  $\text{Ca}^{2+}$  activates also other  $\text{Ca}^{2+}$ -binding proteins such as calmodulins.  $\text{IP}_3$  is specifically degraded by phosphatases to  $\text{IP}_2$ ,  $\text{IP}_1$ , and finally inositol; degradation to inositol can be blocked by lithium ions, and phospholipase C activity determined by measurement of total  $\text{IP}_x$  levels (Berridge, 1993; Clapham, 1995; Mikoshiba, 1997).

#### 1.3.4. Modulation of further signalling proteins

In addition to adenylate cyclase and phospholipase C, multiple effector molecules are reported to be modulated by SRIF receptor subtypes. SRIF receptors induce activation of cGMP-dependent protein kinases (Meriney et al., 1994), and the  $\text{sst}_4$  receptor was found to activate arachidonic acid release and phospholipase  $A_2$  (Shimizu et al., 1996; Schweitzer et al., 1990). Potassium channels are stimulated by the  $\text{sst}_2$  receptor (Wang et al., 1987; 1989; Yatani et al., 1987), calcium channels are inhibited by  $\text{sst}_2$  and  $\text{sst}_5$  receptors (Fujii et al., 1994; Ikeda and Schonfield, 1989; Rosenthal et al., 1988; Tallent et al., 1996; Wang et al., 1990), and  $\text{Na}^+/\text{H}^+$  exchanger proteins are positively or negatively modulated by  $\text{sst}_1$  and  $\text{sst}_5$  receptors (Barber et al., 1989; Hou et al., 1994).

Activation and inhibition of the p42/p44 mitogen-activated protein kinase (= MAPK, Erk1/2) by  $sst_{1-5}$  receptors has been observed in diverse cellular systems, and consequently modulation of the transcription factor elk-1 (Bito et al., 1994; Buscail et al., 1994; 1995; Florio et al., 1994; 1999; Lopez et al., 1997; Todisco et al., 1995; 1997);  $sst_1$  receptor-induced MAPK activation was shown to involve the tyrosine phosphatase SHP-2, the tyrosine kinase c-src, and Ras and Raf-1 (Florio et al., 1999). Stimulation of protein tyrosine phosphatases, particularly SHP-1 and SHP-2, was observed for  $sst_{1-4}$  receptors (Buscail et al., 1994; 1995; Florio et al., 1994; 1999; Reardon et al., 1996; 1997; Lopez et al., 1997; Srikant and Shen, 1996). Further, the recombinantly expressed  $sst_3$  receptor is reported to induce p53 and apoptosis (Sharma et al., 1996).



#### 1.4. Outline of the thesis

The aim of the present study was to characterise ligand binding and ligand-modulated signal transduction pathways of the five different human somatostatin  $sst_{1-5}$  receptor subtypes and of the first non-mammalian somatostatin receptor, the fish  $sst_3$  receptor, all studied in the same environment, i.e. the same cell line. For this purpose, the receptors were stably expressed in CCL39 Chinese hamster lung fibroblast cells, which contain high levels of G-protein isoforms known to couple somatostatin receptors to their effector molecules.

The recently identified CST, which is structurally related to SRIF, was investigated for its ability to bind to the human SRIF receptor subtypes, and pharmacological profiles were established using iodinated CST ( $[^{125}\text{I}][\text{Tyr}^{10}]\text{CST}_{14}$ ), and SRIF/ CST and analogues at cell membrane preparations. Since there is historically great variation in data reported by various groups on the pharmacological profiles of the different mammalian receptor subtypes even when expressed in the same cell line, the affinity profiles using further radioligands ( $[^{125}\text{I}]\text{LTT-SRIF}_{28}$ ,  $[^{125}\text{I}]\text{CGP 23996}$ ,  $[^{125}\text{I}][\text{Tyr}^3]\text{octreotide}$ ) were determined, and compared to each other. The stable and non-hydrolysable GTP-analogue guanylylimidodiphosphate was used to study inhibition of radioligand binding at membrane preparations, and therefore to indirectly examine G-protein coupling of the receptor populations labelled by the various radioligands.

Agonist-induced G-protein activation was investigated at the human SRIF receptors by measuring agonist-stimulated guanosine-5'-O-(3- $[^{35}\text{S}]\text{thio}$ )-triphosphate ( $[^{35}\text{S}]\text{GTP}\gamma\text{S}$ ) binding using microsome preparations; assay conditions were established, and the agonist rank orders of potency and efficacy determined. Inhibition of forskolin-stimulated adenylate cyclase activity by SRIF ligands was examined at human  $sst_{1-5}$  receptors by measuring cellular cyclic adenosine monophosphate (cAMP) levels. Activation of phospholipase C activity mediated by the human SRIF receptor subtypes was indirectly measured by determining total cellular  $[^3\text{H}]\text{-inositolphosphate}$  accumulation; in addition, stimulated intracellular calcium levels were measured using a calcium-dye and by monitoring fluorescence.

The agonist profiles of human  $sst_{1-5}$  receptors obtained in [ $^{35}$ S]GTP $\gamma$ S binding, adenylate cyclase inhibition, and phospholipase C stimulation were compared to each other, and to the affinity profiles determined in competition binding assays using the four distinct radioligands.

To characterise the fish  $sst_3$  receptor cloned from the teleost fish *Apteronotus albifrons*, pharmacological profiles were established in radioligand binding using distinct iodinated ligands, in [ $^{35}$ S]GTP $\gamma$ S binding, in forskolin-stimulated adenylate cyclase inhibition, and in phospholipase C stimulation, and compared to each other, and compared to data obtained at the human somatostatin receptor subtypes. The interest was to elucidate the binding properties as well as the signal transduction machineries in non-mammalian vertebrates. Further, the presence and nature of native somatostatin receptors was studied in various tissues prepared from *Apteronotus albifrons*.

## 2.1. Cell Culture

COS-1 cells (SV40 CV-1 cells, which originate from kidney cells of the African Green Monkey; American Type Culture Collection) and CCL39 cells (established line of Chinese hamster lung fibroblasts; American Type Culture Collection) were cultured in a 1:1 mixture of Dulbecco's Modified Eagle's Medium (DMEM; Seromed, Biochrom, Berlin, Germany; 3.7 g/ l NaHCO<sub>3</sub>; 1.0 g/ l D-glucose; with stable glutamine) and Ham's F-12 Nutrient Mixture (Seromed; 1.176 g/ l NaHCO<sub>3</sub>; with stable glutamine) supplemented with 10 % (v/ v) foetal bovine serum (FBS; Gibco BRL) and penicillin (100 u/ml final concentration)/ streptomycin (100 µg/ ml final concentration) (both from Sigma-Aldrich Chemie, Deisenhofen, Germany) at 37°C, 5 % CO<sub>2</sub> and 95 % relative humidity. For passaging, the cells were detached from the cell culture flask by washing with phosphate-buffered saline (PBS, pH 7.4, Gibco BRL) and by brief incubation with trypsin (0.5 mg/ ml)/ EDTA (0.2 mg/ ml) (Gibco BRL). The cells were passaged every 2 days. For storage, the cells were resuspended in medium containing dimethyl sulfoxide (10 % final concentration), and frozen in liquid nitrogen.

## 2.2. Transient transfection

Transient expression of the fish sst<sub>3</sub> receptor gene in COS-1 cells was carried out by using the diethylaminoethyl (DEAE)-dextran transfection method. Cells were splitted 12- 16 h prior to transfection on culture plates (diameter 10 cm) to obtain a density of approximately 10<sup>4</sup> cells/ plate. For transfection, cells of each plate were covered with 4 ml medium. The transfection mix containing 10- 40 µg pcDNA3-fsst<sub>3</sub> plasmid DNA (G.K.H. Zupanc, Manchester, England), 40 ml HBS buffer pH 7.4 (130 mM NaCl, 0.9 mM NaH<sub>2</sub>PO<sub>4</sub>, 0.8 mM MgSO<sub>4</sub>, 5.4 mM KCl, 1.8 mM CaCl<sub>2</sub>, 25 mM D(+)-glucose, 20 mM HEPES, 5 ng/ ml phenol red) and 80 µl DEAE-dextran (10 mg/ ml) was distributed in each plate. Two hours later, 40 µl chloroquine (10 mM in H<sub>2</sub>O) were added. 6 h after transfection, cells were washed twice with PBS, restored in culture medium, and harvested after additional 32- 36 h.

As a control, cells were transfected in parallel with RSV-lacZII plasmid (constructed by W. Ankenbauer, Heidelberg, Germany) containing the *Escherichia coli*  $\beta$ -galactosidase gene, and harvested 24 h later. Cells were washed twice with PBS, incubated for 10 min at room temperature with 1 % glutaraldehyde in PBS for fixation, washed 3 times with PBS, and incubated overnight in a sealed plate with staining solution (5 mM potassium ferrocyanide, 5 mM potassium ferricyanide, 2 mM  $MgCl_2$ , 1 mg/ml 5-bromo-4-chloro-3-indolyl- $\beta$ -D-galactoside), pH 7.0, at 37°C and 0 %  $CO_2$ . A blue staining can normally be observed by microscopy in roughly 20 % of the cells.

### 2.3. Stable transfection

CCL39 cells were used for stable expression of the human SRIF receptor genes. Cells were splitted 1 day prior to transfection for logarithmic growth.  $1.6 \times 10^8$  cells resuspended in 800  $\mu$ l electroporation buffer (272 mM sucrose, 1 mM  $MgCl_2$ , 7 mM  $Na_2HPO_4/NaH_2PO_4$ ), pH 7.4, were mixed with 10- 80  $\mu$ g DNA pcDNAI-hsst<sub>1</sub>+pNeo, pcDNAI-hsst<sub>2</sub>+pNeo, pcDNAI-hsst<sub>3</sub>+pNeo (G.I. Bell, Chicago, USA), pcDNAI-hsst<sub>4</sub>+pNeo (F. Raulf, Basel, Switzerland), pRc/CMV-hsst<sub>5</sub> (S. Seino, Chiba, Japan), or pcDNA3-fsst<sub>3</sub> (G.K.H. Zupanc, Manchester, England), and incubated on ice for 10 min. Cells were electroporated at 500 V/ 25  $\mu$ F, cooled down at 4°C for 10 min, and supplemented with cell culture medium in 260 ml culture flasks. After 2 days, the antibiotic G418 (geneticin sulphate; Gibco BRL) was added to the cell culture medium (0.4 mg/ml 100 % active G418 final concentration) for selection of SRIF receptor-expressing cells. Receptor expression of single cell-derived colonies was tested by radioligand binding. Stable transfected cells were permanently cultured in G418-containing medium.

### 2.4. Radioligand binding assay

For crude cell membrane preparations, cells were harvested by washing with 10 mM HEPES, pH 7.5, scraping off the culture plates with 4 ml of the same buffer, and centrifugation at 4°C for 5 min at 2500 x g.

The cell pellet was either stored at  $-80^{\circ}\text{C}$  or directly used. The cell preparations were resuspended in binding assay buffer (10 mM HEPES, pH 7.5, 0.5 % (w/v) bovine serum albumin (BSA)) by homogenisation with the Polytron at 50 Hz for 20 s.

For preparation of crude tissue membranes, the different fish tissues were briefly rinsed in 10 mM HEPES, pH 7.5, weighed, resuspended in 10 mM HEPES, pH 7.5, by homogenisation with the Polytron at 50 Hz for 40 s (100 mg/ml each), and stored at  $-80^{\circ}\text{C}$ . Tissue homogenates were diluted in assay buffer to a concentration of 4- 7 mg/ml.

In competition experiments, 150  $\mu\text{l}$  of the cell or tissue homogenate (CCL39 cells:  $\text{hsst}_1$  and  $\text{hsst}_2$ : ca.  $1.5 \times 10^5$  cells/ 4  $\mu\text{g}$  protein,  $\text{hsst}_3$ ,  $\text{hsst}_5$  and  $\text{fsst}_3$ :  $0.75 \times 10^5$  cells/ 2  $\mu\text{g}$  protein, and  $\text{hsst}_4$ :  $4.5 \times 10^5$  cells/ 6  $\mu\text{g}$  protein, depending on the expression level of each receptor; 750  $\mu\text{g}$  brain or 600  $\mu\text{g}$  liver, respectively), were incubated with 50  $\mu\text{l}$  of [ $^{125}\text{I}$ ]LTT-SRIF<sub>28</sub>, [ $^{125}\text{I}$ ][Tyr<sup>10</sup>]CST<sub>14</sub>, [ $^{125}\text{I}$ ]CGP 23996, or [ $^{125}\text{I}$ ][Tyr<sup>3</sup>]octreotide (2175 Ci/mmol; 25- 35 pM; final concentration), in binding assay buffer containing  $\text{MgCl}_2$  (5 mM) and the protease inhibitor bacitracin (5  $\mu\text{g}/\text{ml}$ ), and either 50  $\mu\text{l}$  binding assay buffer (total binding) or with 50  $\mu\text{l}$  of various peptide/ GppNHp concentrations. Non-specific binding was determined in the presence of SRIF<sub>14</sub> (1  $\mu\text{M}$ ). After 1 h at room temperature, the incubation was terminated by vacuum filtration through glass fibre filters pre-soaked in 0.3 % (w/v) polyethyleneimine. The filters were rinsed twice with ice-cold 10 mM Tris/HCl buffer, pH 7.4, and dried. Bound radioactivity was measured in a  $\gamma$ -counter using scintillation liquid (80 % counting efficiency). Data were analysed by non-linear regression curve fitting with the computer program SCTFIT (De Lean, 1979). In saturation experiments, 150  $\mu\text{l}$  of cell homogenates were incubated with 50  $\mu\text{l}$  of 8 different concentrations (approximately 25- 300 pM) of [ $^{125}\text{I}$ ]LTT-SRIF<sub>28</sub>, [ $^{125}\text{I}$ ][Tyr<sup>10</sup>]CST<sub>14</sub>, [ $^{125}\text{I}$ ]CGP 23996, or [ $^{125}\text{I}$ ][Tyr<sup>3</sup>]octreotide, and 50  $\mu\text{l}$  of binding assay buffer (total binding) or 1  $\mu\text{M}$  SRIF<sub>14</sub> (non-specific binding). If GppNHp ( $10^{-5}$  M; final concentration) was used, it was included in each well. Data were analysed using the computer program SCTFIT (De Lean, 1979). Protein concentration was determined according to Bradford (1976) by means of the BioRad Protein Assay Kit with BSA as a standard.

For statistical analysis, data from radioligand binding studies were compared by paired t-Test analysis for individual values using the statistical package in GraphPad Prism. Affinity profiles were compared by correlation and significance indicated by P values; they were also compared one way ANOVA and Dunnett's multiple comparison test.

## 2.5. [<sup>35</sup>S]GTP $\gamma$ S binding assay

Cells were harvested for microsome preparations, by washing with 10 mM HEPES, pH 7.5, scrapping off the culture plates with 4 ml of the same buffer and centrifugation at 4°C for 5 min at 2500 x g. The cell preparations were resuspended in 10 mM HEPES, pH 7.5 by homogenisation with the Polytron at 50 Hz for 20 s, and centrifuged at 4°C for 30 min at 15000 x g. The microsome pellets were resuspended in assay buffer (10 mM HEPES pH 7.4, 100 mM NaCl, 5 mM MgCl<sub>2</sub>, 0.1 mM EDTA pH 8.0, 10  $\mu$ g/ml bacitracin), and either stored at -80°C or directly used.

100  $\mu$ l of the microsome preparation from CCL39 cells (hsst<sub>1</sub>: ca. 3 x 10<sup>5</sup>; hsst<sub>2</sub>, hsst<sub>3</sub> and hsst<sub>4</sub>: 1.5 x 10<sup>5</sup>; hsst<sub>5</sub>, fsst<sub>3</sub>: 0.75 x 10<sup>5</sup> cells, depending on the expression level of each receptor) were incubated with 20  $\mu$ l GDP (1  $\mu$ M; final concentration), and either 10  $\mu$ l assay buffer (total binding) or with 10  $\mu$ l of various peptide concentrations, and with 10  $\mu$ l of [<sup>35</sup>S]GTP $\gamma$ S (200 pM; final concentration) in 96-well Viewplates (Dynatech Laboratories). Non-specific binding was determined by addition of 10  $\mu$ l GTP $\gamma$ S (10  $\mu$ M; final concentration), in all other wells 10  $\mu$ l assay buffer were added. After 5 min preincubation, 50  $\mu$ l wheatgerm agglutinin (WGA) SPA (scintillation proximity assay)-beads were supplemented (1.5 mg beads per well; beads in 50 mM Tris pH 7.4, 0.1 % sodium azide, and diluted 1:3 in assay buffer), the plates sealed, incubated for 1 h at room temperature, and centrifuged for 10 min at 1000 x g. [<sup>35</sup>S]GTP $\gamma$ S bound to a G-protein/ receptor-complex, and thereby to the WGA SPA-beads stimulated those to emit light, which was measured in a  $\beta$ -scintillation counter (Packard TopCount).

Data were calculated and standardised to the level of basal activity (= 100 %). Stimulatory concentration-response curves were analysed by non-linear regression curve fitting using the computer program "GraphPad Prism".  $pK_B$ -values were determined using the Schild-Gaddum-equation.

## 2.6. Adenylate cyclase activity (cAMP accumulation) measurement

In cAMP-Scintillation Proximity Experiments (indirect cAMP measurements), cells were splitted 1 day prior to the experiment in 96-well Viewplates (Dynatech Laboratories) ( $5 \times 10^4$  cells per well). The assay was performed as described for the cAMP-Scintillation Proximity Assay (SPA)-kit (Amersham). Cell culture medium was flicked out, and cells were incubated for 15 min at 37°C (5 % CO<sub>2</sub>, 95 % relative humidity) with 50 µl Minimum Essential Medium (MEM; Gibco BRL; with Earle's salts, without phenol red, with stable glutamine) containing 1 mM isobutylmethylxanthine (IBMX; Sigma) as a phosphodiesterase-inhibitor, either without forskolin (basal enzyme activity) or with 10 µM forskolin (Sigma) and various concentrations of the tested peptides. Experiments were conducted in triplicates. Medium was flicked out, and for cell lysis 50 µl Lysis Reagent I (1 % Dodecyltrimethylammoniumbromide, 0.01 % sodium azide, 0.05 M acetate buffer, pH 5.8) were added to each well, and the plate was shaken for 5 min followed by another incubation period of 5 min. Equal volumes of [<sup>125</sup>I]cAMP (3',5'-cyclic phosphoric acid-2'-O-succinyl-3-[<sup>125</sup>I]-iodotyrosine methyl ester in Lysis Reagent II), of rabbit-anti-cAMP-serum (diluted in Lysis Reagent II), and of SPA anti-rabbit reagent (SPA fluomicrospheres (polyvinyl toluene based beads), diluted in Lysis Reagent II) were mixed, and 150 µl of the mixture was added per well. Plates were sealed and incubated for 15-20 hrs at room temperature. [<sup>125</sup>I]cAMP bound to the rabbit-anti-cAMP-serum/SPA anti-rabbit reagent-complex stimulated the SPA beads to emit light, which was measured in a β-scintillation counter (Packard TopCount).

cAMP of the cell lysate, which competes with [ $^{125}$ I]cAMP in binding to the rabbit-anti-cAMP-serum/ SPA anti-rabbit reagent-complex (radioimmunoassay), was calculated and normalised to the level reached in the presence of forskolin. Forskolin induces a ca. 20-30 fold stimulation of AC in CCL39 cells. Inhibitory concentration-response curves were analysed by non-linear regression curve fitting with the computer program "GraphPad Prism" using the equation  $y = E_{\max}/(1+x/EC_{50})+(100-E_{\max})$ , where y represents the percentage of cAMP produced and x the agonist concentration.  $pK_B$ -values were determined using the Schild-Gaddum-equation.

In direct cAMP measurements, cells were grown to confluence in 24-well plates. Following washing with assay buffer (130 mM NaCl, 5.4 mM KCl, 1.8 mM  $CaCl_2$ , 0.8 mM  $MgSO_4$ , 0.9 mM  $NaH_2PO_4$ , 25 mM glucose, 20 mM HEPES, pH 7.4), the cells were incubated with 6  $\mu$ Ci [ $^3$ H]adenine (1 mCi/ ml) in 500  $\mu$ l assay buffer for 2 h at 37°C, 5 %  $CO_2$  and 95 % relative humidity. When pertussis toxin (PTX; Sigma; 100 ng/ml medium) was used, cells were treated for 24 h before the incubation with 6  $\mu$ Ci [ $^3$ H]adenine. Cells were then washed twice with assay buffer containing 1 mM IBMX (Sigma). The cells were incubated at 37°C in 1 ml assay buffer containing IBMX either without (basal enzyme activity) or with 10  $\mu$ M forskolin (Sigma) and various ligand concentrations. Experiments were conducted in duplicate. After 15 min, cells were extracted with 5 % trichloroacetic acid containing 100  $\mu$ M adenosine triphosphate (ATP) and 100  $\mu$ M cyclic adenosine monophosphate (cAMP).

[ $^3$ H]ATP and [ $^3$ H]cAMP were separated by sequential chromatography on Dowex AG 50W-X4 and alumina columns. Dowex columns were washed with 10 ml  $H_2O$ , then cell-extract and 3 ml  $H_2O$  were loaded, and the eluate ([ $^3$ H]ATP) measured in a  $\beta$ -counter. 8 ml  $H_2O$  were loaded onto the Dowex columns, the eluate was loaded on alumina columns, which had been washed with 10 ml 100  $\mu$ M imidazole, and the flow-through discarded. The [ $^3$ H]cAMP was eluted from the alumina columns with 6 ml 100  $\mu$ M imidazole and measured in a  $\beta$ -counter. The recovery of [ $^3$ H]cAMP, as measured in separate experiments using a [ $^3$ H]cAMP standard, was  $76 \pm 1$  % (n = 5).



Dowex- columns were regenerated with 10 ml 2 N HCl, the alumina columns with 3 ml 1 M imidazole. Data were calculated as cAMP/(cAMP+ATP) ratios and normalised to the level reached in the presence of forskolin. Inhibition concentration-response curves were analysed using the computer program ORIGIN.

## **2.7. Measurement of phosphoinositide turnover (total [<sup>3</sup>H]-IP<sub>x</sub> accumulation)**

2 x 10<sup>5</sup> cells per well were splitted 24 h prior to the experiment on 24-well plates and incubated in 1 ml cell culture medium containing 2 μCi myo-[2-<sup>3</sup>H(N)]-inositol (74 MBq/ ml; American Radiolabelled Chemicals). When pertussis toxin (PTX) was used, cells were pre-treated with the toxin (Sigma; 100 ng/ ml) for at least 3 h during labelling with myo-[2-<sup>3</sup>H(N)]-inositol. Following washing with HBS buffer (130 mM NaCl, 5.4 mM KCl, 1.8 mM CaCl<sub>2</sub>, 0.8 mM MgSO<sub>4</sub>, 0.9 mM NaH<sub>2</sub>PO<sub>4</sub>, 25 mM glucose, 20 mM HEPES, pH 7.4) containing 20 mM LiCl to block inositol monophosphatase activity, the cells were incubated for 5 min at 37° C. Various compound concentrations were added, and the cells were incubated at 37° C for another 50 min. Preliminary experiments were conducted in triplicates, ligand testing was performed in duplicates.

Cells were extracted with 750 μl 10 mM ice-cold formic acid. After 30 min, the extracts containing inositol phosphates and free inositol are diluted into 3 ml of 5 mM NH<sub>4</sub>OH (final pH = 8-9), and applied to AG 1-X8 anion exchange columns (Biorad; 0.7 ml sediment volume/ column). Columns were equilibrated with 4 ml 2.5 mM NH<sub>4</sub>OH, loaded, and washed with 4 ml 40 mM ammonium formate buffer (pH 5) to eliminate free inositol and glycerophosphoinositol. Total inositol phosphates were eluted with 4 ml 2 M ammonium formate buffer (pH 5), and radioactivity was determined by liquid scintillation counting in a β-counter.

The columns were regenerated by washing with 4 ml 2M ammonium formate buffer, 8 ml H<sub>2</sub>O, and 4 ml 2.5 mM NH<sub>4</sub>OH. Stimulatory concentration-response curves were analysed by non-linear regression curve fitting using the computer program "GraphPad Prism". pK<sub>B</sub>-values were determined using the Schild-Gaddum-equation.

## 2.8. Measurement of intracellular $\text{Ca}^{2+}$

$5 \times 10^4$  cells per well were splitted 24 h prior to the experiment on black 96-well plates (Costar). For dye loading, cells were incubated for 1 h at  $37^\circ \text{C}$  (in darkness) with  $100 \mu\text{l}$  dye solution/ well containing  $5 \mu\text{M}$  Fluo-4/ acetoxymethyl ester (Molecular Probes), 0.02 % Pluronic acid (Molecular Probes),  $5 \text{ mM}$  Probenecid (Sigma; freshly prepared),  $20 \text{ mM}$  Hepes pH 7.4, in cell culture medium (DMEM/ F-12 1:1, 10 % FBS). Cells were washed 2x with  $125 \mu\text{l}$  wash solution containing  $2.5 \text{ mM}$  Probenecid,  $20 \text{ mM}$  Hepes pH 7.4, in Hanks Balanced Salt Solution (HBSS; Gibco BRL; with  $1.25 \text{ mM}$   $\text{Ca}^{2+}$ ) to remove extracellular dye, and  $100 \mu\text{l}$  wash solution per well were finally added. Cells were incubated about 30 min at room temperature (darkness) for intracellular enzymatic de-esterification of Fluo-4.

Intracellular calcium was measured using the FLIPR<sup>TM</sup> II system (Fluorometric Imaging Plate Reader; Molecular Devices, USA). Fluorescence excitation was yielded by 480 nm of an argon ion laser; emission was kinetically monitored at 515 nm for 5 min. Various SRIF<sub>14</sub> concentrations were automatically pipetted; 1 unit/ ml f.c. bovine thrombin (Sigma) was used as a positive control. Data were quantified subtracting the minimal from the maximal relative fluorescence units of each curve (well) using FLIPR<sup>TM</sup> II statistical software. Stimulatory concentration-response curves were analysed by non-linear regression curve fitting using the “GraphPad Prism” software.

## 2.9. Ligands

- (1) BIM 23014 (lanreotide; somatuline; D-Nal-c[Cys-Tyr-D-Trp-Lys-Val-Cys]-Thr-NH<sub>2</sub>),
- (2) BIM 23030 (c[Mpr-Tyr-D-Trp-Lys-Val-Cys]-D-Phe-NH<sub>2</sub>),
- (3) BIM 23052 (D-Phe-Phe-Phe-D-Trp-Lys-Thr-Phe-Thr-NH<sub>2</sub>),
- (4) BIM 23056 (D-Phe-Phe-Tyr-D-Trp-Lys-Val-Phe-D-Nal-NH<sub>2</sub>),
- (5) CGP 23996 (c[Asu-Lys-Asn-Phe-Phe-Trp-Lys-Thr-Tyr-Thr-Ser]),

- (6) mouse/ rat CST<sub>14</sub> (cortistatin 14; Pro-c[Cys-Lys-Asn-Phe-Phe-Trp-Lys-Thr-Phe-Ser-Ser-Cys]-Lys),
- (7) [Tyr<sup>10</sup>]CST<sub>14</sub> (Pro-c[Cys-Lys-Asn-Phe-Phe-Trp-Lys-Thr-Tyr-Ser-Ser-Cys]-Lys),
- (8) human CST<sub>17</sub> (cortistatin 17; Asp-Arg-Met-Pro-c[Cys-Arg-Asp-Phe-Phe-Trp-Lys-Thr-Phe-Ser-Ser-Cys]-Lys),
- (9) cycloantagonist (SA; c[Aha-Phe-D-Trp-Lys-Thr(Bzl)]),
- (10) L363,301 (c[Pro-Phe-D-Trp-Lys-Thr-Phe]),
- (11) L362,855 (c[Aha-Phe-Trp-D-Trp-Lys-Thr-Phe]),
- (12) octreotide (SMS 201-995; D-Phe-c[Cys-Phe-D-Trp-Lys-Thr-Cys]-Thr-OH),
- (13) [Tyr<sup>3</sup>]octreotide (SMS 204-090; D-Phe-c[Cys-Tyr-D-Trp-Lys-Thr-Cys]-Thr-OH),
- (14) RC160 (vaptotide; octastatin; D-Phe-c[Cys-Tyr-D-Trp-Lys-Val-Cys]-Trp-NH<sub>2</sub>),
- (15) seglitide (MK678; c[N-Met-Ala-Tyr-D-Trp-Lys-Val-Phe]),
- (16) SRIF<sub>14</sub> (Ala-Gly-c[Cys-Lys-Asn-Phe-Phe-Trp-Lys-Thr-Phe-Thr-Ser-Cys]-OH),
- (17) SRIF<sub>22</sub> (Asp-Asn-Thr-Val-Thr-Ser-Lys-Pro-Leu-Asn-c[Cys-Met-Asn-Tyr-Phe-Trp-Lys-Ser-Arg-Thr-Ala-Cys]-OH),
- (18) SRIF<sub>25</sub> (Ser-Asn-Pro-Ala-Met-Ala-Pro-Arg-Glu-Arg-Lys-Ala-Gly-c[Cys-Lys-Asn-Phe-Phe-Trp-Lys-Thr-Phe-Thr-Ser-Cys]-OH);
- (19) SRIF<sub>28</sub> (Ser-Ala-Asn-Ser-Asn-Pro-Ala-Met-Ala-Pro-Arg-Glu-Arg-Lys-Ala-Gly-c[Cys-Lys-Asn-Phe-Phe-Trp-Lys-Thr-Phe-Thr-Ser-Cys]-OH),
- (20) LTT-SRIF<sub>28</sub> ([Leu<sup>8</sup>,D-Trp<sup>22</sup>,Tyr<sup>25</sup>]-SRIF<sub>28</sub>; Ser-Ala-Asn-Ser-Asn-Pro-Ala-Leu-Ala-Pro-Arg-Glu-Arg-Lys-Ala-Gly-c[Cys-Lys-Asn-Phe-Phe-D-Trp-Lys-Thr-Tyr-Thr-Ser-Cys]-OH),
- (21) [<sup>125</sup>I]CGP 23996 (c[Lys-Asu-Phe-Phe-Trp-Lys-Thr-(<sup>125</sup>I-Tyr)-Thr-Ser]),
- (22) [<sup>125</sup>I][Tyr<sup>10</sup>]CST<sub>14</sub>, [<sup>125</sup>I]Tyr<sup>10</sup>-CST (Pro-c[Cys-Lys-Asn-Phe-Phe-Trp-Lys-Thr-(<sup>125</sup>I-Tyr)-Ser-Ser-Cys]-Lys),
- (23) [<sup>125</sup>I][Tyr<sup>3</sup>]octreotide (D-Phe-c[Cys-(<sup>125</sup>I-Tyr)-D-Trp-Lys-Thr-Cys]-Thr-OH),
- (24) [<sup>125</sup>I]LTT-SRIF<sub>28</sub> ([Leu<sup>8</sup>,D-Trp<sup>22</sup>,<sup>125</sup>I-Tyr<sup>25</sup>]SRIF<sub>28</sub>; Ser-Ala-Asn-Ser-Asn-Pro-Ala-Leu-Ala-Pro-Arg-Glu-Arg-Lys-Ala-Gly-c[Cys-Lys-Asn-Phe-Phe-D-Trp-Lys-Thr-(<sup>125</sup>I-Tyr)-Thr-Ser-Cys]-OH).

Abbreviations: Asu = amino suberic acid; Aha = amino heptanoic acid; Mpr = 3-mercaptopropionic acid; D-Nal = Naphthyl-D-Ala; Bzl = Benzylsubstituent.

5'-Guanylylimidodiphosphate (GppNHp) was from Sigma (St-Louis, Mo). BIM 23014, cycloantagonist SA, LTT-SRIF<sub>28</sub>, SRIF<sub>14</sub>, SRIF<sub>25</sub>, and SRIF<sub>28</sub> were purchased from Bachem AG (Bubendorf, Switzerland), RC160 was purchased from Peninsula Laboratories (Heidelberg, Germany), CST<sub>17</sub> was kindly provided by Drs. JG. Sutcliffe and L. de Lecea (The Scripps Research Institute, La Jolla, CA) or synthesised at ANAWA AG (Wangen, Switzerland); CST<sub>14</sub> and [Tyr<sup>10</sup>]CST<sub>14</sub> were from ANAWA. Other ligands were synthesised at Novartis Pharma AG (Basel, Switzerland). [<sup>125</sup>I]LTT-SRIF<sub>28</sub>, [<sup>125</sup>I][Tyr<sup>10</sup>]CST<sub>14</sub>, [<sup>125</sup>I]CGP 23996, and [<sup>125</sup>I][Tyr<sup>3</sup>]octreotide were custom synthesised from ANAWA AG (Wangen, Switzerland).

## 2.10. Northern blot analysis

Poly(A)<sup>+</sup>-RNA (brain, gut, liver, spleen, stomach) was prepared according to the manuals of Quiagen RNA extraction kits: 4 µg Poly(A)<sup>+</sup>-RNA, and from brain an additional sample of 8 µg Poly(A)<sup>+</sup>-RNA, were diluted 1:1 with loading buffer (20 % formaldehyde, 70 % deionised formamide, 6 % glycerol, 0.5 % bromphenol blue, in 2x MOPS (= 3-[N-morpholino]propanesulfonic acid) buffer) (1x MOPS buffer: 200 mM MOPS, 50 mM NaAc pH 7.0, 10 mM EDTA pH 8.0, pH 7.0 with NaOH). Following 10 min denaturation at 55°C, the samples and the RNA marker (0.2- 9.5 kb) were loaded on a 1 % MOPS-agarose gel (1 % agarose in 1x MOPS buffer, 0.06 % ethidium bromide), and in 1x MOPS buffer separated at 70 V. The quality of the Poly(A)<sup>+</sup>-RNA was checked under UV-light: sharpness of the 28S and 18S ribosomal RNA signals (in fish: 3.5 kb and 1.8 kb, respectively). The RNA was overnight blotted onto a nylon membrane (Hybond<sup>TM</sup>-N, Amersham) in 20x SSC (3 M NaCl, 0.3 M Na<sub>3</sub>-citrate) according to standard protocols (Sambrook et al., 1989), and the membrane was UV-crosslinked (120 mJ/ cm<sup>2</sup>; UV-Stratalinker, Stratagene).

The <sup>32</sup>P-DNA hybridization probe was obtained by specific PCR-amplification: a PCR reaction of 50 µl was carried out in a MicroAmp reaction tube in a GeneAmp PCR System 9600 (Perkin Elmer Cetus).

Final concentrations of the reaction components were 4 ng pcDNA3-fsst<sub>3</sub> plasmid DNA, 200 µM each of dGTP, dCTP, dTTP, 1 µM each of the fsst<sub>3</sub>-specific oligonucleotides 5'-AGGTCCTAAACCGGCCAAG-3' and 5'-ATGAGCACCCCGGCGGCG-3' (206 bp product), 1x PCR-buffer (Stratagene; 1.5 mM MgCl<sub>2</sub>), 10 µCi [ $\alpha$ -<sup>32</sup>P]-dATP and 5 units Taq 2000<sup>TM</sup> DNA polymerase (Stratagene). The PCR conditions were as follows: an initial denaturation step at 95°C for 7 min, during which the enzyme was mixed with other components (Hot Start), then 30 cycles consisting of 95°C for 30 s, 55°C for 30 s, and 72°C for 30 s. For final elongation, the reactions were held at 72°C for 3 min; an in parallel amplified product containing additional 200 µM of dATP and no [ $\alpha$ -<sup>32</sup>P]-dATP was checked on a 1 % agarose gel stained with ethidium bromide. The hybridization probe was filter purified (Millipore; 0.025 µm pore size).

Pre-hybridisation (> 2 h) and hybridisation (overnight) of the nylon membrane were carried out at 43°C in 50 % formamide, 50 mM Tris pH 7.5, 0.8 M NaCl, 1 % SDS, 0.2 % BSA, 0.2 % Ficoll 400, 0.2 % polyvinylpyrrolidone, and 100 µg/ml salmon sperm DNA. For hybridisation, 1.25 x 10<sup>6</sup> dpm/ ml denaturated <sup>32</sup>P-DNA probe were added. The membrane was washed at 65°C three times for 20 min in 1 x SSC, 0.1 % SDS, and exposed to a X-OMAT<sup>TM</sup> autoradiography film (Kodak). As a positive control for the hybridization probe different amounts of pcDNA3-fsst<sub>3</sub> plasmid DNA (10 µg- 1 ng) were pipetted onto a second membrane, denaturated and renatured (see RT-PCR protocol), cross-linked, and hybridized and washed in parallel. The oligonucleotides were purchased from Microsynth (Balgach, Switzerland).

## **2.11. Reverse transcriptase-polymerase chain reaction (RT-PCR)**

Poly(A)<sup>+</sup>-RNA (brain) and total RNA (fsst<sub>3</sub>-expressing CCL39 cells) was prepared according to the manuals of Quiagen RNA extraction kits.

To eliminate potential contamination of the RNA with genomic DNA (since the *fsst<sub>3</sub>* receptor gene contains, like mammalian SRIF receptor genes, no introns) 0.5 µg Poly(A)<sup>+</sup>-RNA from brain and 2 µg total RNA from *fsst<sub>3</sub>* receptor-expressing CCL39 cells (positive control) were incubated for 30 min at 37°C with 0.5 units RQ1 RNase-free-DNase, 20 units rRNasin (Promega) in 25 µl of 10 mM Tris-HCl pH 7.0, 10 mM MgCl<sub>2</sub>, 1 mM DTT, 1 mM EDTA pH 8.0. After addition of 6 µl DNase-Stopmix (50 mM EDTA pH 8.0, 1.5 M NaAc pH 7.0), phenol/ chloroform extraction and ethanol precipitation was performed.

The RNA was denatured by heating for 5 min at 65°C and then reverse transcribed into first strand cDNA by using 500 ng Oligo(dT) primers (Gibco BRL) for Poly(A)<sup>+</sup>-RNA and 3 µg random hexamer primers (Gibco BRL) for total RNA, 20 units rRNasin and 200 units Superscript™ II reverse transcriptase (Gibco BRL) in 20 µl of 1x first strand buffer (Gibco BRL), 250 µM each of dATP, dGTP, dCTP, dTTP, and 10 mM DTT. The reactions were incubated 60 min at 37°C, followed by denaturation for 5 min at 95°C. 3 µl of the first strand cDNA reaction mixture were subjected to PCR amplification. As a control for digestion of genomic DNA, DNase-digested, but not reverse transcribed Poly(A)<sup>+</sup>-RNA (brain), was subjected to PCR in parallel. PCR reactions of 50 µl were carried out in MicroAmp reaction tubes in a GeneAmp PCR System 9600 (Perkin Elmer Cetus). Final concentrations of the reaction components were 200 µM each of dATP, dGTP, dCTP, dTTP, 1 µM each of the *fsst<sub>3</sub>*-specific oligonucleotides 5'-AGGTCCTAAACCGGCCAAG-3' and 5'-ACGTGACGTTTCACGCTTTG-3' (569 bp product), 1x PCR-buffer (Stratagene; 1.5 mM MgCl<sub>2</sub>) and 5 units Taq 2000™ DNA polymerase (Stratagene). The PCR conditions were as follows: an initial denaturation step at 95°C for 2 min, during which the enzyme was mixed with other components (Hot Start), then 40 cycles consisting of 95°C for 20 s, 62°C for 30 s, and 72°C for 90 sec. For final elongation, the reactions were held at 72°C for 7 min. The amplified products were analysed on a 1 % agarose gel stained with ethidium bromide using φX174 RF DNA/Hae III fragments (Gibco BRL) as a molecular weight marker.

Quality and amount of the cDNA was analysed by specific amplification of  $\beta$ -actin with the primers 5'-TCTCGCACACACCTTCTACAA-3' and 5'-GTCTCATGGATACCGCAGGACT-3', which were derived from the  $\beta$ -actin sequence of the teleostean fish *Oryzias latipes*.

To confirm *fsst*<sub>3</sub>-specific amplification, the agarose gel was analysed by Southern Blot. After denaturation (0.5 N NaOH, 1.5 M NaCl) and neutralisation (1.5 N NaOH, 0.5 M Tris pH 7.4) of the gel, the DNA was blotted in 20 x SSC onto a Hybond<sup>TM</sup>-N membrane (Amersham) according to standard protocols (Sambrook et al., 1989), and the membrane was UV-crosslinked with 120 mJ/ cm<sup>2</sup>. The <sup>32</sup>P-DNA probe (206 bp) was obtained by specific PCR-amplification of pcDNA3-*fsst*<sub>3</sub> plasmid DNA with the oligonucleotides 5'-AGGTCCTAAACCGGCCAAG-3' and 5'-ATGAGCACCCCGGCGGCG-3' and filter purification (Millipore; 0.025  $\mu$ m pore size). Pre-hybridisation and hybridisation were carried out at 43°C in 50 % formamide, 50 mM Tris pH 7.5, 0.8 M NaCl, 1 % SDS, 0.2 % BSA, 0.2 % Ficoll 400, 0.2 % polyvinylpyrrolidone, and 100  $\mu$ g/ ml salmon sperm DNA. For hybridisation, 1.25 x 10<sup>6</sup> dpm/ ml denaturated <sup>32</sup>P-DNA probe were added. The membrane was washed at 65°C three times for 20 min in 1 x SSC, 0.1 % SDS, and exposed to a X-OMAT<sup>TM</sup> autoradiography film (Kodak). All oligonucleotides were purchased from Microsynth (Balgach, Switzerland).

## Chapter 3

---

### **[<sup>125</sup>I]Tyr<sup>10</sup>-cortistatin<sub>14</sub> labels all five somatostatin receptors**

---

Sandra Siehler, Klaus Seuwen and Daniel Hoyer,

Naunyn-Schmiedeberg's Archives of Pharmacology (1998) 357: 483-489



### 3.1. Abstract

The recently cloned rat preprocortistatin, which shows homology to the preprosomatostatin peptide, is thought to be enzymatically cleaved to cortistatin<sub>14</sub> (CST<sub>14</sub>) similarly to somatostatin<sub>14</sub> (SRIF<sub>14</sub>). High structural similarity of cortistatin<sub>14</sub> compared to SRIF<sub>14</sub> suggested binding properties to somatostatin receptors similar to SRIF<sub>14</sub>. In the present study, we expressed stably the five human somatostatin receptor subtypes (hsst<sub>1</sub>-hsst<sub>5</sub>) in CCL39 cells (Chinese hamster lung fibroblast cells). The receptors were labelled with an iodinated analogue of CST<sub>14</sub> (<sup>125</sup>I]Tyr<sup>10</sup>-cortistatin<sub>14</sub>, [<sup>125</sup>I]Tyr<sup>10</sup>-CST) to establish the pharmacological profile of hsst<sub>1</sub>-hsst<sub>5</sub> sites labelled with [<sup>125</sup>I]Tyr<sup>10</sup>-CST. In parallel, [Leu<sup>8</sup>,D-Trp<sup>22</sup>,<sup>125</sup>I-Tyr<sup>25</sup>]-SRIF<sub>28</sub> (<sup>125</sup>I]LTT-SRIF<sub>28</sub>) was used as a control at the five recombinant SRIF receptors stably expressed in CCL39 cells. High affinity [<sup>125</sup>I]Tyr<sup>10</sup>-CST binding could be demonstrated to all five recombinant somatostatin receptor subtypes. The pK<sub>d</sub> (-log mol/l) and B<sub>max</sub>-values (fmol/mg) for hsst<sub>1-5</sub> receptors were: 10.02 ± 0.04, 220 ± 30; 9.45 ± 0.09, 340 ± 70; 10.06 ± 0.11, 340 ± 50; 9.67 ± 0.14, 340 ± 110 and 10.33 ± 0.03, 5630 ± 330, respectively. The pharmacological profiles determined with [<sup>125</sup>I]Tyr<sup>10</sup>-CST and [<sup>125</sup>I]LTT-SRIF<sub>28</sub> were very similar at every receptor studied. These data suggest that cortistatin and somatostatin have similar high affinity for SRIF receptors. None of the receptors showed marked selectivity for either CST<sub>14</sub> /CST<sub>17</sub> or the somatostatins. In conclusion, the data show that cortistatin and somatostatin have very similar high affinity to all five recombinant somatostatin receptors. It remains to be seen whether there are specific receptors which bind only somatostatins or cortistatins.

### 3.2. Results

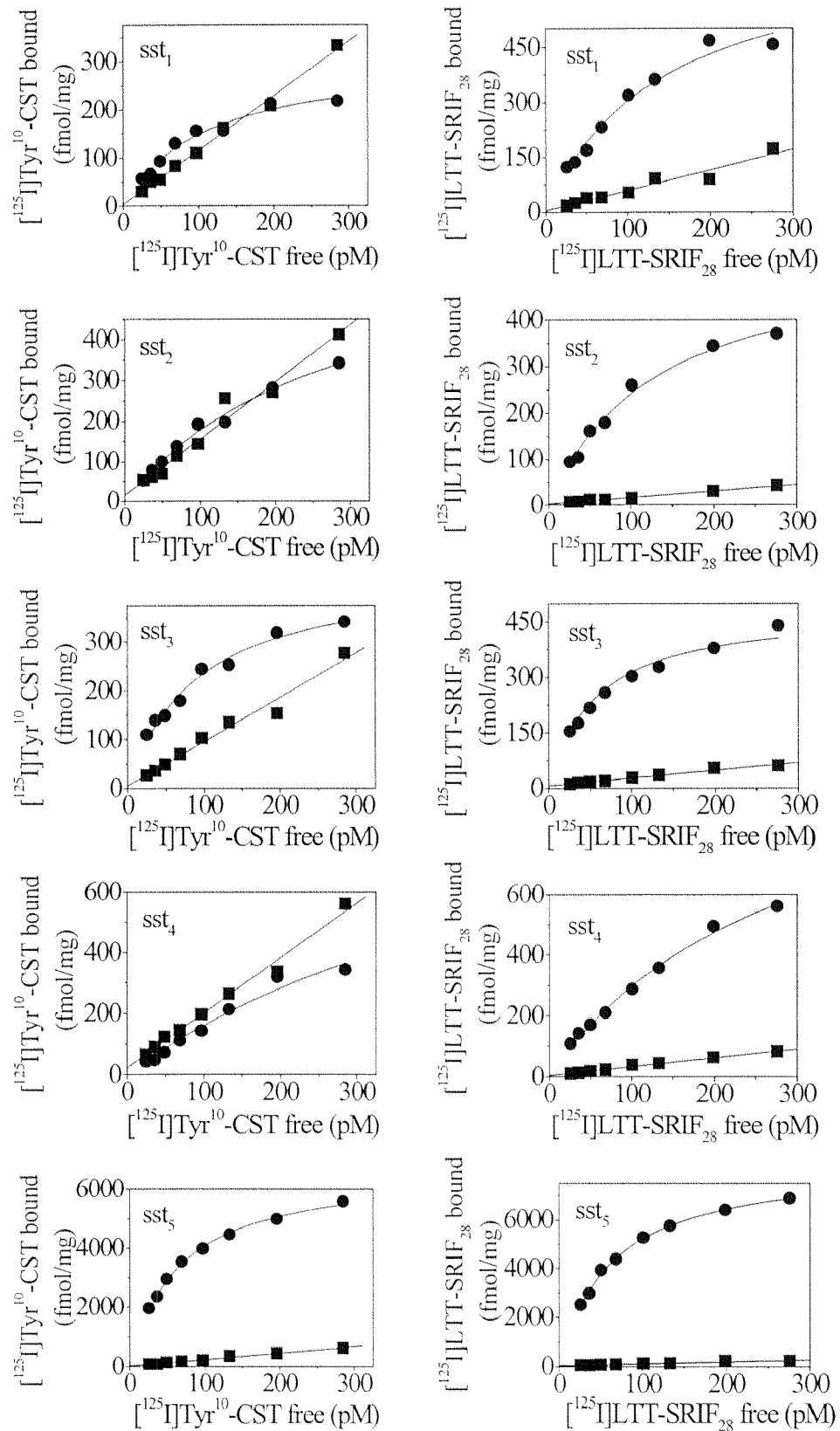
$[^{125}\text{I}]\text{Tyr}^{10}\text{-cortistatin}_{14}$  ( $[^{125}\text{I}]\text{Tyr}^{10}\text{-CST}$ ) specifically bound to the human somatostatin receptors  $\text{sst}_{1-5}$  and was used as a radioligand to determine the pharmacological profile in CCL39 cells. Saturation experiments (table 1) revealed high affinity and saturable binding of  $[^{125}\text{I}]\text{Tyr}^{10}\text{-CST}$  to  $\text{hsst}_{1-5}$  receptors similarly to  $[^{125}\text{I}]\text{LTT-SRIF}_{28}$ . No specific binding and therefore no presence of endogenous SRIF receptors was detectable in non-transfected CCL39 cells (data not shown). RT-PCR revealed expression of  $\text{hsst}_{1-5}$  in the stably transfected cells, but not in non transfected CCL39 cells (data not shown). The saturation isotherms were apparently monophasic suggesting a homogenous population of receptor sites (figure 1). The  $B_{\text{max}}$ -values obtained at each receptor were roughly comparable between the two radioligands. The non specific binding of  $[^{125}\text{I}]\text{Tyr}^{10}\text{-CST}$  was usually higher than that of  $[^{125}\text{I}]\text{LTT-SRIF}_{28}$ , except for  $\text{sst}_3$  receptors which however showed higher expression levels than the other SRIF receptors.

**Table 1:** Comparison of saturation data obtained with  $[^{125}\text{I}]\text{Tyr}^{10}\text{-CST}$  and  $[^{125}\text{I}]\text{LTT-SRIF}_{28}$  at human  $\text{sst}_{1-5}$  receptors

	$[^{125}\text{I}]\text{LTT-SRIF}_{28}$		$[^{125}\text{I}]\text{Tyr}^{10}\text{-CST}$	
	$\text{pK}_d$	$B_{\text{max}}$ [fmol/mg]	$\text{pK}_d$	$B_{\text{max}}$ [fmol/mg]
CCL39/ $\text{hsst}_1$	$9.96 \pm 0.00$	$470 \pm 30$	$10.02 \pm 0.04$	$220 \pm 30$
CCL39/ $\text{hsst}_2$	$9.89 \pm 0.04$	$370 \pm 60$	$9.45 \pm 0.09$	$340 \pm 70$
CCL39/ $\text{hsst}_3$	$10.28 \pm 0.06$	$560 \pm 60$	$10.06 \pm 0.11$	$340 \pm 50$
CCL39/ $\text{hsst}_4$	$9.64 \pm 0.03$	$440 \pm 50$	$9.67 \pm 0.14$	$340 \pm 110$
CCL39/ $\text{hsst}_5$	$10.48 \pm 0.04$	$6950 \pm 220$	$10.33 \pm 0.03$	$5630 \pm 330$

The data represent the mean of  $\text{pK}_d$ -values ( $-\log M$ )  $\pm$  standard error (SEM) of three determinations.

**Figure 1:** Saturation curves using [ $^{125}$ I]Tyr $^{10}$ -CST (left column) and [ $^{125}$ I]LTT-SRIF $_{28}$  (right column) to membranes prepared from CCL39 cells stably expressing human sst $_{1-5}$  receptors.



Crude membrane preparations from sst<sub>1-5</sub> receptor expressing cells were incubated with increasing concentrations of [<sup>125</sup>I]Tyr<sup>10</sup>-CST or [<sup>125</sup>I]LTT-SRIF<sub>28</sub>, and assayed for receptor binding. The plots depict specific (●) and non-specific binding (■) expressed as amount of radioligand bound (fmol/ mg) versus free radioligand concentration (pM). The figures represent one representative example of 3 different experiments.

SRIF<sub>14</sub>, SRIF<sub>28</sub>, CST<sub>14</sub>, CST<sub>17</sub> and the unlabelled Tyr<sup>10</sup>-CST bound with K<sub>d</sub>'s in the nM-range to sst<sub>1-5</sub> receptors. CST<sub>17</sub> which is derived from the human prepropeptide, showed slightly higher affinity at the five human receptors compared to CST<sub>14</sub> which is derived from the rat prepropeptide. The pharmacological profile of human sst<sub>1-5</sub> receptors labelled with [<sup>125</sup>I]Tyr<sup>10</sup>-CST and [<sup>125</sup>I]LTT-SRIF<sub>28</sub> were compared (table 2 & 3, figure 2). The short cyclic SRIF-analogues seglitide, octreotide, RC160 and BIM 23014 bound all with high affinity (< 1 nM) to the sst<sub>2</sub> receptor, but displayed very low affinity to sst<sub>1</sub> and sst<sub>4</sub> receptors. Seglitide showed high affinity for the sst<sub>5</sub> receptor whereas other peptides of this group displayed intermediate affinity. The rank order of potency of compounds for sst<sub>1</sub> sites labelled with [<sup>125</sup>I]Tyr<sup>10</sup>-CST: CST<sub>17</sub> > SRIF<sub>28</sub> ≈ SRIF<sub>14</sub> ≈ > BIM 23052 > CGP 23996 > CST<sub>14</sub> >> octreotide >> seglitide, was similar to that at sst<sub>4</sub> sites: CST<sub>17</sub> > CST<sub>14</sub> = CGP 23996 ≈ SRIF<sub>28</sub> ≈ SRIF<sub>14</sub> ≈ BIM 23052 >> octreotide > seglitide. On the other hand, the affinity rank orders for the other three receptors were typical for the SRIF<sub>1</sub> receptor family, i.e. sst<sub>2</sub>: SRIF<sub>28</sub> ≈ SRIF<sub>14</sub> > seglitide = RC160 > CST<sub>17</sub> ≈ BIM 23014 ≈ octreotide > L362,855 > CST<sub>14</sub> = BIM 23052 = L363,301; sst<sub>3</sub>: SRIF<sub>28</sub> ≈ SRIF<sub>14</sub> ≈ BIM 23052 ≈ CST<sub>17</sub> > CGP 23996 > CST<sub>14</sub> > octreotide > L362,855 > BIM 23014, and sst<sub>5</sub>: CST<sub>17</sub> > SRIF<sub>28</sub> ≈ SRIF<sub>14</sub> ≈ seglitide > CST<sub>14</sub> > octreotide = BIM 23014 > BIM 23030.

The profiles defined using [<sup>125</sup>I]Tyr<sup>10</sup>-CST and [<sup>125</sup>I]LTT-SRIF<sub>28</sub> were comparable independently of the receptor type examined. The sst<sub>3</sub> receptor though, may represent an exception, since some of the compounds (seglitide, octreotide BIM 23052, cycloantagonist) showed an approximately 10 fold higher affinity for [<sup>125</sup>I]Tyr<sup>10</sup>-CST- as compared to [<sup>125</sup>I]LTT-SRIF<sub>28</sub>-labelled sites. The receptor profiles determined with the two radioligands showed high correlation coefficients (see figure 3) at each of the five SRIF receptor subtypes (sst<sub>1</sub>: r = 0.981; sst<sub>2</sub>: r = 0.985; sst<sub>3</sub>: 0.956; sst<sub>4</sub>: 0.985; sst<sub>5</sub>: 0.968).

**Table 2:** Comparison of the pharmacological profiles of human sst<sub>1</sub> and sst<sub>4</sub> receptors labelled with [<sup>125</sup>I]Tyr<sup>10</sup>-CST or [<sup>125</sup>I]LTT-SRIF<sub>28</sub>. The affinity values are expressed as pK<sub>d</sub> ± SEM of 3-4 independent experiments

	CCL39/hsst <sub>1</sub>		CCL39/hsst <sub>4</sub>	
	[ <sup>125</sup> I]LTT-SRIF <sub>28</sub>	[ <sup>125</sup> I]Tyr <sup>10</sup> -CST	[ <sup>125</sup> I]LTT-SRIF <sub>28</sub>	[ <sup>125</sup> I]Tyr <sup>10</sup> -CST
SRIF <sub>14</sub>	9.12 ± 0.05	9.08 ± 0.07	8.91 ± 0.15	8.39 ± 0.28
SRIF <sub>28</sub>	9.22 ± 0.02	9.26 ± 0.07	9.08 ± 0.12	8.44 ± 0.30
seglitide	4.50 ± 0.04	4.32 ± 0.06	5.37 ± 0.08	5.11 ± 0.07
CGP 23996	8.33 ± 0.06	8.31 ± 0.04	8.77 ± 0.03	8.67 ± 0.14
octreotide	6.65 ± 0.05	6.41 ± 0.04	6.40 ± 0.09	5.76 ± 0.08
L362,855	6.25 ± 0.07	6.30 ± 0.07	7.31 ± 0.07	6.76 ± 0.32
L363,301	5.32 ± 0.08	5.38 ± 0.15	5.61 ± 0.03	5.06 ± 0.06
RC160	7.08 ± 0.08	6.96 ± 0.24	7.25 ± 0.05	6.56 ± 0.44
BIM 23030	5.06 ± 0.04	4.85 ± 0.02	5.98 ± 0.04	5.56 ± 0.14
BIM 23014	6.75 ± 0.04	6.66 ± 0.18	6.64 ± 0.07	6.25 ± 0.28
BIM 23056	6.61 ± 0.10	6.46 ± 0.07	7.17 ± 0.10	6.47 ± 0.35
BIM 23052	8.37 ± 0.04	8.62 ± 0.05	8.63 ± 0.04	8.20 ± 0.11
cycloantagonist	7.02 ± 0.00	6.80 ± 0.17	6.48 ± 0.13	6.07 ± 0.26
Tyr <sup>10</sup> -CST	8.56 ± 0.08	9.04 ± 0.13	8.44 ± 0.06	8.17 ± 0.09
CST <sub>14</sub>	8.76 ± 0.06	7.74 ± 0.09	8.76 ± 0.02	8.75 ± 0.14
CST <sub>17</sub>	9.61 ± 0.04	9.61 ± 0.17	9.24 ± 0.02	9.55 ± 0.03

### 3.3. Discussion

The putative neuropeptides CST<sub>14</sub> and CST<sub>17</sub> bound to all five known human somatostatin receptor subtypes with high affinity. There was no preferential affinity of either of the cortistatins to any of the receptors, although the putative human peptide CST<sub>17</sub> showed somewhat higher affinity than its rat equivalent CST<sub>14</sub>.

**Table 3:** Comparison of the pharmacological profiles of human  $sst_2$ ,  $sst_5$  and  $sst_3$  receptors labelled with [ $^{125}$ I]Tyr $^{10}$ -CST or [ $^{125}$ I]LTT-SRIF $_{28}$ . The affinity values are expressed as  $pK_d \pm SEM$  of 3-4 independent experiments

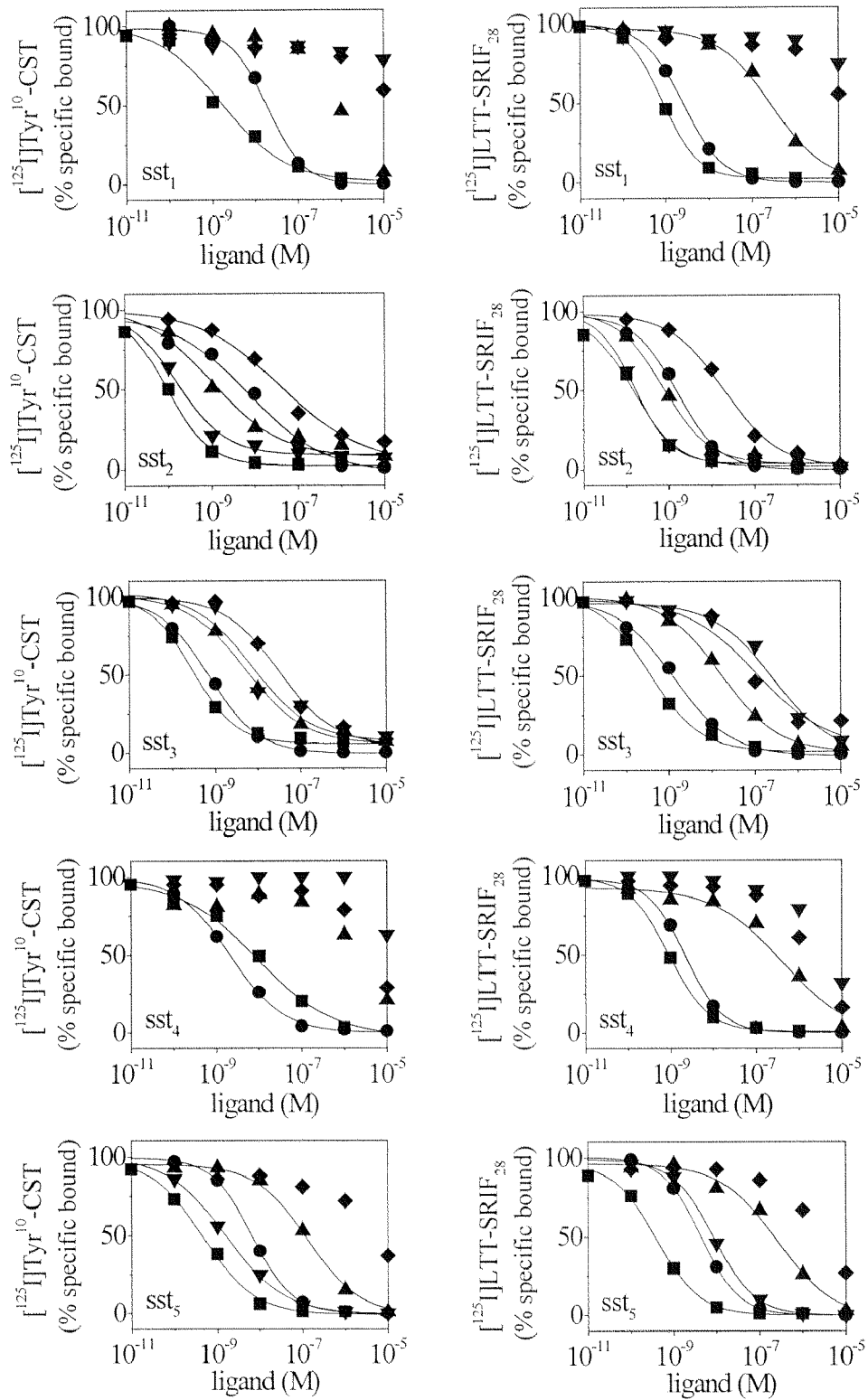
	CCL39/ $hsst_2$		CCL39/ $hsst_5$		CCL39/ $hsst_3$	
	[ $^{125}$ I]LTT-SRIF $_{28}$	[ $^{125}$ I]Tyr $^{10}$ -CST	[ $^{125}$ I]LTT-SRIF $_{28}$	[ $^{125}$ I]Tyr $^{10}$ -CST	[ $^{125}$ I]LTT-SRIF $_{28}$	[ $^{125}$ I]Tyr $^{10}$ -CST
SRIF $_{14}$	10.00 $\pm$ 0.01	10.06 $\pm$ 0.07	9.53 $\pm$ 0.13	9.01 $\pm$ 0.24	9.54 $\pm$ 0.05	9.67 $\pm$ 0.07
SRIF $_{28}$	9.92 $\pm$ 0.03	10.16 $\pm$ 0.11	9.39 $\pm$ 0.22	9.18 $\pm$ 0.19	9.65 $\pm$ 0.04	9.80 $\pm$ 0.08
seglitide	9.96 $\pm$ 0.02	9.62 $\pm$ 0.17	8.70 $\pm$ 0.26	9.14 $\pm$ 0.30	6.88 $\pm$ 0.08	7.89 $\pm$ 0.25
CGP 23996	8.58 $\pm$ 0.07	8.94 $\pm$ 0.02	6.59 $\pm$ 0.41	6.67 $\pm$ 0.24	8.82 $\pm$ 0.05	9.28 $\pm$ 0.19
octreotide	9.19 $\pm$ 0.03	9.11 $\pm$ 0.14	7.17 $\pm$ 0.30	7.31 $\pm$ 0.18	7.88 $\pm$ 0.04	8.60 $\pm$ 0.16
L362,855	8.36 $\pm$ 0.05	8.79 $\pm$ 0.19	7.17 $\pm$ 0.30	7.17 $\pm$ 0.12	7.62 $\pm$ 0.23	8.25 $\pm$ 0.06
L363,301	8.39 $\pm$ 0.11	8.47 $\pm$ 0.18	7.69 $\pm$ 0.13	7.17 $\pm$ 0.15	6.34 $\pm$ 0.06	6.83 $\pm$ 0.08
RC160	9.35 $\pm$ 0.09	9.60 $\pm$ 0.02	7.51 $\pm$ 0.06	7.27 $\pm$ 0.11	7.37 $\pm$ 0.15	7.91 $\pm$ 0.03
BIM 23030	7.77 $\pm$ 0.07	7.66 $\pm$ 0.07	6.02 $\pm$ 0.09	5.56 $\pm$ 0.17	7.17 $\pm$ 0.08	7.85 $\pm$ 0.11
BIM 23014	9.27 $\pm$ 0.06	9.26 $\pm$ 0.07	7.76 $\pm$ 0.13	7.38 $\pm$ 0.19	7.86 $\pm$ 0.41	8.02 $\pm$ 0.14
BIM 23056	6.33 $\pm$ 0.10	6.23 $\pm$ 0.12	7.17 $\pm$ 0.05	6.68 $\pm$ 0.05	6.90 $\pm$ 0.04	7.08 $\pm$ 0.11
BIM 23052	8.30 $\pm$ 0.14	8.50 $\pm$ 0.32	7.92 $\pm$ 0.19	7.45 $\pm$ 0.24	8.42 $\pm$ 0.12	9.55 $\pm$ 0.12
cycloantagonist	5.40 $\pm$ 0.06	5.74 $\pm$ 0.05	6.38 $\pm$ 0.23	6.02 $\pm$ 0.11	6.23 $\pm$ 0.03	7.08 $\pm$ 0.04
Tyr $^{10}$ -CST	8.77 $\pm$ 0.09	8.91 $\pm$ 0.21	8.67 $\pm$ 0.24	8.06 $\pm$ 0.40	8.70 $\pm$ 0.18	8.90 $\pm$ 0.08
CST $_{14}$	8.75 $\pm$ 0.20	8.54 $\pm$ 0.44	8.71 $\pm$ 0.02	8.40 $\pm$ 0.04	9.06 $\pm$ 0.12	9.13 $\pm$ 0.09
CST $_{17}$	9.07 $\pm$ 0.01	9.29 $\pm$ 0.13	9.54 $\pm$ 0.10	9.37 $\pm$ 0.09	9.43 $\pm$ 0.06	9.52 $\pm$ 0.10

When [ $^{125}$ I]Tyr $^{10}$ -CST was used as a radioligand, the data compared well with [ $^{125}$ I]LTT-SRIF $_{28}$  binding, as indicated by the high correlation observed at each of the five SRIF receptors. Some differences could be observed at the  $sst_3$  receptor for a number of compounds, but these may well lie within the experimental variation, although the somatostatins and cortistatins displayed no such differences.

The pharmacological profile established at human recombinant receptors in CCL39 cells reveals some discrepancy to literature data. The cyclic heptapeptide L362,855 reported to be  $sst_5$ -selective (O'Carroll et al., 1994; Raynor et al., 1993a, 1993b; Williams et al., 1997) shows higher affinity to  $sst_2$  receptors in CCL39 cells. Similarly, the linear octapeptide BIM 23052 claimed to be  $sst_5$ -selective (Raynor et al., 1993a, 1993b), shows no selectivity in the present study. Further, we have not been able to reproduce the very high affinity and selectivity for  $sst_3$  receptors which has been reported for BIM 23056. To the contrary, it would appear, that this compound is non-selective and has only intermediate affinity for all five SRIF receptors.  $CST_{14}$  and  $CST_{17}$  bound with similar high affinity to all five receptor subtypes in CCL39 cells, as it was found in  $GH_4$  pituitary cells or at recombinant receptors (De Lecea et al., 1996; 1997a; Fukusumi et al., 1997). According to Fukusumi and colleagues,  $CST_{17}$  and  $CST_{14}$ , were roughly equipotent and displayed about ten-fold lower affinity for the human  $sst_1$  receptor compared to the other receptors. Discrepancies may relate to different radioligands used: [ $^{125}$ I]-Tyr<sup>11</sup>-SRIF<sub>14</sub> (Fukusumi et al., 1997; De Lecea et al., 1996) and [ $^{125}$ I]CGP 23996 (Raynor et al., 1993a). Some variation was also found when comparing with data obtained with [ $^{125}$ I]LTT-SRIF<sub>28</sub> (Patel and Srikant, 1994). On the other hand, the use of different cell systems may also provide some grounds for thought. The expression of the recombinant SRIF receptors is often performed in CHO or COS cells.

Post-transcriptional and post-translational mechanisms, like receptor phosphorylation or glycosylation may vary in different cell systems and hence, could affect the conformation of a receptor-ligand complex. Finally, distinct cell lines may express different sets of G-proteins, which are also suggested to influence the agonist binding properties of receptors (Lefkowitz et al., 1993), since SRIF receptor binding is usually performed with agonist radioligands. For instance, Fukusumi et al. (1997) used CHO cells, where apparently the  $sst_1$  receptor does not couple to adenylate cyclase, whereas it does in CCL39 cells (data not shown). However, the present data were compared with those reported for native  $sst_1$ ,  $sst_2$  and  $sst_4$  receptors described in the human cerebral cortex and in rat lung for the latter (Piwko et al., 1997) and we obtained high correlation coefficients ( $r = 0.93, 0.96$  and  $0.98$ , respectively), suggesting that there is indeed little difference between the receptors expressed recombinantly in CCL39 cells and the native ones.

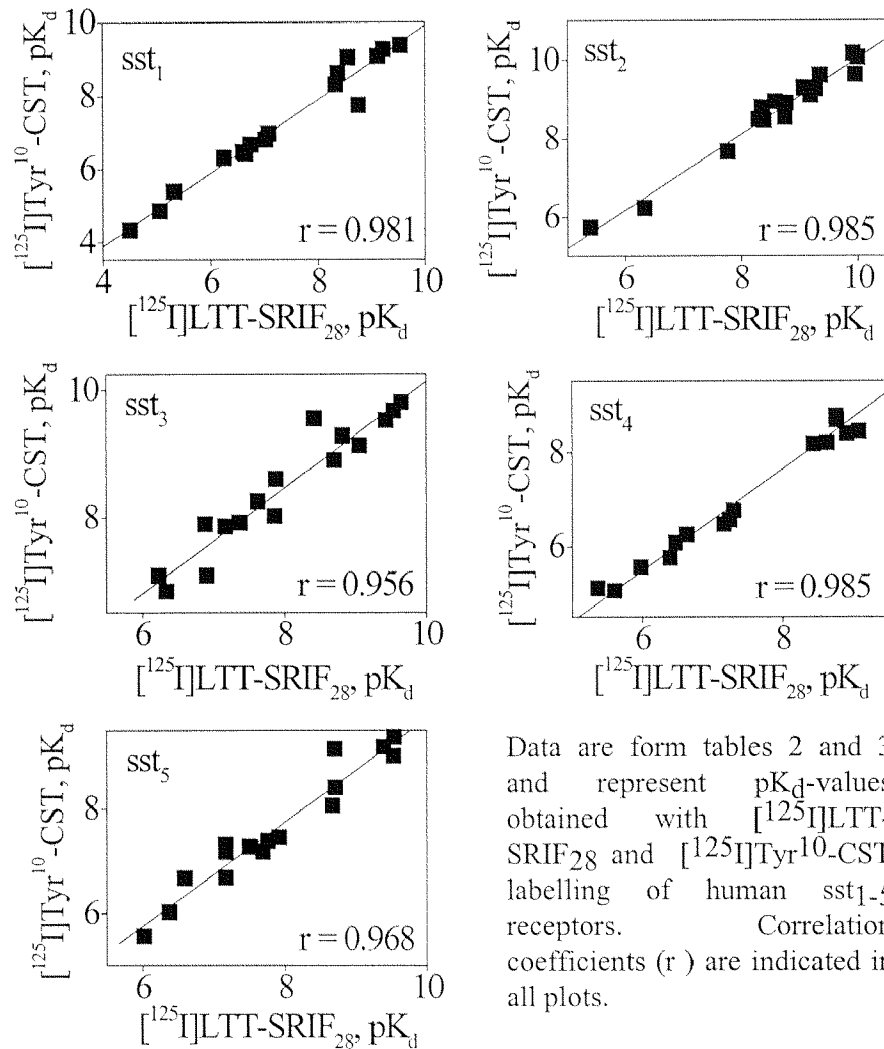
**Figure 2:** Competitive radioligand binding assays performed in membranes prepared from CCL39 cells expressing human  $ss_{1-5}$  receptors.





Crude membrane preparations from sst<sub>1-5</sub> receptor transfected cells were incubated with [<sup>125</sup>I]Tyr<sup>10</sup>-CST or [<sup>125</sup>I]LTT-SRIF<sub>28</sub> and the indicated concentrations of SRIF<sub>14</sub> (■), CST<sub>14</sub> (●), octreotide (▲), seglitide (▼) and BIM 23030 (◆). Data are expressed as percentage of specific binding. The data points represent one representative example of at least 3 different experiments.

**Figure 3:** Correlation between [<sup>125</sup>I]Tyr<sup>10</sup>-CST and [<sup>125</sup>I]LTT-SRIF<sub>28</sub> binding at human recombinant sst<sub>1-5</sub> receptors expressed in CCL39 cells



The existence of the mature rat peptide  $CST_{14}$  has not been documented so far *in vivo*, although a cortistatin prepropeptide was cloned not only from rat, but also from mouse and human. By *in situ* hybridisation, the prepropeptide mRNA has been localised in the cerebral cortex and hippocampus of rat (De Lecea et al., 1996) and mouse (De Lecea et al., 1997b) and in the caudate nucleus and spinal cord of human (De Lecea et al. 1997a; Fukusumi et al., 1997). The homology of preprocortistatin to preprosomatostatin suggests analogous cleavage to mature peptides.  $CST_{14}$  affects neuronal electrical activity and sleep suggesting that the mature peptide is functional and probably different from somatostatin in its actions (De Lecea et al., 1996). Analogous to the rat peptide, the human preprocortistatin may be cleaved to  $CST_{17}$ , which can modulate sleep activity as well (Fukusumi et al., 1997).

The present study shows a close pharmacological similarity between  $CST_{14}$  / $CST_{17}$  and the somatostatins. Indeed,  $CST_{14}$  has been shown to increase potassium conductance similarly to  $SRIF_{14}$  in rat locus coeruleus (Connor et al., 1997).  $CST_{14}$  and  $CST_{17}$  have been reported to have affinities and activities comparable to those of somatostatin at recombinant human SRIF receptor binding and/ or adenylate cyclase activity (Fukusumi et al., 1997).  $CST_{14}$  has also been reported to impair post-training memory in a foot shock avoidance test in mice (Flood et al., 1997). However,  $CST_{14}$  has effects on neuronal depression, sleep modulation and slow wave sleep which do not parallel those of somatostatin (De Lecea et al., 1996).

Administration of  $CST_{17}$  (icv) to rats induced flattening of cortical and hippocampal electroencephalograms (Fukusumi et al., 1997). As some functional responses of  $CST_{14}$  and somatostatin can be differentiated (De Lecea et al., 1996), the existence of yet to be discovered cortistatin receptors may provide a basis for such differences, since the currently known "SRIF" receptors do hardly distinguish between SRIF and cortistatin.

#### 4.1. Abstract

Human somatostatin (somatotropin release inhibiting factor = SRIF) receptor subtypes  $sst_2$  and  $sst_5$  were stably expressed in Chinese hamster lung fibroblast (CCL39) cells. [ $^{125}$ I][Tyr<sup>3</sup>]octreotide labelled with high affinity and in a saturable manner both  $sst_2$  ( $pK_d = 9.89 \pm 0.02$ ,  $B_{max} = 210 \pm 10$  fmol/ mg,  $n = 3$ ) and  $sst_5$  sites ( $pK_d = 9.64 \pm 0.04$ ,  $B_{max} = 920 \pm 170$  fmol/ mg,  $n = 3$ ). The pharmacological profile of  $sst_2$  sites established in CCL39 cells using SRIF and various peptide analogues was very similar to that described previously in CHO cells and in human cortex: SRIF<sub>14</sub> = SRIF<sub>28</sub>  $\geq$  seglitide > BIM 23014 = RC160 > octreotide > CGP 23996  $\geq$  L362,855 > BIM 23052 > L361,301 = cortistatin<sub>14</sub> > BIM 23030 > BIM 23056 > cycloantagonist SA. However, peptides classically perceived as  $sst_2$  receptor selective (e.g. seglitide, octreotide, vapreotide) showed also high affinity for human  $sst_5$  receptors labelled with [ $^{125}$ I][Tyr<sup>3</sup>]octreotide: SRIF<sub>28</sub> > seglitide > SRIF<sub>14</sub> > L361,301 = octreotide > cortistatin<sub>14</sub> = BIM 23014 = BIM 23052 > L362,855 = RC160 > CGP 23996 > BIM 23056 > cycloantagonist SA > BIM 23030. Further radioligand binding studies were performed with [Leu<sup>8</sup>,D-Trp<sup>22</sup>, $^{125}$ I-Tyr<sup>25</sup>]SRIF<sub>28</sub> ([ $^{125}$ I]LTT- SRIF<sub>28</sub>) and [ $^{125}$ I]CGP 23996. At  $sst_2$  receptors,  $B_{max}$ -values determined with [ $^{125}$ I][Tyr<sup>3</sup>]octreotide, [ $^{125}$ I]LTT- SRIF<sub>28</sub> and [ $^{125}$ I]CGP 23996 were in the same range (180- 370 fmol/ mg). 5'-guanylylimidodiphosphate (GppNHp) displaced all three radioligands to the same extent (85 %) and the pharmacological profiles were superimposable. By contrast, at  $sst_5$  receptors  $B_{max}$ -values ranged were very different: [ $^{125}$ I][Tyr<sup>3</sup>]octreotide (920 fmol/mg), [ $^{125}$ I]CGP 23996 (3530 fmol/ mg) and [ $^{125}$ I]LTT-SRIF<sub>28</sub> (6950 fmol/ mg). GppNHp affected [ $^{125}$ I][Tyr<sup>3</sup>]octreotide more than [ $^{125}$ I]CGP 23996 binding, whereas [ $^{125}$ I]LTT-SRIF<sub>28</sub> was much less affected. In addition, the affinity values determined in competition experiments at  $sst_5$  receptors, varied markedly; whereas SRIF<sub>14</sub>, cortistatin<sub>14</sub> and SRIF<sub>28</sub> showed 2, 4 and 8 fold differences in affinity at  $sst_5$  receptors labelled with [ $^{125}$ I][Tyr<sup>3</sup>]octreotide and [ $^{125}$ I]LTT-SRIF<sub>28</sub> compounds such as RC 160, L363,301, L362,855, octreotide or CGP 23996 showed between 42 and 123 fold lower affinity when  $sst_5$  sites were labelled with [ $^{125}$ I]LTT-SRIF<sub>28</sub>. The present data suggest caution to be used when comparing affinity profiles determined in binding studies using different radioligands.

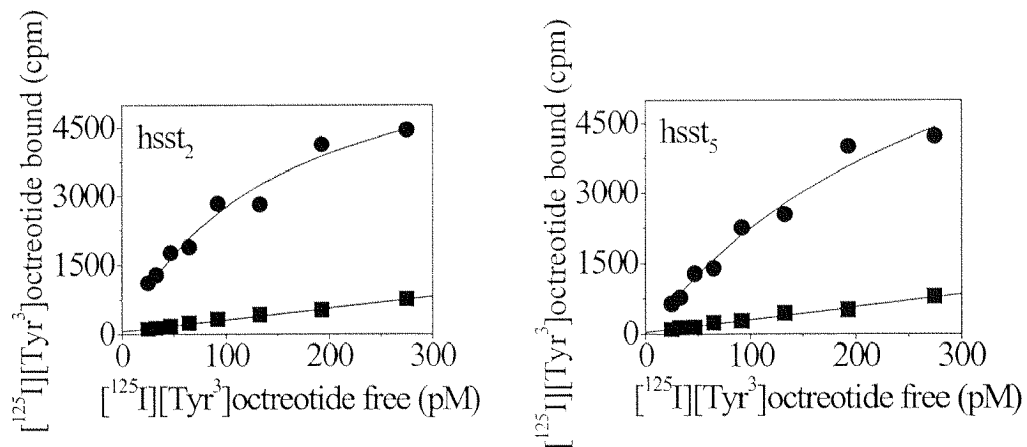
In addition, the present results suggest that effects produced by octreotide and related short chain SRIF analogues on hormone release, modulation of tumour growth and central effects may be mediated by either  $sst_2$  and/or  $sst_5$  receptors.

## 4.2. Results

[ $^{125}\text{I}$ ][Tyr $^3$ ]octreotide showed high specific binding to the human somatostatin receptor subtypes  $sst_2$  and  $sst_5$ , non-specific binding was comparatively low. Saturation experiments performed with [ $^{125}\text{I}$ ][Tyr $^3$ ]octreotide suggested labelling of a single population of binding sites (figure 1) in CCL39 cells expressing human  $sst_2$  ( $pK_d = 9.89 \pm 0.02$ ,  $B_{\max} = 210 \pm 10$  fmol/ mg,  $n = 3$ ) and  $sst_5$  receptors ( $pK_d = 9.64 \pm 0.04$ ,  $B_{\max} = 920 \pm 170$  fmol/ mg,  $n = 3$ ). No specific binding, i.e. no endogenous SRIF receptors could be detected in non-transfected CCL39 cells (data not shown). RT-PCR revealed only expression of either  $hsst_2$  or  $hsst_5$  in the stably transfected cells, but not in non transfected CCL39 cells (data not shown).

[ $^{125}\text{I}$ ][Tyr $^3$ ]octreotide was used to determine the affinity of SRIF and a range of SRIF-analogues in competition studies in CCL39 cells expressing  $hsst_2$  or  $hsst_5$  receptors (table 1; figures 2 + 3); in addition,  $hsst_2$  receptor binding data reported previously (Piwko et al., 1997) obtained in CHO cells and human cerebral cortex are also listed (see table 3). The rank order of potency of [ $^{125}\text{I}$ ][Tyr $^3$ ]octreotide labelled  $hsst_2$  sites was very similar in human cortex and both CHO and CCL39 cells:  $\text{SRIF}_{14} = \text{SRIF}_{28} > \text{seglitide} > \text{BIM 23014} = \text{RC160} > \text{octreotide} > [\text{Tyr}^{10}]\text{cortistatin} > \text{CGP 23996} > \text{L362,855} > \text{BIM 23052} > \text{L361,301} = \text{cortistatin}_{14} > \text{BIM 23030} > \text{BIM 23056} > \text{cycloantagonist}$ . At  $hsst_5$  sites, [ $^{125}\text{I}$ ][Tyr $^3$ ]octreotide defined following rank order of affinity:  $\text{SRIF}_{28} > \text{seglitide} > \text{SRIF}_{14} > [\text{Tyr}^{10}]\text{cortistatin} = [\text{Leu}^8, \text{D-Trp}^{22}, \text{Tyr}^{25}]\text{SRIF}_{28} > \text{L361,301} > \text{octreotide} > \text{cortistatin}_{14} = \text{BIM 23052} = \text{BIM 23014} > \text{L362,855} = \text{RC160} > \text{CGP 23996} > [\text{Tyr}^3]\text{octreotide} > \text{BIM 23056} = \text{cycloantagonist} > \text{BIM 23030}$ . As expected, the  $sst_5$  receptor showed higher affinity for  $\text{SRIF}_{28}$  than  $\text{SRIF}_{14}$ . The short cyclic SRIF-analogues seglitide, octreotide, RC160 and BIM 23014 bound all with high affinity (between 0.1 and 1 nM) to both receptor subtypes.

**Figure 1:** Saturation curves of [ $^{125}$ I][Tyr $^3$ ]octreotide binding to membranes prepared from CCL39 cells stably expressing human sst $_2$  or sst $_5$  receptors.



Crude membrane preparations from sst $_2$  and sst $_5$  expressing cells (6  $\mu$ g or 2  $\mu$ g per assay, respectively) were incubated with increasing concentrations of [ $^{125}$ I][Tyr $^3$ ]octreotide and assayed for receptor binding activity. The plots depict specific ( $\bullet$ ) and non-specific binding ( $\blacksquare$ ) expressed as amount of radioligand bound (cpm/ assay) versus free radioligand concentration (pM). The figure shows one representative example of 3 different experiments.

There was no evidence from competition experiments that two classes of sites fitted the data better than a single class (figure 3). Altogether, the correlation coefficient between both receptor subtypes as labelled with [ $^{125}$ I][Tyr $^3$ ]octreotide (see table 1) is  $r^2 = 0.536$  (data not shown).

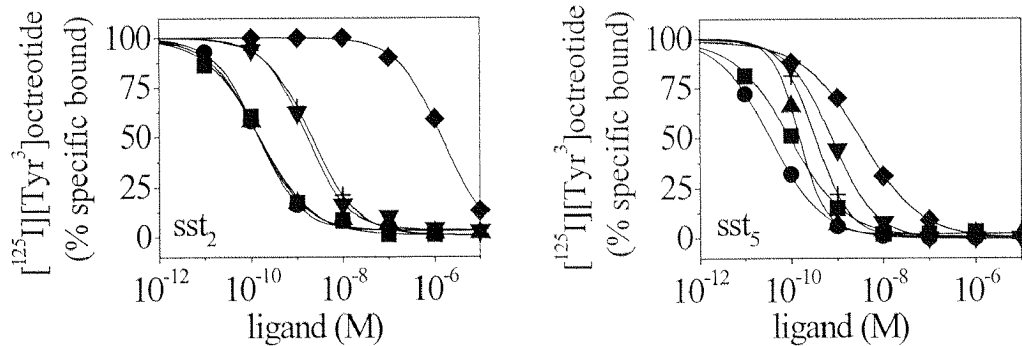
Since [ $^{125}$ I][Tyr $^3$ ]octreotide binding was “atypical”, i.e. a number of ligands displayed very similar affinities for both sst $_2$  and sst $_5$  receptors, further radioligand binding studies were performed with [ $^{125}$ I]LTT-SRIF $_{28}$  and [ $^{125}$ I]CGP 23996 at both sst $_2$  and sst $_5$  receptors expressing CCL39 cells (see table 2). [ $^{125}$ I]LTT-SRIF $_{28}$  and [ $^{125}$ I]CGP 23996 showed high affinity and saturable binding for both sst $_2$  and sst $_5$  receptors. Saturation experiments were compatible with the presence of a homogeneous population of recognition sites. At sst $_2$  receptors,  $B_{max}$ -values determined with [ $^{125}$ I][Tyr $^3$ ]octreotide, [ $^{125}$ I]LTT-SRIF $_{28}$  and [ $^{125}$ I]CGP 23996 were in the same range (180- 370 fmol/ mg).

**Table 1:** Comparison of affinities of SRIF and various SRIF-analogues for human  $ss_{2}$  and  $ss_{5}$  receptors labelled with [ $^{125}$ I][Tyr $^3$ ]octreotide

	CCL39/ $hsst_2$	CCL39/ $hsst_5$
SRIF $_{28}$	9.99 $\pm$ 0.08	10.30 $\pm$ 0.25
seglitide	9.81 $\pm$ 0.13	10.18 $\pm$ 0.22
SRIF $_{14}$	10.01 $\pm$ 0.04	9.87 $\pm$ 0.24
[Tyr $^{10}$ ]cortistatin	9.00 $\pm$ 0.09	9.65 $\pm$ 0.22
L361,301	8.39 $\pm$ 0.08	9.51 $\pm$ 0.14
octreotide	9.10 $\pm$ 0.07	9.48 $\pm$ 0.11
cortistatin $_{14}$	8.35 $\pm$ 0.11	9.34 $\pm$ 0.23
BIM 23014	9.55 $\pm$ 0.03	9.31 $\pm$ 0.10
BIM 23052	8.55 $\pm$ 0.01	9.28 $\pm$ 0.35
L362,855	8.79 $\pm$ 0.06	9.17 $\pm$ 0.10
RC160	9.50 $\pm$ 0.16	9.13 $\pm$ 0.35
CGP 23996	8.95 $\pm$ 0.07	8.68 $\pm$ 0.20
BIM 23056	6.38 $\pm$ 0.11	8.32 $\pm$ 0.17
cycloantagonist SA	5.77 $\pm$ 0.05	8.25 $\pm$ 0.17
BIM 23030	7.94 $\pm$ 0.22	7.45 $\pm$ 0.18

The data represent the mean of  $pK_d$ -values ( $-\log M$ )  $\pm$  standard error of at least three determinations.

**Figure 2:** Competitive radioligand binding on membranes of CCL39 cells expressing human  $ss_2$  or  $ss_5$  receptors.

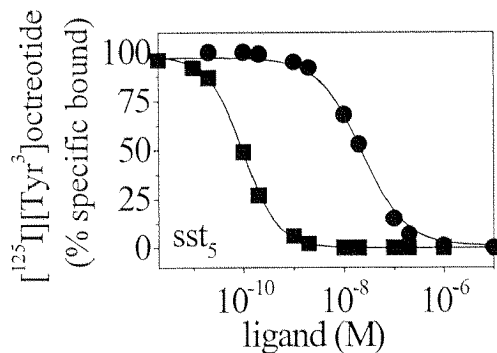


Crude membrane preparations from  $ss_2$  and  $ss_5$  transfected cells (6  $\mu$ g or 2  $\mu$ g per assay, respectively) were incubated with [ $^{125}$ I][Tyr $^3$ ]octreotide and the indicated concentrations of SRIF $_{14}$  (■), SRIF $_{28}$  (●), seglitide (▲), octreotide (▼) and BIM 23056 (◆) and cortistatin $_{14}$  (+). Data are expressed as percentage of specific binding. The figure shows one representative example of at least 3 different experiments.

There were however marked differences in  $B_{max}$ -values at  $ss_5$  receptors (see table 2): [ $^{125}$ I][Tyr $^3$ ]octreotide (920 fmol/mg), [ $^{125}$ I]CGP 23996 (3530 fmol/ mg) and [ $^{125}$ I]LTT-SRIF $_{28}$  (6950 fmol/ mg). In addition, whereas the affinities of the various ligands for  $ss_2$  sites revealed little differences if any (see table 3 and top of figure 4), there were some notable discrepancies in affinity values at the  $ss_5$  receptors, which appeared to be radioligand dependent (see table 4 and bottom of figure 4). These differences are illustrated in figure 4: it can be seen in the top that the competition curves of SRIF $_{14}$  or the ‘‘cycloantagonist’’ at  $ss_2$  receptors are superimposable whichever radioligand is used. At  $ss_5$  receptors, the competition curves obtained with SRIF $_{14}$  show little variations, whereas those of the cycloantagonist are shifted by a factor 10 from one radioligand to the other. Finally, the effects of GppNHp, a non-hydrolysable GTP analogue, were investigated on the binding of the three radioligands at both  $ss_2$  and  $ss_5$  receptors. GppNHp displaced all three radioligands to the same extent (85 %) and similar apparent potency at  $ss_2$  receptors (figure 5), whereas again the effects on  $ss_5$  receptors were radioligand dependent.

Thus, the binding of [ $^{125}$ I][Tyr $^3$ ]octreotide was similarly displaced at sst $_2$  and sst $_5$  receptors, whereas [ $^{125}$ I]CGP 23996 and particularly [ $^{125}$ I]LTT-SRIF $_{28}$  binding were less sensitive to the guanine nucleotide analogue.

**Figure 3:** Competitive displacement by SRIF $_{28}$  and BIM 23056 of radioligand binding at human sst $_5$  receptors.



Crude membrane preparations from human sst $_5$  transfected cells (2  $\mu$ g per assay) were incubated with [ $^{125}$ I][Tyr $^3$ ]octreotide and 12 concentrations of SRIF $_{28}$  (■) or BIM 23056 (●). Data are expressed as percentage of specific binding. The figure shows one representative example of at least 3 different experiments.

### 4.3. Discussion

Octreotide (SMS 201-995, Sandostatin®) is currently used for treatment of acromegaly, various gastro-intestinal disorders and cancer in the gastroenteropancreatic system. In addition, since a number of tumours respond to octreotide treatment, a radiolabelled analogue (octreoscan, Pentetreotide®) is used to visualise SRIF receptor bearing tumours. Octreotide was instrumental in the definition of SRIF receptor subtypes, when Reubi and colleagues (Reubi, 1984; 1985; Reubi and Maurer, 1986) were able to differentiate octreotide-sensitive SRIF binding sites from those which are not sensitive to octreotide, the former were called SS-1 and the latter SS-2. Other ligands were used, such as [ $^{125}$ I]MK 678 and [ $^{125}$ I]CGP 23996 which according to Reisine and colleagues were labelling what was called SRIF-1 and SRIF-2 sites (Raynor et al., 1992) and a number of SRIF $_{14}$  and SRIF $_{28}$  radiolabelled analogues.



**Table 2:** Results of saturation experiments performed with different radioligands at human  $sst_2$  and  $sst_5$  receptors expressed in CCL39 cells

radioligand	$sst_2$ receptors		$sst_5$ receptors	
	$B_{max}$	$pK_d$	$B_{max}$	$pK_d$
$[^{125}I][Tyr^3]octreotide$	$210 \pm 10$	$9.89 \pm 0.02$	$920 \pm 170$	$9.64 \pm 0.04$
$[^{125}I]CGP\ 23996$	$180 \pm 20$	$9.76 \pm 0.06$	$3530 \pm 50$	$9.52 \pm 0.08$
$[^{125}I]LTT-SRIF_{28}$	$370 \pm 60$	$9.89 \pm 0.04$	$6950 \pm 220$	$10.48 \pm 0.04$

The data are expressed as  $B_{max}$  (fmol/ mg) and  $pK_d$ -values ( $-\log \text{ mol/ l}$ )  $\pm$  SEM of at least three experiments. The data represent the mean of  $pK_d$ -values ( $-\log M$ )  $\pm$  standard error of at least three determinations.

The situation became more complex in 1992 when five SRIF receptor were cloned, but at least it was then convincingly demonstrated that SRIF receptor subtypes exist (see Bell and Reisine, 1993; Hoyer et al., 1995a). It was then established that SRIF analogues e.g.  $[^{125}I][Tyr^{11}]SRIF_{14}$  or  $[^{125}I]LTT-SRIF_{28}$  labelled all subtypes. More surprisingly, it was found that  $[^{125}I]CGP\ 23996$  also labelled all receptor subtypes (Raynor et al., 1993a, 1993b). By contrast it seemed that  $[^{125}I]MK\ 678$  or  $[^{125}I][Tyr^3]octreotide$  would only label the currently designated  $sst_2$  receptor (Kluxen et al., 1992; Raynor et al., 1993a). We have investigated that matter further (Schoeffter et al., 1995) and shown that in rat brain and recombinant cells the populations of sites labelled with these two ligands were 1) superimposable with respect to distribution, 2) had close to identical pharmacological profiles in native tissue (e.g. rat brain or human brain, Piwko et al., 1997), 3) that this profile was identical with that of the recombinant  $sst_2$  receptor and 4) that the distribution of sites labelled in the rat or human brain was comparable to that of  $sst_2$  receptor mRNA. Therefore, it was felt adequate to conclude that  $[^{125}I][Tyr^3]octreotide$  and  $[^{125}I]MK\ 678$  labelled sites represent  $sst_2$  receptors.

**Table 3:** Comparison of affinities of SRIF and various SRIF-analogues for human sst<sub>2</sub> receptors labelled with [<sup>125</sup>I][Tyr<sup>3</sup>]octreotide and other radioligands

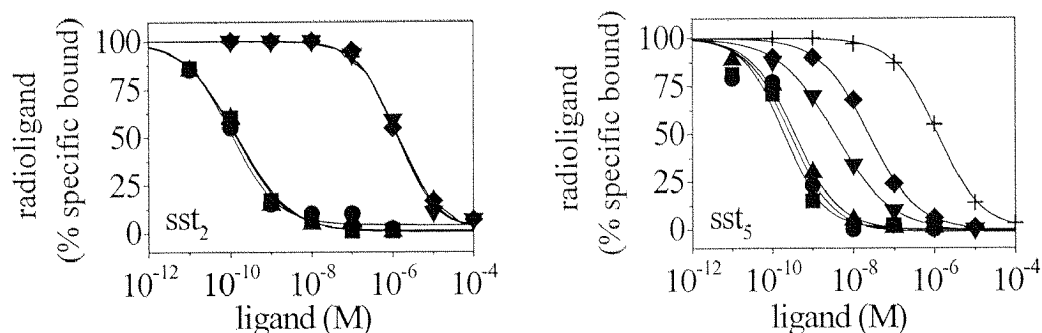
radioligand or tissue	[ <sup>125</sup> I][Tyr <sup>3</sup> ]-octreotide	[ <sup>125</sup> I]LTT-SRIF <sub>28</sub>	[ <sup>125</sup> I]CGP 23996	human cortex	CHO cells hsst <sub>2</sub>
SRIF <sub>14</sub>	10.01 ± 0.04	10.00 ± 0.01	10.10 ± 0.12	10.12	10.50
SRIF <sub>28</sub>	9.99 ± 0.08	9.92 ± 0.03	9.99 ± 0.14	9.66	10.29
seglitide	9.81 ± 0.13	9.96 ± 0.02	9.82 ± 0.07	10.08	10.64
BIM 23014	9.55 ± 0.03	9.27 ± 0.06	9.43 ± 0.09	8.86	9.67
RC160	9.50 ± 0.16	9.35 ± 0.09	9.56 ± 0.06	8.85	10.23
octreotide	9.10 ± 0.07	9.19 ± 0.03	9.16 ± 0.23	8.57	9.90
CGP 23996	8.95 ± 0.07	8.58 ± 0.07	9.06 ± 0.05	8.78	9.62
L362,855	8.79 ± 0.06	8.36 ± 0.05	8.69 ± 0.24	-	-
BIM 23052	8.55 ± 0.01	8.30 ± 0.14	8.76 ± 0.46	7.78	8.73
L361,301	8.39 ± 0.08	8.39 ± 0.11	8.28 ± 0.61	8.32	9.27
cortistatin <sub>14</sub>	8.35 ± 0.11	8.75 ± 0.20	9.04 ± 0.08	-	-
BIM 23030	7.94 ± 0.22	7.77 ± 0.07	7.88 ± 0.03	8.14	9.14
BIM 23056	6.38 ± 0.11	6.33 ± 0.10	6.33 ± 0.14	6.14	6.65
cycloantagonist SA	5.77 ± 0.05	5.40 ± 0.06	5.80 ± 0.17	5.43	5.90

Human cortex and CHO cell data are from Piwko et al. (1997). The data represent the mean of pK<sub>D</sub>-values (-log M) ± standard error of at least three determinations.

On the other hand, we have established that under specific salt conditions (120 mM NaCl) the binding sites labelled with [ $^{125}$ I][Tyr $^{11}$ ]SRIF $_{14}$  in rat cortex (Hoyer et al., 1995b) had a pharmacological profile that could not be distinguished from that of recombinantly expressed sst $_1$  receptors (although the sst $_4$  profile is very close). Thus, one could assume that the so called SS-2 sites of Reubi (1984;1985) corresponded to sst $_1$  receptors, although in the lung, sst $_4$  receptor show a similar profile (Schloos et al., 1997). However, a number of findings are disturbing: there is indeed great variation in the data reported by different groups (Raynor et al., 1993a, 1993b; Bruns et al., 1994; Patel and Srikant, 1994) on the pharmacological profile of the different receptors, as illustrated at the Ciba Foundation meeting (see Patel et al., 1995; Bruns et al., 1995 and the discussions therein). For instance, it has been reported that [ $^{125}$ I]CGP 23996 (Czernik & Petrack, 1983) was labelling so called SRIF-2 sites with profiles and distribution different from SRIF-1 sites (Raynor and Reisine, 1989; Raynor et al., 1992b; 1993a; Martin et al., 1991), whereas Epelbaum et al. (1985) had noticed that the pharmacology and distribution of the sites labelled with [ $^{125}$ I]CGP 23996 was very similar to that of sites labelled with [ $^{125}$ I][D-Trp $^8$ ]SRIF $_{14}$  and this is fully justified since [ $^{125}$ I]CGP 23996 was found later to label all five cloned SRIF receptors.

The present paper shows clearly that [ $^{125}$ I][Tyr $^3$ ]octreotide labels recombinant human sst $_5$  receptors with high affinity, although the radioligand was thought to label exclusively sst $_2$  receptors (Hoyer et al., 1994b; Piwko et al., 1997; Schoeffter et al., 1995). The pharmacological profile of [ $^{125}$ I][Tyr $^3$ ]octreotide labelled human sst $_2$  receptors is very similar in transfected CCL39 and CHO cells and native tissue, i.e. human cerebral cortex. On the other hand, [ $^{125}$ I][Tyr $^3$ ]octreotide-labelled human sst $_5$  sites bound SRIF $_{28}$  preferentially compared to SRIF $_{14}$ , and somewhat surprisingly, showed very high affinity for the SRIF-analogues octreotide, seglitide, RC160, BIM 23014, BIM 23052 and BIM 23056. Due to these “atypical” features, the pharmacological profiles of sst $_2$  and sst $_5$  receptors expressed in CCL39 cells were further investigated by using [ $^{125}$ I]LTT-SRIF $_{28}$  and [ $^{125}$ I]CGP 23996.

**Figure 4:** Binding of [ $^{125}$ I][Tyr $^3$ ]octreotide, [ $^{125}$ I]CGP 23996 and [ $^{125}$ I]LTT-SRIF $_{28}$  at sst $_2$  and sst $_5$  receptors is differently affected by SRIF $_{14}$  and the cycloantagonist SA.



Crude membrane preparations from sst $_2$  and sst $_5$  transfected cells (6  $\mu$ g or 2  $\mu$ g per assay, respectively) were incubated with [ $^{125}$ I][Tyr $^3$ ]octreotide or [ $^{125}$ I]CGP 23996 or [ $^{125}$ I]LTT-SRIF $_{28}$  and the indicated concentrations of SRIF $_{14}$  (■, ●, and ▲ for each radioligand, respectively), and cycloantagonist SA (▼, ◆, and +, respectively). Data are expressed as percentage of specific binding. The figure is representative of at least 3 different experiments.

There were differences in  $B_{\max}$ -values (see table 2): at sst $_2$  receptors, [ $^{125}$ I][Tyr $^3$ ]octreotide, [ $^{125}$ I]CGP 23996 and [ $^{125}$ I]LTT-SRIF $_{28}$  labelled about the same number of sites (180- 370 fmol/ mg); by contrast, the differences were particularly marked at sst $_5$  receptors, where [ $^{125}$ I][Tyr $^3$ ]octreotide labelled 920 fmol/ mg, [ $^{125}$ I]CGP 23996 recognised 3530 fmol/ mg and [ $^{125}$ I]LTT-SRIF $_{28}$  6950 fmol/ mg, i.e. seven fold a higher value than [ $^{125}$ I][Tyr $^3$ ]octreotide. Obviously, such discrepancies have already been reported for peptide receptors e.g. Neurokinin NK1 or opiate receptors (see Hjorth et al., 1996; Schwartz et al., 1996), but were mainly related to the actual nature of the radioligands used, i.e. agonists versus antagonists. Such a point can however, not be made here, since the three radioligands and the non-labelled peptides used behave essentially as agonists (with the limitation that none of the actual radioligands exists as cold iodinated form) when assayed in second messenger tests (inhibition of cAMP production). It is commonly assumed that agonists label a high affinity state of the receptor whereas antagonists label all receptors (high and low affinity states), although it can be debated whether two affinity states exists or whether the receptor-ligand-G protein complex exist under multiple forms.

In the present case, we have evaluated the effects of GppNHp on the binding of all three radioligands. GppNHp reduced the binding to  $sst_2$  receptors to the same extent as would be expected, since all three ligands define binding sites with similar profile and similar receptor density. Similarly, the binding of [ $^{125}$ I][Tyr<sup>3</sup>]-octreotide to  $sst_5$  receptors was highly sensitive to GppNHp, whereas that of [ $^{125}$ I]CGP 23996 was less affected, and [ $^{125}$ I]LTT-SRIF<sub>28</sub> binding only weakly inhibited by GppNHp. The data are consistent with [ $^{125}$ I][Tyr<sup>3</sup>]-octreotide labelling only a minor part of the  $sst_5$  receptor population which shows high affinity for many of the agonists tested and is almost entirely inhibited by GppNHp. [ $^{125}$ I]CGP 23996 labels significantly more sites, which show intermediate affinity for the synthetic ligands and is only partly affected by GppNHp. By contrast, [ $^{125}$ I]LTT-SRIF<sub>28</sub> labels a very large number of receptors (6950 fmol/ mg compared to 920 fmol/ mg for [ $^{125}$ I][Tyr<sup>3</sup>]-octreotide); but this binding is only little affected by GppNHp and shows low affinity for most of the synthetic analogues of SRIF. Yet, the sites labelled by all three ligands have high affinity for the endogenous peptides (SRIF and cortistatin, see tables and figure 4).

This kind of behaviour is very common for “antagonist” ligands (see Teitler et al., 1990), much less so for agonists binding. However, whereas the binding of [ $^{125}$ I] pancreatic peptide (PP) to NPY<sub>4</sub> receptors (Walker et al., 1997) is very sensitive to GppNHp, the binding of [ $^{125}$ I]peptide YY (PYY) is not affected by the guanine nucleotide; PP and PYY are considered as the endogenous agonists. Similarly to the present case, [ $^{125}$ I]PYY represented only a very minor fraction of the sites labelled by [ $^{125}$ I]PP at NPY<sub>4</sub> receptors (Walker et al., 1997). Obviously, one could invoke other reasons to explain apparent differences in  $B_{max}$ -values in cells expressing homogeneous populations of recombinant G-protein receptors such as receptor dimerisation which could be differently affected by agonists as is suggested for dopamine D<sub>2</sub>,  $\beta_2$  adrenoceptors or metabotropic glutamate type 5 receptors (see Hebert et al., 1996; Romano et al., 1996), but there is as yet no positive evidence for such behaviour with SRIF receptors.

**Table 4:** Comparison of affinities of SRIF and various SRIF-analogues for human  $sst_5$  receptors labelled with [ $^{125}$ I][Tyr $^3$ ]octreotide and other radioligands

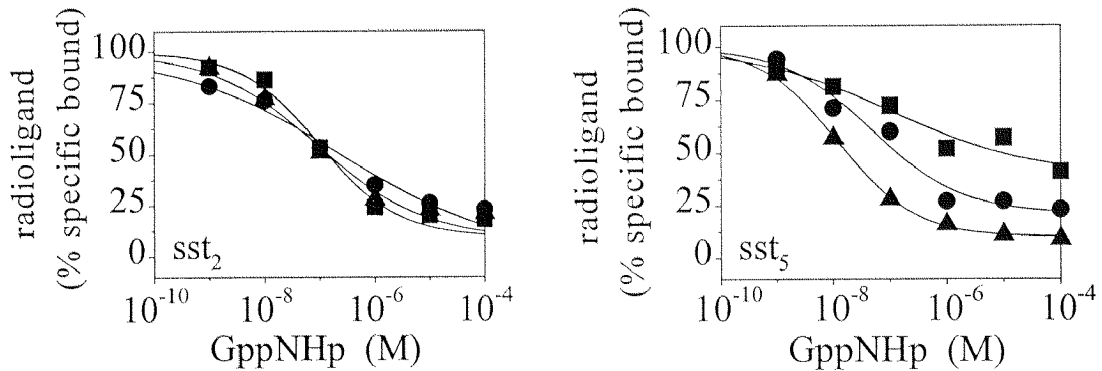
radioligand	[ $^{125}$ I][Tyr $^3$ ] octreotide	[ $^{125}$ I]LTT- SRIF $_{28}$	[ $^{125}$ I]CGP 23996
SRIF $_{28}$	10.30 $\pm$ 0.25	9.39 $\pm$ 0.22	10.15 $\pm$ 0.23
seglitide	10.18 $\pm$ 0.22	8.70 $\pm$ 0.26	10.22 $\pm$ 0.35
SRIF $_{14}$	9.87 $\pm$ 0.24	9.53 $\pm$ 0.13	9.82 $\pm$ 0.19
[Tyr $^{10}$ ]cortistatin	9.65 $\pm$ 0.22	8.67 $\pm$ 0.24	9.77 $\pm$ 0.24
[Leu $^8$ ,D-Trp $^{22}$ ,Tyr $^{25}$ ]SRIF $_{28}$	9.60 $\pm$ 0.02	8.47 $\pm$ 0.02	9.70 $\pm$ 0.21
L361,301	9.51 $\pm$ 0.14	7.69 $\pm$ 0.13	8.77 $\pm$ 0.09
octreotide	9.48 $\pm$ 0.11	7.17 $\pm$ 0.30	8.96 $\pm$ 0.10
cortistatin $_{14}$	9.34 $\pm$ 0.23	8.71 $\pm$ 0.02	9.24 $\pm$ 0.07
BIM 23014	9.31 $\pm$ 0.10	7.76 $\pm$ 0.13	9.07 $\pm$ 0.04
BIM 23052	9.28 $\pm$ 0.35	7.92 $\pm$ 0.19	9.59 $\pm$ 0.14
L362,855	9.17 $\pm$ 0.10	7.17 $\pm$ 0.30	8.72 $\pm$ 0.04
RC160	9.13 $\pm$ 0.35	7.51 $\pm$ 0.06	8.72 $\pm$ 0.25
CGP 23996	8.68 $\pm$ 0.20	6.59 $\pm$ 0.41	8.26 $\pm$ 0.08
[Tyr $^3$ ]octreotide	8.41 $\pm$ 0.06	6.49 $\pm$ 0.01	8.03 $\pm$ 0.05
BIM 23056	8.32 $\pm$ 0.17	7.17 $\pm$ 0.05	7.77 $\pm$ 0.09
cycloantagonist SA	8.25 $\pm$ 0.17	6.38 $\pm$ 0.23	7.77 $\pm$ 0.06
BIM 23030	7.45 $\pm$ 0.18	6.02 $\pm$ 0.09	7.09 $\pm$ 0.05

The data represent the mean of  $pK_D$ -values ( $-\log M$ )  $\pm$  standard error of at least three determinations.

As can be taken from table 3, the use of different radioligands has apparently little influence on the affinity of the tested compounds at  $hsst_2$  receptors. Indeed, the correlation coefficients of the profiles defined with the three radioligands are very high:  $r^2 = 0.972-0.975$ , and the individual values almost identical. In addition, the data are very comparable to those reported previously with the  $hsst_2$  receptors expressed in CHO cells and native receptors of human cerebral cortex ( $r^2 = 0.939- 0.947$ , see Piwko et al., 1997). By contrast, the profile determined for human  $sst_5$  receptors appeared to be rather radioligand-dependent (table 4). Thus, whereas the affinity values determined using [ $^{125}I$ ]CGP 23996 or [ $^{125}I$ ][Tyr<sup>3</sup>]octreotide were similar, affinity values determined using [ $^{125}I$ ]LTT-SRIF<sub>28</sub> were clearly lower for some compounds: octreotide, seglitide, L363,301, BIM 23014, BIM 23030, BIM 23052, BIM 23056, CGP 23996, L362,855, RC160, [Tyr<sup>3</sup>]octreotide and cycloantagonist (SA) showed up to 100 fold lower affinities. These affinity values were so markedly low that one would not expect [Tyr<sup>3</sup>]octreotide or CGP 23996 to label the human  $sst_5$  receptors at the low concentrations used here (between 25 and 30 pM, whereas the affinity for the non labelled compounds are about 1000 fold lower). The correlation coefficient obtained when comparing the three  $sst_5$  binding profiles were respectively 0.773, 0.833 and 0.922, lower than observed at  $sst_2$  receptors. On the other hand, the putative endogenous peptides SRIF<sub>14/28</sub> and cortistatin were little affected by the use of different radioligands since the differences in affinity values were about 2, 4 and 8 fold to the most between the extreme values.

Based on the present results, it would appear that the pharmacological profiles of some G-protein coupled receptors may be radioligand-dependent. The surprising findings are that in two similar situations (i.e.  $sst_2$  and  $sst_5$  receptors expressed in the same CCL39 cells), the results can be so different. Probably, the various agonists are able to induce different kinds of receptor conformations, although this does not apply to every receptor within one family.

**Figure 5:** Binding of [ $^{125}$ I][Tyr $^3$ ]octreotide, [ $^{125}$ I]CGP 23996 and [ $^{125}$ I]LTT-SRIF $_{28}$  at sst $_2$  and sst $_5$  receptors is differently affected by the stable guanine nucleotide GppNHp.



Crude membrane preparations from sst $_2$  and sst $_5$  transfected cells (6  $\mu$ g or 2  $\mu$ g per assay, respectively) were incubated with [ $^{125}$ I][Tyr $^3$ ]octreotide ( $\blacktriangle$ ), [ $^{125}$ I]CGP 23996 ( $\bullet$ ) or [ $^{125}$ I]LTT-SRIF $_{28}$  ( $\blacksquare$ ) and the indicated concentrations of GppNHp at sst $_2$  receptors (top) and sst $_5$  receptors (bottom). Data are expressed as percentage of specific binding. One representative example of at least 3 independent experiments.

Post-transcriptional and post-translational modifications, such as protein phosphorylation or glycosylation, may be cell type-specific and as such may affect receptor conformation and influence the binding properties. Coupling to different G-protein isoforms, which may show different expression pattern depending on the cells, could also be implicated in receptor binding properties (Lefkowitz et al., 1993). In any case, the labelling by [ $^{125}$ I][Tyr $^3$ ]octreotide with similar affinity of human sst $_2$  and sst $_5$  receptors and the very high affinity of small cyclic peptides for the sst $_5$  receptor suggests that in addition to sst $_2$  receptors, sst $_5$  receptors could be responsible for mediating a number of effects of short SRIF analogues which may have been assigned primarily to sst $_2$  receptors. Similarly, in vivo labelling by octreotide analogues may represent both sst $_2$  and sst $_5$  receptor sites. Finally, from the present data, it is not all too surprising to see differences in affinity reported by different groups at the same recombinant receptor and data obtained by different investigators may not be immediately comparable.



## 5.1. Abstract

Human somatostatin receptor subtypes 1-5 ( $ss_{1-5}$ ) were characterised using the agonist radioligands [ $^{125}$ I]LTT-SRIF<sub>28</sub>, [ $^{125}$ I][Tyr<sup>10</sup>]CST<sub>14</sub>, [ $^{125}$ I]CGP 23996 and [ $^{125}$ I][Tyr<sup>3</sup>]octreotide in stably transfected CCL39 Chinese hamster lung fibroblast cells. The radioligands used labelled saturable and high affinity populations of sites in each instance; at  $ss_{1-4}$  receptors  $B_{max}$ -values were roughly equivalent. By contrast, at  $ss_5$  receptors  $B_{max}$ -values determined with [ $^{125}$ I]CGP 23996 and [ $^{125}$ I][Tyr<sup>3</sup>]octreotide were significantly lower (two and eight fold) compared to [ $^{125}$ I]LTT-SRIF<sub>28</sub> and [ $^{125}$ I][Tyr<sup>10</sup>]CST<sub>14</sub>.

Experiments were performed with the stable GTP-analogue guanylylimidodiphosphate (GppNHp) to establish guanine nucleotide sensitivity of agonist binding to  $ss_{1-5}$  receptors. The sensitivity towards GppNHp was quite variable depending on receptor and/or ligand. At  $ss_1$  and  $ss_4$  receptors, GppNHp produced little effect overall, whereas binding to  $ss_3$  and  $ss_2$  receptors was reduced by 70 and > 80 %, respectively. At  $ss_5$  receptors, the binding of [ $^{125}$ I]LTT-SRIF<sub>28</sub> and [ $^{125}$ I][Tyr<sup>10</sup>]CST<sub>14</sub> was only slightly affected by GppNHp, while [ $^{125}$ I]CGP 23996 and [ $^{125}$ I][Tyr<sup>3</sup>]octreotide binding was almost entirely inhibited. Thus, [ $^{125}$ I][Tyr<sup>3</sup>]octreotide labelled about 26-fold less  $ss_5$  receptors than [ $^{125}$ I]LTT-SRIF<sub>28</sub>, in the presence of 10  $\mu$ M GppNHp. These discrepancies in guanine nucleotide sensitivity, were confirmed in GppNHp competition experiments.

Competition studies were performed at the five receptors labelled with the different radioligands to establish their respective pharmacological profiles: the rank order of affinity was largely radioligand-independent at  $ss_{1-4}$  receptors, in contrast to  $ss_5$  receptors, where it was radioligand-dependent. Thus, the pharmacological profile of [ $^{125}$ I][Tyr<sup>10</sup>]CST<sub>14</sub>- and [ $^{125}$ I]CGP23996-labelled  $ss_5$  sites correlated highly significantly, but did not correlate with the affinity profiles defined with [ $^{125}$ I]CGP 23996 and [ $^{125}$ I][Tyr<sup>3</sup>]octreotide binding to  $ss_5$  receptors.

Depending on the agonist radioligand used and the receptor studied, it would appear that binding can be essentially to a guanine nucleotide sensitive state (e.g.  $ss_2$  or  $ss_3$ ), a guanine nucleotide insensitive state ( $ss_1$  or  $ss_4$ ) or a mixture of both ( $ss_5$ ); in the latter case, each radioligand defining a more or less different rank order of affinity at the same receptor.

In summary, the differences in agonist receptor binding and guanine nucleotide sensitivity cannot be explained by the ternary complex model or its variations, but rather suggest the existence of multiple agonist-specific receptor states, which vary from one receptor to another.

## 5.2. Results

### Saturation experiments

$[^{125}\text{I}]\text{LTT-SRIF}_{28}$ ,  $[^{125}\text{I}][\text{Tyr}^{10}]\text{CST}_{14}$  and  $[^{125}\text{I}]\text{CGP 23996}$  labelled human  $ss_{1-5}$  receptors in CCL39 cells with high affinity and in a saturable manner (see figure 1 and table 1); non-specific binding was low for each radioligand. No specific binding was found for any of the radioligands used here in non-transfected cells; RT-PCR confirmed the expression of the respective SRIF receptor subtypes in the stably transfected CCL39 cells, and the absence of expression in the non-transfected cells (data not shown).  $[^{125}\text{I}][\text{Tyr}^3]\text{octreotide}$  labelled  $ss_2$  and  $ss_5$  receptors with high affinity, whereas the low affinity of the radioligand for  $ss_3$  receptors precluded any further binding studies;  $ss_1$  and  $ss_4$  receptors could not be labelled with  $[^{125}\text{I}][\text{Tyr}^3]\text{octreotide}$  (data not shown). Saturation curves suggested the labelling of a single population of receptor binding sites.

Receptor densities ( $B_{\max}$ -values) obtained with [ $^{125}$ I]LTT-SRIF<sub>28</sub>, [ $^{125}$ I][Tyr<sup>10</sup>]CST<sub>14</sub>, [ $^{125}$ I]CGP 23996 (and [ $^{125}$ I][Tyr<sup>3</sup>]octreotide) were similar at sst<sub>1-4</sub> receptors (see table 1), but rather divergent at human sst<sub>5</sub> receptors ( $pK_d = 10.48 \pm 0.04$ ,  $10.33 \pm 0.03$ ,  $9.52 \pm 0.08$  and  $9.64 \pm 0.04$ , respectively;  $B_{\max} = 6950 \pm 220$ ,  $5630 \pm 330$ ,  $3530 \pm 50$  and  $920 \pm 170$  fmol/mg protein, respectively). Thus, [ $^{125}$ I][Tyr<sup>3</sup>]octreotide labelled almost 8-fold less sst<sub>5</sub> receptor sites than [ $^{125}$ I]LTT-SRIF<sub>28</sub>, whereas at sst<sub>2</sub> receptors [ $^{125}$ I][Tyr<sup>3</sup>]octreotide and the other radioligands labelled similar densities (see table 1). Similarly, there were no profound differences in  $B_{\max}$ -values at either sst<sub>1</sub> or sst<sub>3</sub> receptors, although there is tendency for [ $^{125}$ I]LTT-SRIF<sub>28</sub> to label more sites than for example [ $^{125}$ I]CGP 23996.

### Effects of GppNHp

To examine, whether differences in receptor densities - especially at sst<sub>5</sub> receptors - may be explained by the radioligands labelling different affinity states of the receptor, the effects of the non-hydrolysable GTP-analogue GppNHp on radioligand binding were investigated. First, saturation experiments were performed with the different radioligands in the presence of 10  $\mu$ M GppNHp (table 1). The affinities of the four radioligands at sst<sub>1-5</sub> receptors were very similar whether saturation experiments were performed with or without GppNHp. At sst<sub>4</sub> receptors, GppNHp produced no significant changes in  $B_{\max}$ -values for any of the radioligands. At sst<sub>1-3</sub> receptors, the effects of GppNHp on  $B_{\max}$ -values were limited to a 2-fold decrease if at all. At sst<sub>5</sub> receptors  $B_{\max}$ -values determined with [ $^{125}$ I]LTT-SRIF<sub>28</sub> and [ $^{125}$ I][Tyr<sup>10</sup>]CST<sub>14</sub> were not affected by GppNHp; in marked contrast,  $B_{\max}$ -values defined by [ $^{125}$ I]CGP 23996 and [ $^{125}$ I][Tyr<sup>3</sup>]octreotide were 3-4 fold lower in the presence compared to the absence of GppNHp (figure 1 and table 1). In other words, in the presence of GppNHp, [ $^{125}$ I][Tyr<sup>3</sup>]octreotide labelled about 24- 26 fold less sst<sub>5</sub> receptor sites ( $B_{\max} = 270 \pm 90$  fmol/mg) compared to [ $^{125}$ I]LTT-SRIF<sub>28</sub> and [ $^{125}$ I][Tyr<sup>10</sup>]CST<sub>14</sub> ( $B_{\max} = 6560 \pm 560$  and  $6960 \pm 760$ , respectively) (table 1). Similarly, [ $^{125}$ I]CGP 23996 labelled about 7 times less sst<sub>5</sub> receptor sites than the latter two radioligands.

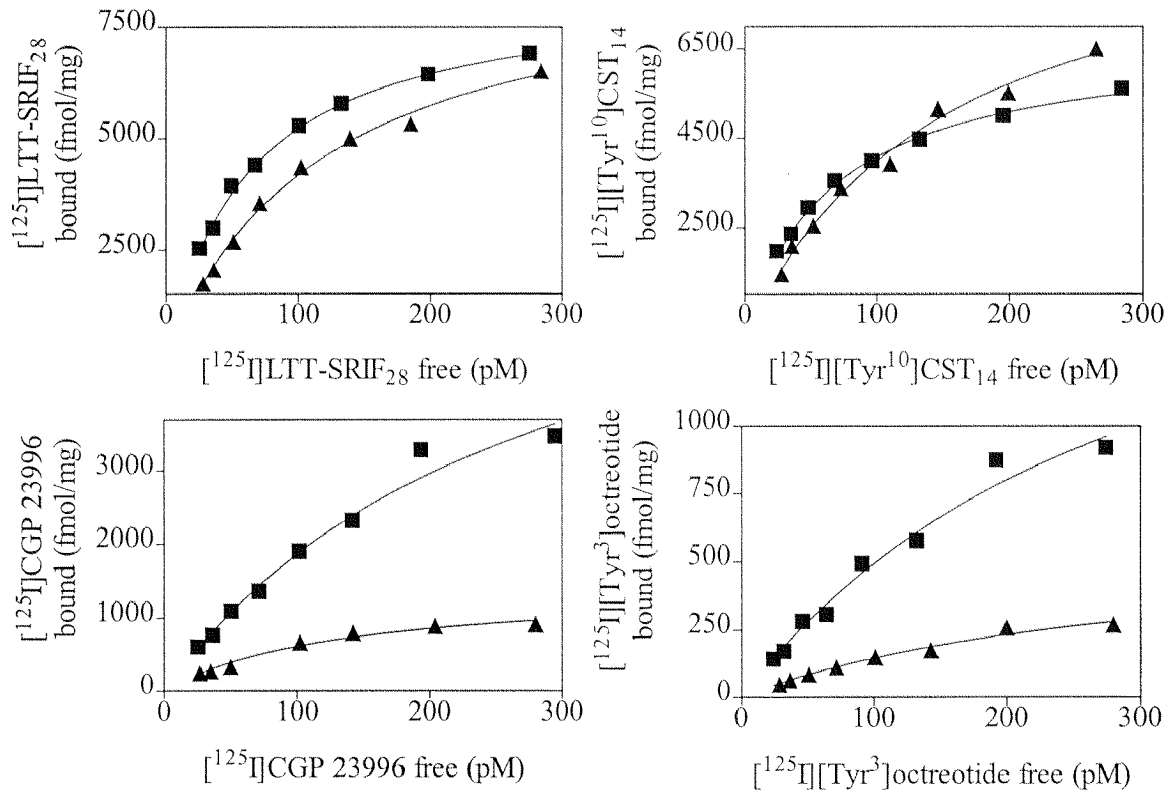
**Table 1:** Comparison of saturation experiments in the absence or the presence of GppNHp ( $10^{-5}$  M) using [ $^{125}$ I]LTT-SRIF<sub>28</sub>, [ $^{125}$ I][Tyr<sup>10</sup>]CST<sub>14</sub>, [ $^{125}$ I]CGP 23996 and [ $^{125}$ I][Tyr<sup>3</sup>]octreotide at human sst<sub>1-5</sub> receptors

	[ $^{125}$ I]LTT-SRIF <sub>28</sub>		[ $^{125}$ I][Tyr <sup>10</sup> ]CST <sub>14</sub>		[ $^{125}$ I]CGP 23996		[ $^{125}$ I][Tyr <sup>3</sup> ]octreotide	
	pK <sub>d</sub>	B <sub>max</sub> [fmol/mg]	pK <sub>d</sub>	B <sub>max</sub> [fmol/mg]	pK <sub>d</sub>	B <sub>max</sub> [fmol/mg]	pK <sub>d</sub>	B <sub>max</sub> [fmol/mg]
hsst <sub>1</sub>	9.96 ± 0.00	470 ± 30	10.02 ± 0.04	220 ± 30	9.63 ± 0.09	260 ± 30	-	-
hsst <sub>1</sub> + GppNHp	10.15 ± 0.09	200 ± 20	9.75 ± 0.13	320 ± 50	9.33 ± 0.13	310 ± 60	-	-
hsst <sub>2</sub>	9.89 ± 0.04	370 ± 60	9.45 ± 0.09	340 ± 70	9.76 ± 0.06	180 ± 20	9.89 ± 0.02	210 ± 10
hsst <sub>2</sub> + GppNHp	10.21 ± 0.06	160 ± 20	9.93 ± 0.13	140 ± 30	9.53 ± 0.13	130 ± 10	9.93 ± 0.23	170 ± 40
hsst <sub>3</sub>	10.28 ± 0.06	560 ± 60	10.06 ± 0.11	340 ± 50	9.76 ± 0.05	270 ± 40	-	-
hsst <sub>3</sub> + GppNHp	10.41 ± 0.06	220 ± 20	9.68 ± 0.08	360 ± 70	9.54 ± 0.06	110 ± 10	-	-
hsst <sub>4</sub>	9.64 ± 0.03	440 ± 50	9.67 ± 0.14	340 ± 110	9.35 ± 0.03	690 ± 50	-	-
hsst <sub>4</sub> + GppNHp	9.51 ± 0.03	520 ± 20	9.62 ± 0.08	450 ± 60	9.56 ± 0.07	790 ± 100	-	-
hsst <sub>5</sub>	10.48 ± 0.04	6950 ± 220	10.33 ± 0.03	5630 ± 330	9.52 ± 0.08	3530 ± 50	9.64 ± 0.04	920 ± 170
hsst <sub>5</sub> + GppNHp	10.18 ± 0.11	6560 ± 560	10.48 ± 0.14	6960 ± 760	9.82 ± 0.08	930 ± 270	9.80 ± 0.25	270 ± 90

The data are expressed as the mean of pK<sub>d</sub>-values (-log M) or B<sub>max</sub>-values ± SEM of 3 different experiments.

In a second series of experiments, a range of increasing GppNHp concentrations were used to inhibit the binding of the radioligands to human sst<sub>1-5</sub> receptors (table 2; figure 2). Overall, at sst<sub>1</sub> and especially sst<sub>4</sub> receptors, radioligand binding was relatively little affected by GppNHp (see figure 2, table 2). At sst<sub>3</sub> and especially sst<sub>2</sub> receptors (E<sub>max</sub>-values = 82- 89 %, pEC<sub>50</sub>'s = 6.76- 7.32), the effects were rather similar independently of the radioligand tested.

**Figure 1:** Guanine nucleotide sensitivity of [ $^{125}$ I]LTT-SRIF<sub>28</sub>, [ $^{125}$ I][Tyr<sup>10</sup>]CST<sub>14</sub>, [ $^{125}$ I]CGP 23996 or [ $^{125}$ I][Tyr<sup>3</sup>]octreotide binding to membranes prepared from CCL39 cells stably expressing sst<sub>5</sub> receptors.



Crude membrane preparations (2  $\mu$ g per assay) were incubated with increasing concentrations of the radioligand in the absence (■) or presence (▲) of GppNHp (10<sup>-5</sup> M; final concentration), and assayed for receptor binding. The plots depict specific binding expressed as amount of radioligand bound (fmol/mg) versus free radioligand concentration (pM). The figures show one representative example of three different experiments.

By contrast, at sst<sub>5</sub> receptors, whereas [ $^{125}$ I]LTT-SRIF<sub>28</sub> and [ $^{125}$ I][Tyr<sup>10</sup>]CST<sub>14</sub> binding was only moderately inhibited ( $E_{\max}$  = 47  $\pm$  6 % and 31  $\pm$  6 %, pEC<sub>50</sub> = 5.87  $\pm$  0.30 and 4.81  $\pm$  0.36, respectively), [ $^{125}$ I]CGP 23996 binding, and especially [ $^{125}$ I][Tyr<sup>3</sup>]octreotide binding were almost entirely blocked ( $E_{\max}$  = 76  $\pm$  1 % and 88  $\pm$  1 %, pEC<sub>50</sub> = 6.89  $\pm$  0.20 and 7.77  $\pm$  0.14 respectively) by GppNHp.

## Competition experiments

The pharmacological profiles of the five SRIF receptors were determined in classical competition assays. SRIF<sub>14</sub>, SRIF<sub>28</sub> and CST<sub>17</sub> and their analogues bound nanomolar affinity to hsst<sub>1-5</sub> receptors (pK<sub>d</sub>'s = 8.39 - 10.21) (tables 3(A)-(E); figure 4). The rank order of affinity at sst<sub>1</sub> sites was similar for all three radioligands: CST<sub>17</sub> ≥ SRIF<sub>28</sub> ≈ LTT-SRIF<sub>28</sub> ≈ SRIF<sub>14</sub> ≈ CST<sub>14</sub> > [Tyr<sup>10</sup>]CST<sub>14</sub> ≈ CGP 23996 ≈ BIM 23052 >> octreotide > seglitide. Also at sst<sub>4</sub> sites the affinity profiles were comparable for the three radioligands: CST<sub>17</sub> ≈ LTT-SRIF<sub>28</sub> ≥ SRIF<sub>28</sub> ≈ SRIF<sub>14</sub> ≈ CST<sub>14</sub> ≈ CGP 23996 > [Tyr<sup>10</sup>]CST<sub>14</sub> ≈ BIM 23052 >> octreotide > seglitide.

The SRIF<sub>1</sub> receptors revealed different types of behaviour, with affinity values almost identical whichever radioligand used at sst<sub>2</sub> receptors: SRIF<sub>28</sub> ≈ SRIF<sub>14</sub> ≈ seglitide ≈ LTT-SRIF<sub>28</sub> > RC160 ≈ BIM 23014 ≥ CST<sub>17</sub> ≈ octreotide > CST<sub>14</sub> ≈ [Tyr<sup>10</sup>]CST<sub>14</sub>. At sst<sub>3</sub> binding was also largely comparable although [<sup>125</sup>I]LTT-SRIF<sub>28</sub> labelled sites tended to show somewhat lower affinity for the synthetic analogues: SRIF<sub>28</sub> ≈ SRIF<sub>14</sub> ≈ LTT-SRIF<sub>28</sub> ≈ CST<sub>17</sub> ≥ BIM 23052 ≥ CST<sub>14</sub> ≈ [Tyr<sup>10</sup>]CST<sub>14</sub> ≈ CGP 23996 > octreotide > seglitide. At sst<sub>5</sub> sites, virtually every radioligand showed a separate profile; especially the two natural ligands defined very low affinity values for the synthetic peptides with CGP23996 and octreotide having only micromolar affinity, although their radioactive analogues labelled these sites with sub-nanomolar affinity: (a) [<sup>125</sup>I]LTT-SRIF<sub>28</sub> and [<sup>125</sup>I][Tyr<sup>10</sup>]CST<sub>14</sub>: CST<sub>17</sub> ≥ SRIF<sub>14</sub> ≈ SRIF<sub>28</sub> > seglitide ≈ LTT-SRIF<sub>28</sub> ≈ CST<sub>14</sub> ≈ [Tyr<sup>10</sup>]CST<sub>14</sub> >> BIM 23052 ≈ BIM 23014 > octreotide, (b) [<sup>125</sup>I]CGP 23996: SRIF<sub>28</sub> ≈ CST<sub>17</sub> ≈ seglitide > SRIF<sub>14</sub> ≈ LTT-SRIF<sub>28</sub> ≈ [Tyr<sup>10</sup>]CST<sub>14</sub> ≈ BIM 23052 > CST<sub>14</sub> > BIM 23014 ≈ octreotide, (c) [<sup>125</sup>I][Tyr<sup>3</sup>]octreotide: SRIF<sub>28</sub> ≈ seglitide ≥ SRIF<sub>14</sub> ≈ CST<sub>17</sub> > LTT-SRIF<sub>28</sub> ≈ [Tyr<sup>10</sup>]CST<sub>14</sub> > L363,301 ≈ octreotide ≈ CST<sub>14</sub> ≈ BIM 23052 ≈ BIM 23014.

**Table 2:** Effects of GppNHp (max.  $10^{-4}$  M) on [ $^{125}$ I]LTT-SRIF<sub>28</sub>, [ $^{125}$ I][Tyr<sup>10</sup>]CST<sub>14</sub>, [ $^{125}$ I]CGP 23996 and [ $^{125}$ I][Tyr<sup>3</sup>]octreotide binding to human sst<sub>1-5</sub> receptors: comparison of pEC<sub>50</sub>-values (-log M) or E<sub>max</sub>-values [% inhibition] ± SEM of three experiments

	[ $^{125}$ I]LTT-SRIF <sub>28</sub>		[ $^{125}$ I][Tyr <sup>10</sup> ]CST <sub>14</sub>		[ $^{125}$ I]CGP 23996		[ $^{125}$ I][Tyr <sup>3</sup> ]octreotide	
	E <sub>max</sub>	pEC <sub>50</sub>	E <sub>max</sub>	pEC <sub>50</sub>	E <sub>max</sub>	pEC <sub>50</sub>	E <sub>max</sub>	pEC <sub>50</sub>
CCL39/ hsst <sub>1</sub>	39 ± 0	6.67 ± 0.28	63 ± 3	6.62 ± 0.23	34 ± 4	6.24 ± 0.07	-	-
CCL39/ hsst <sub>2</sub>	82 ± 1	6.97 ± 0.05	83 ± 4	7.32 ± 0.16	82 ± 3	6.76 ± 0.10	89 ± 3	7.07 ± 0.17
CCL39/ hsst <sub>3</sub>	68 ± 3	6.91 ± 0.21	83 ± 1	7.74 ± 0.12	76 ± 6	7.64 ± 0.23	-	-
CCL39/ hsst <sub>4</sub>	44 ± 2	6.89 ± 0.08	36 ± 7	6.17 ± 0.04	8 ± 2	(-)	-	-
CCL39/ hsst <sub>5</sub>	47 ± 6	5.87 ± 0.30	31 ± 6	4.81 ± 0.36	76 ± 1	6.89 ± 0.20	88 ± 1	7.77 ± 0.14

At SRIF<sub>2</sub> - sst<sub>1</sub> and sst<sub>4</sub> - receptors all affinity profiles highly significantly correlated (correlation coefficients  $r = 0.926- 0.987$ ) (table 4). At SRIF<sub>1</sub> receptors, the situation was less clear cut. Interestingly, at human sst<sub>5</sub> receptors the affinity profiles of the pairs [ $^{125}$ I]LTT-SRIF<sub>28</sub> and [ $^{125}$ I][Tyr<sup>10</sup>]CST<sub>14</sub>, or [ $^{125}$ I]CGP 23996 and [ $^{125}$ I][Tyr<sup>3</sup>]octreotide correlated highly significantly ( $r = 0.942$  and  $0.916$ , respectively), whereas the pharmacological profiles of [ $^{125}$ I]CGP 23996 and [ $^{125}$ I][Tyr<sup>3</sup>]octreotide revealed lower correlations with those of the other two radioligands ( $r = 0.767- 0.898$ ).

### 5.3. Discussion

The purpose of this study was to compare agonist-receptor interactions at various human somatostatin receptors using classical radioligand binding studies.

**Table 3:** Comparison of the pharmacological profiles of human sst<sub>1-5</sub> receptors defined with [<sup>125</sup>I]LTT-SRIF<sub>28</sub>, [<sup>125</sup>I][Tyr<sup>10</sup>]CST<sub>14</sub>, [<sup>125</sup>I]CGP 23996 or [<sup>125</sup>I][Tyr<sup>3</sup>]octreotide. The affinity values are expressed as pK<sub>d</sub>-values (-log M) ± SEM of 3 determinations

**Table 3(A)** CCL39/hsst<sub>1</sub>

	[ <sup>125</sup> I]LTT-SRIF <sub>28</sub>	[ <sup>125</sup> I][Tyr <sup>10</sup> ]CST <sub>14</sub>	[ <sup>125</sup> I]CGP 23996
SRIF <sub>14</sub>	9.12 ± 0.05	9.08 ± 0.07	8.95 ± 0.11
SRIF <sub>28</sub>	9.22 ± 0.02	9.26 ± 0.07	9.38 ± 0.06
LTT-SRIF <sub>28</sub>	9.22 ± 0.11	9.28 ± 0.01	9.13 ± 0.13
CST <sub>17</sub>	9.61 ± 0.04	9.61 ± 0.17	9.48 ± 0.08
CST <sub>14</sub>	8.76 ± 0.06	7.74 ± 0.09	9.07 ± 0.29
[Tyr <sup>10</sup> ]CST <sub>14</sub>	8.56 ± 0.08	9.04 ± 0.13	8.32 ± 0.06
seglitide	4.50 ± 0.04	4.32 ± 0.06	4.87 ± 0.03
CGP 23996	8.33 ± 0.06	8.31 ± 0.04	8.45 ± 0.09
octreotide	6.65 ± 0.05	6.41 ± 0.04	6.23 ± 0.08
[Tyr <sup>3</sup> ]octreotide	5.57 ± 0.07	5.82 ± 0.10	5.69 ± 0.13
L362,855	6.25 ± 0.07	6.30 ± 0.07	6.08 ± 0.16
L363,301	5.32 ± 0.08	5.38 ± 0.15	5.66 ± 0.15
RC 160	7.08 ± 0.08	6.96 ± 0.24	6.65 ± 0.24
BIM 23030	5.06 ± 0.04	4.85 ± 0.02	5.17 ± 0.06
BIM 23014	6.75 ± 0.04	6.66 ± 0.18	6.41 ± 0.24
BIM 23056	6.61 ± 0.10	6.46 ± 0.07	6.56 ± 0.25
BIM 23052	8.37 ± 0.04	8.62 ± 0.05	8.17 ± 0.07
cycloantagonist SA	7.02 ± 0.00	6.80 ± 0.17	6.48 ± 0.25



**Table 3(B)** CCL39/hsst<sub>4</sub>

	[ <sup>125</sup> I]LTT-SRIF <sub>28</sub>	[ <sup>125</sup> I][Tyr <sup>10</sup> ]CST <sub>14</sub>	[ <sup>125</sup> I]CGP 23996
SRIF <sub>14</sub>	8.91 ± 0.15	8.39 ± 0.28	8.87 ± 0.08
SRIF <sub>28</sub>	9.08 ± 0.12	8.44 ± 0.30	9.06 ± 0.09
LTT-SRIF <sub>28</sub>	9.16 ± 0.01	9.13 ± 0.02	9.37 ± 0.20
CST <sub>17</sub>	9.24 ± 0.02	9.55 ± 0.30	9.26 ± 0.02
CST <sub>14</sub>	8.76 ± 0.02	8.75 ± 0.14	8.57 ± 0.03
[Tyr <sup>10</sup> ]CST <sub>14</sub>	8.44 ± 0.06	8.17 ± 0.09	8.30 ± 0.03
seglitide	5.37 ± 0.08	5.11 ± 0.07	5.04 ± 0.05
CGP 23996	8.77 ± 0.03	8.67 ± 0.14	8.62 ± 0.03
octreotide	6.40 ± 0.09	5.76 ± 0.08	6.02 ± 0.09
[Tyr <sup>3</sup> ]octreotide	6.29 ± 0.06	6.17 ± 0.08	5.89 ± 0.06
L362,855	7.31 ± 0.07	6.76 ± 0.32	7.08 ± 0.11
L363,301	5.61 ± 0.03	5.06 ± 0.06	5.64 ± 0.40
RC 160	7.25 ± 0.05	6.56 ± 0.44	6.97 ± 0.26
BIM 23030	5.98 ± 0.04	5.56 ± 0.14	5.53 ± 0.11
BIM 23014	6.64 ± 0.07	6.25 ± 0.28	6.52 ± 0.05
BIM 23056	7.17 ± 0.10	6.47 ± 0.35	7.04 ± 0.07
BIM 23052	8.63 ± 0.04	8.20 ± 0.11	8.13 ± 0.06
cycloantagonist SA	6.48 ± 0.13	6.07 ± 0.26	6.29 ± 0.07

The somatostatin field is notorious for rather strong disagreements about the degree of selectivity of various SRIF analogues for one or the other somatostatin receptor reported by some authors which could not be confirmed by others (see discussions in Chadwick et al, 1995, Bruns et al, 1995; Patel, 1997).

**Table 3(C)** CCL39/hsst<sub>2</sub>

	[ <sup>125</sup> I]LTT-SRIF <sub>28</sub>	[ <sup>125</sup> I][Tyr <sup>10</sup> ]CST <sub>14</sub>	[ <sup>125</sup> I]CGP 23996	[ <sup>125</sup> I][Tyr <sup>3</sup> ]octreotide
SRIF <sub>14</sub>	10.00 ± 0.01	10.06 ± 0.07	10.10 ± 0.12	10.01 ± 0.04
SRIF <sub>28</sub>	9.92 ± 0.03	10.16 ± 0.11	9.99 ± 0.14	9.99 ± 0.08
LTT-SRIF <sub>28</sub>	9.70 ± 0.25	8.90 ± 0.29	10.06 ± 0.07	9.17 ± 0.02
CST <sub>17</sub>	9.07 ± 0.01	9.29 ± 0.13	9.33 ± 0.15	8.85 ± 0.10
CST <sub>14</sub>	8.75 ± 0.20	8.54 ± 0.44	9.04 ± 0.08	8.35 ± 0.11
[Tyr <sup>10</sup> ]CST <sub>14</sub>	8.77 ± 0.09	8.91 ± 0.21	8.93 ± 0.04	9.00 ± 0.09
seglitide	9.96 ± 0.02	9.62 ± 0.17	9.82 ± 0.07	9.81 ± 0.13
CGP 23996	8.58 ± 0.07	8.94 ± 0.02	9.06 ± 0.05	8.95 ± 0.07
octreotide	9.19 ± 0.03	9.11 ± 0.14	9.16 ± 0.23	9.10 ± 0.07
[Tyr <sup>3</sup> ]octreotide	8.43 ± 0.23	7.10 ± 0.11	9.48 ± 0.23	8.66 ± 0.10
L362,855	8.36 ± 0.05	8.79 ± 0.19	8.69 ± 0.24	8.79 ± 0.06
L363,301	8.39 ± 0.11	8.47 ± 0.18	8.28 ± 0.61	8.39 ± 0.08
RC 160	9.35 ± 0.09	9.60 ± 0.02	9.56 ± 0.06	9.50 ± 0.16
BIM 23030	7.77 ± 0.07	7.66 ± 0.07	7.88 ± 0.03	7.94 ± 0.22
BIM 23014	9.27 ± 0.06	9.26 ± 0.07	9.43 ± 0.09	9.55 ± 0.03
BIM 23056	6.33 ± 0.10	6.23 ± 0.12	6.33 ± 0.14	6.38 ± 0.11
BIM 23052	8.30 ± 0.14	8.50 ± 0.32	8.76 ± 0.46	8.55 ± 0.01
cycloantagonist SA	5.40 ± 0.06	5.74 ± 0.05	5.80 ± 0.17	5.77 ± 0.05

To avoid problems, which could be generated by species differences and/ or the use of different expression systems and/ or of different radioligands, it was decided to deal only with human recombinant receptors, all expressed in the same cellular system, i.e. stably transfected CCL39 Chinese hamster lung fibroblast cells and with the same radioligands.

**Table 3(D)** CCL39/hsst<sub>5</sub>

	[ <sup>125</sup> I]LTT-SRIF <sub>28</sub>	[ <sup>125</sup> I][Tyr <sup>10</sup> ]CST <sub>14</sub>	[ <sup>125</sup> I]CGP 23996	[ <sup>125</sup> I][Tyr <sup>3</sup> ]octreotide
SRIF <sub>14</sub>	9.53 ± 0.13	9.01 ± 0.24	9.82 ± 0.19	9.87 ± 0.24
SRIF <sub>28</sub>	9.39 ± 0.22	9.18 ± 0.19	10.15 ± 0.23	10.30 ± 0.25
LTT-SRIF <sub>28</sub>	8.47 ± 0.02	8.12 ± 0.01	9.70 ± 0.21	9.60 ± 0.02
CST <sub>17</sub>	9.54 ± 0.10	9.37 ± 0.09	10.21 ± 0.16	9.85 ± 0.04
CST <sub>14</sub>	8.71 ± 0.02	8.40 ± 0.04	9.24 ± 0.07	9.34 ± 0.23
[Tyr <sup>10</sup> ]CST <sub>14</sub>	8.67 ± 0.24	8.06 ± 0.40	9.77 ± 0.24	9.65 ± 0.22
seglitide	8.70 ± 0.26	9.14 ± 0.30	10.22 ± 0.35	10.18 ± 0.22
CGP 23996	6.59 ± 0.41	6.67 ± 0.24	8.26 ± 0.08	8.68 ± 0.20
octreotide	7.17 ± 0.30	7.31 ± 0.18	8.96 ± 0.10	9.48 ± 0.11
[Tyr <sup>3</sup> ]octreotide	6.49 ± 0.01	6.00 ± 0.07	8.03 ± 0.05	8.41 ± 0.06
L362,855	7.17 ± 0.30	7.17 ± 0.12	8.72 ± 0.04	9.17 ± 0.10
L363,301	7.69 ± 0.13	7.17 ± 0.15	8.77 ± 0.09	9.51 ± 0.14
RC 160	7.51 ± 0.06	7.27 ± 0.11	8.72 ± 0.25	9.13 ± 0.35
BIM 23030	6.02 ± 0.09	5.56 ± 0.17	7.09 ± 0.05	7.45 ± 0.18
BIM 23014	7.76 ± 0.13	7.38 ± 0.19	9.07 ± 0.04	9.31 ± 0.10
BIM 23056	7.17 ± 0.05	6.68 ± 0.05	7.77 ± 0.09	8.32 ± 0.17
BIM 23052	7.92 ± 0.19	7.45 ± 0.24	9.59 ± 0.14	9.28 ± 0.35
cycloantagonist SA	6.38 ± 0.23	6.02 ± 0.11	7.77 ± 0.06	8.25 ± 0.17

Further, whenever practical, experiments were run in parallel. In three additional reports (Siehler and Hoyer, submitted (b), (c), (d), we investigate in with the same models, agonist-stimulated GTPγS binding, inhibition of adenylate cyclase and stimulation of PLC activities.

**Table 3(E)** CCL39/hsst<sub>3</sub>

	[ <sup>125</sup> I]LTT-SRIF <sub>28</sub>	[ <sup>125</sup> I][Tyr <sup>10</sup> ]CST <sub>14</sub>	[ <sup>125</sup> I]CGP 23996
SRIF <sub>14</sub>	9.54 ± 0.05	9.67 ± 0.07	9.71 ± 0.08
SRIF <sub>28</sub>	9.65 ± 0.04	9.80 ± 0.08	9.94 ± 0.17
LTT-SRIF <sub>28</sub>	9.84 ± 0.12	9.26 ± 0.03	10.09 ± 0.13
CST <sub>17</sub>	9.43 ± 0.06	9.52 ± 0.10	9.88 ± 0.04
CST <sub>14</sub>	9.06 ± 0.12	9.13 ± 0.09	9.27 ± 0.01
[Tyr <sup>10</sup> ]CST <sub>14</sub>	8.70 ± 0.18	8.90 ± 0.08	9.02 ± 0.25
seglitide	6.88 ± 0.08	7.89 ± 0.25	7.68 ± 0.15
CGP 23996	8.82 ± 0.05	9.28 ± 0.19	9.15 ± 0.04
octreotide	7.88 ± 0.04	8.60 ± 0.16	8.44 ± 0.01
[Tyr <sup>3</sup> ]octreotide	6.84 ± 0.25	6.20 ± 0.10	7.90 ± 0.00
L362,855	7.62 ± 0.23	8.25 ± 0.06	8.29 ± 0.04
L363,301	6.34 ± 0.06	6.83 ± 0.08	6.97 ± 0.13
RC 160	7.37 ± 0.15	7.91 ± 0.03	7.82 ± 0.15
BIM 23030	7.17 ± 0.08	7.85 ± 0.11	7.64 ± 0.20
BIM 23014	7.86 ± 0.41	8.02 ± 0.14	7.93 ± 0.11
BIM 23056	6.90 ± 0.04	7.08 ± 0.11	7.20 ± 0.10
BIM 23052	8.42 ± 0.12	9.55 ± 0.12	9.71 ± 0.02
cycloantagonist SA	6.23 ± 0.03	7.08 ± 0.04	6.88 ± 0.13

The radioligands used here, are as far as known, agonists at SRIF receptors or at least closely linked to compounds known as agonists, since the true "cold" iodinated equivalents of the ligands are not available. Thus, [<sup>125</sup>I]LTT-SRIF<sub>28</sub>, [<sup>125</sup>I][Tyr<sup>10</sup>]CST<sub>14</sub> are analogues of the natural somatostatin-28 and cortistatin-14, whereas [<sup>125</sup>I]CGP 23996 and [<sup>125</sup>I][Tyr<sup>3</sup>]octreotide are analogues of the synthetic peptide agonists CGP 23996 and octreotide.

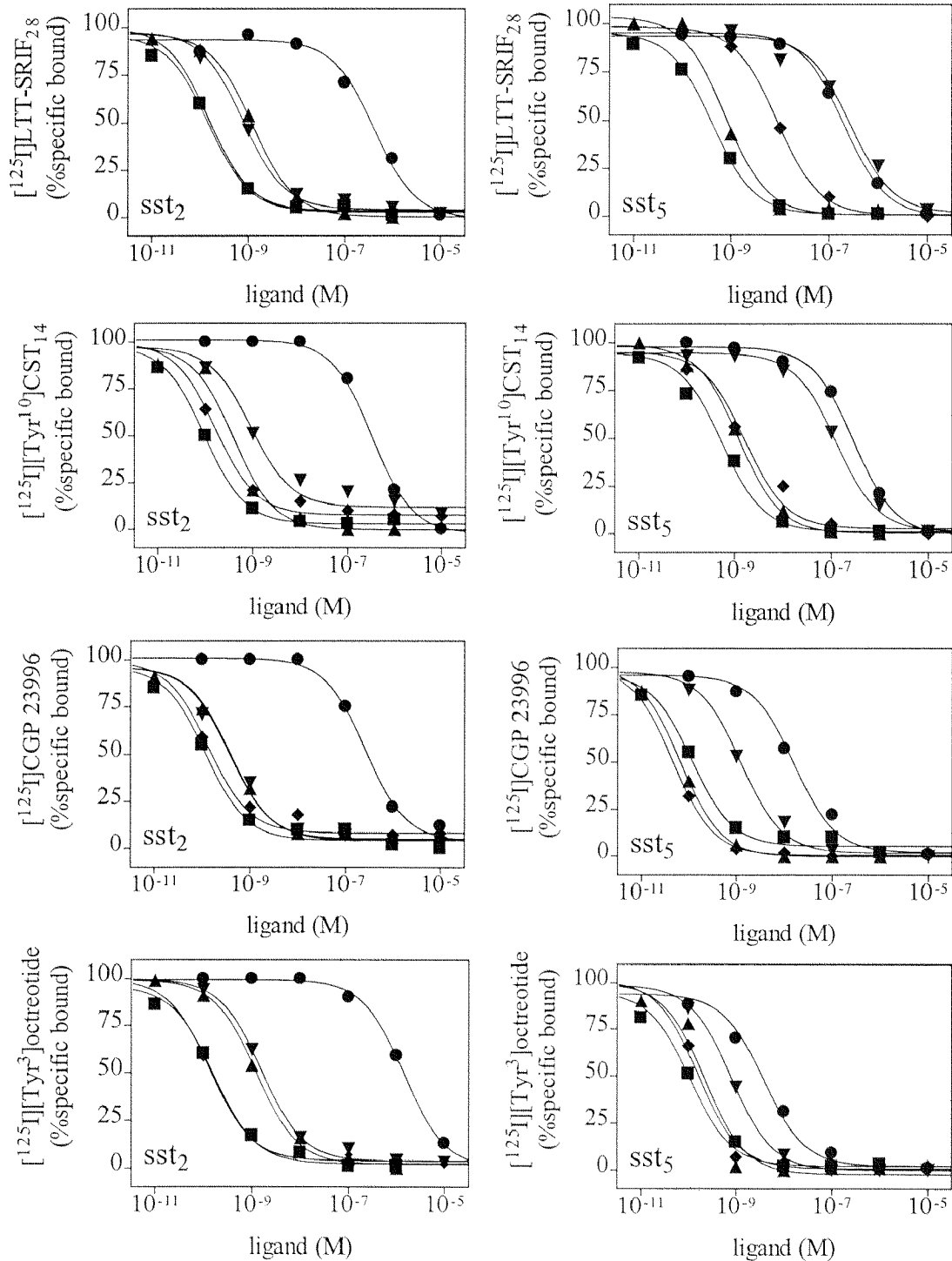
The four analogues are full or close to full agonists in adenylate cyclase experiments performed in these cells; therefore, it may be anticipated that such compounds determine the same  $B_{\max}$ -values at a given receptor and share a number of features. All four radioligands showed high affinity and saturable binding, and altogether the levels of non-specific binding and noise were low.

The first surprise of this study comes from saturation experiments: at the five receptors and as may be anticipated, the natural analogues [ $^{125}\text{I}$ ]LTT-SRIF<sub>28</sub> and [ $^{125}\text{I}$ ][Tyr<sup>10</sup>]CST<sub>14</sub> labelled similar receptor densities, although there is somewhat less binding for the cortistatin analogue at sst<sub>1</sub> and sst<sub>3</sub> receptors. By contrast, the synthetic peptide [ $^{125}\text{I}$ ]CGP 23996 labelled only about half of the sites recognised by [ $^{125}\text{I}$ ]LTT-SRIF<sub>28</sub>, except at sst<sub>4</sub> receptors. Similarly, [ $^{125}\text{I}$ ][Tyr<sup>3</sup>]octreotide labelled only about half sst<sub>2</sub> and almost 8-fold less sst<sub>5</sub> receptor sites compared to [ $^{125}\text{I}$ ]LTT-SRIF<sub>28</sub>, as if the ligands recognise different states (or combinations thereof) of the receptors.

To further investigate the possibility of multiple agonist receptor states, the effects of the non-hydrolysable GTP-analogue GppNHp on [ $^{125}\text{I}$ ]LTT-SRIF<sub>28</sub>, [ $^{125}\text{I}$ ]CGP 23996, [ $^{125}\text{I}$ ][Tyr<sup>10</sup>]CST<sub>14</sub> and [ $^{125}\text{I}$ ][Tyr<sup>3</sup>]octreotide binding to sst<sub>1-5</sub> receptors were investigated in both "competition" and saturation experiments. At sst<sub>1-4</sub> receptors, differences in  $B_{\max}$ -values were rather limited following co-incubation with GppNHp. By contrast, the large differences in  $B_{\max}$ -values at sst<sub>5</sub> receptors labelled with [ $^{125}\text{I}$ ]LTT-SRIF<sub>28</sub>, [ $^{125}\text{I}$ ][Tyr<sup>10</sup>]CST<sub>14</sub>, [ $^{125}\text{I}$ ]CGP 23996 and [ $^{125}\text{I}$ ][Tyr<sup>3</sup>]octreotide ( $B_{\max}$  = 6950, 5630, 3530 and 920 fmol/ mg, respectively) were amplified when GppNHp (10  $\mu\text{M}$ ) was added: on the one hand, [ $^{125}\text{I}$ ]LTT-SRIF<sub>28</sub> and [ $^{125}\text{I}$ ][Tyr<sup>10</sup>]CST<sub>14</sub> binding were almost GppNHp-insensitive (6560 and 6960 fmol/ mg, respectively), suggesting the labelling of primarily G-protein uncoupled receptors. On the other hand,  $B_{\max}$ -values for [ $^{125}\text{I}$ ]CGP 23996 and [ $^{125}\text{I}$ ][Tyr<sup>3</sup>]octreotide were reduced 3- 4 fold (930 and 270 fmol/ mg, respectively), suggesting predominantly binding to G-protein-coupled receptor states.

In "competition" experiments, GppNHp affected radioligand binding to rather different extents even at the same receptor subtype. At SRIF<sub>2</sub> (sst<sub>1</sub> and sst<sub>4</sub>) receptors, the radioligands appear to bind to a mixture of G-protein-coupled and -uncoupled receptor states.

**Figure 2:** Competition experiments performed in membranes prepared from CCL39 cells expressing human  $sst_2$  or  $sst_5$  receptors.



Crude membrane preparations from  $sst_2$  or  $sst_5$  receptor transfected cells were incubated with  $[^{125}\text{I}]\text{LTT-SRIF}_{28}$ ,  $[^{125}\text{I}][\text{Tyr}^{10}]\text{CST}_{14}$ ,  $[^{125}\text{I}]\text{CGP 23996}$  or  $[^{125}\text{I}][\text{Tyr}^3]\text{octreotide}$  and the indicated concentrations of SRIF<sub>14</sub> (■), CST<sub>17</sub> (▼), octreotide (▲), seglitide (◆) and BIM 23056 (●). Data are expressed as percentage of specific binding. The graphs show one example of at least 3 different experiments.

In particular, [<sup>125</sup>I]CGP 23996 seemed to recognise only uncoupled sst<sub>4</sub> receptors, since its binding was not significantly affected by GppNHp, whereas it was reduced by 30- 60 % with the other ligands. Of notice, the little effect produced by GppNHp on [<sup>125</sup>I]LTT-SRIF<sub>28</sub> and [<sup>125</sup>I][Tyr<sup>10</sup>]CST<sub>14</sub> binding, illustrating that natural ligands do not necessarily recognise receptors in a high affinity (G-protein-coupled) state only or primarily. At SRIF<sub>1</sub> receptors, the situations were quite variable. Thus, sst<sub>2</sub> and sst<sub>3</sub> receptors seem to be essentially recognised in a coupled state by all tested radioligands, since the effects of GppNHp rather marked, > 80 % inhibition for all four ligands at sst<sub>2</sub> receptors, and 70- 80 % inhibition at sst<sub>3</sub> receptors. In marked contrast, the sst<sub>5</sub> receptor binding of [<sup>125</sup>I]LTT-SRIF<sub>28</sub> and [<sup>125</sup>I][Tyr<sup>10</sup>]CST<sub>14</sub>, of which B<sub>max</sub>-values were high and ligand affinities lower, was only moderately inhibited by GppNHp, suggesting again binding to a mixed population of G-protein-coupled and -uncoupled receptor states. On the other hand, the sst<sub>5</sub> receptor binding of [<sup>125</sup>I]CGP 23996, and especially [<sup>125</sup>I][Tyr<sup>3</sup>]octreotide, of which B<sub>max</sub>-values were low and ligand affinities high, was almost entirely inhibited by GppNHp suggesting binding to essentially G-protein-coupled receptor states. Not only were the maximal effects of GppNHp different and dependent on ligand and receptor, but also the potency of GppNHp varied rather markedly, with apparent pEC<sub>50</sub>-values ranging from 4.81 to 7.77 at sst<sub>5</sub> binding, i.e. up to 1000-fold difference.

Subsequently, we compared the binding profiles of the three (or when feasible four) radioligands in competition studies with a number of rather varied structures including analogues of the natural SRIF and CST, as well as cyclic and linear peptides known to have affinity for one or the other member of the SRIF receptor family. In essence, affinities obtained in competition assays were almost superimposable at sst<sub>1-4</sub> receptors whichever the radioligand used, although this has to be qualified. By contrast, at sst<sub>5</sub> receptors, highest affinity values were determined using [<sup>125</sup>I][Tyr<sup>3</sup>]octreotide, which defined the lowest B<sub>max</sub>-values and was most sensitive to GppNHp. Similarly, higher affinities were measured with [<sup>125</sup>I]CGP 23996-labelled sites, which labelled also a relatively low receptor density. Altogether, lower affinities were determined when using the hormone analogues [<sup>125</sup>I]LTT-SRIF<sub>28</sub> and [<sup>125</sup>I][Tyr<sup>10</sup>]CST<sub>14</sub>, which both labelled high receptor densities.

**Table 4:** Correlation coefficients (r) of correlation analyses between affinity profiles (pK<sub>d</sub>-values) obtained by using [<sup>125</sup>I]LTT-SRIF<sub>28</sub>, [<sup>125</sup>I][Tyr<sup>10</sup>]CST<sub>14</sub>, [<sup>125</sup>I]CGP 23996 and [<sup>125</sup>I][Tyr<sup>3</sup>]octreotide at human sst<sub>1-5</sub> receptors. Data used for correlation are shown in Tables 4(A)-(E).

**Table 4(A)** CCL39/hsst<sub>1</sub>

	[ <sup>125</sup> I]LTT-SRIF <sub>28</sub>	[ <sup>125</sup> I][Tyr <sup>10</sup> ]CST <sub>14</sub>
[ <sup>125</sup> I][Tyr <sup>10</sup> ]CST <sub>14</sub>	0.966	-
[ <sup>125</sup> I]CGP 23996	0.971	0.926

**Table 4(B)** CCL39/hsst<sub>4</sub>

	[ <sup>125</sup> I]LTT-SRIF <sub>28</sub>	[ <sup>125</sup> I][Tyr <sup>10</sup> ]CST <sub>14</sub>
[ <sup>125</sup> I][Tyr <sup>10</sup> ]CST <sub>14</sub>	0.969	-
[ <sup>125</sup> I]CGP 23996	0.987	0.960

**Table 4(C)** CCL39/hsst<sub>2</sub>

	[ <sup>125</sup> I]LTT-SRIF <sub>28</sub>	[ <sup>125</sup> I][Tyr <sup>10</sup> ]CST <sub>14</sub>	[ <sup>125</sup> I]CGP 23996
[ <sup>125</sup> I][Tyr <sup>10</sup> ]CST <sub>14</sub>	0.874	-	-
[ <sup>125</sup> I]CGP 23996	0.978	0.761	-
[ <sup>125</sup> I][Tyr <sup>3</sup> ]octreotide	0.954	0.888	0.924

**Table 4(D)** CCL39/hsst<sub>5</sub>

	[ <sup>125</sup> I]LTT-SRIF <sub>28</sub>	[ <sup>125</sup> I][Tyr <sup>10</sup> ]CST <sub>14</sub>	[ <sup>125</sup> I]CGP 23996
[ <sup>125</sup> I][Tyr <sup>10</sup> ]CST <sub>14</sub>	0.942	-	-
[ <sup>125</sup> I]CGP 23996	0.850	0.896	-
[ <sup>125</sup> I][Tyr <sup>3</sup> ]octreotide	0.767	0.843	0.916



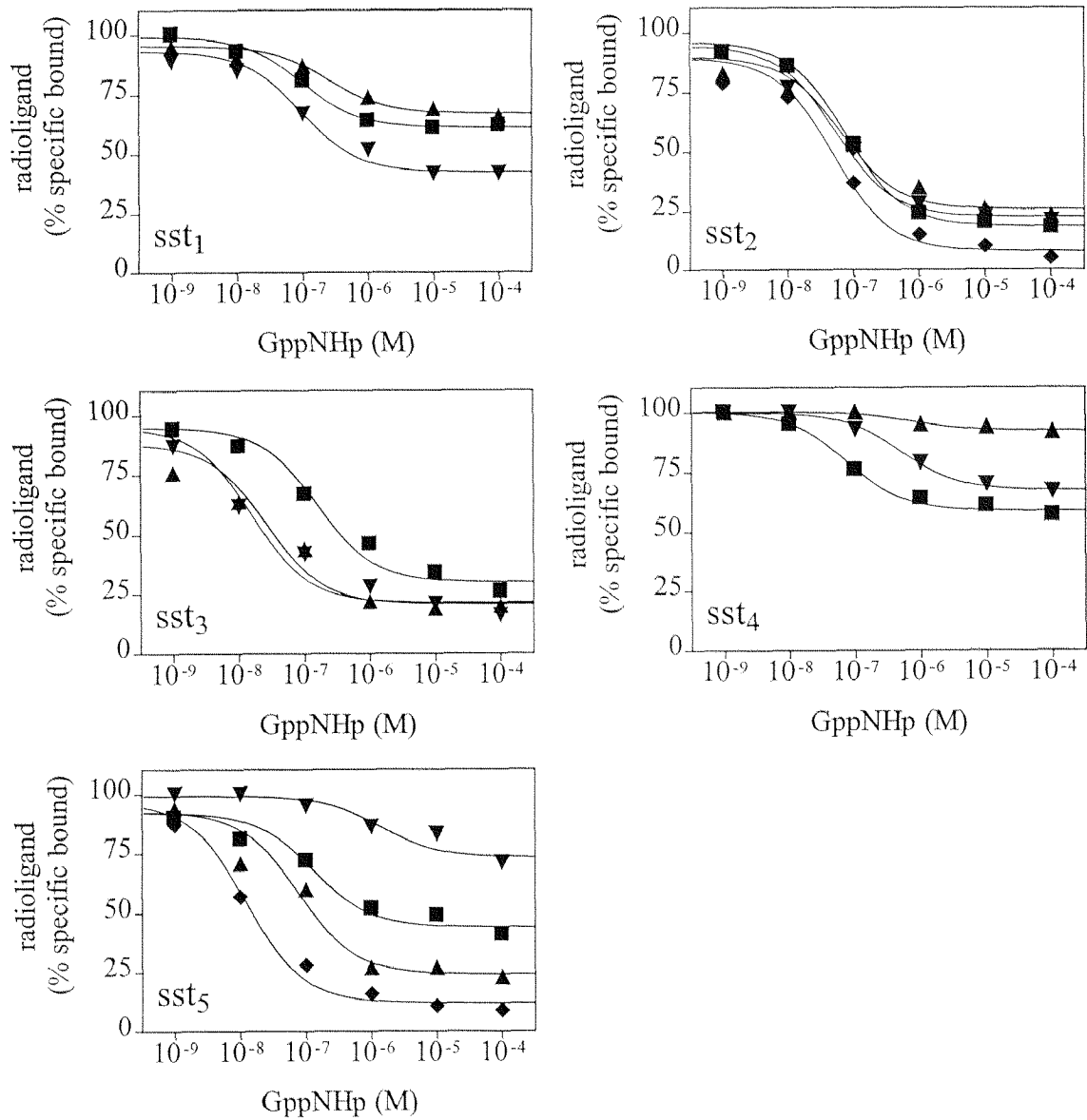
**Table 4(E)** CCL39/hsst<sub>3</sub>

	[ <sup>125</sup> I]LTT-SRIF <sub>28</sub>	[ <sup>125</sup> I][Tyr <sup>10</sup> ]CST <sub>14</sub>
[ <sup>125</sup> I][Tyr <sup>10</sup> ]CST <sub>14</sub>	0.839	-
[ <sup>125</sup> I]CGP 23996	0.932	0.829

Thus, the affinity profiles of human sst<sub>1,4</sub> receptors determined with [<sup>125</sup>I]LTT-SRIF<sub>28</sub>, [<sup>125</sup>I][Tyr<sup>10</sup>]CST<sub>14</sub>, [<sup>125</sup>I]CGP 23996 and [<sup>125</sup>I][Tyr<sup>3</sup>]octreotide correlated highly significantly. This was much less conspicuous at sst<sub>5</sub> receptors: for instance, the profile of [<sup>125</sup>I]CGP 23996 and [<sup>125</sup>I][Tyr<sup>3</sup>]octreotide correlated significantly, but not when compared to the profiles of [<sup>125</sup>I]LTT-SRIF<sub>28</sub> or [<sup>125</sup>I][Tyr<sup>10</sup>]CST<sub>14</sub>. Indeed, the absolute affinity values could easily vary by a factor 100 or higher depending on the radioligand used, but also and more surprisingly the rank order of affinity did also vary rather markedly. A number of discrepancies became apparent when comparing homologous versus heterologous binding. Thus it is not always evident that heterologous displacement studies will predict which ligand may turn into a good radioligand; in other words, affinities may be well underestimated when competing [Tyr<sup>3</sup>]octreotide or CGP 23996 for sites labelled with [<sup>125</sup>I]LTT-SRIF<sub>28</sub> or [<sup>125</sup>I][Tyr<sup>10</sup>]CST<sub>14</sub>. In several cases, the resulting affinity values would not predict the high affinity that can be obtained with the corresponding radioligands, [<sup>125</sup>I]CGP 23996 and [<sup>125</sup>I][Tyr<sup>3</sup>]octreotide.

Similar findings have been made at NK receptors, to the extent that it was not expected to label NK1 receptors with either NKA or NKB, since these peptides have low affinity for NK1 receptors labelled with Substance P. Yet contrary to all expectations [<sup>3</sup>H]NKA or [<sup>3</sup>H]NKB label NK1 receptors with high affinity, questioning some of the points made about the selectivity of these ligands or senktide (Hastrup and Schwartz, 1996). Similarly, it was not expected that [<sup>125</sup>I][Tyr<sup>3</sup>]octreotide would label sst<sub>5</sub> receptor based on its affinity for the receptor labelled with [<sup>125</sup>I]LTT-SRIF<sub>28</sub> or [<sup>125</sup>I][Tyr<sup>10</sup>]CST<sub>14</sub>. This may be another illustration that each ligand may induce a somewhat different agonist receptor complex.

**Figure 3:** Effects of GppNHp on radioligand binding at human sst<sub>1-5</sub> receptors.

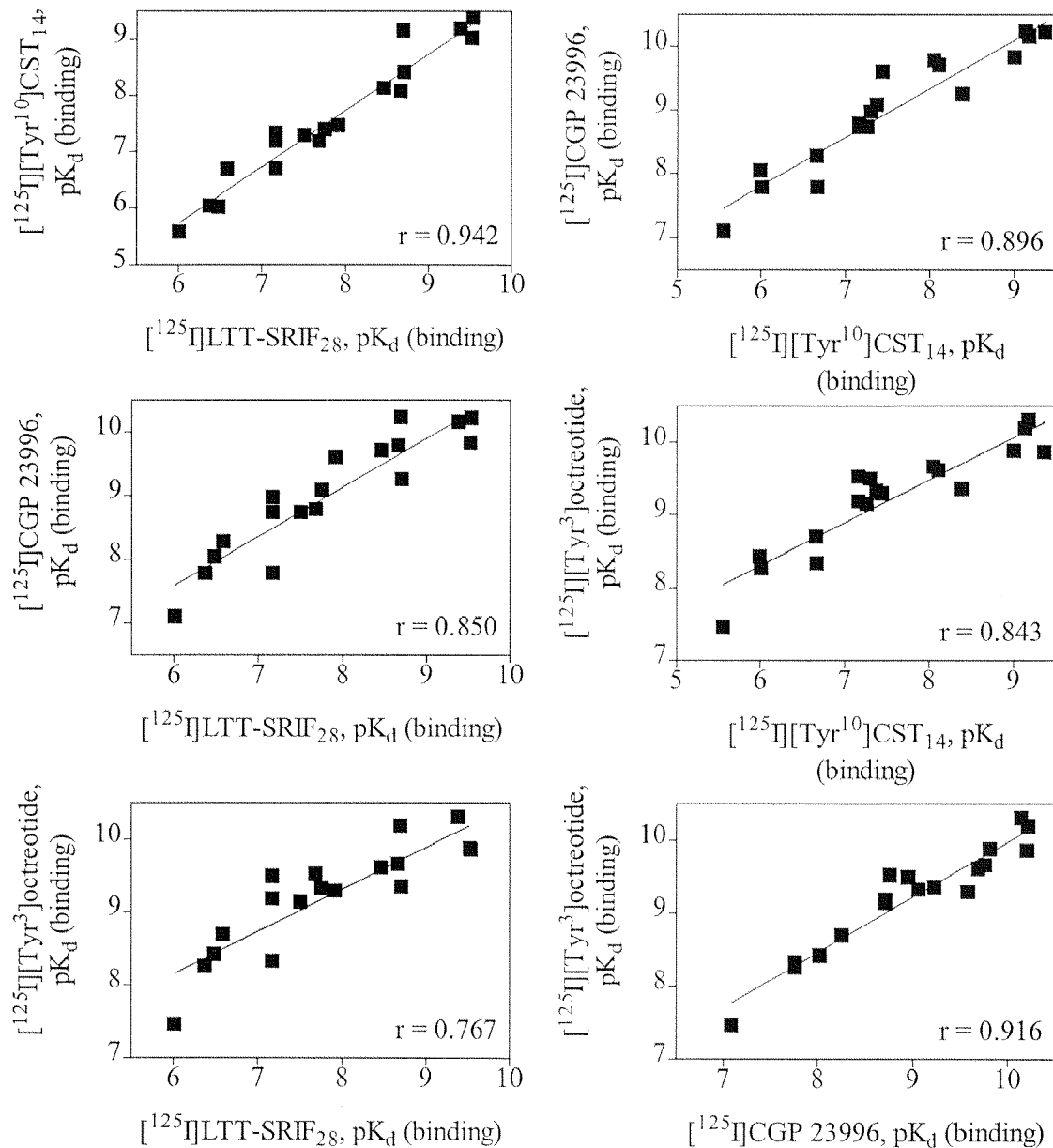


Crude membrane preparations from sst<sub>1-5</sub> receptor transfected cells were incubated with [<sup>125</sup>I]LTT-SRIF<sub>28</sub> (■), [<sup>125</sup>I][Tyr<sup>10</sup>]CST<sub>14</sub> (▼), [<sup>125</sup>I]CGP 23996 (▲) or [<sup>125</sup>I][Tyr<sup>3</sup>]octreotide (◆) and the indicated concentrations of GppNHp. Data are expressed as percentage of specific binding. One representative example of at least 3 different experiments is shown.

Overall it remains to be seen whether the notion of high and low affinity states is useful at all; if two states were to exist and the ligands differentiate between these, one would expect biphasic competition curves, however these were not observed. One may wonder why endogenous peptides such as SRIF<sub>28</sub> or CST may bind to G-protein-uncoupled SRIF receptors; to be functionally relevant this suggest G-protein-independent signalling pathways. A Na<sup>+</sup>/H<sup>+</sup> exchanger regulatory factor (NHERF) binds to the  $\beta_2$ -adrenergic receptors to mediate inhibition of a Na<sup>+</sup>/H<sup>+</sup> exchanger without involving any G-protein (Hall et al., 1998). SRIF receptors were found to inhibit Na<sup>+</sup>/H<sup>+</sup> exchanger activity in a pertussis toxin-insensitive manner (Barber et al., 1989; Hou et al., 1994), an effect, which might also involve NHERF or NHERF-like proteins, in the absence of G-protein coupling.

According to the “ternary complex model”, agonists bind with high affinity to G-protein-coupled receptors, which stabilises the receptor/ G-protein complex, and with low affinity to non-coupled receptors. Antagonists on the other hand, bind with the same affinity to both, G-protein-coupled and non-coupled receptors (De Lean et al., 1980). The ternary complex model was extended to the “allosteric ternary complex model”, since mutants of adrenergic and other receptors were shown to be constitutively active and thereby couple to G-proteins even in the absence of any ligand (Samama et al., 1993; Lefkowitz et al., 1993). However, the various versions of these models do not explain the present results, since all four tested radioligands are shown to behave as full agonists in second messenger studies at sst<sub>1,5</sub> receptors (De Lecea et al., 1996; Hoyer et al., 1994b), but nevertheless show depending on the radioligand and the SRIF receptor subtype “antagonist” behaviour in binding to receptors coupled and non-coupled to G-proteins. The results may rather be explained by assuming multiple agonist-specific receptor conformations, which have already been suggested for  $\beta_2$ -adrenergic receptors as in adenylate cyclase assays the G-protein dissociation rate was agonist-specific (Krumins et al., 1997). Another study at Y<sub>4</sub> receptors supports this model: iodinated pancreatic polypeptide, which is an endogenous agonist at rat Y<sub>4</sub> receptors as peptide YY is, labelled about 26-fold more rat Y<sub>4</sub> receptor sites in COS cells than iodinated peptide YY.

**Figure 4:** Comparison of affinity profiles defined by [ $^{125}$ I]LTT-SRIF<sub>28</sub>, [ $^{125}$ I][Tyr<sup>10</sup>]CST<sub>14</sub>, [ $^{125}$ I]CGP 23996 and [ $^{125}$ I][Tyr<sup>3</sup>]octreotide at human recombinant sst<sub>5</sub> receptors expressed in CCL39 cells.



Data are from tables 3(A)-(E) and compare pK<sub>d</sub>-values of human sst<sub>5</sub> receptors obtained in radioligand binding assays. Correlation coefficients (r) are indicated in the plots.

Binding of the pancreatic polypeptide was rather insensitive to GppNHp, whereas binding of peptide YY was efficiently inhibited by GppNHp ( $E_{\max} = 78 \pm 4 \%$ ) (Walker et al., 1997).

Addition of 20  $\mu\text{M}$  GTP $\gamma$ S to rat  $\text{sst}_1$  receptors immunoprecipitated in complex with [ $^{125}\text{I}$ ][Tyr $^{11}$ ]SRIF $_{14}$  induced dissociation of the iodinated ligand, but roughly 30 % of the ligand/ receptor complex was insensitive to GTP $\gamma$ S (Gu et al., 1995) suggesting binding of [ $^{125}\text{I}$ ][Tyr $^{11}$ ]SRIF $_{14}$  to G-protein-coupled and -uncoupled receptors as observed with [ $^{125}\text{I}$ ]LTT-SRIF $_{28}$  in our study.

In conclusion, our study shows, that different agonists may bind a given receptor with different features; G-protein-coupled receptors therefore might not only exist in a G-protein-coupled state with high affinity for agonists and in a G-protein-uncoupled state with low affinity for agonists, but rather in multiple agonist-specific receptor states. As shown for [ $^{125}\text{I}$ ]LTT-SRIF $_{28}$  and [ $^{125}\text{I}$ ][Tyr $^{10}$ ]CST $_{14}$ , some agonists seem to bind not only G-protein-coupled receptors, but also G-protein-uncoupled receptors with high affinity as suggested by their low GppNHp-sensitivity, while other agonists like [ $^{125}\text{I}$ ]CGP 23996 and [ $^{125}\text{I}$ ][Tyr $^3$ ]octreotide seem to bind mostly the G-protein-coupled receptor conformation. Since the SRIF receptors were overexpressed in CCL39 cells, the receptor level compared to the G-protein level is probably higher and therefore the ratio of G-protein-uncoupled receptors to G-protein-coupled receptors is higher than in vivo, but nevertheless G-protein-coupled and -uncoupled receptors in an equilibrium are also existent in vivo.

Ultimately, the data also show that depending on the radioligand used, large differences in affinity can be determined and thus it is not surprising that the so-called selectivity ratios reported from one or another group may be entirely different; for instance, seglitide shows the rank order  $\text{sst}_2 > \text{sst}_5 > \text{sst}_3$  when defined with [ $^{125}\text{I}$ ]LTT-SRIF $_{28}$  but the rank order  $\text{sst}_5 > \text{sst}_2 > \text{sst}_3$  when determined with [ $^{125}\text{I}$ ]CGP 23996, and if one starts comparing different radioligand the situation is even more complex.

## Chapter 6

---

### Characterisation of human recombinant somatostatin receptors: 2) modulation of GTP $\gamma$ S binding

---

Sandra Siehler and Daniel Hoyer,

Naunyn-Schmiedeberg's Archives of Pharmacology, submitted

## 6.1. Abstract

G-protein activation by somatostatin (SRIF), cortistatin (CST) and analogues of these neuropeptides was investigated at human somatostatin receptor subtypes 1-5 (sst<sub>1-5</sub>) stably expressed in CCL39 Chinese hamster lung fibroblast cells by measuring agonist-stimulated [<sup>35</sup>S]GTP $\gamma$ S binding.

[<sup>35</sup>S]GTP $\gamma$ S binding was performed in the presence of 100 mM NaCl and 1  $\mu$ M GDP, although higher E<sub>max</sub> and/ or pEC<sub>50</sub> values may have been obtained under other conditions, but at the expense of lower absolute stimulation or signal/ noise ratio.

SRIF<sub>14</sub> stimulated [<sup>35</sup>S]GTP $\gamma$ S binding to 162 %, 220 %, 148 % and 266 % of control levels via sst<sub>2</sub>, sst<sub>3</sub>, sst<sub>4</sub> and sst<sub>5</sub> receptors, respectively. At sst<sub>1</sub> receptors, SRIF<sub>14</sub> produced only a limited stimulation (E<sub>max</sub> = 115 %). Hence sst<sub>1</sub> receptors were not subjected to further [<sup>35</sup>S]GTP $\gamma$ S binding experiments. [<sup>35</sup>S]GTP $\gamma$ S binding assays were then performed with sst<sub>2-5</sub> receptors.

Most of the peptide analogues stimulated [<sup>35</sup>S]GTP $\gamma$ S binding in sst<sub>2-5</sub> receptor expressing cells. BIM 23056 behaved as an antagonist on SRIF<sub>14</sub>-induced [<sup>35</sup>S]GTP $\gamma$ S binding with apparent pK<sub>B</sub>-value of 6.33 and 5.84 at hsst<sub>3</sub> and hsst<sub>5</sub> receptors, respectively, whereas neither agonism nor antagonism could be shown (at 1  $\mu$ M) at sst<sub>2</sub> or sst<sub>4</sub> receptors. The effect at sst<sub>5</sub> receptors was not surmountable and needs further investigations. The so-called "antagonist" SA, was devoid of antagonist activity at sst<sub>2</sub> or sst<sub>3</sub> receptors, whereas it was almost a full agonist at sst<sub>4</sub> and sst<sub>5</sub> receptor mediated [<sup>35</sup>S]GTP $\gamma$ S binding.

The [<sup>35</sup>S]GTP $\gamma$ S binding profiles of hsst<sub>2-5</sub> receptors were compared to their respective radioligand binding profiles. For sst<sub>4</sub> and sst<sub>5</sub> receptors, the rank order of affinity of all tested radioligands correlated highly significantly with [<sup>35</sup>S]GTP $\gamma$ S binding (r = 0.814 - 0.897). At sst<sub>3</sub> receptors, [<sup>35</sup>S]GTP $\gamma$ S correlated somewhat less with binding profiles obtained with [<sup>125</sup>I][Tyr<sup>10</sup>]CST<sub>14</sub> and [<sup>125</sup>I]CGP 23996 than with [<sup>125</sup>I]LTT-SRIF<sub>28</sub> (r = 0.743, 0.757 and 0.882, respectively).

At sst<sub>2</sub> receptors, [<sup>35</sup>S]GTPγS binding correlated with [<sup>125</sup>I]LTT-SRIF<sub>28</sub>, [<sup>125</sup>I]CGP 23996 and [<sup>125</sup>I][Tyr<sup>3</sup>]octreotide binding profiles ( $r = 0.596- 0.699$ ), but not with [<sup>125</sup>I][Tyr<sup>10</sup>]CST<sub>14</sub> binding.

The present [<sup>35</sup>S]GTPγS binding data combined to previous radioligand binding results obtained in cells expressing human SRIF receptors, suggest that at any given receptor, agonists' rank orders of potency (not to mention absolute affinity values which vary profoundly) are not as strictly ordered as may be anticipated. We are investigating these aspects further by analysing additional signalling pathways.

## 6.2. Results

### Assay conditions

The conditions for [<sup>35</sup>S]GTPγS binding assays were established at hsst<sub>5</sub> receptors using SRIF<sub>14</sub> as the agonist and a Mg<sup>2+</sup>-concentration of 5 mM. Initially, 100 mM NaCl were added to determine the optimal GDP-concentration (table 1(A); figure 1). SRIF<sub>14</sub> did not stimulate [<sup>35</sup>S]GTPγS binding in the absence of GDP. Basal levels of specifically bound [<sup>35</sup>S]GTPγS decreased with increasing GDP concentrations (from 0.1 to 30 μM), whereas the agonist-stimulated [<sup>35</sup>S]GTPγS binding increased to reach a maximum at 30 μM GDP ( $E_{\max} = 475 \pm 54 \%$ ). In parallel, an increase of the GDP-concentration was accompanied by a decrease of the pEC<sub>50</sub>-value of SRIF<sub>14</sub> (from 8.82 to 8.06, see table 1 and figure 1). Therefore, a GDP-concentration of 1 μM was considered as optimal with respect to absolute stimulation but also signal to noise ratio and apparent potency ( $E_{\max} = 266 \pm 19 \%$ ; pEC<sub>50</sub> = 8.39 ± 0.12). This set-up was used to determine the optimal NaCl-concentration (table 1(B); figure 2). The maximal stimulation of [<sup>35</sup>S]GTPγS binding increased with increasing NaCl concentrations ( $E_{\max} = 339 \pm 50 \%$ ), whereas specific bound [<sup>35</sup>S]GTPγS decreased in parallel.



**Table 1:** Stimulation of [<sup>35</sup>S]GTPγS binding by SRIF<sub>14</sub> at human sst<sub>5</sub> receptors: influence of different GDP or NaCl concentrations on the pEC<sub>50</sub>-value and the maximal stimulation. pEC<sub>50</sub>'s (-log M) and E<sub>max</sub>-values [% stimulation over basal level (= 100 %) ± SEM of three experiments are shown

GDP [μM]	pEC <sub>50</sub>	E <sub>max</sub>
0	(-)	101 ± 2
0.1	8.82 ± 0.05	167 ± 5
0.3	8.80 ± 0.07	178 ± 7
1	8.39 ± 0.12	266 ± 19
5	8.43 ± 0.07	371 ± 48
10	8.38 ± 0.01	430 ± 68
30	8.29 ± 0.04	475 ± 54
100	8.06 ± 0.08	308 ± 24

**Table 1(A)**

Variation of the GDP concentration  
(100 mM NaCl)

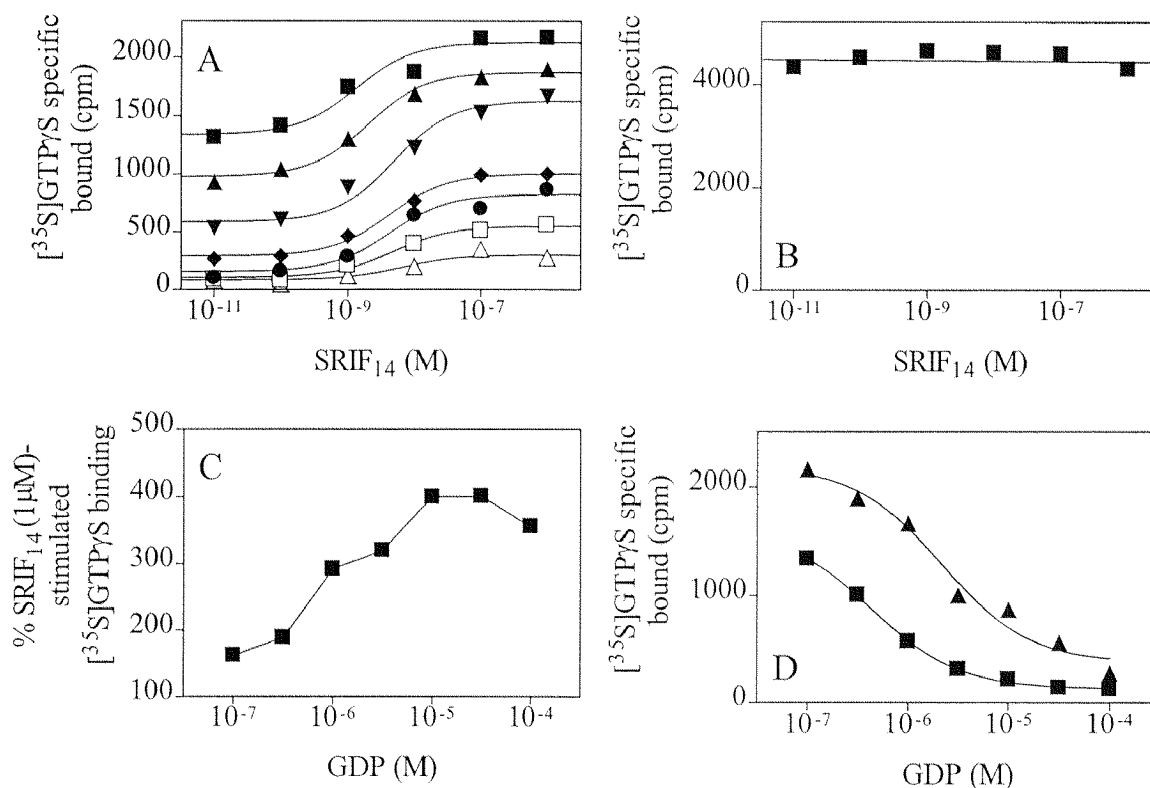
NaCl [mM]	pEC <sub>50</sub>	E <sub>max</sub>
10	9.18 ± 0.08	138 ± 11
25	9.09 ± 0.11	152 ± 4
50	8.92 ± 0.05	203 ± 8
100	8.39 ± 0.12	266 ± 19
150	8.08 ± 0.21	304 ± 20
200	7.90 ± 0.16	339 ± 50
300	7.39 ± 0.17	336 ± 68

**Table 1(B)**

Variation of the NaCl concentration  
(1 μM GDP)

In addition, an increase in the sodium chloride level (from 10 to 300 mM) markedly reduced the potency of SRIF<sub>14</sub> to stimulate [<sup>35</sup>S]GTPγS binding (pEC<sub>50</sub> = 9.18 to 7.39). Therefore, 100 mM NaCl was considered as optimal, although higher E<sub>max</sub> and/ or lower EC<sub>50</sub>-values may have been obtained under other conditions, but at the expense of lesser absolute agonist-induced stimulation or signal/ noise.

**Figure 1:** Effect of GDP concentration on [ $^{35}$ S]GTP $\gamma$ S binding to microsome preparations from CCL39 cells expressing human sst $_5$  receptors using 100 mM NaCl.



(A) Microsomes (2  $\mu$ g per assay) were incubated with [ $^{35}$ S]GTP $\gamma$ S (0.2 nM), the indicated concentrations of SRIF $_{14}$  and a fixed GDP concentration. Each curve represents a different GDP concentration: 0.1  $\mu$ M (■), 0.3  $\mu$ M (▲), 1  $\mu$ M (▼), 5  $\mu$ M (◆), 10  $\mu$ M (●), 30  $\mu$ M (□), or 100  $\mu$ M (Δ).

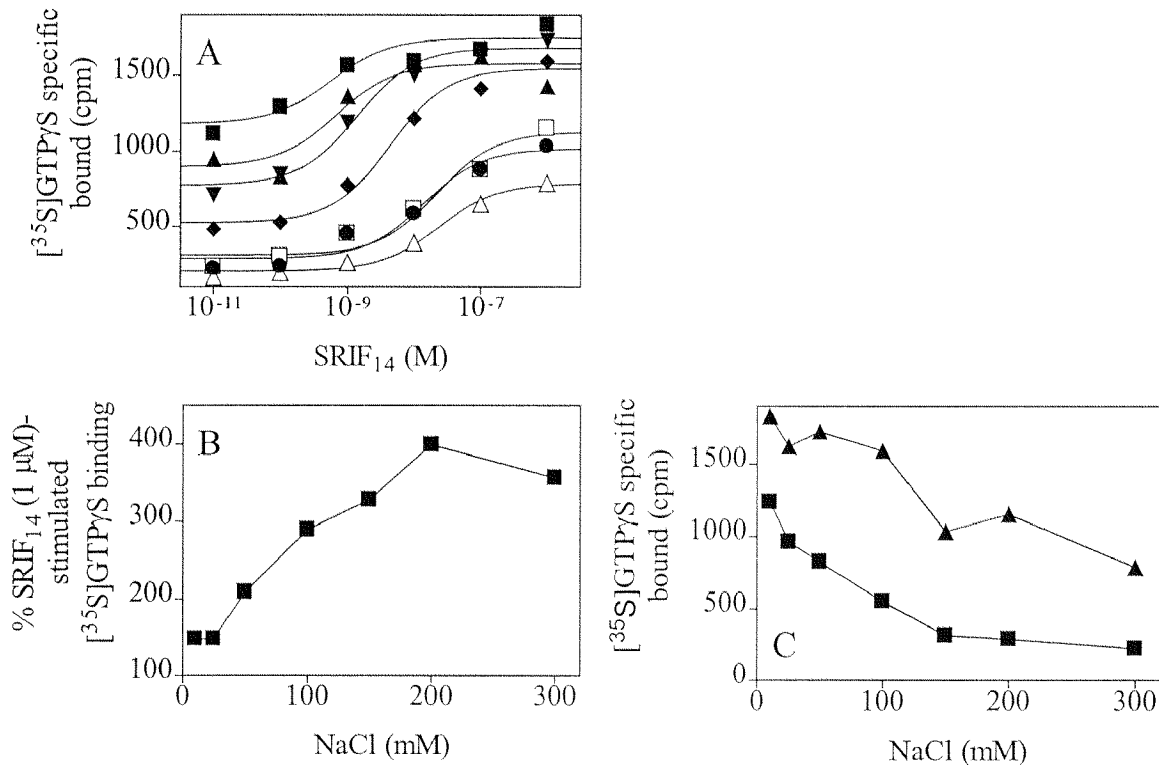
(B) Microsomes were incubated with [ $^{35}$ S]GTP $\gamma$ S, the indicated concentrations of SRIF $_{14}$ , and in the absence of GDP (■).

(C) % stimulation of [ $^{35}$ S]GTP $\gamma$ S binding by 1  $\mu$ M SRIF $_{14}$  with the indicated GDP concentrations. Data represent the percentage of basal [ $^{35}$ S]GTP $\gamma$ S binding at each GDP concentration.

(D) Specific [ $^{35}$ S]GTP $\gamma$ S binding in the absence (■) or presence (▲) of 1  $\mu$ M SRIF $_{14}$  using the indicated GDP concentrations.

The data points show one representative example of 3 independent determinations.

**Figure 2:** Effect of sodium chloride concentration on [ $^{35}$ S]GTP $\gamma$ S binding to microsome preparations from sst $_5$  receptor expressing CCL39 cells using 1  $\mu$ M GDP.



(A) Microsomes (2  $\mu$ g per assay) were incubated with [ $^{35}$ S]GTP $\gamma$ S (0.2 nM), the indicated concentrations of SRIF $_{14}$  and a fixed NaCl concentration. Each curve represents a different NaCl concentration: 10 mM (■), 25 mM (▲), 50 mM (▼), 100 mM (◆), 150 mM (●), 200 mM (□), or 300 mM (Δ).

(B) % stimulation of [ $^{35}$ S]GTP $\gamma$ S binding by 1  $\mu$ M SRIF $_{14}$  with the indicated NaCl concentrations. Data represent the percentage of basal [ $^{35}$ S]GTP $\gamma$ S binding at each NaCl concentration.

(C) Specific [ $^{35}$ S]GTP $\gamma$ S binding in the absence (■) or presence (▲) of 1  $\mu$ M SRIF $_{14}$  using the indicated NaCl concentrations.

The data points represent one representative example of 3 different experiments.

**Table 2:** Stimulation of [<sup>35</sup>S]GTPγS binding by SRIF, CST, and various analogues at human sst<sub>2-5</sub> receptors: comparison of pEC<sub>50</sub> values (-log M) and E<sub>max</sub>-values [% stimulation] ± SEM of 3 independent determinations

Table 2(A)	CCL39/hsst <sub>2</sub>		CCL39/hsst <sub>3</sub>	
	E <sub>max</sub>	pEC <sub>50</sub>	E <sub>max</sub>	pEC <sub>50</sub>
SRIF <sub>14</sub>	162 ± 3	6.95 ± 0.05	220 ± 8	7.32 ± 0.11
SRIF <sub>28</sub>	172 ± 7	6.14 ± 0.03	225 ± 6	6.96 ± 0.06
LTT-SRIF <sub>28</sub>	168 ± 9	6.78 ± 0.20	243 ± 5	7.44 ± 0.19
CST <sub>17</sub>	137 ± 5	5.83 ± 0.15	188 ± 12	6.59 ± 0.15
[Tyr <sup>10</sup> ]CST <sub>14</sub>	124 ± 4	6.28 ± 0.27	151 ± 10	6.83 ± 0.27
seglitide	185 ± 5	7.39 ± 0.09	159 ± 2	5.78 ± 0.02
CGP 23996	159 ± 8	6.06 ± 0.09	197 ± 18	7.14 ± 0.08
octreotide	158 ± 11	6.52 ± 0.34	150 ± 19	6.70 ± 0.30
[Tyr <sup>3</sup> ]octreotide	181 ± 3	6.57 ± 0.14	156 ± 4	5.76 ± 0.07
L362,855	132 ± 1	5.65 ± 0.03	128 ± 2	6.27 ± 0.29
BIM 23056	78 ± 1	(-)	88 ± 2	(-)
BIM 23052	133 ± 5	5.91 ± 0.27	212 ± 5	6.29 ± 0.04
cycloantagonist SA	102 ± 2	(-)	116 ± 6	(-)

These optimised conditions were used in [<sup>35</sup>S]GTPγS binding assays performed with sst<sub>2-5</sub> receptors. SRIF<sub>14</sub> stimulated [<sup>35</sup>S]GTPγS binding at sst<sub>2</sub>, sst<sub>3</sub>, sst<sub>4</sub> and sst<sub>5</sub> receptors to 162 %, 220 %, 148 % and 266 % respectively, of control levels (table 2; figure 3). At sst<sub>1</sub> receptors SRIF<sub>14</sub> produced only a slight stimulation (E<sub>max</sub> = 115 %), which was not increased by using 5 μM GDP (data not shown); hence sst<sub>1</sub> receptors were not subjected to further [<sup>35</sup>S]GTPγS binding experiments.

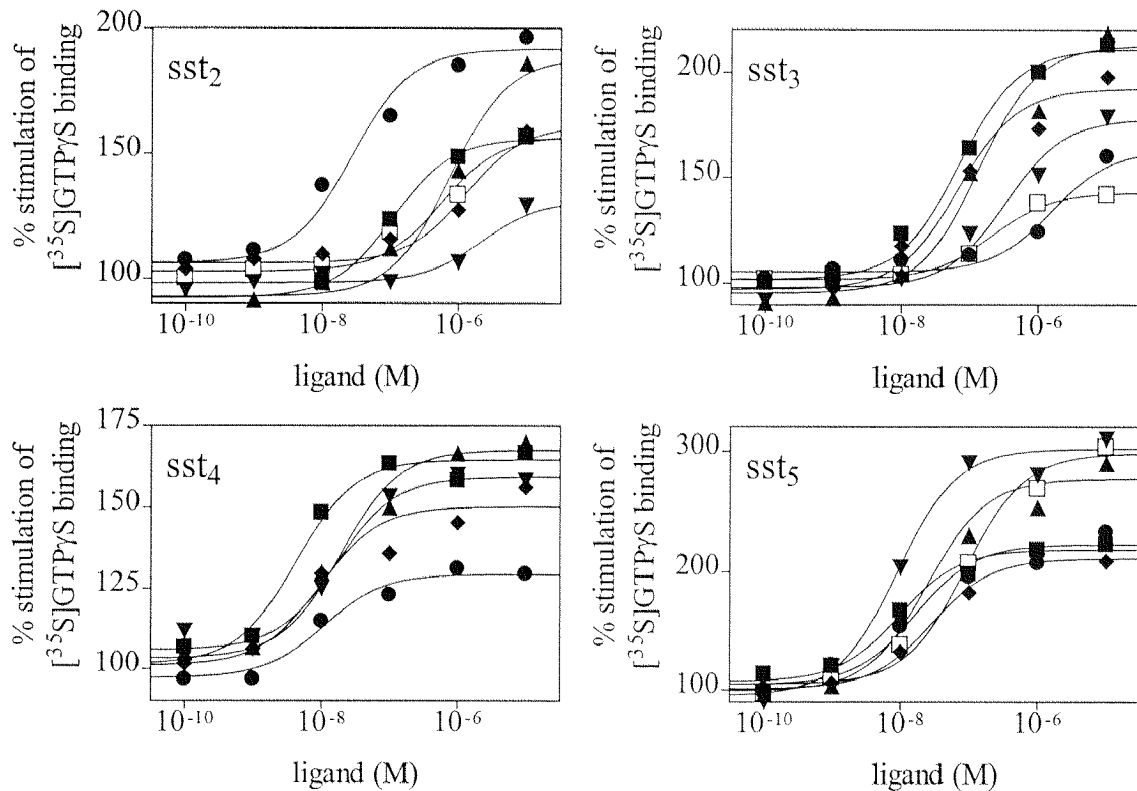
Table 2(B)	CCL39/hsst <sub>4</sub>		CCL39/hsst <sub>5</sub>	
	E <sub>max</sub>	pEC <sub>50</sub>	E <sub>max</sub>	pEC <sub>50</sub>
SRIF <sub>14</sub>	148 ± 3	8.05 ± 0.17	266 ± 19	8.39 ± 0.12
SRIF <sub>28</sub>	145 ± 8	7.58 ± 0.13	268 ± 14	7.65 ± 0.08
LTT-SRIF <sub>28</sub>	149 ± 3	7.12 ± 0.26	278 ± 6	7.63 ± 0.09
CST <sub>17</sub>	146 ± 12	7.66 ± 0.07	231 ± 7	7.94 ± 0.09
[Tyr <sup>10</sup> ]CST <sub>14</sub>	142 ± 3	7.02 ± 0.22	215 ± 19	7.43 ± 0.08
seglitide	N.D.	N.D.	240 ± 18	7.89 ± 0.10
CGP 23996	151 ± 4	8.12 ± 0.07	211 ± 9	7.12 ± 0.31
octreotide	126 ± 2	5.67 ± 0.21	278 ± 13	6.89 ± 0.09
[Tyr <sup>3</sup> ]octreotide	131 ± 10	5.49 ± 0.03	220 ± 1	6.56 ± 0.17
L362,855	N.D.	N.D.	231 ± 16	6.29 ± 0.02
BIM 23056	98 ± 3	(-)	100 ± 12	(-)
BIM 23052	154 ± 1	6.42 ± 0.11	266 ± 12	6.80 ± 0.14
cycloantagonist SA	126 ± 5	5.57 ± 0.05	222 ± 5	5.82 ± 0.08

### Hsst<sub>2</sub> receptors

Interestingly, SRIF<sub>14</sub> revealed higher potencies than SRIF<sub>28</sub> in stimulating [<sup>35</sup>S]GTPγS binding at sst<sub>2-5</sub> receptors, although their affinities determined in radioligand binding studies are not distinguishable (Siehler et al., submitted (a)). SRIF<sub>14</sub> showed an E<sub>max</sub> of 162 % at sst<sub>2</sub> receptors. Most of the compounds tested had similar efficacy to SRIF<sub>14</sub>, except cortistatin analogues, L362,855 and BIM 23052, which acted as partial agonists.

BIM 23056 did not stimulate [<sup>35</sup>S]GTPγS binding at any of the receptor subtypes, and the cycloantagonist SA was also devoid of activity at sst<sub>2</sub> and sst<sub>3</sub> receptors. Since BIM 23056 and the SA compound revealed no or only very low agonist activities at [<sup>35</sup>S]GTPγS binding, both peptides were tested for their potential antagonist activity on SRIF<sub>14</sub>-stimulated [<sup>35</sup>S]GTPγS binding (table 3; figure 4).

**Figure 3:** Stimulation of specific [ $^{35}$ S]GTP $\gamma$ S binding to microsome preparations from CCL39 cells expressing human sst $_{2-5}$  receptors by SRIF analogues.



Microsomes of transfected cells (sst $_2$ , sst $_3$ , sst $_4$ : 4  $\mu$ g protein; sst $_5$ : 2  $\mu$ g protein) were incubated with [ $^{35}$ S]GTP $\gamma$ S (0.2 nM), the indicated concentrations of SRIF $_{14}$  (■), SRIF $_{28}$  (▲), CST $_{17}$  (▼), CGP 23996 (◆), seglitide (●), or octreotide ( $\Delta$ ) in the presence of 5 mM MgCl $_2$ , 1  $\mu$ M GDP, and 100 mM NaCl. Graphs represent the percentage of specific [ $^{35}$ S]GTP $\gamma$ S binding stimulated by 10  $\mu$ M SRIF $_{14}$ , which was included in each experiment. The data points show one representative example of 3 different experiments performed in triplicates.

No antagonist activity could be measured for the “cycloantagonist” SA at sst $_{2-5}$  receptors, but rather a slightly increased pEC $_{50}$  of SRIF $_{14}$  when tested in the presence of SA (1  $\mu$ M final concentration). BIM 23056 (1  $\mu$ M) was devoid of effect and may have to be tested at higher concentrations.

The following rank order of potency in stimulating [ $^{35}\text{S}$ ]GTP $\gamma$ S binding at sst<sub>2</sub> receptors was observed: seglitide > SRIF<sub>14</sub> > LTT-SRIF<sub>28</sub> > octreotide  $\approx$  [Tyr<sup>3</sup>]octreotide > [Tyr<sup>10</sup>]CST<sub>14</sub> > SRIF<sub>28</sub> > CGP 23996 > BIM 23052  $\approx$  CST<sub>17</sub> > L362,855. The [ $^{35}\text{S}$ ]GTP $\gamma$ S binding profiles of human sst<sub>2</sub> receptors were correlated to their pharmacological profiles determined in radioligand binding experiments (tables 4 and 5; figure 5).

The [ $^{35}\text{S}$ ]GTP $\gamma$ S binding profile correlated modestly with [ $^{125}\text{I}$ ]LTT-SRIF<sub>28</sub>, [ $^{125}\text{I}$ ]CGP 23996 and [ $^{125}\text{I}$ ][Tyr<sup>3</sup>]octreotide binding profiles ( $r = 0.596- 0.699$ ), and not at all with [ $^{125}\text{I}$ ][Tyr<sup>10</sup>]CST<sub>14</sub> binding.

### Hsst<sub>3</sub> receptors

SRIF<sub>14</sub> displayed an E<sub>max</sub> of 220 % at sst<sub>3</sub> receptors. The somatostatin analogues, CGP 23996 and BIM 23052 had similar efficacy to SRIF<sub>14</sub>. The cortistatin and octreotide analogues, seglitide, and L362,855 acted as partial agonists whereas BIM 23056 and SA were virtually devoid of activity. BIM 23056 (1  $\mu\text{M}$  final concentration) behaved as an antagonist on SRIF<sub>14</sub>-stimulated [ $^{35}\text{S}$ ]GTP $\gamma$ S binding ( $\text{pK}_b = 6.33 \pm 0.24$ ) whereas SA at 1  $\mu\text{M}$  showed no antagonism. The following rank order of potency in stimulating [ $^{35}\text{S}$ ]GTP $\gamma$ S binding was observed at sst<sub>3</sub> receptors: LTT-SRIF<sub>28</sub>  $\approx$  SRIF<sub>14</sub> > CGP 23996 > SRIF<sub>28</sub> > [Tyr<sup>10</sup>]CST<sub>14</sub>  $\approx$  octreotide  $\approx$  CST<sub>17</sub> > BIM 23052  $\approx$  L362,855 > seglitide > [Tyr<sup>3</sup>]octreotide. The [ $^{35}\text{S}$ ]GTP $\gamma$ S binding profile of human sst<sub>3</sub> receptors was compared to their pharmacological profiles determined in radioligand binding experiments (tables 4 and 5; figure 5). The affinities obtained with [ $^{125}\text{I}$ ][Tyr<sup>10</sup>]CST<sub>14</sub> and [ $^{125}\text{I}$ ]CGP 23996 correlated somewhat less with [ $^{35}\text{S}$ ]GTP $\gamma$ S binding than affinities obtained with [ $^{125}\text{I}$ ]LTT-SRIF<sub>28</sub> ( $r = 0.743, 0.757$  and  $0.882$ , respectively).

Hsst<sub>4</sub> receptors

SRIF<sub>14</sub> displayed an E<sub>max</sub> of 148 % at sst<sub>4</sub> receptors. Most of the compounds tested had similar efficacy to SRIF<sub>14</sub>, except octreotide analogues, and SA which acted as partial agonists. BIM 23056, at 1 μM, did not stimulate [<sup>35</sup>S]GTPγS binding, but was also devoid of antagonist activity. The following rank order of potency in stimulating [<sup>35</sup>S]GTPγS binding was observed at sst<sub>4</sub> receptors: CGP 23996 > SRIF<sub>14</sub> > CST<sub>17</sub> ≈ SRIF<sub>28</sub> > LTT-SRIF<sub>28</sub> ≈ [Tyr<sup>10</sup>]CST<sub>14</sub> > BIM 23052 > octreotide ≈ [Tyr<sup>3</sup>]octreotide ≈ cycloantagonist SA. The [<sup>35</sup>S]GTPγS binding profile of human sst<sub>4</sub> receptors was correlated to the pharmacological profiles determined in radioligand binding experiments (tables 4 and 5; figure 5). The radioligand binding profiles of all tested radioligands correlated well with corresponding [<sup>35</sup>S]GTPγS binding profile (r = 0.867 - 0.897).

**Table 3:** Antagonistic activity of BIM 23056 and cycloantagonist SA (10<sup>-6</sup> M final concentration) on SRIF<sub>14</sub>-stimulated [<sup>35</sup>S]GTPγS binding at human sst<sub>2,5</sub> receptors: comparison of pEC<sub>50</sub>-values (-log M), E<sub>max</sub>-values [% stimulation], and pK<sub>B</sub>-values ± SEM of 3 independent determinations

	SRIF <sub>14</sub>		SRIF <sub>14</sub> + cycloantagonist SA			SRIF <sub>14</sub> +BIM 23056		
	E <sub>max</sub>	pEC <sub>50</sub>	E <sub>max</sub>	pEC <sub>50</sub>	pK <sub>B</sub>	E <sub>max</sub>	pEC <sub>50</sub>	pK <sub>B</sub>
CCL39/ hsst <sub>2</sub>	162 ± 3	6.95 ± 0.05	171 ± 6	7.53 ± 0.06	-	169 ± 5	7.74 ± 0.04	-
CCL39/ hsst <sub>3</sub>	220 ± 8	7.32 ± 0.11	161 ± 8	7.38 ± 0.06	-	153 ± 8	6.72 ± 0.17	6.33 ± 0.24
CCL39/ hsst <sub>4</sub>	148 ± 3	8.05 ± 0.17	126 ± 4	8.67 ± 0.09	-	126 ± 1	8.73 ± 0.13	-
CCL39/ hsst <sub>5</sub>	266 ± 19	8.39 ± 0.12	158 ± 5	8.85 ± 0.03	-	137 ± 7	8.19 ± 0.04	5.84 ± 0.17



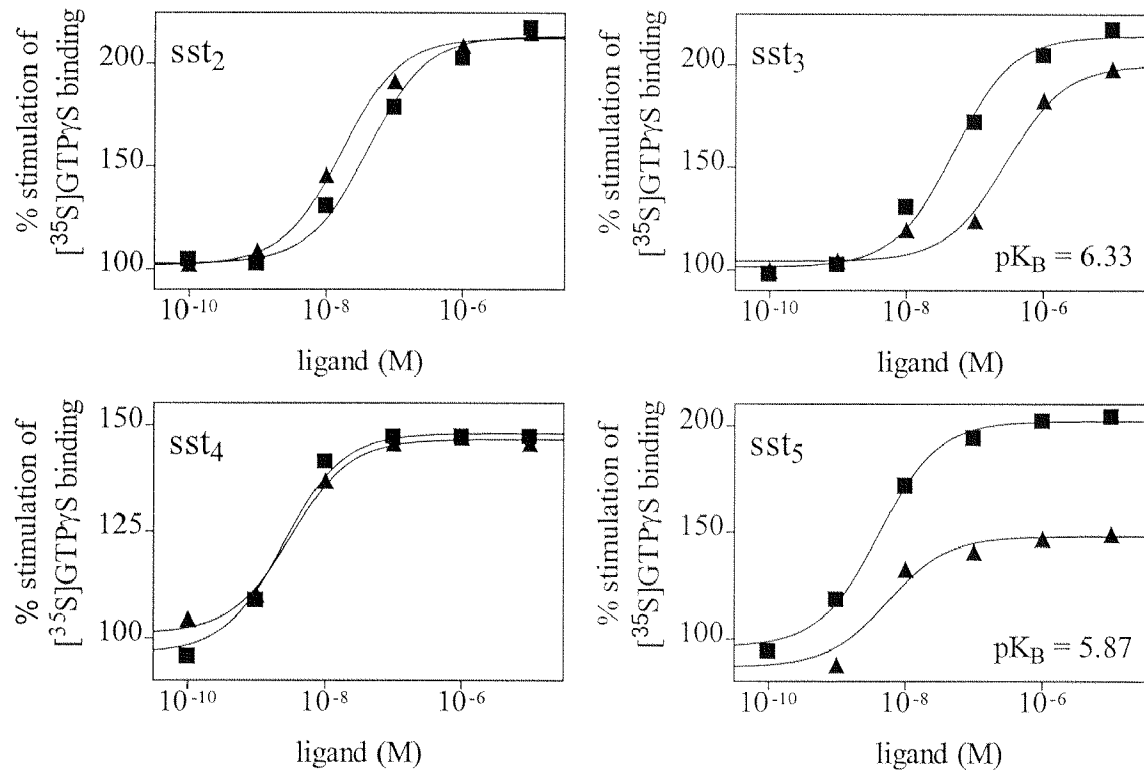
## Hsst<sub>5</sub> receptors

SRIF<sub>14</sub> displayed an E<sub>max</sub> of 255 % at sst<sub>5</sub> receptors. All compounds tested were close to full agonists compared to SRIF<sub>14</sub>, the least efficacious compounds showing about 70 % intrinsic activity. Only BIM 23056 was devoid of agonist activity. When tested as an antagonist, an apparent pK<sub>B</sub> of 5.84 was determined, but the antagonism appeared to be non competitive. The following rank order of potency in stimulating [<sup>35</sup>S]GTPγS binding at sst<sub>5</sub> receptors was observed: SRIF<sub>14</sub> > CST<sub>17</sub> ≈ seglitide > SRIF<sub>28</sub> ≈ LTT-SRIF<sub>28</sub> > [Tyr<sup>10</sup>]CST<sub>14</sub> > CGP 23996 > octreotide ≈ BIM 23052 > [Tyr<sup>3</sup>]octreotide > L362,855 > SA. [<sup>35</sup>S]GTPγS binding profiles of human sst<sub>5</sub> receptors were correlated to their pharmacological profiles determined in radioligand binding experiments (tables 4 and 5; figure 5). At sst<sub>5</sub> receptors, the binding profiles of all tested radioligands correlated highly with their corresponding [<sup>35</sup>S]GTPγS binding profile (r = 0.814 - 0.874).

### 6.3. Discussion

We have reported previously some rather marked differences in B<sub>max</sub>-values and ligand affinities at human sst<sub>5</sub> receptors stably expressed in CCL39 cells using the four agonist radioligands [<sup>125</sup>I]LTT-SRIF<sub>28</sub>, [<sup>125</sup>I][Tyr<sup>10</sup>]CST<sub>14</sub>, [<sup>125</sup>I]CGP 23996 and [<sup>125</sup>I][Tyr<sup>3</sup>]octreotide. On the other hand, such differences were not observed at human sst<sub>1,4</sub> receptors expressed in the same cells (Siehler et al., 1998a, submitted (a)), although a similar situation was noticed with the fish sst<sub>3</sub> receptor (Siehler et al, 1999). The non-hydrolysable GTP-analogue guanylylimidodiphosphate (GppNHp) inhibited radioligand binding to various degrees even at a single receptor subtype.

**Figure 4:** Antagonist activity of BIM 23056 on SRIF<sub>14</sub>-stimulated [<sup>35</sup>S]GTPγS binding at human SRIF receptor subtypes.



Microsomes of SRIF receptor transfected CCL39 cells were incubated with [<sup>35</sup>S]GTPγS (0.2 nM), the indicated concentrations of SRIF<sub>14</sub> and either without (■) or with BIM 23056 (▲) (1 μM final concentration), in the presence of 5 mM MgCl<sub>2</sub>, 1 μM GDP, and 100 mM NaCl. Graphs show the percentage of specific [<sup>35</sup>S]GTPγS binding stimulated by 10 μM SRIF<sub>14</sub>, which was included in each experiment. The curves represent one example of 3 different experiments performed in triplicates. pK<sub>B</sub>-values ± SEM are shown in the graphs.

The data suggested, that [<sup>125</sup>I][Tyr<sup>3</sup>]octreotide and [<sup>125</sup>I]CGP 23996, which defined higher ligand affinities, label predominantly a G-protein-coupled sst<sub>5</sub> receptor population, and therefore lower receptor densities; whereas the agonists [<sup>125</sup>I]LTT-SRIF<sub>28</sub> and [<sup>125</sup>I][Tyr<sup>10</sup>]CST<sub>14</sub> seemed to label G-protein-coupled and -uncoupled sst<sub>5</sub> receptors i.e. higher receptor densities (Siehler et al., submitted (a)), in spite of the fact, that the non-iodinated ligands behave as full agonists in second messenger experiments (De Lecea et al., 1996; Hoyer et al., 1994b).

In addition, we noticed that rank orders of affinity defined with the different radioligands at the same receptors may vary to a significant extent. These data do not fit to the allosteric ternary complex model (De Lean et al., 1980; Lefkowitz et al., 1993; Samama et al., 1993), but rather suggest various agonist-specific receptor states.

Therefore, [<sup>35</sup>S]GTPγS binding was established at sst<sub>5</sub> receptors. Increasing GDP or NaCl concentrations lead to decreased pEC<sub>50</sub>'s for SRIF<sub>14</sub>, whereas E<sub>max</sub> was increased. GTPγS has a higher affinity than GDP for the agonist/ receptor/ G-protein complex, but high GDP concentrations will inhibit GTPγS binding (Gilman, 1987). Hence, higher agonist concentrations might be needed to stimulate [<sup>35</sup>S]GTPγS binding in the presence of high GDP; on the other hand, such conditions allow a better gain in the system (signal/ noise).

Sodium ions are thought to increase the receptor/ G-protein interactions (Costa et al., 1990), and thereby might increase ligand-stimulated [<sup>35</sup>S]GTPγS binding. On the other hand, agonist binding to SRIF receptors is regulated by sodium binding to an allosteric receptor site: while receptors of the SRIF<sub>2</sub>-family (sst<sub>1</sub>, sst<sub>4</sub>) are less sodium-sensitive, sodium ions inhibit agonist binding to SRIF<sub>1</sub>-family members (sst<sub>2</sub>, sst<sub>3</sub>, sst<sub>5</sub>) (Horstman et al., 1990; Raynor et al., 1993a; 1993b; Reubi and Maurer, 1986). All five SRIF receptor subtypes reveal a conserved aspartate residue in the second or third transmembrane domain; upon exchange of this residue at sst<sub>2</sub> and sst<sub>3</sub> receptors, the inhibition of agonist binding by sodium was abolished (Nehring et al., 1995; Kong et al., 1993). Eventually, 1 μM GDP and 100 mM NaCl were considered to be optimal for the study of agonist-stimulated [<sup>35</sup>S]GTPγS binding via SRIF receptors.

SRIF<sub>14</sub> stimulated [<sup>35</sup>S]GTPγS binding to 162 %, 220 %, 148 % and 266 % respectively of control levels at sst<sub>2</sub>, sst<sub>3</sub>, sst<sub>4</sub> and sst<sub>5</sub> receptors. By contrast, although coupling of sst<sub>1</sub> receptors to inhibition of adenylate cyclase activity is reported (Hoyer et al., 1994b; Patel et al., 1994), stimulation of [<sup>35</sup>S]GTPγS binding was almost not detectable at sst<sub>1</sub> receptors. The expression levels of the diverse G-protein subunits vary between different cell lines, and might be partially responsible for apparently deficient G-protein-coupling as has been reported for sst<sub>1</sub> receptors (see Hoyer et al, 1995a, 1995b).

**Table 4:** Human  $ss_{2,5}$  receptors: comparison of affinities ( $pK_d$ 's) of the receptors labelled with [ $^{125}I$ ]LTT-SRIF<sub>28</sub>, [ $^{125}I$ ][Tyr<sup>10</sup>]CST<sub>14</sub>, [ $^{125}I$ ]CGP 23996 or [ $^{125}I$ ][Tyr<sup>3</sup>]octreotide (Siehl et al., submitted (a)), and potencies ( $pEC_{50}$ 's) in stimulation of [ $^{35}S$ ]GTP $\gamma$ S binding (table 2); data are expressed as  $pK_d$ 's or  $pEC_{50}$ 's ( $-\log M$ ) or  $E_{max}$ -values [% stimulation] of 3 determinations

**Table 4(A)** CCL39/ $hsst_2$

	[ $^{125}I$ ]LTT-SRIF <sub>28</sub>	[ $^{125}I$ ][Tyr <sup>10</sup> ]CST <sub>14</sub>	[ $^{125}I$ ]CGP 23996	[ $^{125}I$ ][Tyr <sup>3</sup> ]octreotide	[ $^{35}S$ ]GTP $\gamma$ S	
	$pK_d$	$pK_d$	$pK_d$	$pK_d$	$E_{max}$	$pEC_{50}$
SRIF <sub>14</sub>	10.00	10.06	10.10	10.01	162	6.95
SRIF <sub>28</sub>	9.92	10.16	9.99	9.99	172	6.14
LTT-SRIF <sub>28</sub>	9.70	8.90	10.06	9.17	168	6.78
CST <sub>17</sub>	9.07	9.29	9.33	8.85	137	5.83
[Tyr <sup>10</sup> ]CST <sub>14</sub>	8.77	8.91	8.93	9.00	124	6.28
seglitide	9.96	9.62	9.82	9.81	185	7.39
CGP 23996	8.58	8.94	9.06	8.95	159	6.06
octreotide	9.19	9.11	9.16	9.10	158	6.52
[Tyr <sup>3</sup> ]octreotide	8.43	7.10	9.48	8.66	181	6.57
L362,855	8.36	8.79	8.69	8.79	132	5.65
BIM 23056	6.33	6.23	6.33	6.38	78	(-)
BIM 23052	8.30	8.50	8.76	8.55	133	5.91
cycloantagonist SA	5.40	5.74	5.80	5.77	102	(-)

However, negative coupling of  $ss_1$  receptors to adenylate cyclase activity could be measured in CCL39 cells (Siehl and Hoyer, submitted (c)), which might be explained by an amplification effect in the signalling cascade, since a single G-protein may activate or inhibit many effector molecules such as adenylate cyclase (Birnbauer and Birnbauer, 1995).

**Table 4(B)** CCL39/hsst<sub>3</sub>

	[ <sup>125</sup> I]LTT-SRIF <sub>28</sub>	[ <sup>125</sup> I][Tyr <sup>10</sup> ]CST <sub>14</sub>	[ <sup>125</sup> I]CGP 23996	[ <sup>35</sup> S]GTPγS	
	pK <sub>d</sub>	pK <sub>d</sub>	pK <sub>d</sub>	E <sub>max</sub>	pEC <sub>50</sub>
SRIF <sub>14</sub>	9.54	9.67	9.71	220	7.32
SRIF <sub>28</sub>	9.65	9.80	9.94	225	6.96
LTT-SRIF <sub>28</sub>	9.84	9.26	10.09	243	7.44
CST <sub>17</sub>	9.43	9.52	9.88	188	6.59
[Tyr <sup>10</sup> ]CST <sub>14</sub>	8.70	8.90	9.02	151	6.83
seglitide	6.88	7.89	7.68	159	5.78
CGP 23996	8.82	9.28	9.15	197	7.14
octreotide	7.88	8.60	8.44	150	6.70
[Tyr <sup>3</sup> ]octreotide	6.84	6.20	7.90	156	5.76
L362,855	7.62	8.25	8.29	128	6.27
BIM 23056	6.90	7.08	7.20	88	(-)
BIM 23052	8.42	9.55	9.71	212	6.29
cycloantagonist SA	6.23	7.08	6.88	116	(-)

The pEC<sub>50</sub>-values determined in [<sup>35</sup>S]GTPγS binding are obviously much lower than the respective pK<sub>d</sub>-values determined in radioligand binding assays, especially for sst<sub>2</sub> and sst<sub>3</sub> receptors. This may be due to the rather low density of receptors expressed in the CCL39 cells used here.

SRIF<sub>14</sub> stimulates [<sup>35</sup>S]GTPγS binding with a higher potency than SRIF<sub>28</sub>, at all four receptors. In CCL39 cells, SRIF<sub>14</sub> and SRIF<sub>28</sub> bind with similar high affinity to human sst<sub>3</sub> receptors (Siehler et al., 1998a, 1998b). In other studies, SRIF<sub>28</sub> shows higher affinity than SRIF<sub>14</sub> in radioligand and [<sup>35</sup>S]GTPγS binding assays at human sst<sub>3</sub> receptors expressed in CHO (e.g. Williams et al., 1997).

**Table 4(C)** CCL39/hsst<sub>4</sub>

	[ <sup>125</sup> I]LTT-SRIF <sub>28</sub>	[ <sup>125</sup> I][Tyr <sup>10</sup> ]CST <sub>14</sub>	[ <sup>125</sup> I]CGP 23996	[ <sup>35</sup> S]GTPγS	
	pK <sub>d</sub>	pK <sub>d</sub>	pK <sub>d</sub>	E <sub>max</sub>	pEC <sub>50</sub>
SRIF <sub>14</sub>	8.91	8.39	8.87	148	8.05
SRIF <sub>28</sub>	9.08	8.44	9.06	145	7.58
LTT-SRIF <sub>28</sub>	9.16	9.13	9.37	149	7.12
CST <sub>17</sub>	9.24	9.55	9.26	146	7.66
[Tyr <sup>10</sup> ]CST <sub>14</sub>	8.44	8.17	8.30	142	7.02
CGP 23996	8.77	8.67	8.62	151	8.12
octreotide	6.40	5.76	6.02	126	5.67
[Tyr <sup>3</sup> ]octreotide	6.29	6.17	5.89	131	5.49
BIM 23056	7.17	6.47	7.04	98	(-)
BIM 23052	8.63	8.20	8.13	154	6.42
cycloantagonist SA	6.48	6.07	6.29	126	5.57

The relative potency of CST<sub>17</sub> in stimulating [<sup>35</sup>S]GTPγS binding is equivalent to that of SRIF<sub>28</sub> and moderately lower than that of SRIF<sub>14</sub> at the receptors investigated here. Similarly, CST<sub>17</sub> has been reported to bind with similar high affinity to all SRIF receptor subtypes (Siehler et al., 1998a). Therefore, it cannot be decided which receptor subtype(s) may mediate the cortistatin-specific effects on neuronal depression and sleep modulation (De Lecea et al., 1996; Fukusumi et al., 1997). Although octreotide and seglitide show high affinity for sst<sub>5</sub> receptors (Siehler et al., 1998a), the relative potency of the two compounds compared to somatostatins in [<sup>35</sup>S]GTPγS binding, suggest octreotide and seglitide to be relatively more selective for sst<sub>2</sub> receptors. Nevertheless, octreotide, when used to inhibit growth of hormone-secreting tumours (Lamberts et al., 1991), might activate sst<sub>2</sub> and sst<sub>5</sub> receptors when both receptor subtypes are expressed.

**Table 4(D)** CCL39/hsst<sub>5</sub>

	[ <sup>125</sup> I]LTT-SRIF <sub>28</sub>	[ <sup>125</sup> I][Tyr <sup>10</sup> ]CST <sub>14</sub>	[ <sup>125</sup> I]CGP 23996	[ <sup>125</sup> I][Tyr <sup>3</sup> ]octreotide	[ <sup>35</sup> S]GTPγS	
	pK <sub>d</sub>	pK <sub>d</sub>	pK <sub>d</sub>	pK <sub>d</sub>	E <sub>max</sub>	pEC <sub>50</sub>
SRIF <sub>14</sub>	9.53	9.01	9.82	9.87	255	8.39
SRIF <sub>28</sub>	9.39	9.18	10.15	10.30	268	7.65
LTT-SRIF <sub>28</sub>	8.47	8.12	9.70	9.60	278	7.63
CST <sub>17</sub>	9.54	9.37	10.21	9.85	231	7.94
[Tyr <sup>10</sup> ]CST <sub>14</sub>	8.67	8.06	9.77	9.65	215	7.43
seglitide	8.70	9.14	10.22	10.18	240	7.89
CGP 23996	6.59	6.67	8.26	8.68	211	7.12
octreotide	7.17	7.31	8.96	9.48	278	6.89
[Tyr <sup>3</sup> ]octreotide	6.49	6.00	8.03	8.41	220	6.56
L362,855	7.17	7.17	8.72	9.17	231	6.29
BIM 23056	7.17	6.68	7.77	8.32	100	(-)
BIM 23052	7.92	7.45	9.59	9.28	266	6.80
cycloantagonist SA	6.38	6.02	7.77	8.25	222	5.82

BIM 23056 behaves as an antagonist on SRIF<sub>14</sub>-induced [<sup>35</sup>S]GTPγS binding with apparent pK<sub>B</sub>-value of 6.33 at hsst<sub>3</sub> receptors and 5.84 at hsst<sub>5</sub> receptors; whereas neither agonism nor antagonism could be shown (at 1 μM) at sst<sub>2</sub> or sst<sub>4</sub> receptors. The antagonism at sst<sub>5</sub> receptors is not surmountable and needs further investigations. The so-called antagonist SA, is devoid of antagonist activity at sst<sub>2</sub> or sst<sub>3</sub> receptors, whereas it is almost a full agonist at sst<sub>4</sub> and sst<sub>5</sub> receptors. BIM 23056 was previously described as sst<sub>3</sub>-selective agonist (Patel & Srikant, 1994), but this is not replicated here. BIM 23056 was already reported as a competitive hsst<sub>5</sub> receptor-antagonist on [<sup>35</sup>S]GTPγS binding in CHO-K1 cells, with a higher pK<sub>B</sub> (= 7.44) (Williams et al., 1997). In the same sst<sub>5</sub> receptor-expressing cells BIM 23056 was described to potently antagonise SRIF<sub>14</sub>-induced phosphoinositide stimulation as well as SRIF<sub>14</sub>-induced increase of intracellular Ca<sup>2+</sup> (pK<sub>B</sub> = 7.4 and 8.0, respectively) (Wilkinson et al., 1996; 1997).

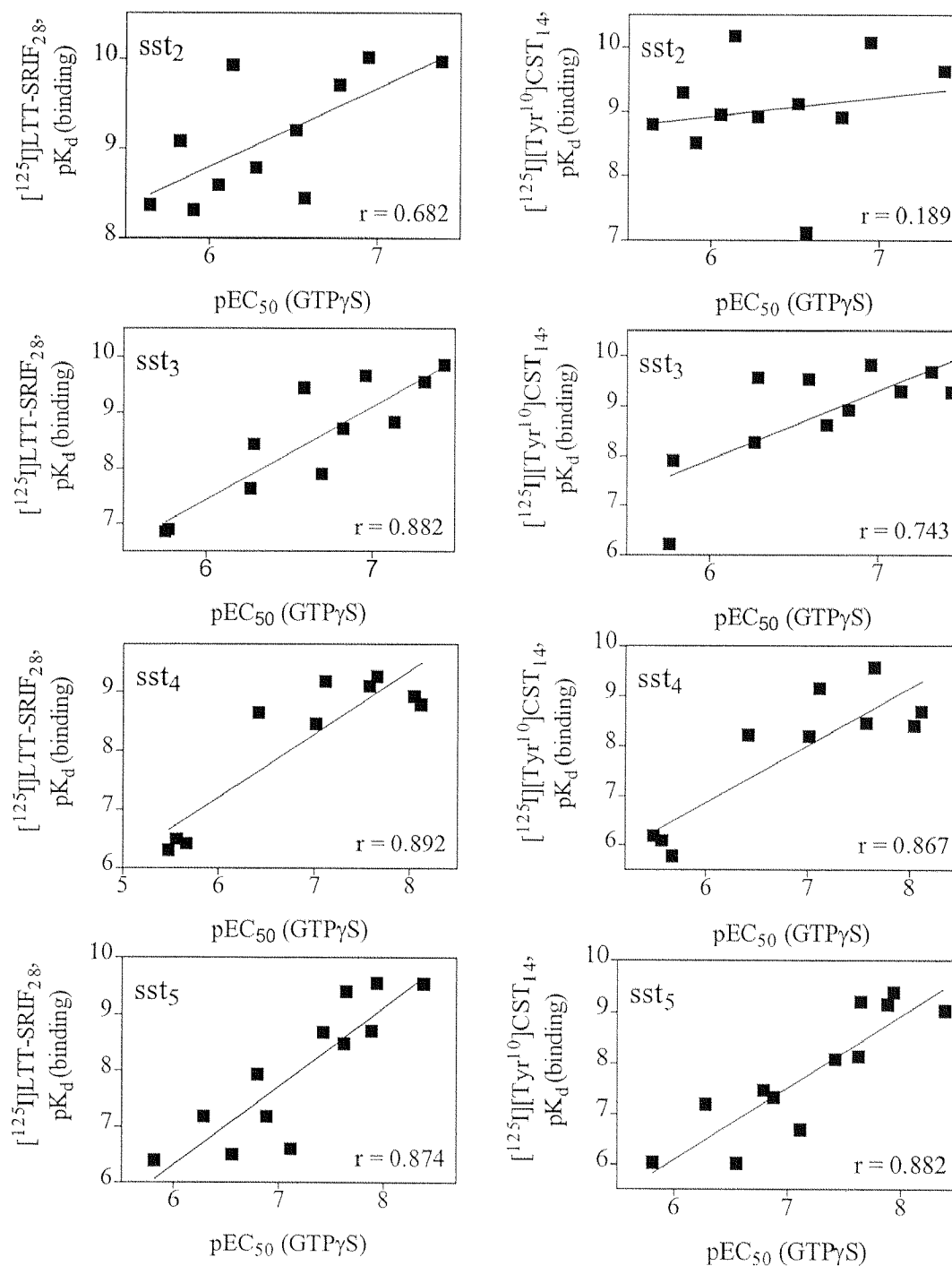
**Table 5:** Correlation coefficients (r) of correlation analyses between [<sup>125</sup>I]LTT-SRIF<sub>28</sub>, [<sup>125</sup>I][Tyr<sup>10</sup>]CST<sub>14</sub>, [<sup>125</sup>I]CGP 23996 or [<sup>125</sup>I][Tyr<sup>3</sup>]octreotide binding (pK<sub>d</sub>) and stimulation of [<sup>35</sup>S]GTPγS binding (pEC<sub>50</sub>) at human sst<sub>2,5</sub> receptors. Data used for correlation are shown in table 4(A)-(D).

	[ <sup>125</sup> I]LTT-SRIF <sub>28</sub>	[ <sup>125</sup> I][Tyr <sup>10</sup> ]CST <sub>14</sub>	[ <sup>125</sup> I]CGP 23996	[ <sup>125</sup> I][Tyr <sup>3</sup> ]octreotide
CCL39/ hsst <sub>2</sub>	0.682	0.189	0.699	0.596
CCL39/ hsst <sub>3</sub>	0.882	0.743	0.757	-
CCL39/ hsst <sub>4</sub>	0.892	0.867	0.897	-
CCL39/ hsst <sub>5</sub>	0.874	0.882	0.831	0.814

Evidently, G-protein coupling as measured in radioligand binding or second messenger experiments and G-protein activation measured by [<sup>35</sup>S]GTPγS binding may be rather divergent at times. The two GTP-analogues GppNHp and GTPγS have different G-protein binding properties: GTPγS binds to recombinant G<sub>o</sub> or G<sub>11</sub> with higher affinity than GppNHp; in line with the present data, GTPγS activates G<sub>o</sub> more potently than does GppNHp. In addition, when compared to GTP both non-hydrolysable GTP-analogues tend to hyperactivate G-proteins, and therefore are different from the naturally occurring and hydrolysable GTP (Rebois et al., 1997; Remmers and Neubig, 1996). The correlation between radioligand and [<sup>35</sup>S]GTPγS binding is reasonably good at sst<sub>3</sub>, sst<sub>4</sub> and sst<sub>5</sub> receptors, which may be surprising in the latter case, since radioligand binding has shown some rather marked differences when the profiles determined by the different radioligands are compared at hsst<sub>5</sub>. Also rather surprising, is the fact that at sst<sub>2</sub> receptors, the correlations are not particularly impressive (especially with [<sup>125</sup>I][Tyr<sup>10</sup>]CST<sub>14</sub> binding), although it should be kept in mind that the ranges were rather narrow between the most and least potent compounds.



**Figure 5:** Human recombinant  $sst_{2-5}$  receptors expressed in CCL39 cells: correlation between [ $^{125}$ I]LTT-SRIF $_{28}$  (left column) or [ $^{125}$ I][Tyr $^{10}$ ]CST $_{14}$  (right column) binding and agonist-stimulated [ $^{35}$ S]GTP $\gamma$ S binding.



Data are from table 4(A)-(D), and represent pK<sub>d</sub>-values derived from radioligand binding of human  $sst_{2-5}$  receptors and pEC<sub>50</sub>-values obtained from [ $^{35}$ S]GTP $\gamma$ S binding assays. Correlation coefficients (r) are indicated in all plots.

However, what appears to be clear is that the individual rank orders of potency determined using either method do not fit very well, and correlations are only obtained because altogether there is a general agreement at a given receptor more than an exact replication from one test to another. This suggests that at any given receptor, agonists' rank orders of potency (not to mention absolute affinity values which vary profoundly) are not as well defined as may be anticipated. We are investigating these aspects further by analysing additional signalling pathways.

## 7.1. Abstract

The five human somatostatin receptor subtypes (hsst<sub>1-5</sub>) were stably expressed in CCL39 cells (Chinese hamster lung fibroblast cells) to study the inhibition of forskolin-stimulated adenylate cyclase (FSAC) activity induced by somatostatin (SRIF), cortistatin (CST) and SRIF peptide analogues. Inhibition of FSAC was observed with all five receptors, although the maximal effects produced by SRIF<sub>14</sub> varied from around 40 (sst<sub>1</sub>, sst<sub>2</sub>, sst<sub>4</sub>) to 67 % (sst<sub>3</sub>, sst<sub>5</sub>) reflecting to some extent differences in receptor density. SRIF<sub>28</sub> was slightly more potent than SRIF<sub>14</sub> to inhibit FSAC at all five receptors, although the potency of the natural peptides SRIF<sub>14</sub>, SRIF<sub>28</sub> and CST<sub>17</sub> was generally similar with pEC<sub>50</sub>-values ranging from 7.5 to 8.7 depending on receptor and ligand.

At SRIF<sub>1</sub> receptors (sst<sub>2</sub>, sst<sub>3</sub>, sst<sub>5</sub>) most of the peptide analogues displayed full agonism (with some exceptions e.g. BIM 23056 at sst<sub>1,3</sub> and sst<sub>5</sub> receptors, and L362,855 and cycloantagonist SA at sst<sub>3</sub> receptors), whereas at SRIF<sub>2</sub> receptors these analogues tended to behave as partial agonists. BIM 23056 was an antagonist at sst<sub>3</sub> receptors (pK<sub>B</sub> = 6.33), but not at other receptors.

The AC inhibition profiles of sst<sub>1-5</sub> receptors were compared with the different radioligand binding profiles as well as with [<sup>35</sup>S]GTPγS binding profile for sst<sub>2,5</sub> receptors. High correlations were observed between FSAC inhibition, radioligand binding and [<sup>35</sup>S]GTPγS binding profiles at sst<sub>3</sub>, sst<sub>4</sub> and sst<sub>5</sub> receptors; by contrast, correlation coefficients at sst<sub>1</sub> and sst<sub>2</sub> receptors were low, and the binding profiles of [<sup>125</sup>I][Tyr<sup>10</sup>]CST<sub>14</sub> correlated poorly. In line with these findings, the FSAC inhibition and [<sup>35</sup>S]GTPγS binding correlated poorly at sst<sub>2</sub> receptors (sst<sub>1</sub> receptors show no significant induction of [<sup>35</sup>S]GTPγS binding). The apparent lack of or weak relationship between FSAC, radioligand or [<sup>35</sup>S]GTPγS binding observed for some SRIF receptors, suggest that different active states may exist for these receptors, which may favour one of transduction cascade over others.

## 7.2. Results

Inhibition of forskolin-stimulated adenylate cyclase (FSAC) activity was determined using a radioimmunoassay measuring intracellular cyclic adenosine monophosphate (cAMP) levels in cells expressing one of the five SRIF receptors (tables 1A & 1B; figure 1).

### SRIF<sub>1</sub> receptors

#### Sst<sub>2</sub> receptors:

The most potent agonist at sst<sub>2</sub> receptors was seglitide (pEC<sub>50</sub> = 10.03) and the rank order of potencies was: seglitide > [Tyr<sup>3</sup>]octreotide > SRIF<sub>28</sub> > octreotide ≈ LTT-SRIF<sub>28</sub> > SRIF<sub>14</sub> ≈ CST<sub>17</sub> > CGP 23996 > L362,855 ≈ [Tyr<sup>10</sup>]CST<sub>14</sub> ≈ BIM 23052. Most of the peptides showed full or close to full agonism with intrinsic activities of 85- 110 % compared to that of SRIF<sub>14</sub>, which inhibited FSAC by 33 ± 1 %. Interestingly, CST<sub>17</sub> had only low efficacy (44 % of SRIF<sub>14</sub>), whereas BIM 23056 and the “cycloantagonist” were almost devoid of agonism. These two compounds however did not produce significant antagonism when tested at 1 μM against SRIF<sub>14</sub> (not shown).

#### Sst<sub>5</sub> receptors:

At sst<sub>5</sub> receptors, the most potent agonist was again seglitide (pEC<sub>50</sub> = 9.33). The rank order of potency was: seglitide > SRIF<sub>28</sub> ≈ CST<sub>17</sub> > SRIF<sub>14</sub> > LTT-SRIF<sub>28</sub> > [Tyr<sup>10</sup>]CST<sub>14</sub> ≈ octreotide > BIM 23052 ≈ [Tyr<sup>3</sup>]octreotide > CGP 23996 > L362,855 > BIM 23056 > cycloantagonist SA. Similarly to sst<sub>2</sub> receptors, most compounds displayed full agonism with intrinsic activities in the range 80- 120 % of SRIF<sub>14</sub>, which inhibited FSAC by 62 ± 2 %. Octreotide was less potent at sst<sub>5</sub> than at sst<sub>2</sub> receptors. BIM 23056 displayed partial agonism (47 %). Neither, BIM 23056 nor SA did produce significant antagonism when tested at 1 μM against SRIF<sub>14</sub> (not shown).

**Table 1:** Inhibition of forskolin-stimulated adenylate cyclase activity by human  $ssst_{1-5}$  receptors

Table 1(A)	CCL39/ $hsst_1$		CCL39/ $hsst_4$	
	$E_{max}$	$pEC_{50}$	$E_{max}$	$pEC_{50}$
SRIF <sub>14</sub>	100 ± 7	8.21 ± 0.09	100 ± 5	8.53 ± 0.21
SRIF <sub>28</sub>	114 ± 10	8.29 ± 0.12	100 ± 5	8.53 ± 0.16
LTT-SRIF <sub>28</sub>	100 ± 7	7.18 ± 0.02	78 ± 11	7.85 ± 0.08
CST <sub>17</sub>	62 ± 3	8.13 ± 0.14	65 ± 5	8.30 ± 0.17
[Tyr <sup>10</sup> ]CST <sub>14</sub>	100 ± 3	6.82 ± 0.05	86 ± 5	7.61 ± 0.13
CGP 23996	97 ± 17	7.18 ± 0.20	95 ± 5	8.27 ± 0.20
octreotide	38 ± 0	(-)	78 ± 3	6.00 ± 0.25
[Tyr <sup>3</sup> ]octreotide	14 ± 7	(-)	81 ± 5	5.79 ± 0.19
BIM 23056	55 ± 17	(-)	86 ± 3	7.06 ± 0.08
BIM 23052	104 ± 7	6.69 ± 0.03	105 ± 3	7.20 ± 0.23
cycloantagonist SA	79 ± 7	6.48 ± 0.05	73 ± 0	6.03 ± 0.07

Sst<sub>3</sub> receptors:

The most potent antagonist to inhibit forskolin-stimulated cAMP production in  $ssst_3$  receptor-expressing cells was LTT-SRIF<sub>28</sub> ( $pEC_{50} = 8.40$ ). The rank order was: LTT-SRIF<sub>28</sub> > SRIF<sub>28</sub> > CGP 23996 ≈ SRIF<sub>14</sub> > CST<sub>17</sub> ≈ BIM 23052 > octreotide > [Tyr<sup>10</sup>]CST<sub>14</sub> ≈ L362,855 ≈ seglitide > cycloantagonist SA ≈ [Tyr<sup>3</sup>]octreotide. Similarly to the activities measured at the other two SRIF<sub>1</sub> receptors, most of the compounds displayed full agonism when compared to SRIF<sub>14</sub> (67 ± 8 % inhibition of FSAC), in the range 80- 100 %. There were two noticeable exceptions, BIM 23056 and the cycloantagonist SA with values around 30 %. SA did not produce significant antagonism when tested at 1 μM against SRIF<sub>14</sub>, whereas BIM 23056 at 1 μM produced a shift in the CRC with an apparent  $pK_B$  of 6.33 ± 10 (figure 2).

Table 1(B)	CCL39/hsst <sub>2</sub>		CCL39/hsst <sub>5</sub>		CCL39/hsst <sub>3</sub>	
	E <sub>max</sub>	pEC <sub>50</sub>	E <sub>max</sub>	pEC <sub>50</sub>	E <sub>max</sub>	pEC <sub>50</sub>
SRIF <sub>14</sub>	100 ± 11	8.36 ± 0.22	100 ± 10	8.33 ± 0.24	100 ± 14	7.76 ± 0.17
SRIF <sub>28</sub>	111 ± 7	8.72 ± 0.12	109 ± 4	8.45 ± 0.12	94 ± 11	8.19 ± 0.20
LTT-SRIF <sub>28</sub>	111 ± 7	8.33 ± 0.05	106 ± 4	7.84 ± 0.17	97 ± 5	8.40 ± 0.20
CST <sub>17</sub>	44 ± 11	8.15 ± 0.10	92 ± 0	8.38 ± 0.26	75 ± 3	7.47 ± 0.07
[Tyr <sup>10</sup> ]CST <sub>14</sub>	107 ± 7	6.80 ± 0.19	109 ± 10	7.69 ± 0.10	84 ± 3	6.80 ± 0.16
seglitide	107 ± 15	10.03 ± 0.13	119 ± 12	9.33 ± 0.25	89 ± 11	6.68 ± 0.12
CGP 23996	100 ± 7	7.79 ± 0.07	112 ± 6	7.07 ± 0.04	89 ± 3	7.84 ± 0.16
octreotide	104 ± 4	8.44 ± 0.21	123 ± 4	7.68 ± 0.17	97 ± 2	7.01 ± 0.01
[Tyr <sup>3</sup> ]octreotide	115 ± 7	9.70 ± 0.16	118 ± 4	7.30 ± 0.04	81 ± 2	6.31 ± 0.01
L362,855	137 ± 4	6.87 ± 0.04	143 ± 4	6.81 ± 0.17	58 ± 17	6.70 ± 0.05
BIM 23056	22 ± 7	(-)	47 ± 8	6.60 ± 0.04	26 ± 2	(-)
BIM 23052	122 ± 29	6.74 ± 0.13	125 ± 10	7.40 ± 0.11	104 ± 2	7.43 ± 0.17
cycloantagonist SA	37 ± 4	(-)	100 ± 6	5.69 ± 0.04	32 ± 8	6.38 ± 0.08

Comparison of pEC<sub>50</sub> values (-log M) or E<sub>max</sub>-values [% inhibition] ± SEM of three or more experiments; E<sub>max</sub>-values were normalized to the maximal inhibition reached by SRIF<sub>14</sub> (E<sub>max</sub> = 100 % inhibition).

SRIF<sub>2</sub> receptors

Sst<sub>1</sub> receptors:

The most potent agonist to inhibit cAMP production via sst<sub>1</sub> receptors was SRIF<sub>28</sub> (pEC<sub>50</sub> = 8.33) and the rank order of potency was: SRIF<sub>28</sub> > CST<sub>17</sub> > SRIF<sub>14</sub> > LTT-SRIF<sub>28</sub> ≈ CGP 23996 > [Tyr<sup>10</sup>]CST<sub>14</sub> ≈ BIM 23052 > cycloantagonist SA. When taking SRIF<sub>14</sub> as the reference full agonist (39 ± 4 % inhibition of FSAC), most other analogues acted as partial agonists (including CST<sub>17</sub>) with efficacy values ranging from 14 to 80 % the least efficacious being octreotide and [Tyr<sup>3</sup>]octreotide.

BIM 23056 and SA did not produce significant antagonism when tested at 1  $\mu$ M against SRIF<sub>14</sub> (not shown).

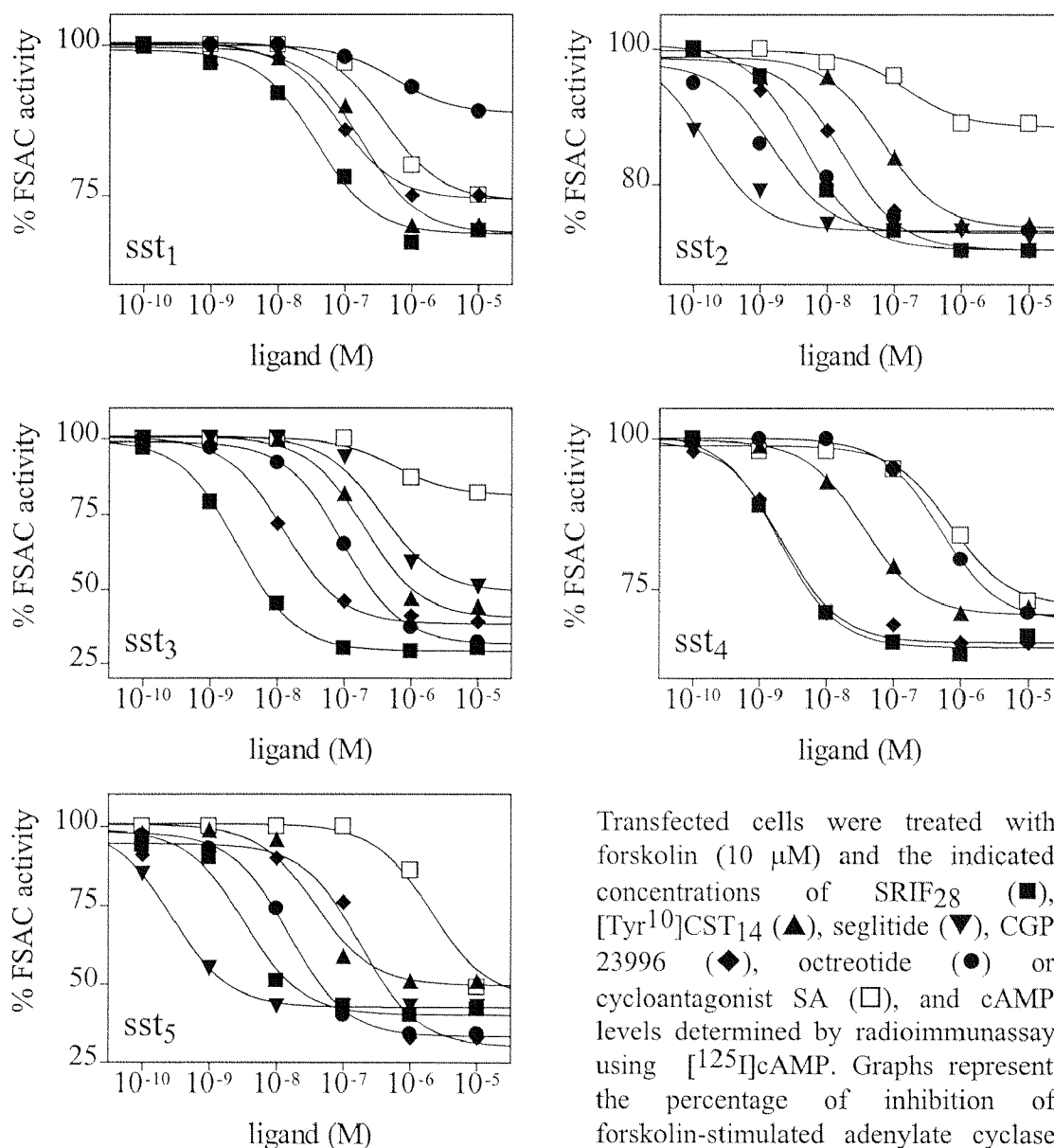
Sst<sub>4</sub> receptors:

Inhibition of cAMP production in sst<sub>4</sub> receptor-expressing CCL39 cells showed SRIF<sub>28</sub> to be the most potent agonist (pEC<sub>50</sub> = 8.45) and was characterised by the rank order of potency: SRIF<sub>28</sub> > CST<sub>17</sub>  $\approx$  CGP 23996 > SRIF<sub>14</sub> > LTT-SRIF<sub>28</sub> > [Tyr<sup>10</sup>]CST<sub>14</sub> > BIM 23052 > BIM 23056 > cycloantagonist SA  $\approx$  octreotide > [Tyr<sup>3</sup>]octreotide. None of the compounds tested had an intrinsic activity lower than 65 % of that of SRIF<sub>14</sub> (37  $\pm$  3 %), thus all compounds were very efficacious partial or full agonists.

Comparison of inhibition of FSAC at sst<sub>1,5</sub> with radioligand binding

The pharmacological profiles determined in radioligand binding and inhibition of FSAC assays were compared for all five SRIF receptors (table 2; figure 3). At hsst<sub>5</sub> receptors, the binding profiles of all four radioligands correlated highly significantly with the FSAC profile, although somewhat less for [<sup>125</sup>I]LTT-SRIF<sub>28</sub> binding. Similarly, at sst<sub>3</sub> and sst<sub>4</sub> receptors, the binding profiles of [<sup>125</sup>I]LTT-SRIF<sub>28</sub>, [<sup>125</sup>I][Tyr<sup>10</sup>]CST<sub>14</sub> and [<sup>125</sup>I]CGP 23996 correlated highly significantly with the inhibition of FSAC (correlation coefficient  $r = 0.83 - 0.95$ , table 3). At hsst<sub>1</sub> receptors, binding and inhibition of FSAC were statistically significant, although the correlation coefficients were rather modest (0.67- 0.80). The least convincing comparisons were established with the hsst<sub>2</sub> receptor: thus, [<sup>125</sup>I]LTT-SRIF<sub>28</sub>, [<sup>125</sup>I]CGP 23996 and [<sup>125</sup>I][Tyr<sup>3</sup>]octreotide binding correlated modestly with sst<sub>2</sub> receptor mediated inhibition of FSAC ( $r = 0.43 - 0.67$ ), whereas the [<sup>125</sup>I][Tyr<sup>10</sup>]CST<sub>14</sub> profile showed no correlation at all. The very poor correlation stems actually from [Tyr<sup>3</sup>]octreotide, which behaved as a rather weak ligand at [<sup>125</sup>I]LTT-SRIF<sub>28</sub> and especially [<sup>125</sup>I][Tyr<sup>10</sup>]CST<sub>14</sub> labelled sites, yet was one of the most potent agonists at FSAC.

**Figure 1:** Inhibition of forskolin-stimulated adenylate cyclase (FSAC) activity by SRIF peptides in CCL39 cells expressing human *sst*<sub>1-5</sub> receptors.



Transfected cells were treated with forskolin (10  $\mu$ M) and the indicated concentrations of SRIF<sub>28</sub> (■), [Tyr<sup>10</sup>]CST<sub>14</sub> (▲), seglitide (▼), CGP 23996 (◆), octreotide (●) or cycloantagonist SA (□), and cAMP levels determined by radioimmunoassay using [<sup>125</sup>I]cAMP. Graphs represent the percentage of inhibition of forskolin-stimulated adenylate cyclase activity. The data points represent one representative example of 3 different experiments. The mean of the pEC<sub>50</sub>-values  $\pm$  SEM of 3 determinations are shown in table 1.



### Comparison of inhibition of FSAC at sst<sub>1-5</sub> with [<sup>35</sup>S]GTPγS binding

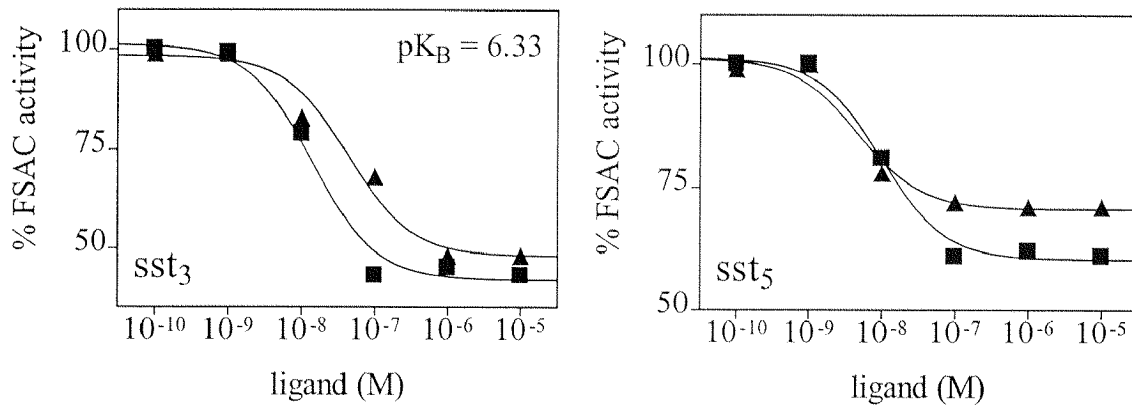
Inhibition of FSAC profiles and [<sup>35</sup>S]GTPγS binding profiles at human sst<sub>2-5</sub> receptors (table 2; figure 4) revealed statistically significant correlations at sst<sub>4</sub> receptors ( $r = 0.98$ , table 3) > sst<sub>5</sub> and sst<sub>3</sub> receptors ( $r = 0.88$  and  $0.83$ , respectively) > sst<sub>2</sub> receptors ( $r = 0.72$ ). [<sup>35</sup>S]GTPγS binding did not produce robust data with hsst<sub>1</sub> receptors. It can also be seen from table 2 that the rank orders of efficacy were more or less divergent depending on the receptor type.

### 7.3. Discussion

There are three main signalling pathways known so far to be modulated by somatostatin receptors: the adenylate cyclase/ protein kinase A-pathway, the phospholipase C/ IP<sub>3</sub>-pathway, and the Ras/ Raf/ MAP kinase (mitogen-activated protein kinase)-pathway. In the present study, we measured the inhibition of forskolin-stimulated AC activity; forskolin stimulates directly and non selectively adenylate cyclases, although it is not established, whether all known AC isoforms are affected (Seamon et al., 1986). Thus, inhibition of forskolin-stimulated adenylate cyclase activity (FSAC) was determined in CCL39 cells expressing one of the five SRIF receptors. The maximal inhibition of cAMP production obtained via sst<sub>3</sub> and sst<sub>5</sub> receptors (e.g. for SRIF<sub>14</sub>:  $E_{max} = 67$  and  $62$  %, respectively) was larger than that produced by sst<sub>1</sub>, sst<sub>2</sub> and sst<sub>4</sub> receptors (SRIF<sub>14</sub>:  $E_{max} = 39$ ,  $33$  and  $37$  %, respectively). The natural peptides SRIF<sub>14</sub>, SRIF<sub>28</sub> and CST<sub>17</sub> were similarly potent to inhibit FSAC activity at human sst<sub>1-5</sub> receptors ( $pEC_{50}$ 's =  $8.11$ - $8.72$ ), although SRIF<sub>14</sub> and CST<sub>17</sub> were less potent at sst<sub>1</sub> receptors ( $pEC_{50} = 7.41$ ) and sst<sub>3</sub> receptors respectively ( $pEC_{50} = 7.47$ ).

Overall, SRIF<sub>28</sub> seems to be slightly more potent and efficacious than SRIF<sub>14</sub> to inhibit cAMP production at the human SRIF receptor subtypes, whereas CST<sub>17</sub> tended to show only partial agonism.

**Figure 2:** Antagonistic activity of BIM 23056 on SRIF<sub>14</sub>-inhibited forskolin-stimulated adenylate cyclase (FSAC) activity at human sst receptor subtypes.



CCL39 cells transfected with sst<sub>3</sub> or sst<sub>5</sub> receptors were treated with forskolin (10  $\mu$ M), the indicated concentrations of SRIF<sub>14</sub>, and either without (■) or with BIM 23056 (▲) (1  $\mu$ M final concentration), and cAMP levels measured as described. Graphs show the percentage of inhibition of forskolin-stimulated adenylate cyclase activity. The data points represent one representative example of 3 different experiments. pK<sub>B</sub>-values  $\pm$  SEM are shown in the graphs.

BIM 23056 and the peptide SA inhibited FSAC with low efficacy; the E<sub>max</sub>-values of these peptides especially at SRIF<sub>1</sub> receptors (sst<sub>2</sub>, sst<sub>3</sub>, sst<sub>5</sub>) were very low. Therefore, the possible antagonism by both peptides on SRIF<sub>14</sub>-inhibited FSAC was studied. SA did not antagonise the effect of SRIF<sub>14</sub> at a concentration of 1  $\mu$ M, whereas BIM 23056 showed sst<sub>3</sub> receptor antagonism (pK<sub>B</sub> = 6.33), but not at the other four SRIF receptor subtypes.

In previous studies, SRIF<sub>28</sub>, CGP 23996, octreotide, and cycloantagonist SA revealed a similar cAMP inhibition profile at hsst<sub>1</sub> receptors expressed in HEK293 cells (Hoyer et al., 1995b); similarly for SRIF<sub>14</sub>, SRIF<sub>28</sub>, seglitide, CGP 23996, octreotide, BIM 23052 and cycloantagonist SA at hsst<sub>2</sub> receptors expressed in CHO cells (Schoeffter et al., 1995), although all pEC<sub>50</sub>'s were somewhat higher compared to the present study carried out in CCL39 cells.

**Table 2:** Human  $ss_{1,5}$  receptors: comparison of affinities ( $pK_d$ 's) of the receptors labelled with  $[^{125}I]$ LTT-SRIF<sub>28</sub>,  $[^{125}I]$ [Tyr<sup>10</sup>]CST<sub>14</sub>,  $[^{125}I]$ CGP 23996 or  $[^{125}I]$ [Tyr<sup>3</sup>]octreotide, efficacies ( $pEC_{50}$ 's) in stimulation of  $[^{35}S]$ GTP $\gamma$ S specific binding, and efficacies in inhibition of forskolin-stimulated adenylate cyclase (FSAC) activity (table 1).

**Table 2(A)** CCL39/hsst<sub>1</sub>

	$[^{125}I]$ LTT- SRIF <sub>28</sub>	$[^{125}I]$ [Tyr <sup>10</sup> ] CST <sub>14</sub>	$[^{125}I]$ CGP 23996	inhibition of FSAC activity	
	$pK_d$	$pK_d$	$pK_d$	$E_{max}$	$pEC_{50}$
SRIF <sub>14</sub>	9.12	9.08	8.95	100	8.21
SRIF <sub>28</sub>	9.22	9.26	9.38	114	8.29
LTT-SRIF <sub>28</sub>	9.22	9.28	9.13	100	7.18
CST <sub>17</sub>	9.61	9.61	9.48	62	8.13
[Tyr <sup>10</sup> ]CST <sub>14</sub>	8.56	9.04	8.32	100	6.82
CGP 23996	8.33	8.31	8.45	97	7.18
octreotide	6.65	6.41	6.23	38	(-)
[Tyr <sup>3</sup> ]octreotide	5.57	5.82	5.69	14	(-)
BIM 23056	6.61	6.46	6.56	55	(-)
BIM 23052	8.37	8.62	8.17	104	6.69
cycloantagonist SA	7.02	6.80	6.48	79	6.48

This difference may be due to methodology, since here cAMP levels were determined indirectly in a radioimmunoassay, while in previous studies formation of  $[^3H]$ cAMP was measured directly; when the latter method was applied to hsst<sub>5</sub> receptors expressed in CCL39 cells, SRIF<sub>28</sub>, seglitide and octreotide produced  $pEC_{50}$ -values of  $9.15 \pm 0.08$ ,  $9.66 \pm 0.09$  and  $8.46 \pm 0.11$ , respectively (data not shown).

**Table 2(B)** CCL39/hsst<sub>4</sub>

	[ <sup>125</sup> I] LTT- SRIF <sub>28</sub>	[ <sup>125</sup> I] [Tyr <sup>10</sup> ] CST <sub>14</sub>	[ <sup>125</sup> I] CGP 23996	stimulation of [ <sup>35</sup> S]GTPγS binding		inhibition of FSAC activity	
	pK <sub>d</sub>	pK <sub>d</sub>	pK <sub>d</sub>	E <sub>max</sub>	pEC <sub>50</sub>	E <sub>max</sub>	pEC <sub>50</sub>
SRIF <sub>14</sub>	8.91	8.39	8.87	100	8.05	100	8.53
SRIF <sub>28</sub>	9.08	8.44	9.06	94	7.58	100	8.53
LTT-SRIF <sub>28</sub>	9.16	9.13	9.37	102	7.12	78	7.85
CST <sub>17</sub>	9.24	9.55	9.26	96	7.66	65	8.30
[Tyr <sup>10</sup> ]CST <sub>14</sub>	8.44	8.17	8.30	88	7.02	86	7.61
CGP 23996	8.77	8.67	8.62	106	8.12	95	8.27
octreotide	6.40	5.76	6.02	54	5.67	78	6.00
[Tyr <sup>3</sup> ]octreotide	6.29	6.17	5.89	65	5.49	81	5.79
BIM 23056	7.17	6.47	7.04	-4	(-)	86	7.06
BIM 23052	8.63	8.20	8.13	113	6.42	105	7.20
cycloantagonist SA	6.48	6.07	6.29	54	5.57	73	6.03

The ability of a ligand-receptor complex to inhibit AC activity may vary with cell type-specific expression of G-protein isoforms and AC isoforms. Sst<sub>1</sub> receptors expressed in CHO cells are reported to inhibit AC activity by coupling to G<sub>13</sub>; by contrast, according to some authors (Kagimoto et al., 1994; Kubota et al., 1994), sst<sub>2</sub> receptors did not couple to AC inhibition in CHO cells; only after co-transfection of G<sub>11</sub>, which is not endogenously expressed in CHO cells, inhibition of FSAC was observed. In HEK293 cells, in which G<sub>11</sub> is endogenously expressed, sst<sub>2</sub> receptors did not couple to AC (Law et al., 1993), although they activate G<sub>13</sub>; in these cells, as well as in CHO cells, sst<sub>3</sub> receptors couple via G<sub>11</sub> proteins to AC inhibition (Law et al., 1994). Sst<sub>2</sub> receptors expressed in GH<sub>4</sub>C<sub>1</sub> cells couple via G<sub>12</sub> and G<sub>13</sub> proteins to AC (Tallent and Reisine, 1992), but when expressed in AtT20 cells they mediate AC inhibition via G<sub>11</sub> like in CHO cells (Yajima et al., 1993).

Table 2(C) CCL39/hsst<sub>2</sub>

	[ <sup>125</sup> I] LTT- SRIF <sub>28</sub>	[ <sup>125</sup> I] [Tyr <sup>10</sup> ] CST <sub>14</sub>	[ <sup>125</sup> I] CGP 23996	[ <sup>125</sup> I] [Tyr <sup>3</sup> ] octreo tide	stimulation of [ <sup>35</sup> S]GTPγS binding		inhibition of FSAC activity	
	pK <sub>d</sub>	pK <sub>d</sub>	pK <sub>d</sub>	pK <sub>d</sub>	E <sub>max</sub>	pEC <sub>50</sub>	E <sub>max</sub>	pEC <sub>50</sub>
SRIF <sub>14</sub>	10.00	10.06	10.10	10.01	100	6.95	100	8.36
SRIF <sub>28</sub>	9.92	10.16	9.99	9.99	116	6.14	111	8.72
LTT-SRIF <sub>28</sub>	9.70	8.90	10.06	9.17	110	6.78	111	8.33
CST <sub>17</sub>	9.07	9.29	9.33	8.85	60	5.83	44	8.15
[Tyr <sup>10</sup> ]CST <sub>14</sub>	8.77	8.91	8.93	9.00	39	6.28	107	6.80
seglitide	9.96	9.62	9.82	9.81	137	7.39	107	10.03
CGP 23996	8.58	8.94	9.06	8.95	95	6.06	100	7.79
octreotide	9.19	9.11	9.16	9.10	94	6.52	104	8.44
[Tyr <sup>3</sup> ]octreotide	8.43	7.10	9.48	8.66	131	6.57	115	9.70
L362,855	8.36	8.79	8.69	8.79	52	5.65	137	6.87
BIM 23056	6.33	6.23	6.33	6.38	-35	(-)	22	(-)
BIM 23052	8.30	8.50	8.76	8.55	53	5.91	122	6.74
cycloantagonist SA	5.40	5.74	5.80	5.77	3	(-)	37	(-)

More surprisingly perhaps, hsst<sub>5</sub> receptors expressed in CHO cells were found to inhibit FSAC at low concentrations, but to stimulate AC activity via G<sub>s</sub> at high agonist concentrations (Carruthers et al., 1999); this stimulatory effect on AC activity at high agonist concentrations was not obvious at human sst<sub>5</sub> receptors expressed in CCL39 cells. The differential expression of the nine types of AC's has not been studied in cell lines, and it may vary from one clone to another.

G<sub>i</sub> is known to inhibit mainly AC types I, V and VI. In vivo, AC type I is specifically expressed in neurones, whereas type V and VI are ubiquitous (for review, Birnbaumer and Birnbaumer, 1995; Taussig et al., 1993; 1994). Thus, AC type V and VI might be the isoforms inhibited by somatostatin receptors in CCL39 cells.

**Table 2(D)** CCL39/hsst<sub>5</sub>

	[ <sup>125</sup> I] LTT- SRIF <sub>28</sub>	[ <sup>125</sup> I] [Tyr <sup>10</sup> ] CST <sub>14</sub>	[ <sup>125</sup> I] CGP 23996	[ <sup>125</sup> I] [Tyr <sup>3</sup> ] octreo tide	stimulation of [ <sup>35</sup> S]GTPγS binding		inhibition of FSAC activity	
	pK <sub>d</sub>	pK <sub>d</sub>	pK <sub>d</sub>	pK <sub>d</sub>	E <sub>max</sub>	pEC <sub>50</sub>	E <sub>max</sub>	pEC <sub>50</sub>
SRIF <sub>14</sub>	9.53	9.01	9.82	9.87	100	8.39	100	8.33
SRIF <sub>28</sub>	9.39	9.18	10.15	10.30	101	7.65	109	8.45
LTT-SRIF <sub>28</sub>	8.47	8.12	9.70	9.60	107	7.63	106	7.84
CST <sub>17</sub>	9.54	9.37	10.21	9.85	79	7.94	92	8.38
[Tyr <sup>10</sup> ]CST <sub>14</sub>	8.67	8.06	9.77	9.65	69	7.43	109	7.69
seglitide	8.70	9.14	10.22	10.18	84	7.89	119	9.33
CGP 23996	6.59	6.67	8.26	8.68	67	7.12	112	7.07
octreotide	7.17	7.31	8.96	9.48	107	6.89	123	7.68
[Tyr <sup>3</sup> ]octreotide	6.49	6.00	8.03	8.41	72	6.56	118	7.30
L362,855	7.17	7.17	8.72	9.17	79	6.29	143	6.81
BIM 23056	7.17	6.68	7.77	8.32	0	(-)	47	6.60
BIM 23052	7.92	7.45	9.59	9.28	100	6.80	125	7.40
cycloantagonist SA	6.38	6.02	7.77	8.25	74	5.82	100	5.69

Inhibition of AC in CCL39 cells was more pronounced via hsst<sub>3</sub> and sst<sub>5</sub> than by sst<sub>1</sub>, sst<sub>2</sub> and sst<sub>4</sub> receptors. In contrast, in CHO cells expressing the human sst<sub>1-5</sub> receptors, the AC inhibition was highest with sst<sub>1</sub> receptors, and lowest at sst<sub>3</sub> receptors (Patel et al., 1994). Thus, it cannot be concluded, that one or the other SRIF receptor shows higher ability to inhibit FSAC, as this varies with cell lines, receptor density, and presumably G<sub>i</sub> and/or AC subtype expression.

We have previously reported differences in B<sub>max</sub>- and affinity values at human sst<sub>5</sub> receptors labelled with [<sup>125</sup>I]LTT-SRIF<sub>28</sub>, [<sup>125</sup>I][Tyr<sup>10</sup>]CST<sub>14</sub>, [<sup>125</sup>I]CGP 23996 and [<sup>125</sup>I][Tyr<sup>3</sup>]octreotide. In addition, the binding of the radioligands to the same receptor subtype was differently sensitive to GppNHp (Siehler et al., 1998a; 1998b; 1999; submitted (a)).

**Table 2(E)** CCL39/hsst<sub>3</sub>

	[ <sup>125</sup> I] LTT- SRIF <sub>28</sub>	[ <sup>125</sup> I] [Tyr <sup>10</sup> ] CST <sub>14</sub>	[ <sup>125</sup> I] CGP 23996	stimulation of [ <sup>35</sup> S]GTPγS binding		inhibition of FSAC activity	
	pK <sub>d</sub>	pK <sub>d</sub>	pK <sub>d</sub>	E <sub>max</sub>	pEC <sub>50</sub>	E <sub>max</sub>	pEC <sub>50</sub>
SRIF <sub>14</sub>	9.54	9.67	9.71	100	7.32	100	7.76
SRIF <sub>28</sub>	9.65	9.80	9.94	104	6.96	94	8.19
LTT-SRIF <sub>28</sub>	9.84	9.26	10.09	119	7.44	97	8.40
CST <sub>17</sub>	9.43	9.52	9.88	73	6.59	75	7.47
[Tyr <sup>10</sup> ]CST <sub>14</sub>	8.70	8.90	9.02	43	6.83	84	6.80
seglitide	6.88	7.89	7.68	49	5.78	89	6.68
CGP 23996	8.82	9.28	9.15	81	7.14	89	7.84
octreotide	7.88	8.60	8.44	42	6.70	97	7.01
[Tyr <sup>3</sup> ]octreotide	6.84	6.20	7.90	47	5.76	81	6.31
L362,855	7.62	8.25	8.29	23	6.27	58	6.70
BIM 23056	6.90	7.08	7.20	-10	(-)	26	(-)
BIM 23052	8.42	9.55	9.71	93	6.29	104	7.43
cycloantagonist SA	6.23	7.08	6.88	13	(-)	32	6.38

The data are expressed as pK<sub>d</sub>'s or pEC<sub>50</sub>'s (-log M), or E<sub>max</sub>-values values [% stimulation or inhibition, normalized to the E<sub>max</sub> of SRIF<sub>14</sub> = 100 %] of at least 3 determinations.

These differences could not be explained by the agonist or antagonist nature of the ligands, since all four “cold” ligands displayed nearly full agonism at inhibiting FSAC activity. However, the more surprising findings may come from the comparison between FSAC, radioligand and [<sup>35</sup>S]GTPγS binding.

**SRIF<sub>2</sub> receptors:** Sst<sub>1</sub> receptors reveal a good agreement between FSAC and radioligand binding, although the three radioligands were not affected profoundly by GppNHp and no robust [<sup>35</sup>S]GTPγS binding could be documented. Thus, EC<sub>50</sub>-values were 25 to 100 fold lower than K<sub>d</sub>'s, but overall there was a similar rank order of potency; and most compounds display partial agonism.

**Table 3:** Correlation coefficients (r) of linear regression analyses between the pharmacological profile of inhibition of forskolin-stimulated adenylate cyclase (FSAC) activity and either the affinity profiles of [<sup>125</sup>I]LTT-SRIF<sub>28</sub>, [<sup>125</sup>I][Tyr<sup>10</sup>]CST<sub>14</sub>, [<sup>125</sup>I]CGP 23996 and [<sup>125</sup>I][Tyr<sup>3</sup>]octreotide, or the pharmacological profile of stimulation of [<sup>35</sup>S]GTPγS binding for human sst<sub>1-5</sub> receptors

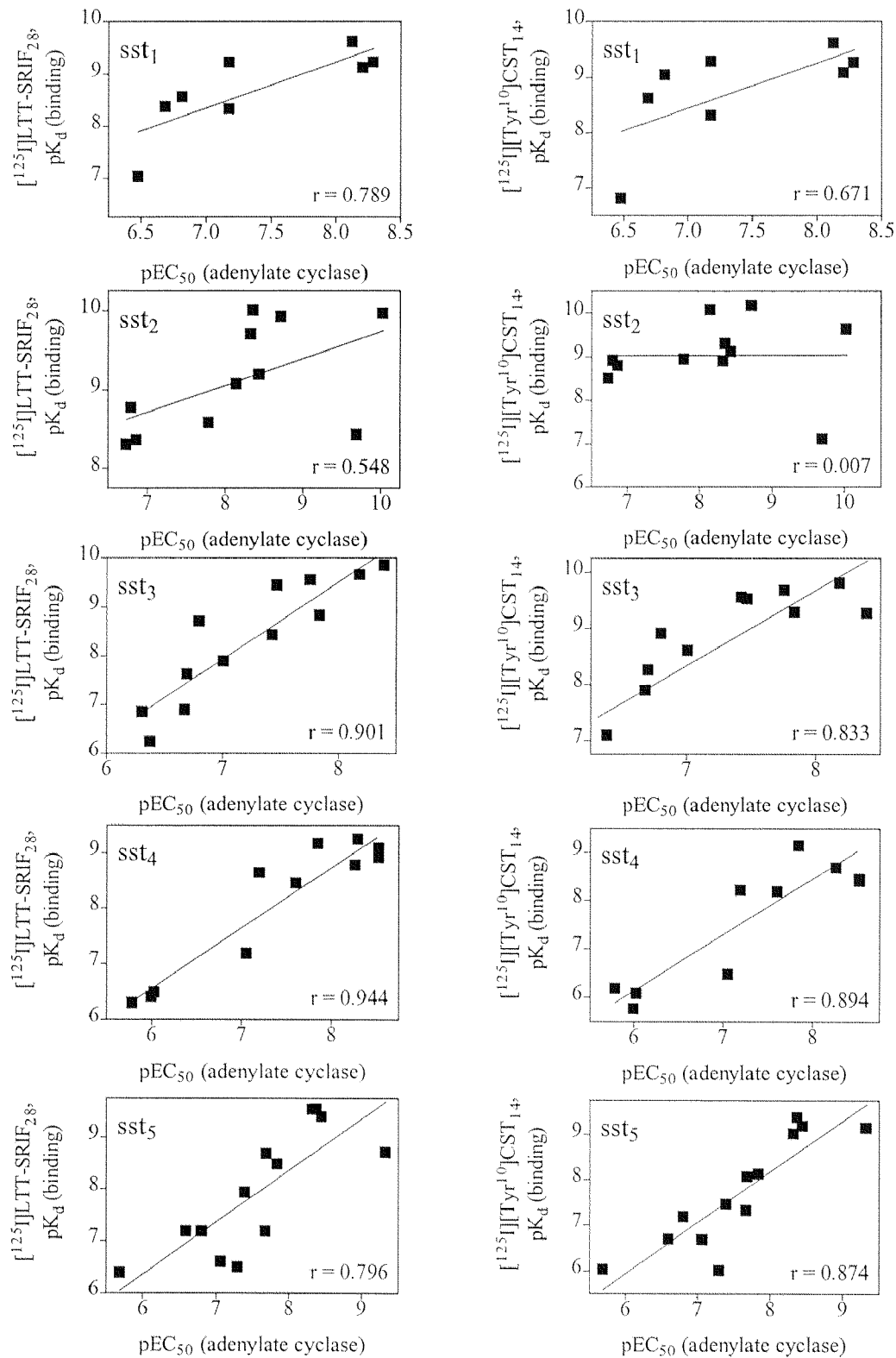
	[ <sup>125</sup> I]LTT-SRIF <sub>28</sub>	[ <sup>125</sup> I][Tyr <sup>10</sup> ]CST <sub>14</sub>	[ <sup>125</sup> I]CGP 23996	[ <sup>125</sup> I][Tyr <sup>3</sup> ]octreotide	[ <sup>35</sup> S]GTPγS binding
CCL39/ hsst <sub>1</sub>	0.789	0.671	0.795	-	-
CCL39/ hsst <sub>2</sub>	0.548	0.007	0.669	0.428	0.716
CCL39/ hsst <sub>3</sub>	0.901	0.833	0.874	-	0.827
CCL39/ hsst <sub>4</sub>	0.944	0.894	0.951	-	0.976
CCL39/ hsst <sub>5</sub>	0.796	0.874	0.871	0.888	0.876

Data used for correlation analyses are presented in tables 2(A)-(E).

Sst<sub>4</sub> receptors: although at sst<sub>4</sub>, like at sst<sub>1</sub> receptors, binding was not much affected by GppNHp, there is almost a perfect agreement between inhibition of FSAC and radioligand binding data, which show about 10 fold higher affinity. Thus at SRIF<sub>2</sub> receptors, values determined in radioligand binding studies, [<sup>35</sup>S]GTPγS binding and inhibition of FSAC appear to be rather predictive. **SRIF<sub>1</sub> receptors:** Sst<sub>2</sub> receptors showed a perfect agreement between the profiles defined by the four radioligands [<sup>125</sup>I]CGP 23996, [<sup>125</sup>I][Tyr<sup>3</sup>]octreotide, [<sup>125</sup>I]LTT-SRIF<sub>28</sub> and [<sup>125</sup>I][Tyr<sup>10</sup>]CST<sub>14</sub>, which were all markedly GppNHp sensitive. However, both [<sup>35</sup>S]GTPγS binding and inhibition of FSAC are only rather modestly stimulated via sst<sub>2</sub> receptors in these cells. EC<sub>50</sub>-values obtained in the two tests do not compare well, differences range from 25 to 1300 fold in favour of FSAC (see [Tyr<sup>3</sup>]octreotide, CST<sub>17</sub>, seglitide or even SRIF<sub>28</sub> which are markedly less potent in [<sup>35</sup>S]GTPγS binding). Surprisingly, the intrinsic activities are comparable and many compounds display full agonism except BIM23056 and SA.



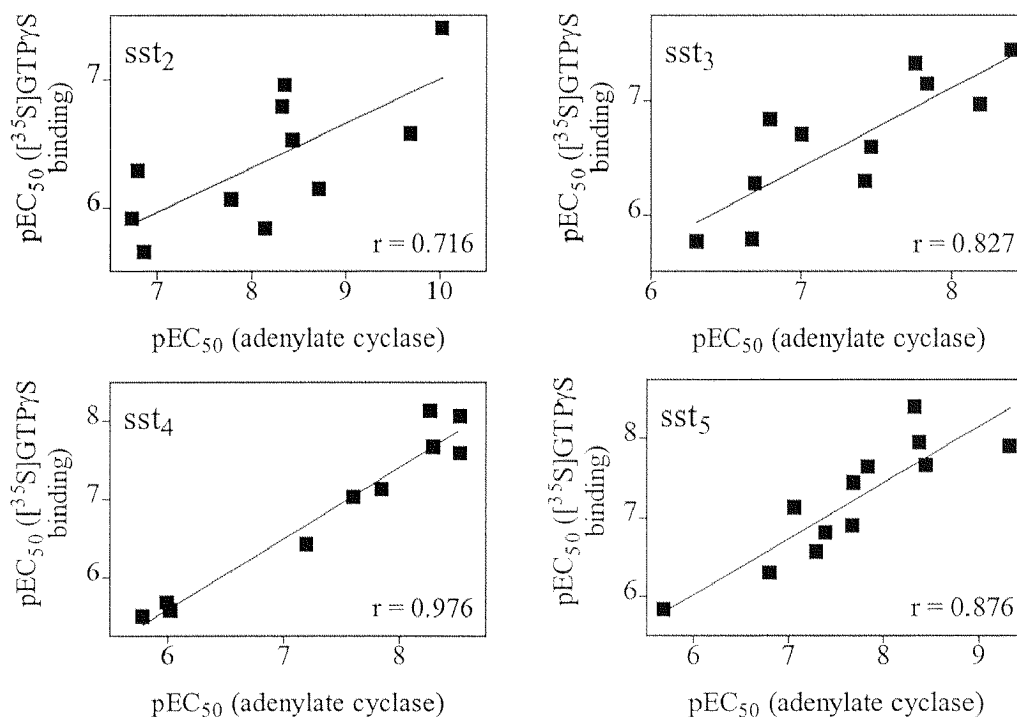
**Figure 3:** Human recombinant sst<sub>1-5</sub> receptors expressed in CCL39 cells: correlation analyses between [<sup>125</sup>I]LTT-SRIF<sub>28</sub> (left column) or [<sup>125</sup>I][Tyr<sup>10</sup>]CST<sub>14</sub> binding (right column) and inhibition of forskolin-stimulated adenylate cyclase activity.



Data are from tables 2(A)-(E) and represent  $pK_d$ -values obtained with radioligand labeling of human  $sst_{1-5}$  receptors and  $pEC_{50}$ -values obtained with adenylate cyclase activity assays. Correlation coefficients ( $r$ ) are indicated in all plots.

The comparison with radioligand binding is even less convincing:  $K_d$ 's are about 10 to 100 fold higher than  $EC_{50}$ 's in FSAC, with marked exception: [Tyr<sup>3</sup>]octreotide and seglitide are more potent at FSAC than at any binding sites.  $Sst_3$  receptors:  $pEC_{50}$ -values determined at [<sup>35</sup>S]GTP $\gamma$ S binding and inhibition of FSAC are very similar although somewhat higher at FSAC. In both cases, the efficacy of the compounds is very significant (up to 250 % stimulation of [<sup>35</sup>S]GTP $\gamma$ S binding and 70 % inhibition of FSAC), although full agonism is more common at the latter. There is a reasonably good correlation with binding although the cortistatin analogues, for instance, show very high affinity in binding when their effect on FSAC is about 100- 400 fold lower, especially when considering [<sup>125</sup>I]CGP 23996 and [<sup>125</sup>I][Tyr<sup>10</sup>]CST<sub>14</sub> binding data.  $Sst_5$  receptors: the same comments can be made for  $sst_5$  receptors; the peptides show good overall efficacy in stimulating [<sup>35</sup>S]GTP $\gamma$ S binding and in inhibiting FSAC, many compounds display full agonism, the intrinsic activity of the peptides are similar in both tests as well as their absolute  $pEC_{50}$ -values, and therefore a good correlation is seen between the two tests. [<sup>125</sup>I]CGP 23996 and [<sup>125</sup>I][Tyr<sup>3</sup>]octreotide were strongly GppNHp sensitive and affinity values are about 80- 120 fold higher than effects at FSAC. In both cases rank orders of affinity correlate well. [<sup>125</sup>I]LTT-SRIF<sub>28</sub> and [<sup>125</sup>I][Tyr<sup>10</sup>]CST<sub>14</sub>, which were much less GppNHp sensitive and labelled 8 and 2 fold more sites than [<sup>125</sup>I]CGP 23996 and [<sup>125</sup>I][Tyr<sup>3</sup>]octreotide, show absolute affinity values which are in rather good agreement with FSAC data with differences of 10 or less. However, seglitide by far the most potent in FSAC ranks 4<sup>th</sup> -6<sup>th</sup> in binding. Thus, at SRIF<sub>1</sub> receptors, radioligand binding data tends to overestimate affinities systematically at  $sst_2$ , and to a significant extent at  $sst_3$  and  $sst_5$ ; in the case of the two latter receptors, there are good to very significant correlations between FSAC activity, [<sup>35</sup>S]GTP $\gamma$ S, and radioligand binding.

**Figure 4:** Human  $sst_{2-5}$  receptors stably expressed in CCL39 cells: linear regression analyses between the pharmacological profiles of inhibition of forskolin-stimulated adenylate cyclase (FSAC) activity and of stimulation of [ $^{35}$ S]GTP $\gamma$ S specific binding.



Data are from tables 2(A)-(E) and represent pEC<sub>50</sub>-values obtained from adenylate cyclase activity assays and [ $^{35}$ S]GTP $\gamma$ S binding assays with  $sst_{2-5}$  receptors. Correlation coefficients (r) are indicated in all plots.

However for all three receptors, there are manifest discrepancies between one or the other test such as with seglitide and octreotide analogues, which are very potent in second messengers, but less so in binding or with cortistatin, for which depending on the receptor the reverse is true.

Altogether, it should be clear, that neither radioligand nor [ $^{35}$ S]GTP $\gamma$ S binding provide an absolute predictor for the pharmacological profile of a receptor as determined in adenylate cyclase experiments, be it absolute or relative potency and/ or efficacy. The affinity values are often very high compared to more “functional” values, and neither the rank orders of affinities nor the intrinsic activities are entirely superimposable.

This varies obviously with ligand, receptor, second messenger and there might be many reasons, even technical, since all tests are not performed under identical conditions; however, one may suggest that such diversity may be linked to the existence of multiple agonist-specific receptor conformations, each of which may couple preferentially to one or the other intracellular pathways within the signal transduction network. The switch of the G-protein coupled receptors from one signalling pathway to another might be regulated by receptor phosphorylation: phosphorylation of the  $\beta_2$ -adrenergic receptor by protein kinase A couples the receptor to the MAPK-pathway via  $G_i$  proteins, whereas the non-phosphorylated receptor is coupled to the AC/ protein kinase A-pathway via  $G_s$  proteins (Daaka et al., 1997). It remains to be seen, whether the coupling of somatostatin receptors to signal transduction cascades is regulated by similar phosphorylation mechanisms. However, one cannot rule out, that ligands may lead to receptor trafficking simply because the conformation of the ligand-receptor-complex may show preference for one or the other G-proteins, and subsequently messenger cascades (see Berg et al., 1998a, 1998b, 1998c ; Leff et al., 1997, 1998; Scaramellini et al., 1998). If so, a number of discrepancies that have been reported between recombinant and native systems may be partly explained.

## 8.1. Abstract

[<sup>3</sup>H]-total phosphoinositide (IP<sub>x</sub>) accumulation, a measure of phospholipase C (PLC) activity, induced by somatostatin (SRIF)- and cortistatin (CST)-analogues was studied at human somatostatin receptor subtypes 1-5 (hsst<sub>1-5</sub>) recombinantly expressed in CCL39 (Chinese hamster lung fibroblast) cells.

SRIF<sub>14</sub> (10 μM) stimulated total [<sup>3</sup>H]-IP<sub>x</sub> production 200 % and 1070 % over basal levels, and increased intracellular Ca<sup>2+</sup> ([Ca<sup>2+</sup>]<sub>i</sub>) 1600 % and 2790 %, in cells expressing hsst<sub>3</sub> and hsst<sub>5</sub> receptors, respectively. The SRIF<sub>14</sub>-stimulated IP<sub>x</sub> production was partly blocked by 100 ng/ml pertussis toxin (PTX) (30 % and 15 % inhibition, respectively). At hsst<sub>1</sub>, hsst<sub>2</sub>, and hsst<sub>4</sub> receptors, only weak or no stimulation of PLC activity was found (E<sub>max</sub> = 114 %, 122 %, and 102 %, respectively). Consequently, hsst<sub>3</sub> and hsst<sub>5</sub> receptors were subjected to more detailed studies to establish pharmacological profiles of PLC stimulation.

At hsst<sub>3</sub> receptors, the efficacies of most ligands were in the same range (E<sub>max</sub> = 218-267 %). At hsst<sub>5</sub> receptors E<sub>max</sub>-values varied over a broad range, seglitide, CST<sub>17</sub>, SRIF<sub>28</sub> displaying almost full agonism compared to SRIF<sub>14</sub>, whereas octreotide and BIM 23052 showed very low partial agonism. BIM 23056 behaved as an antagonist on SRIF<sub>14</sub>-induced total [<sup>3</sup>H]-IP<sub>x</sub> accumulation with a pK<sub>B</sub>-value of 6.74 at hsst<sub>3</sub> receptors, and of 6.94 at hsst<sub>5</sub> receptors. The putative cycloantagonist SA showed weak antagonist activity on SRIF<sub>14</sub>-induced total [<sup>3</sup>H]-IP<sub>x</sub> levels at hsst<sub>3</sub> (pK<sub>B</sub> = 5.85), but not at hsst<sub>5</sub> receptors.

The [<sup>3</sup>H]-IP<sub>x</sub> accumulation profiles at sst<sub>3</sub>/sst<sub>5</sub> receptors were compared to their respective radioligand binding ([<sup>125</sup>I]LTT-SRIF<sub>28</sub>, [<sup>125</sup>I][Tyr<sup>10</sup>]CST<sub>14</sub>, [<sup>125</sup>I]CGP 23996, [<sup>125</sup>I][Tyr<sup>3</sup>]octreotide binding), to [<sup>35</sup>S]GTPγS binding, and to forskolin-stimulated adenylate cyclase (FSAC) inhibition profiles determined previously in CCL39 cells (Siehler et al., submitted (a); Siehler and Hoyer, submitted (b), (c)).

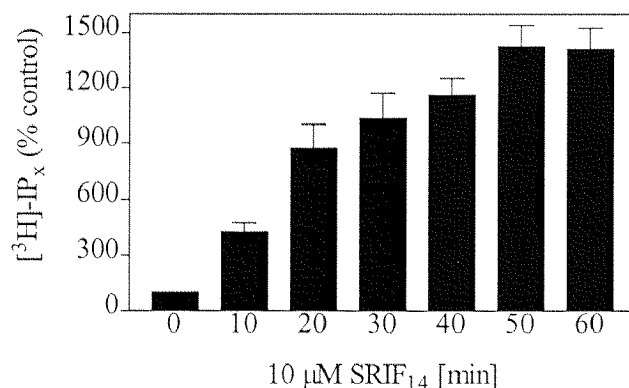
The different affinity profiles correlated relatively well at both receptor subtypes with PLC activation ( $ss_{t_3}$ :  $r = 0.90- 0.97$ ;  $ss_{t_5}$ :  $r = 0.80- 0.87$ ). However, [ $^{35}$ S]GTP $\gamma$ S binding correlated only minimally with stimulation of [ $^3$ H]-IP $_x$  levels at  $ss_{t_5}$  receptors ( $r = 0.59$ ), but rather well at  $ss_{t_3}$  receptors ( $r = 0.80$ ). A moderate correlation was also observed between inhibition of FSAC activity and stimulation of PLC activity for  $hsst_3$  and  $hsst_5$  receptors with correlation coefficients of 0.85 and 0.70, respectively.

In summary, most SRIF analogues behave as full agonists at  $hsst_3$  receptors and agonist-induced phosphoinositide turnover correlates well with radioligand binding, [ $^{35}$ S]GTP $\gamma$ S binding and inhibition of adenylate cyclase activity, all measured in CCL39 cells. By contrast, at  $hsst_5$  receptors, most SRIF analogues behave as intermediate or very low partial agonists (although receptor levels are very high) and the agonist-induced phosphoinositide turnover correlates rather poorly with radioligand binding, [ $^{35}$ S]GTP $\gamma$ S binding or inhibition of adenylate cyclase activity, all measured in the same cell line, suggesting either that PLC activity is irrelevant at the  $ss_{t_5}$  receptor or that receptor trafficking may have taken place.

## 8.2. Results

To study the activation of phospholipase C (PLC) activity via human  $ss_{t_{1-5}}$  receptors stably expressed in CCL39 cells, total [ $^3$ H]-IP $_x$  accumulation was determined using an anion exchange column assay. The assay was performed in the presence of 20 mM LiCl to block inositolmonophosphate phosphatase activity. Therefore, total [ $^3$ H]-IP $_x$  accumulation measures predominantly inositolmonophosphate and only trace amounts of di- or triphosphorylated inositol, which are dephosphorylated to IP $_1$  by their specific phosphatases. 10  $\mu$ M SRIF $_{14}$  induced a time-dependent increase of total [ $^3$ H]-IP $_x$  for up to 60 min at human  $ss_{t_5}$  receptors. The stimulation over basal level (100 %) reached  $427 \pm 45$  % after 10 min and  $1408 \pm 119$  % after 60 min (table 1; figure 1).

**Figure 1:** Stimulation of total [ $^3\text{H}$ ]-IP $_x$  accumulation by SRIF $_{14}$  in CCL39 cells expressing human sst $_5$  receptors.

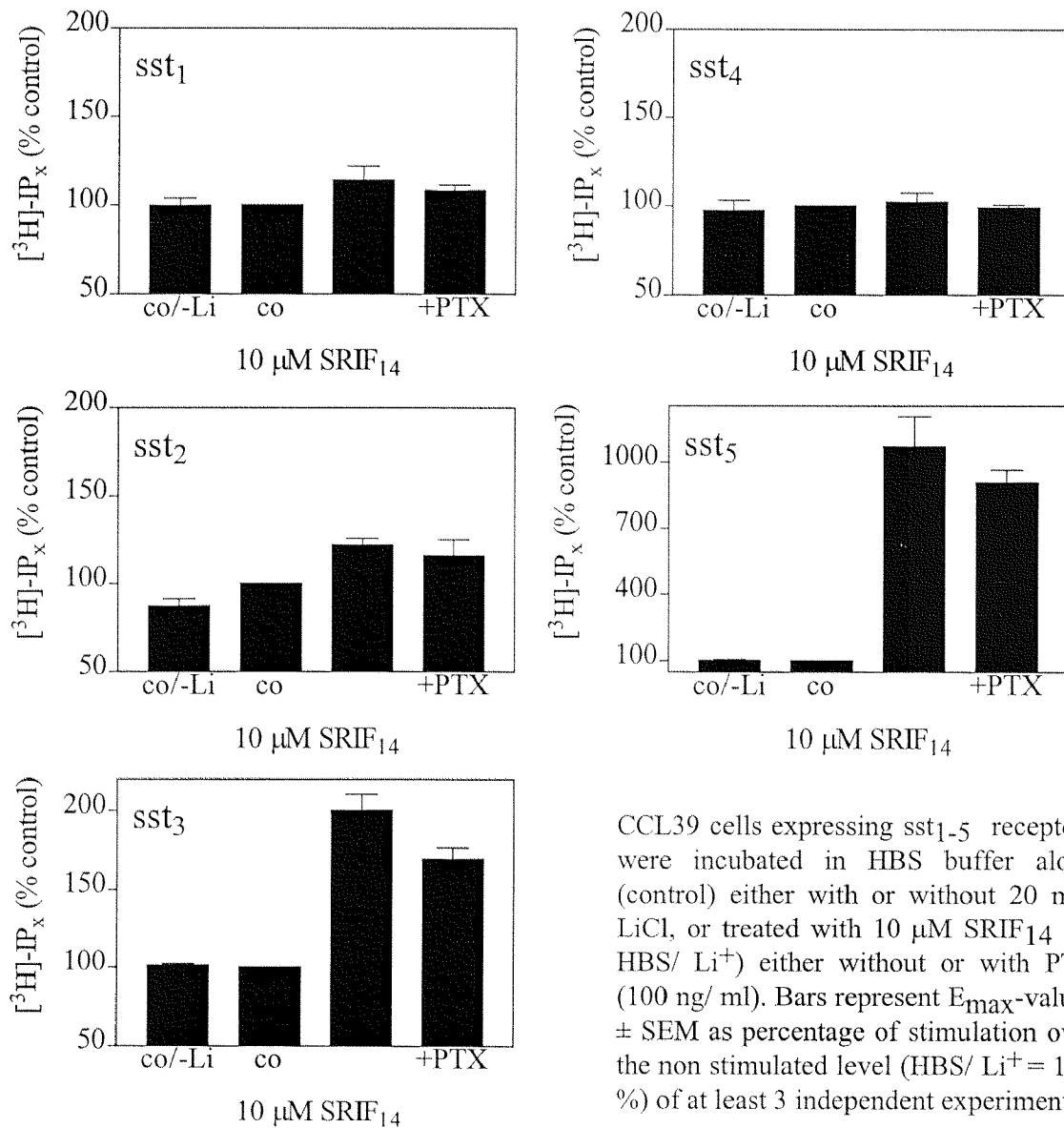


Transfected cells were treated for 10, 20, 30, 40, 50 or 60 min with 10  $\mu\text{M}$  SRIF $_{14}$  in HBS buffer containing 20 mM LiCl, or with the buffer alone (control). Bars represent  $E_{\text{max}}$ -values  $\pm$  SEM, which were calculated as percentage stimulation over the control level (= 100 %) of 3 independent experiments.

Since the maximal effect was reached after 50 minutes, all subsequent experiments were performed with a 50 min treatment time.

SRIF $_{14}$ -stimulated [ $^3\text{H}$ ]-IP $_x$  accumulation via hsst $_3$  and hsst $_5$  receptors ( $200 \pm 10$  % and  $1069 \pm 134$  %, respectively) was only partially affected by the addition of 100 ng/ml pertussis toxin ( $30 \pm 6$  % and  $15 \pm 7$  % inhibition, respectively). Cells were pre-incubated with pertussis toxin 3- 5 hrs prior to the experiment, since longer treatment times with PTX inhibited cell proliferation to various degrees at the different cell clones. By contrast, SRIF $_{14}$ -induced total [ $^3\text{H}$ ]-IP $_x$  accumulation was not significant at human sst $_4$  receptors ( $102 \pm 5$  %), and only marginal at sst $_1$  and sst $_2$  receptors ( $114 \pm 8$  % and  $122 \pm 4$  %, respectively), which were therefore not subjected to further studies (table 2; figure 2).

The pharmacological profiles of total [ $^3\text{H}$ ]-IP $_x$  accumulation were established at human sst $_3$  and sst $_5$  receptors using a number of SRIF and CST analogues (table 3; figure 3).

**Figure 2:** Stimulation of total [ $^3\text{H}$ ]-IP $_x$  accumulation via recombinant human sst $_{1-5}$ .

At sst $_3$  receptors, the  $E_{\text{max}}$ -values were about in the same range (218- 267 %) with the exception of [Tyr $^3$ ]octreotide, L362,855, and BIM 23056, which revealed lower efficacy; the so-called cycloantagonist SA displayed no significant agonist activity. In comparison, at human sst $_5$  receptors,  $E_{\text{max}}$ -values ranged from full agonism to low partial agonism: 1141 % (SRIF $_{14}$ ), followed by 788- 862 % (seglitide, CST $_{17}$ , SRIF $_{28}$ ), down to 289 % (octreotide), 191 % (BIM 23052) and 123 % (BIM 23056); the cycloantagonist SA had no agonist activity.



The  $pEC_{50}$ -values were intermediate to low compared to radioligand binding at both receptor subtypes ( $pEC_{50} = 5.53- 7.90$ ). The rank order of ligand potency for  $ss_{t_3}$  was: LTT-SRIF<sub>28</sub> > SRIF<sub>14</sub> > BIM 23052  $\approx$  CST<sub>17</sub>  $\approx$  SRIF<sub>28</sub> > [Tyr<sup>10</sup>]CST<sub>14</sub>  $\approx$  CGP 23996 > L362,855 > octreotide > seglitide > [Tyr<sup>3</sup>]octreotide > BIM 23056. The rank order of ligand potency for  $ss_{t_5}$  was: CST<sub>17</sub> > seglitide  $\approx$  SRIF<sub>14</sub> > SRIF<sub>28</sub> > BIM 23052  $\approx$  L362,855 > LTT-SRIF<sub>28</sub> > [Tyr<sup>10</sup>]CST<sub>14</sub> > octreotide > BIM 23056  $\approx$  [Tyr<sup>3</sup>]octreotide > CGP 23996.

SRIF<sub>14</sub> induced via human  $ss_{t_3}$  and  $ss_{t_5}$  receptors a maximal increase of intracellular  $Ca^{2+}$  ( $[Ca^{2+}]_i$ ) of  $1603 \pm 217$  % and  $2792 \pm 709$  % over the basal level, with  $pEC_{50}$ -values of  $6.87 \pm 0.22$  and  $6.27 \pm 0.04$ , respectively (figure 4). As in total [<sup>3</sup>H]-IP<sub>x</sub> accumulation measurements, SRIF<sub>14</sub> induced  $[Ca^{2+}]_i$  was not significant at  $ss_{t_4}$  receptors ( $97 \pm 3$  % of controls), and rather moderate at  $ss_{t_1}$  and  $ss_{t_2}$  receptors ( $123 \pm 5$  % and  $502 \pm 10$  %, respectively).

BIM 23056 and SA were examined for antagonism, since their efficacy was very low at both receptor subtypes. BIM 23056 antagonised SRIF<sub>14</sub>-stimulated total [<sup>3</sup>H]-IP<sub>x</sub> levels at  $ss_{t_3}$  and  $ss_{t_5}$  receptors with an apparent  $pK_B$  of  $6.74 \pm 0.10$  and  $6.94 \pm 0.19$ , respectively (table 4; figure 5). Cyloantagonist SA showed antagonist activity on SRIF<sub>14</sub>-induced IP<sub>x</sub> levels only at  $ss_{t_3}$  receptors ( $pK_B = 5.85 \pm 0.07$ ), but not at  $ss_{t_5}$  receptors (final concentration of 1  $\mu$ M).

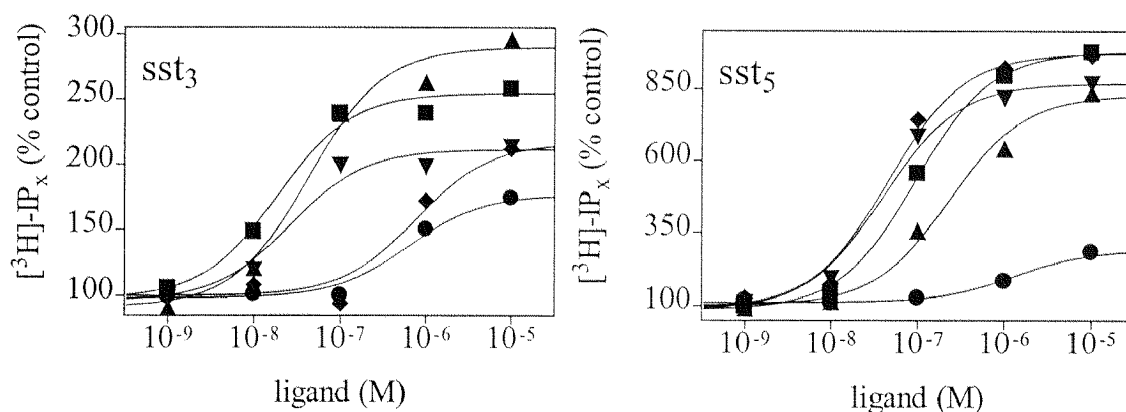
Sst<sub>3</sub>/  $ss_{t_5}$  receptor-modulated PLC activity was compared to data obtained previously in radioligand binding assays using different radioligands ([<sup>125</sup>I]LTT-SRIF<sub>28</sub>, [<sup>125</sup>I][Tyr<sup>10</sup>]CST<sub>14</sub>, [<sup>125</sup>I]CGP 23996, [<sup>125</sup>I][Tyr<sup>3</sup>]octreotide), in [<sup>35</sup>S]GTP $\gamma$ S binding experiments, and in adenylate cyclase activity (FSAC) (Siehler et al., submitted (a); Siehler and Hoyer, submitted (b), (c)) (table 5), and correlated to each other (table 6; figure 6; figure 7; figure 8). Overall,  $pEC_{50}$ -values determined at PLC activity were lower compared to affinity values of the ligands at  $ss_{t_3}$ /  $ss_{t_5}$  receptors, and lower or comparable to  $pEC_{50}$ -values obtained in GTP $\gamma$ S binding or FSAC experiments.

**Table 1:** Activation of total [ $^3\text{H}$ ]-IP<sub>x</sub> accumulation by SRIF, CST, and analogues by human sst<sub>3</sub> and sst<sub>5</sub> receptors

	CCL39/hsst <sub>3</sub>		CCL39/hsst <sub>5</sub>	
	E <sub>max</sub>	pEC <sub>50</sub>	E <sub>max</sub>	pEC <sub>50</sub>
SRIF <sub>14</sub>	100 ± 26	7.71 ± 0.18	100 ± 20	7.22 ± 0.10
SRIF <sub>28</sub>	98 ± 10	7.36 ± 0.22	66 ± 13	6.90 ± 0.20
LTT-SRIF <sub>28</sub>	87 ± 18	7.90 ± 0.08	21 ± 6	6.45 ± 0.11
CST <sub>17</sub>	89 ± 15	7.38 ± 0.09	71 ± 7	7.39 ± 0.00
[Tyr <sup>10</sup> ]CST <sub>14</sub>	78 ± 16	7.05 ± 0.05	46 ± 3	6.31 ± 0.05
seglitide	77 ± 6	6.01 ± 0.12	73 ± 8	7.27 ± 0.04
CGP 23996	87 ± 10	7.05 ± 0.14	16 ± 2	5.53 ± 0.02
octreotide	71 ± 17	6.27 ± 0.09	18 ± 2	6.00 ± 0.12
[Tyr <sup>3</sup> ]octreotide	47 ± 5	5.79 ± 0.14	11 ± 3	5.76 ± 0.10
L362,855	31 ± 4	6.61 ± 0.08	3 ± 0	6.78 ± 0.08
BIM 23056	21 ± 5	5.62 ± 0.22	2 ± 0	5.81 ± 0.06
BIM 23052	81 ± 18	7.44 ± 0.04	9 ± 1	6.80 ± 0.08
cycloantagonist SA	7 ± 2	(-)	2 ± 0	(-)

Comparison of pEC<sub>50</sub>-values (-log M) and E<sub>max</sub>-values [% activation] ± SEM of 3 different determinations; E<sub>max</sub>-values were normalised to the maximal stimulation reached by SRIF<sub>14</sub> (E<sub>max</sub> = 100 % stimulation).

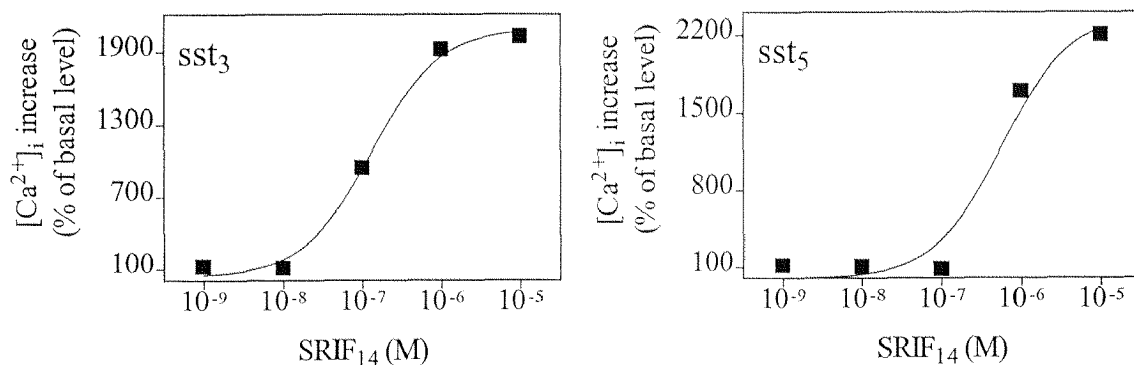
**Figure 3:** Activation of total [ $^3\text{H}$ ]-IP $_x$  accumulation by SRIF, CST, and analogues by human sst $_3$  and sst $_5$  receptors expressed in CCL39 cells.



CCL39 cells were incubated with 2  $\mu\text{Ci}$  myo-[2- $^3\text{H}$ (N)]-inositol, treated with the indicated concentrations of SRIF $_{14}$  (■), SRIF $_{28}$  (▲), CST $_{17}$  (▼), seglitide (◆) or octreotide (●), and total [ $^3\text{H}$ ]-IP $_x$  levels determined by anion exchange chromatography. Graphs represent the percentage of activation over the control level, and one representative example of at least 3 different determinations; the mean of the pEC $_{50}$ -values  $\pm$  are shown in table 3.

The various radioligand affinity profiles correlated at both studied receptor subtypes highly significantly, with their respective PLC activation profile although the correlation coefficients were higher for sst $_3$  than for sst $_5$  (sst $_3$ :  $r = 0.90- 0.97$ ; sst $_5$ :  $r = 0.80- 0.87$ ) (figure 6). In general, all correlation coefficients were lower at human sst $_5$  receptors compared to human sst $_3$  receptors. Thus, [ $^{35}\text{S}$ ]GTP $\gamma\text{S}$  binding correlated weakly with stimulation of total [ $^3\text{H}$ ]-IP $_x$  levels at sst $_5$  receptors ( $r = 0.59$ ), but well at sst $_3$  receptors (figure 7). A significant correlation was observed between inhibition of forskolin-stimulated AC activity and stimulation of PLC activity for both receptors (figure 8). Further, whereas the rank order of efficacy was rather comparable at hsst $_3$  receptor mediated effects, this was not the case at hsst $_5$  receptors.

**Figure 4:** SRIF<sub>14</sub>-induced increase of intracellular Ca<sup>2+</sup> at human sst<sub>3</sub> and sst<sub>5</sub> receptors expressed in CCL39 cells.



CCL39 cells were loaded with 5  $\mu$ M Fluo-4 dye, treated with the indicated SRIF<sub>14</sub> concentrations, and emitted fluorescence was kinetically monitored using the FLIPR<sup>TM</sup> II system. Graphs show the percentage of [Ca<sup>2+</sup>]<sub>i</sub> increase over the control level, and one representative example of 3 different experiments.

### 8.3. Discussion

We have stably expressed the five human SRIF receptors in CCL39 cells (Siehl et al, 1998a, 1998b). These clones have been used previously to characterise radioligand binding, agonist-stimulated [<sup>35</sup>S]GTP $\gamma$ S binding and inhibition of forskolin-stimulated adenylate cyclase activity. Similar studies were performed with a fish sst<sub>3</sub> receptor also expressed in CCL39 cells (Siehl et al, 1999). These studies revealed some atypical features of the pharmacological profiles of some of the receptors examined, especially hsst<sub>5</sub> and fsst<sub>3</sub>. Thus, affinity and B<sub>max</sub>-values appeared to depend on the radioligand used ([<sup>125</sup>I]LTT-SRIF<sub>28</sub>, [<sup>125</sup>I][Tyr<sup>10</sup>]CST<sub>14</sub>, [<sup>125</sup>I]CGP 23996, [<sup>125</sup>I][Tyr<sup>3</sup>] octreotide, Siehl et al., 1998a; 1998b, 1999, submitted (a)), although the non-iodinated analogue of all radioligands showed full agonism in second messenger assays (De Lecea et al., 1996; Hoyer et al., 1995b; Siehl and Hoyer, submitted (b), (c)).

**Table 2:** Antagonist activity of BIM 23056 ( $10^{-6}$  M) and cycloantagonist SA ( $10^{-6}$  M) on stimulation of total [ $^3$ H]-IP<sub>x</sub> accumulation by human sst<sub>3</sub> and sst<sub>5</sub> receptors

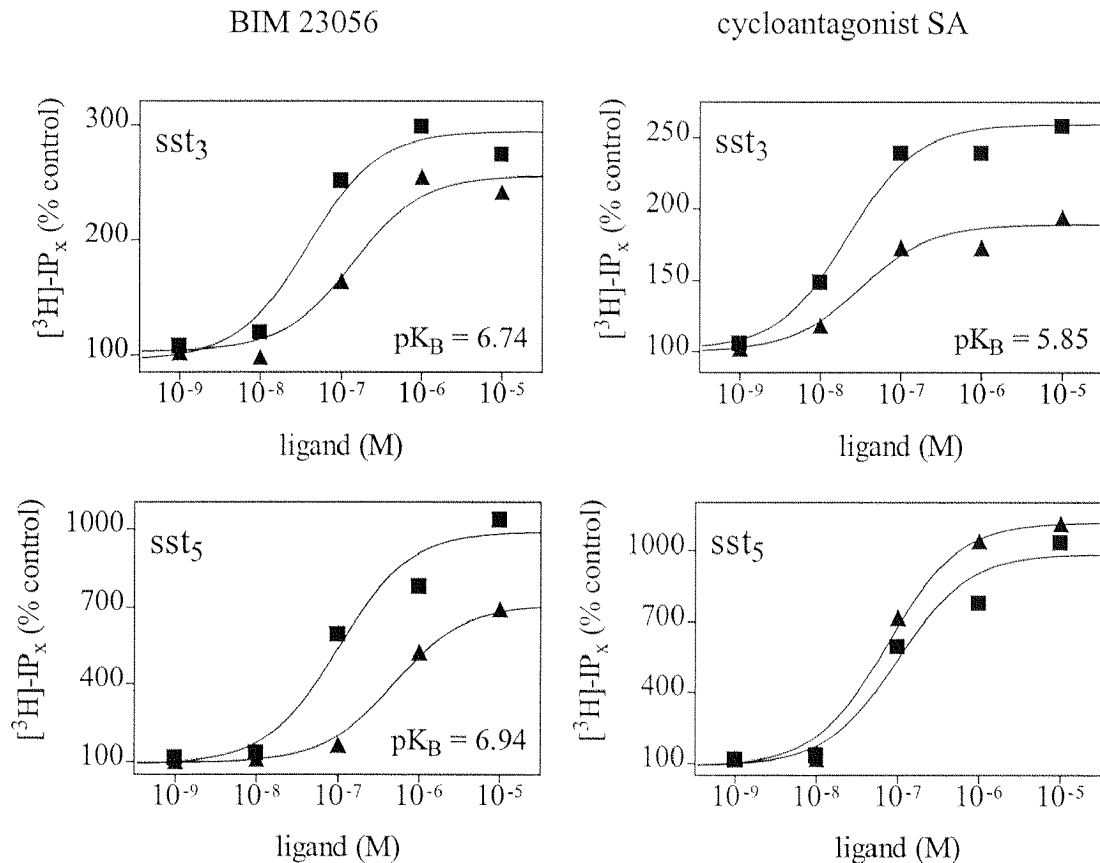
	SRIF <sub>14</sub>		SRIF <sub>14</sub> +BIM 23056			SRIF <sub>14</sub> + cycloantagonist SA		
	E <sub>max</sub>	pEC <sub>50</sub>	E <sub>max</sub>	pEC <sub>50</sub>	pK <sub>B</sub>	E <sub>max</sub>	pEC <sub>50</sub>	pK <sub>B</sub>
CCL39/ hsst <sub>3</sub>	100 ± 16	7.71 ± 0.18	113 ± 15	6.70 ± 0.12	6.74 ± 0.10	87 ± 16	7.37 ± 0.07	5.85 ± 0.07
CCL39/ hsst <sub>5</sub>	100 ± 20	7.22 ± 0.10	43 ± 8	6.28 ± 0.09	6.94 ± 0.19	76 ± 13	7.15 ± 0.02	-

Comparison of pEC<sub>50</sub>-values (-log M), E<sub>max</sub>-values [% stimulation], and pK<sub>B</sub>-values ± SEM of 3 independent determinations; E<sub>max</sub>-values were normalised to the stimulation reached by SRIF<sub>14</sub> (= 100 %).

Similarly, the rank orders of potency and/ or efficacy determined in [ $^{35}$ S]GTP $\gamma$ S binding and adenylate cyclase activation were not entirely consistent for a given receptor (Siehler and Hoyer, submitted (b), (c)). Thus, the data indicated quite some variability in the "pharmacological profile" of a given receptor depending on the agonist used and/ or the system studied (radioligand binding or second messenger).

In contrast to the predictions made by the allosteric ternary complex model (De Lean et al., 1980; Lefkowitz et al., 1993; Samama et al., 1993), these data suggested agonists to label G-protein-coupled or G-protein-coupled/ and -uncoupled receptor states, and that each agonist-specific receptor conformation triggers specifically the linked signalling cascades as may be suggested by Berg et al., 1998a, 1998b, 1998c, Leff et al., 1997, 1998 and Scaramellini et al., 1998.

**Figure 5:** Antagonist activity of BIM 23056 and cycloantagonist SA on SRIF<sub>14</sub>-induced total [<sup>3</sup>H]-IP<sub>x</sub> accumulation at human sst<sub>3</sub> and sst<sub>5</sub> receptors.



CCL39 cells were incubated with myo-[2-<sup>3</sup>H(N)]-inositol, treated with the indicated concentrations of SRIF<sub>14</sub>, and either without (■) or with BIM 23056 or cycloantagonist SA (▲) (1 μM f. c.), and total [<sup>3</sup>H]-IP<sub>x</sub> levels measured as described. Graphs show the % of induction of total [<sup>3</sup>H]-IP<sub>x</sub> accumulation over the control level. The data points represent one example of 3 different experiments. pK<sub>B</sub>-values ± SEM are shown in the graphs.

To further examine these aspects, inositol phosphate accumulation measurements were established at human SRIF receptors to determine phospholipase C (PLC) activity at the five human SRIF receptors expressed in CCL39 cells. At hsst<sub>5</sub> receptors, SRIF<sub>14</sub> produced a maximal 11 to 14 fold stimulation of PLC activity after 50 min at 37°C, conditions which were used in all further experiments.

By comparison, Wilkinson et al., (1997) reported a 2-fold induction by SRIF<sub>14</sub> of IP<sub>x</sub> levels via hsst<sub>5</sub> receptors expressed in CHO cells.

Under the conditions used, SRIF<sub>14</sub> induced a stimulation of total [<sup>3</sup>H]-IP<sub>x</sub> accumulation via hsst<sub>3</sub> and hsst<sub>5</sub> receptors of 200 % and 1069 %, respectively. By contrast SRIF<sub>14</sub> increased only minimally IP<sub>x</sub> levels in CCL39 cells expressing hsst<sub>1</sub> and sst<sub>2</sub> receptors (114 % and 122 %). These results were confirmed by measurement of [Ca<sup>2+</sup>]<sub>i</sub>, which is increased by PLC-induced IP<sub>3</sub> molecules: SRIF<sub>14</sub> induced an [Ca<sup>2+</sup>]<sub>i</sub> increase via sst<sub>3</sub> and sst<sub>5</sub> receptors of 1600 % and 2790 %, but only of 120 % and 500 % via sst<sub>1</sub> and sst<sub>2</sub> receptors, respectively. It has been reported that SRIF<sub>14</sub> induced about 130 % stimulation of [<sup>3</sup>H]-IP<sub>x</sub> in COS-7 cells expressing hsst<sub>1</sub> receptors (Akbar et al., 1994; Tomura et al., 1994), but no stimulation in F<sub>4</sub>C<sub>1</sub> rat pituitary cells expressing rodent sst<sub>1</sub> receptors (Chen et al., 1997). On the other hand, SRIF<sub>14</sub> has been reported to produce almost a 6-fold activation of PLC activity at mouse sst<sub>2</sub> receptors, and SRIF<sub>14</sub> produced even a 10-fold stimulation of PLC activity at human sst<sub>2</sub> receptors when expressed COS cells (Akbar et al., 1994; Chen et al., 1997; Tomura et al., 1994). In our hands, human sst<sub>4</sub> receptors failed to mediate significant IP<sub>x</sub> production and [Ca<sup>2+</sup>]<sub>i</sub> increase in CCL39 cells. This may not be surprising, since stimulation of rat sst<sub>4</sub> receptors also failed to induce IP<sub>3</sub> synthesis or Ca<sup>2+</sup> mobilisation (Bito et al., 1994); on the other hand, human sst<sub>4</sub> receptors were reported to induce IP<sub>3</sub> synthesis 1.7-fold by SRIF<sub>14</sub> when expressed in COS-7 cells (Akbar et al., 1994). Such rather drastic differences are probably explained by the use of different cell lines, in which a number of mechanisms are cell-specific such as: (a) the receptor may post-translationally modified, e.g. glycosylated or phosphorylated, (b) the expression and respective levels of G-protein isoforms; (c) the expression of the four PLC<sub>β</sub>-isoenzymes (Exton et al., 1996), (d) the presence or absence of different RGS proteins (regulators of G-protein signalling), e.g. RGS2 selectively blocks G<sub>q</sub>α-mediated activation of PLC<sub>β1</sub>, (e) expression and levels of RAMPs (receptor-activity-modifying proteins), which modulate receptor activity by regulation of the receptor glycosylation pattern, (f) receptor activity might be cell-specifically modulated by receptor heterodimerisation (Heximer et al., 1997; Kaupmann et al., 1998; Lefkowitz et al., 1993; McLatchie et al., 1998; Roush et al., 1996).

**Table 3:** Human sst<sub>3</sub> and sst<sub>5</sub> receptors: comparison of ligand potencies (pEC<sub>50</sub>-values) to activate total [<sup>3</sup>H]-IP<sub>x</sub> accumulation (a) with affinities (pK<sub>d</sub>'s) of the receptors labelled with [<sup>125</sup>I]LTT-SRIF<sub>28</sub>, [<sup>125</sup>I][Tyr<sup>10</sup>]CST<sub>14</sub>, [<sup>125</sup>I]CGP 23996 or [<sup>125</sup>I][Tyr<sup>3</sup>]octreotide, (b) with potencies (pEC<sub>50</sub>'s) to stimulate [<sup>35</sup>S]GTPγS specific binding, and (c) potencies to inhibit forskolin-stimulated adenylate cyclase (FSAC) activity.

**Table 3(A)** CCL39/hsst<sub>3</sub>

	[ <sup>125</sup> I] LTT- SRIF <sub>28</sub>	[ <sup>125</sup> I] [Tyr <sup>10</sup> ] CST <sub>14</sub>	[ <sup>125</sup> I] CGP 23996	[ <sup>35</sup> S]GTPγS		FSAC activity		total [ <sup>3</sup> H]IP <sub>x</sub>	
	pK <sub>d</sub>	pK <sub>d</sub>	pK <sub>d</sub>	E <sub>max</sub>	pEC <sub>50</sub>	E <sub>max</sub>	pEC <sub>50</sub>	E <sub>max</sub>	pEC <sub>50</sub>
SRIF <sub>14</sub>	9.54	9.67	9.71	100	7.32	100	7.76	100	7.71
SRIF <sub>28</sub>	9.65	9.80	9.94	104	6.96	94	8.19	98	7.36
LTT-SRIF <sub>28</sub>	9.84	9.26	10.09	119	7.44	97	8.40	87	7.90
CST <sub>17</sub>	9.43	9.52	9.88	73	6.59	75	7.47	89	7.38
[Tyr <sup>10</sup> ]CST <sub>14</sub>	8.70	8.90	9.02	43	6.83	84	6.80	78	7.05
seglitide	6.88	7.89	7.68	49	5.78	89	6.68	77	6.01
CGP 23996	8.82	9.28	9.15	81	7.14	89	7.84	87	7.05
octreotide	7.88	8.60	8.44	42	6.70	97	7.01	71	6.27
[Tyr <sup>3</sup> ]octreotide	6.84	6.20	7.90	47	5.76	81	6.31	47	5.79
L362,855	7.62	8.25	8.29	23	6.27	58	6.70	31	6.61
BIM 23056	6.90	7.08	7.20	-10	(-)	26	(-)	21	5.62
BIM 23052	8.42	9.55	9.71	93	6.29	104	7.43	81	7.44
cycloantagonist SA	6.23	7.08	6.88	13	(-)	32	6.38	7	(-)

Obviously, neither the effects of RAMPs, nor receptor dimerisation have been documented for any of the SRIF receptors, but this may only be a matter of time.



**Table 3(B)** CCL39/hsst<sub>5</sub>

	[ <sup>125</sup> I] LTT- SRIF <sub>28</sub>	[ <sup>125</sup> I] [Tyr <sup>10</sup> ] CST <sub>14</sub>	[ <sup>125</sup> I] CGP 23996	[ <sup>125</sup> I] [Tyr <sup>3</sup> ] octreo tide	[ <sup>35</sup> S]GTPγS		FSAC activity		total [ <sup>3</sup> H]IP <sub>x</sub>	
	pK <sub>d</sub>	pK <sub>d</sub>	pK <sub>d</sub>	pK <sub>d</sub>	E <sub>max</sub>	pEC <sub>50</sub>	E <sub>max</sub>	pEC <sub>50</sub>	E <sub>max</sub>	pEC <sub>50</sub>
SRIF <sub>14</sub>	9.53	9.01	9.82	9.87	100	8.39	100	8.33	100	7.22
SRIF <sub>28</sub>	9.39	9.18	10.15	10.30	101	7.65	109	8.45	66	6.90
LTT-SRIF <sub>28</sub>	8.47	8.12	9.70	9.60	107	7.63	106	7.84	21	6.45
CST <sub>17</sub>	9.54	9.37	10.21	9.85	79	7.94	92	8.38	71	7.39
[Tyr <sup>10</sup> ]CST <sub>14</sub>	8.67	8.06	9.77	9.65	69	7.43	109	7.69	46	6.31
seglitide	8.70	9.14	10.22	10.18	84	7.89	119	9.33	73	7.27
CGP 23996	6.59	6.67	8.26	8.68	67	7.12	112	7.07	16	5.53
octreotide	7.17	7.31	8.96	9.48	107	6.89	123	7.68	18	6.00
[Tyr <sup>3</sup> ]octreotide	6.49	6.00	8.03	8.41	72	6.56	118	7.30	11	5.76
L362,855	7.17	7.17	8.72	9.17	79	6.29	143	6.81	3	6.78
BIM 23056	7.17	6.68	7.77	8.32	0	(-)	47	6.60	2	5.81
BIM 23052	7.92	7.45	9.59	9.28	100	6.80	125	7.40	9	6.80
cycloantagonist SA	6.38	6.02	7.77	8.25	74	5.82	100	5.69	2	(-)

The data are expressed as pK<sub>d</sub>'s or pEC<sub>50</sub>'s (-log M), or E<sub>max</sub>-values [% stimulation or inhibition, respectively; normalised to E<sub>max</sub> of SRIF<sub>14</sub> = 100 %] of at least 3 determinations.

The hsst<sub>3</sub> and hsst<sub>5</sub> receptors mediated stimulation of total [<sup>3</sup>H]-IP<sub>x</sub> accumulation was partially blocked by PTX treatment (30 % and 15 %, respectively) suggesting that G<sub>i</sub>/ G<sub>o</sub> proteins are only marginally involved in the response measured, especially at sst<sub>5</sub> receptors. Along these lines, Akbar et al. (1994) reported a 2.7-fold increase of total IP<sub>x</sub> levels at hsst<sub>3</sub> receptors and a 12-fold increase at hsst<sub>5</sub> receptors in COS cells, which were blocked via PTX by 70 % and 35 %.

**Table 4:** Human sst<sub>3</sub> and sst<sub>5</sub> receptors expressed in CCL39 cells: correlation coefficients (r) and P-values from linear regression analyses between the pharmacological profile of stimulation of total [<sup>3</sup>H]-IP<sub>x</sub> accumulation and (a) the affinity profiles of [<sup>125</sup>I]LTT-SRIF<sub>28</sub>, [<sup>125</sup>I][Tyr<sup>10</sup>]CST<sub>14</sub>, [<sup>125</sup>I]CGP 23996 and [<sup>125</sup>I][Tyr<sup>3</sup>]octreotide, or (b) the profile of stimulation of [<sup>35</sup>S]GTP<sub>γ</sub>S binding, or (c) the profile of inhibition of forskolin-stimulated adenylate cyclase (FSAC) activity

	CCL39/ hsst <sub>3</sub>		CCL39/ hsst <sub>5</sub>	
	r	P	r	P
[ <sup>125</sup> I]LTT-SRIF <sub>28</sub>	0.946	< 0.0001	0.833	0.0008
[ <sup>125</sup> I][Tyr <sup>10</sup> ]CST <sub>14</sub>	0.896	< 0.0001	0.867	0.0003
[ <sup>125</sup> I]CGP 23996	0.967	< 0.0001	0.842	0.0006
[ <sup>125</sup> I][Tyr <sup>3</sup> ]octreotide	-	-	0.803	0.0017
[ <sup>35</sup> S]GTP <sub>γ</sub> S binding	0.799	0.0032	0.585	0.0589
inhibition of FSAC activity	0.849	0.0010	0.717	0.0087

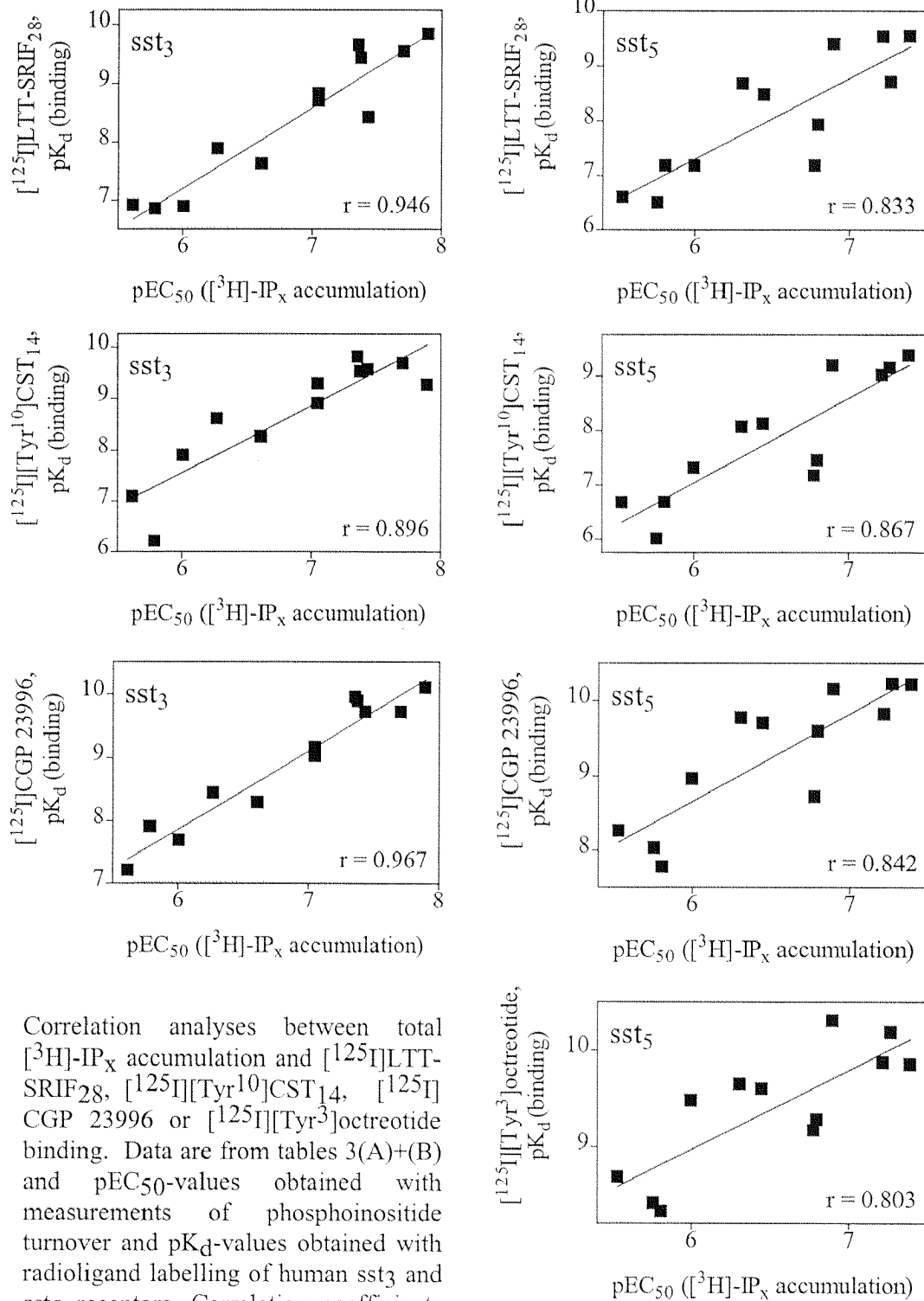
Data used for correlation analyses are presented in tables 3(A)+(B).

Similarly, Murthy et al. (1996) reported a 2.4-fold increase of PLC<sub>β3</sub> activity at guinea pig sst<sub>3</sub> receptors, which was inhibited via PTX by 86 %. At hsst<sub>5</sub> receptors expressed in CHO cells, PTX treatment resulted in 92 % inhibition IP<sub>x</sub> levels (Wilkinson et al., 1997). The marked inhibition of PLC activation by PTX described in some instances may be due to the prolonged PTX treatment of the cells (≥ 18 hrs). Such conditions however, inhibited cell proliferation of CCL39 cells and we limited pre-treatment time to 3 hours.

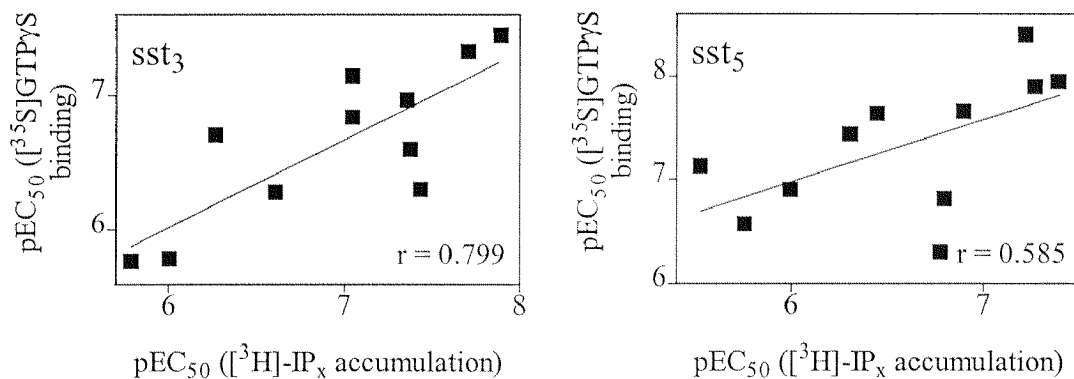
At both  $hsst_3$  and  $hsst_5$  receptors,  $SRIF_{14}$  ( $pEC_{50} = 7.71$  and  $7.22$ ) was somewhat more potent in stimulating total  $[^3H]$ -IP<sub>x</sub> production than  $SRIF_{28}$  ( $7.36$  and  $6.90$ ). A lower potency of  $SRIF_{14}$  compared to that of  $SRIF_{28}$  was reported at  $hsst_5$  receptors expressed in CHO cells ( $pEC_{50} = 6.48$  and  $6.83$ , Wilkinson et al., 1997), but overall it still remains to be seen whether  $sst_5$  receptors show indeed some selectivity for  $SRIF_{28}$  over  $SRIF_{14}$  as initially claimed. Potencies of  $SRIF_{14}$  to induce  $[Ca^{2+}]_i$  increase via  $hsst_3$  and  $hsst_5$  receptors were lower than those obtained measuring PLC activity ( $pEC_{50} = 6.87$  and  $6.27$ ).

In CCL39 cells expressing  $hsst_3$  receptors, most agonists stimulated  $[^3H]$ -IP<sub>x</sub> production to a similar extent (218- 267 % of basal), in other words most compounds acted as full or nearly full agonists, except BIM 23056 or cycloantagonist SA, which had essentially antagonist activity. By contrast, at  $hsst_5$  receptors, the efficacy of the studied ligands varied over a broad range (1141 % for  $SRIF_{14}$  to 118 % = cycloantagonist SA). Thus, whereas  $SRIF_{14}$  was a full agonist on total  $[^3H]$ -IP<sub>x</sub> accumulation, the other peptides behaved as partial agonists. Less extreme variations were also observed at the human  $sst_5$  receptor in  $[^{35}S]$ GTP $\gamma$ S binding and adenylate cyclase inhibition (Siehl and Hoyer, submitted (b), (c)).

BIM 23056 antagonised  $SRIF_{14}$ -stimulated accumulation of phosphoinositide levels with an apparent  $pK_B$  of 6.74 at  $hsst_3$ , and 6.94 at  $hsst_5$  receptors. Wilkinson et al. (1996; 1997) found for BIM 23056 a similar  $pK_B$  of 7.4 at  $hsst_5$  receptors on  $SRIF_{14}$ -induced phosphoinositide turnover, and a  $pK_B$  of 8.0 on  $SRIF_{14}$ -induced increase of intracellular  $Ca^{2+}$ . In addition, in previous studies we found BIM 23056 to antagonise  $SRIF_{14}$ -induced  $[^{35}S]$ GTP $\gamma$ S binding at  $hsst_3$  and  $hsst_5$  receptors (6.33 and 5.84, respectively), as well as  $SRIF_{14}$ -induced inhibition of forskolin-stimulated adenylate cyclase activity at  $hsst_3$  ( $pK_B = 6.33$ ), but not at  $hsst_5$  receptors (Siehl and Hoyer, submitted (b), (c)). Cycloantagonist SA, which revealed no significant activity on stimulation of PLC at both receptor subtypes, showed antagonism on  $SRIF_{14}$ -stimulated phosphoinositide turnover at  $hsst_3$  receptors ( $pK_B = 5.85$ ), but not at  $hsst_5$  receptors in this assay, nor in  $[^{35}S]$ GTP $\gamma$ S binding or adenylate cyclase at both receptor subtypes.

**Figure 6:** Human recombinant sst<sub>3</sub> and sst<sub>5</sub> receptors expressed in CCL39 cells.

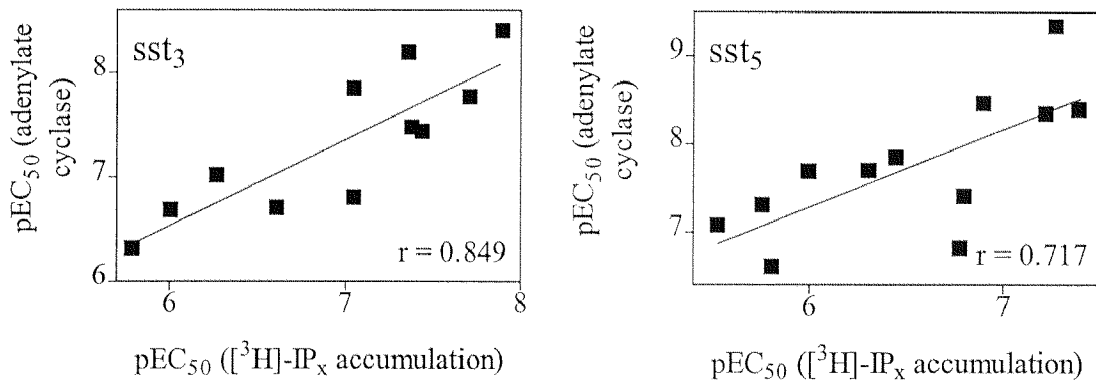
**Figure 7:** Human  $sst_3$  and  $sst_5$  receptors stably expressed in CCL39 cells.



Linear regression analysis between the pharmacological profiles of total  $[^3H]-IP_x$  measurements and of  $[^{35}S]GTP\gamma S$  specific binding experiments. Data are from tables 3(A)+(B) and represent  $pEC_{50}$ -values. Correlation coefficients ( $r$ ) are given in all plots.

However, these values have to be taken with care as the antagonism produced does not seem to be competitive in nature.

A comparison between the rank orders of potency determined at  $hsst_3$  and  $hsst_5$  receptors for  $[^3H]-IP_x$  accumulation on the one hand, and radioligand binding profiles,  $[^{35}S]GTP\gamma S$  binding and adenylate cyclase activity on the other (Siehler et al., submitted (a); Siehler and Hoyer, submitted (b), (c)) resulted in correlation coefficients, which were high for  $hsst_3$  receptors ( $r = 0.799- 0.967$ ), and lower for  $hsst_5$  receptors ( $r = 0.585- 0.867$ ). This may have been expected, since radioligand binding studies performed with various agonists resulted in more homogeneous results at  $sst_3$  receptors compared to  $sst_5$  receptors. Thus, when comparing  $[^{35}S]GTP\gamma S$  binding and phosphoinositide turnover, the low correlation ( $r = 0.585$ ) might suggest either 1) that some signalling pathways are preferred with respect to others (e.g.  $[^{35}S]GTP\gamma S$  binding and inhibition of adenylate cyclase activity correlated much better,  $r = 0.856$ ), or 2) that different signal transduction pathways activated by the same somatostatin receptor may apparently display a different recognition profile, e.g. some agonists may induce preferential coupling to one or another pathway/ G-protein.

**Figure 8:** CCL39 cells expressing human  $sst_3$  and  $sst_5$  receptors.

Correlation analysis between the pharmacological profiles of total [<sup>3</sup>H]-IP<sub>x</sub> accumulation and of adenylate cyclase activity measurements. Data (pEC<sub>50</sub>-values) used for analyses are from tables 3(A)+(B). Correlation coefficients (r) are shown in both graphs.

This cannot be demonstrated here since the incubation conditions are not identical in the different test systems, but is suggested (see also Berg et al, 1998a, 1998b; Leff et al., 1997, 1998).

On the other hand, it cannot be excluded, that coupling of  $sst_3/sst_5$  receptors to the phosphoinositide/ PLC pathway might be due to receptor overexpression as reported for other recombinantly expressed receptors (Cotecchia et al., 1990), and coupling to PLC might not play a role in a normal physiological environment for SRIF receptors. This may hold true for  $sst_5$  receptors which in these cells are expressed at high levels (up to 7000 fmol/ mg) whereas the other four receptors are expressed at similar levels (between 300- 400 fmol/ mg); however, of the “low” expressors,  $sst_3$  was able to couple efficiently to PLC activity.

The expression of PLC<sub>β</sub> isoenzymes has not been studied in CCL39 cells, but since somatostatin receptors couple efficiently to G<sub>i/o</sub> proteins (for review: Meyerhof, 1998), they probably activate PLC<sub>β2</sub> and/or PLC<sub>β3</sub>.

Further, since the response mediated by  $sst_3/sst_5$  receptors was in both cases only partially affected by addition of PTX, which blocks  $G_i/G_o$  signalling, coupling to  $G_q$ -protein family members may also be anticipated:  $G_q\alpha$  mediates activation of  $PLC_{\beta 1}$ ,  $PLC_{\beta 3}$ , and  $PLC_{\beta 4}$ , while  $G_{11}\alpha$  mediates activation of  $PLC_{\beta 1}$  and  $PLC_{\beta 3}$  (Berridge, 1993; for review: Exton, 1996). The phosphoinositide/ PLC pathway is an important  $Ca^{2+}$  signalling machinery triggered by G-protein-coupled receptors, although another pathway independent of PLC, and involving sphingosine kinase activation is described for muscarinic acetylcholine receptors (Meyer zu Heringhof et al., 1998). Thus, in rat AR42J pancreas cells endogenously expressing  $sst_2$  receptors SRIF<sub>14</sub> induced increases of intracellular calcium levels, but no stimulation of  $IP_3$  production (Taylor, 1995), meaning that modulation of intracellular calcium levels by somatostatin receptors not only involves PLC activation, but also modulation of cell-surface  $Ca^{2+}$  channels (Meyerhof, 1998), and/ or might also involve stimulation of the sphingosine kinase pathway.

In summary,  $hsst_3$  and  $hsst_5$  receptors appear to be able to couple rather efficiently to PLC activity and  $[Ca^{2+}]_i$  increase in CCL39 cells. The effect on PLC activity is only marginally affected by PTX, i.e. the G-proteins involved are not primarily  $G_o/G_i$ , suggesting that  $G_q$  may play a major role. This is important since the other parameters measured previously,  $[^{35}S]GTP\gamma S$  binding (presumably) and inhibition of adenylate cyclase activity are essentially the result of coupling to  $G_i$ -proteins. It appears, that at  $sst_3$  receptors most SRIF analogues behave as full agonists and that the agonist-induced phosphoinositide turnover correlates well with radioligand binding,  $[^{35}S]GTP\gamma S$  binding and inhibition of adenylate cyclase activity, all measured in the same cell line. Pretty much the opposite statement can be made about  $sst_5$  receptors: at  $sst_5$  receptors, most SRIF analogues behave as moderate or very low partial agonists (although the expression levels are very high) and the agonist-induced phosphoinositide turnover correlates rather poorly with radioligand binding,  $[^{35}S]GTP\gamma S$  binding or inhibition of adenylate cyclase activity all measured in the same cell line, suggesting either that PLC activity is irrelevant at the  $sst_5$  receptor or that receptor trafficking may have taken place.

If so, this would explain difference in both rank orders of potency and rank orders of efficacy observed when comparing data obtained at the same receptor, but using different tests.



## 9.1. Abstract

The actions of the various forms of somatostatin (SRIF), including those of the tetradecapeptide SRIF<sub>14</sub>, are mediated by specific receptors. In mammals, five subtypes of SRIF receptors, termed sst<sub>1-5</sub>, have been cloned. By using a combination of reverse transcriptase polymerase chain reaction and genomic library screening in the gymnotiform fish *Apteronotus albifrons*, we have isolated a gene encoding the first-known non-mammalian SRIF receptor. The deduced amino acid sequence displays 59 % identity with the human sst<sub>3</sub> receptor protein; hence, we have called the gene '*Apteronotus sst<sub>3</sub>*'. The predicted protein consists of 494 amino-acid residues exhibiting a putative seven-transmembrane domain topology typical of G-protein-coupled receptors. A signal corresponding to the *Apteronotus sst<sub>3</sub>* receptor was detected in brain after amplification of poly(A)<sup>+</sup>-RNA by reverse transcriptase-polymerase chain reaction, but not by Northern Blot analysis or *in situ* hybridization, thus suggesting a low level of expression. Membranes prepared from CCL39 cells stably expressing the *Apteronotus sst<sub>3</sub>* receptor gene bound [<sup>125</sup>I][Leu<sup>8</sup>,D-Trp<sup>22</sup>,<sup>125</sup>I-Tyr<sup>25</sup>]SRIF<sub>28</sub> with high affinity and in a saturable manner ( $B_{\max} = 4470$  fmol/ mg protein;  $pK_d = 10.5$ ). SRIF<sub>14</sub> and various synthetic SRIF receptor agonists produced a dose-dependent inhibition of radioligand binding, with the following rank order of potency: SRIF<sub>14</sub>  $\approx$  SRIF<sub>28</sub> > BIM 23052 > octreotide > BIM 23056. Under low stringent conditions, an *Apteronotus sst<sub>3</sub>* probe hybridized to multiple DNA fragments in *Hind*III or *Eco*RI digests of *A. albifrons* DNA, indicating that the *Apteronotus sst<sub>3</sub>* receptor is a member of a larger family of *Apteronotus* SRIF receptors.

## 9.2. Methods

Standard procedures were carried out as described in Sambrook et al. (1989). Subsequent to subcloning of appropriate DNA fragments into pGEM-3Z vector (Promega Biotec, Madison, Wisconsin), DNA sequencing was performed by the dideoxynucleotide chain termination procedure, using Sequenase® Version 2.0 DNA Sequencing Kit (United States Biochemical, Cleveland, Ohio). Both strands were sequenced.

### 9.2.1. Cloning of *A. albifrons* sst<sub>3</sub> receptor

DNA was extracted from liver tissue of adult *A. albifrons* (Teleostei, Gymnotiformes) obtained from a tropical fish importer (Aquarium Glaser, Rodgau, Germany). Total RNA was isolated from brain tissue using TRIzol® Reagent (Gibco BRL, Gaithersburg, Maryland). For reverse transcriptase-polymerase chain reaction (RT-PCR), cDNA was prepared from total RNA by means of mouse Moloney leukemia virus reverse transcriptase (Gibco BRL) and random hexamer oligonucleotide primers (Perkin-Elmer Corp., Norwalk, Connecticut). sst receptor-related sequences in the cDNA were amplified through PCR (Saiki et al., 1985) with the degenerate primers 5'-GACCGCTA(C/T)(G/C)TGGC(C/T)GTGGT(G/A)CA(T/C)C-3' and 5'-ATGGGGTT(T/G)GC(A/G)CAGCTGTT(A/G/C/T)GCATA-3'. The following temperature profile was employed: an initial denaturing step at 94°C for 5 min, and then 35 cycles consisting of 1 min each at 94°C for denaturing, 55°C for annealing, and 72°C for extension.

A resulting 504 basepair PCR product was subcloned into the *Hind*II site of pGEM-3Z and sequenced. Analysis of this sequence showed that it was most similar to that of the human sst<sub>3</sub> receptor. Mammalian sst receptor genes lack introns, at least in their protein coding regions, and we assumed that the organization of the *A. albifrons* sst<sub>3</sub> receptor gene would be similar. Thus, the remainder of the *A. albifrons* sst<sub>3</sub> receptor sequence was determined by the analysis of genomic clones.

Fragments of the *A. albifrons* sst<sub>3</sub> receptor gene were isolated through inverse PCR technique using *Pst*I-digested *A. albifrons* genomic DNA and the primers 5'-GTGTAGACGATGAACGCTGC-3' and 5'-CCATTCTACATACTCAACAT-3' which generated a 513 basepair PCR product. The two overlapping PCR products obtained by cDNA amplification and inverse PCR were ligated together to generate a fragment of 860 basepairs. This fragment was <sup>32</sup>P-labeled by nick translation and used as a probe to perform a Southern blotting using *Bgl*II digested genomic DNA. A 2.8 kb band was positive. It is likely that this band contained two kinds of fragments, because there was a *Bgl*II site in the probe. An *A. albifrons* genomic DNA library with inserts of size-selected 2.8 kb fragments digested with *Bgl*II was made and screened with the same probe by a plaque hybridization technique. DNA was prepared from plaque-purified clones and sequenced.

A construct encoding *A. albifrons* sst<sub>3</sub> receptor suitable for expression studies was generated by PCR amplification. A 1523 basepair fragment (nucleotides 107-1629) was amplified using specific primers with a *Hind*III linker sequence on the forward primer and *Xba*I linker sequence on the reverse primer. The PCR product was subcloned into the *Hind*III-*Xba*I sites of pcDNA3.1 (+) (Invitrogen, San Diego, California). The sequence of the insert in this clone, pAa-sst<sub>3</sub>, was confirmed.

### 9.2.2. Fish tissues

Black ghosts (*Apteronotus albifrons*), teleost fish of the order Gymnotiformes, were obtained from local pet shops. The fish were sacrificed with a lethal dose of MS-222 (3-aminobenzoic acid ethyl ester; Sigma Chemical Company) dissolved in aquarium water; brain, liver, heart, spleen, stomach and gut were rapidly removed and snap-frozen in isopentane at -45°C. The organs of individual animals were pooled and kept frozen until further use.

### 9.3. Results

#### Isolation of *Apteronotus sst*<sub>3</sub> receptor gene

SRIF receptor clones were isolated from adult *A. albifrons* total brain RNA by RT-PCR (Higuchi, 1990) using degenerate primers based on regions of sequence homology amongst mouse *sst*<sub>1-3</sub> receptors. The upstream and downstream primers corresponded to conserved regions between the third and fourth putative transmembrane domains, and in the seventh transmembrane domain, respectively. An amplified band was subcloned and sequenced. Sequence analysis of one clone revealed a 504 basepair insert that was similar to mammalian *sst* receptors, and less similar to other G-protein-coupled receptors.

Through inverse PCR (Innis et al., 1990; Ochman et al., 1988, 1990), an additional 357 basepair sequence was obtained, and the overlapping PCR products were ligated together to generate an 860 basepair fragment. This fragment was <sup>32</sup>P labeled and used in Southern blot analysis as a probe for *Bgl*III digested genomic DNA. A 2.8 kb band was revealed (data not shown). 5×10<sup>5</sup> plaques of a size-selected library of *A. albifrons* genomic DNA which contained 2.8 kb *Bgl*III fragments were screened. Two clones, λfsst3-A and λfsst3-B, obtained from 21 positive plaques, were sequenced.

#### Amino acid sequence of *Apteronotus sst*<sub>3</sub> receptor

The sequence of the inserts of λfsst3-A and λfsst3-B displayed an open reading frame of 1482 basepairs, thus predicting the sequence of a protein of 494 amino acids (mol wt, 54,696) (figure 1). Hydropathic analysis of this protein sequence demonstrated seven hydrophobic, putatively membrane-spanning domains separated by stretches of hydrophilic amino acids, a feature characteristic of G-proteins (Dohlman et al., 1991; Probst et al., 1992). Comparison of the sequence of the *A. albifrons* gene with those of other G-protein-coupled receptors showed that it was most similar to mammalian *sst*<sub>3</sub> receptor genes, hence designated '*Apteronotus sst*<sub>3</sub>'. It lacks introns in the protein coding region.

The sequence of the protein encoded by the *Apteronotus* sst<sub>3</sub> receptor gene exhibits 59 % (72 %), 58 % (71 %), and 56 % (69 %) identity (similarity) with the sequences of human (Yamada et al., 1992b), mouse (Yasuda et al., 1992), and rat sst<sub>3</sub> (Meyerhof et al., 1992), respectively (figure 2). The *Apteronotus*-specific peptide sequence diverged most at the amino and carboxyl termini from the corresponding regions of the mammalian receptors. Greatest similarity was found in the region between the amino terminus of the first transmembrane domain and the carboxyl terminus of the seventh transmembrane domain. In this region, the protein sequence showed 71 % (82 %), 70 % (80 %), and 70 % (80 %) identity (similarity) with the corresponding sequences of the human, mouse, and rat sst<sub>3</sub> receptors, respectively. There are several long stretches of sequences in these regions which are completely identical (figure 2).

Analysis of the sequence of *Apteronotus* sst<sub>3</sub> demonstrated many features that are conserved among G-protein-coupled receptors (Dohlmann et al., 1991; Findlay and Eliopoulos, 1990; Probst et al., 1992). This includes several conserved amino acids in the transmembrane segments and the highly conserved sequence Asp<sup>158</sup>-Arg-Tyr (DRY) at the NH<sub>2</sub>-terminal end of the second intracellular loop.

A consensus sequence pointing to a potential site for coupling to G-proteins (Okamoto and Nishimoto, 1992) is located in the 26-residue region of Val<sup>248</sup> to Arg<sup>273</sup>, which comprises the third cytoplasmic loop; it is composed of two basic residues at the amino-terminal side (K<sup>249</sup>VR) and the R<sup>269</sup>KITR motif at the carboxyl-terminal end of the loop. Three consensus sites for serine phosphorylation could be identified in the first (Ser<sup>91</sup>) and third intracellular loop (Ser<sup>261</sup> and Ser<sup>267</sup>) of the *Apteronotus* sst<sub>3</sub> receptor: The sequences RXS<sup>91</sup>X, XRXXS<sup>261</sup>X, and XRRXS<sup>267</sup>X (the phosphate-accepting serine is indicated by S, whereas the determinant arginine residues are marked by R, and the less essential residues by X) match the recognitions motifs of the multifunctional calmodulin-dependent protein kinase II. In addition, the sequence XRRXS<sup>267</sup> matches the recognition sequence of cAMP-dependent protein kinase A (Kemp and Pearson, 1990; Kennelly and Krebs, 1991). Two cysteines located at positions Cys<sup>134</sup> and Cys<sup>208</sup> might form a disulfide bond between the first and second extracellular loop. The presence of such a disulfide bridge has been shown in other G-protein-coupled receptors to be essential for ligand binding activity (Strosberg, 1991).

**Figure 1:** Nucleotide and predicted amino acid sequences of *A. albifrons* sst<sub>3</sub> receptor gene and protein.

1	CTTAAGCTCAACGTTCTTCCCTTTACAGCTAACAAACAATATTTACGCCAAAGAGCCAGGGGCTATAACAGTTTCTCATTGCGTTTTTTGCAGGCAGCATGGGCAGGT	
112	CCTAARCCGGCCRAAG     ATG GAG GCG CCC ATA ACG GCT GCG GTG TTT GGA TAC GAG GAC CCT CGT TCC TGG GAC TCC AAC GTT TCT Met Glu Ala Pro Ile Thr Ala Ala Val Phe Gly Tyr Glu Asp Pro Arg Ser Trp Asp Ser <u>Asn</u> Val Ser	23
196	TCT CTC CCC GCC CAC CCG GCC TTT CCC CTC CCC CCA GGC CAC GCC CTC CTC CCC GAC GGG TCT CCG CAG AAC TGG ACG GAG GGC Ser Leu Pro Ala His Pro Ala Phe Pro Leu Pro Pro Gly His Ala Leu Leu Pro Asp Gly Ser Pro Gln <u>Asn</u> Trp Thr Glu Gly	51
280	GAT GGG GCG GGT TTC TCT CCG AGC GCC GCC GGG GTG CTC ATC CCT CTT GTC TAC ATC GCC GTA TGC GTC GTA GGC CTC GCG GGG Asp Gly Ala Gly Phe Ser Pro Ser Ala Ala Gly <u>Val Leu Ile Pro Leu Val Tyr Ile Ala Val Cys Val Val Gly Leu Gly Gly</u>	79
364	AAC ACG CTG GTC ATC CAC ATC GTC CTG CGC TAC TCT CAC GTG CAG TCG GTC ACT AAC ATC TAC ATC CTG AAC CTC GCC ATA GCC <u>Asn Thr Leu Val Ile His Ile Val Leu Arg Tyr Ser</u> His Val Gln Ser Val Thr Asn Ile Tyr Ile Leu Asn Leu Ala Ile Ala	107
448	GAC GAG CTC TTC ATG CTT GGC CTG CCC TTC CTG GCT GTA CAG AAC GCG CTC CTC TCC TGG CCG TTC GGC TCG CTG ATG TGC CCG Asp Glu Leu Phe <u>Met Leu Gly Leu Pro Phe Leu Ala Val Gln Asn Ala Leu Leu Ser Trp Pro Phe Gly Ser Leu Met Cys Arg</u>	135
532	CTG GTC ATG ACC GTG GAC GCC ATC AAC CAG TTC ACC AGC ATC TTC TGC CTG ACA GTG ATG AGC ATC GAC CGC TAT GTG GCC GTG <u>Leu Val Met Thr Val Asp Ala Ile Asn Gln Phe Thr Ser Ile Phe Cys Leu Thr Val Met Ser Ile Asp Arg Tyr Val Ala Val</u>	163
616	GTG CAT CCC TCC GCT CCT CCA GGT GGC GCC GTC CTC TGG TGG CCA AAG CGT GAA CGT CAC GTG TGG GCC GTC TCC TTC GTG GTG Val His Pro Ser Ala Pro Pro Gly Gly Ala Val Leu Trp Trp Pro Lys Arg Glu Arg His <u>Val Trp Ala Val Ser Phe Val Val</u>	191
700	GTC CTG CCG GTG GTG GTG TTC GCC GAC GTG CTG CAG GAC GAC CCG AAC TGC AGC ATC GTG TGG CCC GAG CCG GCG GAG GTC TGG Val Leu Pro Val Val Val Phe Ala <u>Asp Val Leu Gln Asp Asp Arg Asn</u> Cys Ser Ile Val Trp Pro Glu Pro Ala Glu Val Trp	219
784	AAA GCA GCG TTC ATC GTC TAC ACC GCC ACG GTG GGC TTC TTC TGC CCC CTA CTG GTG ATC TGC CTG TGT TAC CTG CTC ATC GTG Lys Ala Ala Phe <u>Ile Val Tyr Thr Ala Thr Val Gly Phe Cys Pro Leu Leu Val Ile Cys Leu Cys Tyr Leu Leu Ile Val</u>	247
868	GTG AAG GTG CCG ACG TCC GGG CCG CCG GTG CCG GCC ACG TCT GTG CGA CGC CGT AAG TCC GAG CGA AAG ATC ACG CCG ATG GTG Val Lys Val Arg Thr Ser Gly Arg Arg Val Arg Ala Thr <u>Ser Val Arg Arg Arg Lys Ser</u> Glu Arg Lys Ile Thr Arg <u>Met Val</u>	275
952	GTG ATA GTG GTA GCC GTG TTC GTG CTC TGT TGG CTG CCA TTC TAC ATA CTC AAC ATT GTC AAC CTG TTG GTT CTC CTT CCT GGG Val Ile Val Val Ala Val Phe Val Leu Cys Trp Leu Pro Phe Tyr Ile Leu Asn Ile Val Asn Leu Leu Val Leu Leu Pro Gly	303
1036	GAG TTT CGT GGC CTC TAT TAC TTT GTG GTG GTT CTG TCT TAT GCC AAC AGC TGT GCC AAT CCC ATT TTG TAT GGA TTC CTC TCA Glu Phe Arg Gly <u>Leu Tyr Tyr Phe Val Val Val Leu Ser Tyr Ala Asn Ser Cys Ala Asn Pro Ile Leu Tyr Gly Phe Leu Ser</u>	331
1120	GAC AAC TTT AAG AGA GGT TTC CCG AAA GCA CTG TGC CCG TCA ACC AGA CCG GTA GAC AAT CAG GAA TTG CAG CAG GGC ACC ATG Asp Asn Phe Lys Arg Gly Phe Arg Lys Ala Leu Cys Arg Ser Thr Arg Arg Val Asp Asn Gln Glu Leu Gln Gln Gly Thr Met	359
1204	GGA AAC CAT ACG CTG CCA CTT GAG GAA ATG AAG AGA GAT CTG GAA CCC AGG GAG TGC CTG AGA GAA ACC TGC ACA GAG ACG CAG Gly Asn His Thr Leu Pro Leu Glu Glu Met Lys Arg Asp Leu Glu Pro Arg Glu Cys Leu Arg Glu Thr Cys Thr Glu Thr Gln	387
1288	TGT GAG AGA GAT GAA GAA GGA GAG GAA GAG GAG GAA GTA GAA ATA GGA TAT ATG GAG AAC GCC ACC CCG TTG AAT GAA ATC TAT Cys Glu Arg Asp Glu Glu Gly Glu Glu Glu Val Glu Ile Gly Tyr Met Glu Asn Ala Thr Arg Leu Asn Glu Ile Tyr	415
1372	AAG TCT GTG CAG AAT GGC TGC GGA AAT GGG CAC ATG GAG GGC ACT AGG ACC ATG TTC GCA CAT GGG GCA GAT GGT CAT GCT GCA Lys Ser Val Gln Asn Gly Cys Gly Asn Gly His Met Glu Gly Thr Arg Thr Met Phe Ala His Gly Ala Asp Gly His Ala Ala	443
1456	GGC CAC GGT AGT GAA TCC AGA ACT CAG GGG AAC AGG GGG CAT ATA AGT CCG ATG ACC TCT GGA CCT GTT CCT GCT CTC AGT GGA Gly His Gly Ser Glu Ser Arg Thr Gln Gly Asn Arg Gly His Ile Ser Pro Met Thr Ser Gly Pro Val Pro Ala Leu Ser Gly	471
1540	GCT CAG AAG GAG AAC GTC AAA GCT CTG CCA GAG GAA ACA ACG GAT ACA ATC CTG GAA ATT AGT TAC TTG     TGAGCTCTATAAAC Ala Gln Lys Glu Asn Val Lys Ala Leu Pro Glu Glu Thr Thr Asp Thr Ile Leu Glu Ile Ser Tyr Leu	494
1624	GTATGACAGAACTTATTTTAAACCTTTTCAAAAACCCATCAAAAGTGAATGCTAATGATAAATATTCCTTTGAGAATGTGAATCATCAGCAGTTGTCTTGTATGTTTA	
1735	ATATCTGTTCAAAATATATTAATTTTGTGTAGGCTTTAAGAGTAAGCTATATATATTTGAATTAAGTTCACTGAGACAGTTACAGCTGAATTAATGTTTAGTCTGAGAA	
1846	GCAAGTGTCCCATTAAGAGTGGTGATAACAGTTTTTGTGACTTAATCAGTTGTAGAAATCAATAGATTTTGCACAAAGTTTAAATATT	

The nucleotide sequence is numbered on the left; the amino acid sequence is indicated on the right. The seven putative transmembrane domains were assigned on the basis of a Kyte and Doolittle hydrophobicity plot and are shown in bold and underlined. The three potential N-glycosylation sites at positions Asn<sup>21</sup>, Asn<sup>47</sup>, and Asn<sup>207</sup> are underlined. The potential phosphorylation sites at Ser<sup>91</sup>, Ser<sup>261</sup>, and Ser<sup>267</sup> in the first and third cytoplasmic loops are marked by double underlining. Two cysteines located at positions Cys<sup>134</sup> and Cys<sup>208</sup> might form a disulfide bond between the first and second extracellular loop; these residues are printed in italics.

The cysteine at position Cys<sup>343</sup> is a potential palmitoylation site. It may attach the receptor's carboxyl terminus to the cell membrane via a palmitoyl anchor, thus producing a fourth cytoplasmic loop.

The extracellular domains contain consensus sequences of the types NXS or NXT (N, asparagine; X, any amino acid except proline and aspartic acid; S, serine; T, threonine) for *N*-glycosylation (Kornfeld and Kornfeld, 1985) at Asn<sup>21</sup>, Asn<sup>47</sup>, and Asn<sup>207</sup>. Polysaccharides *N*-linked to Asn residues have been shown to play a role in promoting high affinity agonist binding to SRIF receptors (Rens-Domiano and Reisine, 1991).

### Southern blotting

Hybridization under a low stringent condition of Southern blots of *Hind*III or *Eco*RI digests of genomic DNA of *A. albifrons* with a <sup>32</sup>P-labeled fragment of the *Apteronotus sst<sub>3</sub>* receptor gene showed strongly labeled bands at 12 kb (figure 3). In addition, faintly hybridizing DNA fragments of 5 and 2.3 kb in *Hind*III digests as well as of 2.8 and 0.9 kb in *Eco*RI digests were evident. The presence of these weakly hybridizing fragments suggested that there is a family of *sst* receptors in *A. albifrons*, similar to the mammalian somatostatinergic receptors.

### Northern blotting and RT-PCR

To check whether the cloned *Apteronotus sst<sub>3</sub>* receptor is expressed in tissues of *A. albifrons*, poly(A)<sup>+</sup>-RNA from brain, liver, heart, spleen, and stomach was prepared and subjected to Northern Blot analysis. No signal could be detected, not even in brain from which the receptor was cloned. Similarly, several attempts to localize the *Apteronotus sst<sub>3</sub>* by *in situ* hybridization failed, although various approaches were employed. Therefore, poly(A)<sup>+</sup>-RNA was used for RT-PCR, which is more sensitive than Northern Blot analysis. After high amplification (40 cycles), a weak signal was observed in brain (figure 4); this was confirmed by Southern Blot hybridization. In the other tissues, the rather high background could not be reduced, although the cDNA was of good quality, as shown by amplification of  $\beta$ -actin (data not shown).

Figure 2: Comparison of the amino acid sequences of *Apteronotus* sst<sub>3</sub> and human sst<sub>3</sub> receptors.

Fish sst <sub>3</sub>	1	MEAPITAAVFGYEDPRSDSNVSSLPAHFAFPLPPGHALLPDGSPQNWTEGDGAGFSPAAGVLIPLVYIAVGVVGLGNTLVIHIVLRYSHVQSVTNI	99
Human sst <sub>3</sub>	1	MDMLHPSSVSTTSEPENASSAWPPD:ATLGNVSA::GPSAGLAVS::GVLIPLVLVVGVVGLLGNLSLVIYVVLRHRTASPSVTNV	81
		<----- TM1 ----->	
Fish sst <sub>3</sub>		YILNLAIADELFMGLGLPFLAVQNALSMPPFGSLMCLRLVMTVDAINQFTSI FCLTVMSIDRYAVVHP::SAPPGGAVLWPKRERHVMWAVFVVLPLVWVFA	199
Human sst <sub>3</sub>		YILNLAIADELFMGLGLPFLAAQNALSMPFGSLMCLRLVMAVDGINQFTSIFCLTVMSVDRYLAVVHP:TRSARWRTPAVARTVSA.AVWVASAVVVLPLVVVFS	182
		<----- TM2 -----> <----- TM3 -----> <----- TM4 ----->	
Fish sst <sub>3</sub>		DVLQDDRNCSIVMPEPAEVMKAAFIVYTATVGVFFCPLLVI CLCYLLIIVKVRTSGRRVRATSV:RRRKSERKIKTRMVIIVVAVFVLCWLPFFYILLNIVNLLVL	300
Human sst <sub>3</sub>		GVPRGMSTCHMQMPEPAAAWRAGFIIYTAALGVFGPILLVI CLCYLLIIVKRSAGRRVWAPSCQRRRSERRVTRMVAVALFVLCWMPFFYILLNIVNVVCP	284
		<----- TM5 -----> <----- TM6 ----->	
Fish sst <sub>3</sub>		LPGE::FRGLYYFVVVLSYANS CANP ILYGFLSDNFKRGRKALCRSTRVDNQLQQGTMGNHTLPLEEMKRDLEPRECLRETCTETQCERDEEGEREEV	400
Human sst <sub>3</sub>		LPEEPAFFGLYFLVVALPYANS CANP ILYGFLSYRFGQFRVLLRPSRRVRSQE:EE	356
		<----- TM7 ----->	
Fish sst <sub>3</sub>		EIGYMENATRLNEIYKSVQNGCGNHMEGTRTMFAHGADGHAAGHSGESRTQGNRGHIS:PMTSGVPVALSGAQKENVKALPEETTD:IIIIEISYL	494
Human sst <sub>3</sub>		:EE	418

The single-letter code for the amino acids is used. Gaps (represented by colons) have been introduced to maximize alignment. The invariant amino acid residues are shown in boldface type. The seven putative transmembrane domains (TM1- TM7) of the *Apteronotus* sst<sub>3</sub> protein are indicated.



### Pharmacological properties of *Apteronotus* sst<sub>3</sub> receptor

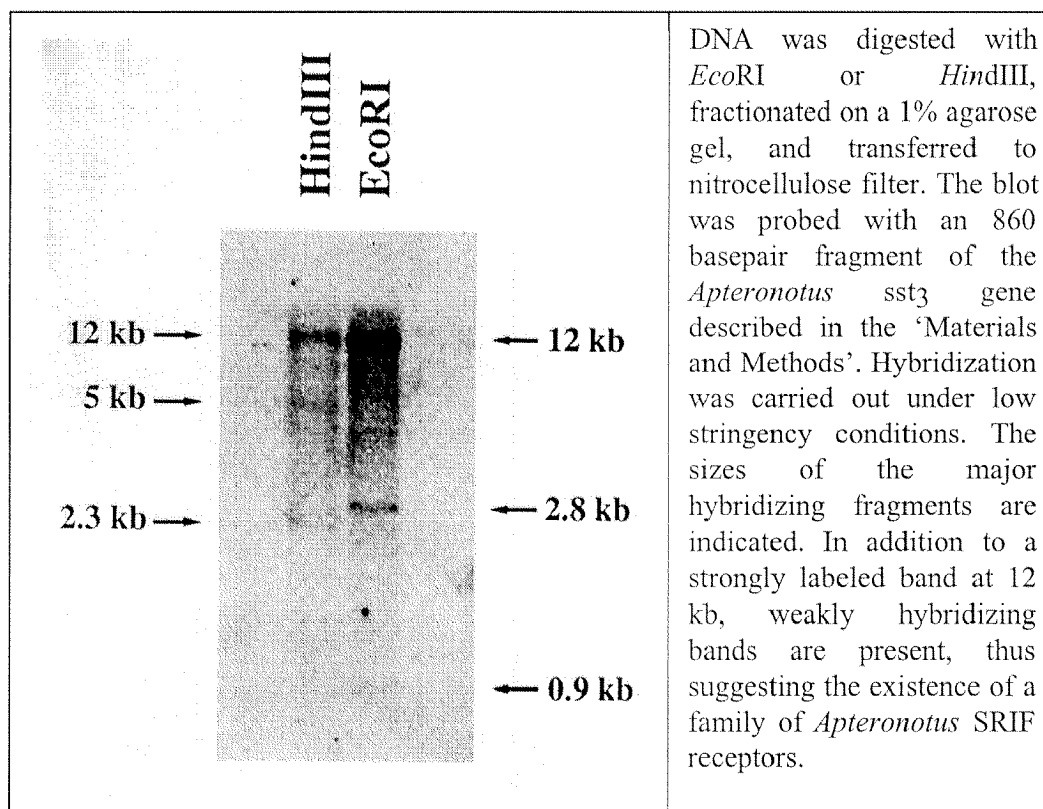
To characterize the protein product encoded by the cloned *Apteronotus* sst<sub>3</sub> receptor gene, the corresponding DNA was transfected and stably expressed in CCL39 cells. Saturation experiments performed with [<sup>125</sup>I]LTT-SRIF<sub>28</sub> revealed the presence of a high density of binding sites ( $B_{\max} = 4470 \pm 130$  fmol/ mg protein,  $pK_d = 10.51 \pm 0.12$ ). Non-specific binding was very low (figure 5). The saturation curve displayed an apparent monophasic course as confirmed by linear Scatchard plot (not shown).

Further characterization of the putative SRIF receptor expressed in CCL39 cells was carried out by radioligand-binding-competition analysis using SRIF<sub>14</sub> and SRIF<sub>28</sub>, as well as the SRIF analogues octreotide, BIM 23052, and BIM 23056 (figure 6; table 1). These peptides exhibited the following rank order of binding potency: SRIF<sub>14</sub>  $\approx$  SRIF<sub>28</sub> > BIM 23052 > octreotide > BIM 23056. Competition curves were monophasic as shown in Figure 6, thus suggesting the presence of a single population of SRIF binding sites. Non-transfected cells did not display significant levels of specific binding.

### 9.4. Discussion

In this paper, we report, to our knowledge for the first time, the cloning and pharmacological characterization of a non-mammalian SRIF receptor. By using a combination of RT-PCR and genomic library screening, the gene encoding this receptor was isolated from the gymnotiform fish *A. albifrons*. Existence of SRIF receptors in this teleost has been suggested by receptor binding autoradiography using the non-selective ligand [<sup>125</sup>I]Tyr<sup>0</sup>-D-Trp<sup>8</sup>-SRIF<sub>14</sub> (Zupanc et al., 1994). As the structure of the cloned receptor resembles the mammalian sst<sub>3</sub> receptor subtype, we have termed it '*Apteronotus* sst<sub>3</sub> receptor'.

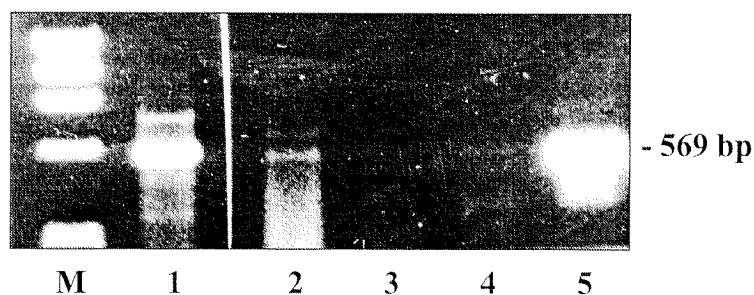
**Figure 3:** Southern blot analysis of genomic DNA of *A. albifrons*.



#### Molecular characterization of the cloned *Apteronotus sst<sub>3</sub>* receptor

Comparison of the fish *sst<sub>3</sub>* receptor with its mammalian homologues points to many conserved features. Almost 60 % of the amino acid residues are invariant compared to the protein encoded by the human *sst<sub>3</sub>* receptor gene (cf. Yasuda et al., 1992). An even higher degree of identity is found in the region between the amino terminus of the first transmembrane domain and the carboxyl terminus of the seventh transmembrane domain; within this segment, more than 70 % of the amino acid residues are identical. The same tendency of the sequences to be most similar in the region of the seven alpha-helical transmembrane regions and to be most divergent at the amino and carboxyl ends has been found in the three mammalian *sst<sub>3</sub>* receptors (Meyerhof et al., 1992; Yamada et al., 1992b; Yasuda et al., 1992) and in the other subtypes of SRIF receptors (for reviews, see Hoyer et al., 1994b; Reisine and Bell, 1995).

**Figure 4:** RT-PCR with Poly(A)<sup>+</sup>RNA prepared from *Apteronotus* brain.

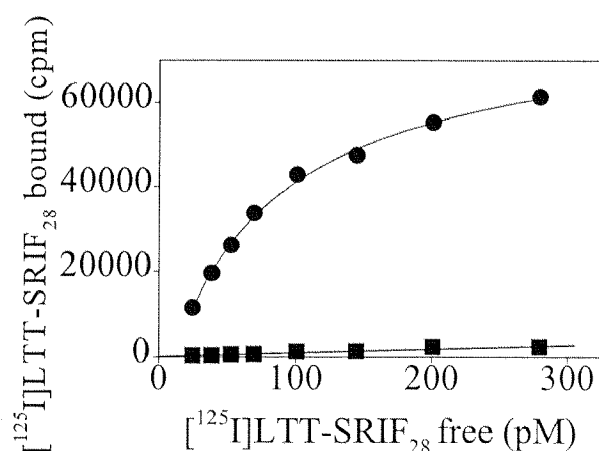


PCR products were separated on a 1% agarose gel and stained with ethidium bromide. M, molecular weight marker ( $\phi$ -X174 RF DNA/*Hae*III fragments; 1353, 1078, 872, 603, 310, 281, 271, 234, 194, 118, 72 bp); (1) cDNA from *Apteronotus sst3* expressing CCL39 cells (positive control); (2) cDNA from *Apteronotus* brain; (3) poly(A)<sup>+</sup>RNA from *Apteronotus* brain (negative control); (4) H<sub>2</sub>O (negative control); (5) pcDNA3-*Apteronotus sst3* plasmid DNA (positive control).

The high similarity and identity scores especially in the putative transmembrane regions are good indicators to decide whether receptors are, indeed, homologous subtypes, or whether they are just members of the same subfamily (cf. Hoyer et al., 1994a). In the present case, the *Apteronotus sst3* receptor is, based on sequence identity/ similarity, clearly homologous to the *sst3* receptor identified in mammalian species.

The cloning of the *Apteronotus sst3* receptor gene provides the opportunity to search for highly conserved structural features of SRIF receptors among a much broader scale of species within the vertebrate phylum than previously available. It is very likely that such structures are also functionally important. A highly conserved amino acid is the tyrosine in position 290 of the *Apteronotus sst3* receptor. This residue is also present within the sixth transmembrane domain of the mammalian *sst1-4*, but not of the mammalian *sst5*, where it is exchanged by phenylalanine (for sequence comparison, see Bell and Reisine, 1993; Hoyer et al., 1994b; Patel et al., 1995; Reisine, 1995; Reisine and Bell, 1995; Florio et al., 1996; Patel et al., 1996; Schindler et al., 1996; Patel, 1997).

**Figure 5:** Saturation isotherm of [ $^{125}$ I]LTT-SRIF<sub>28</sub> binding to membranes prepared from CCL39 cells stably expressing *Apteronotus sst*<sub>3</sub>.



Crude membrane preparations (4  $\mu$ g/ assay) were incubated with increasing concentrations of [ $^{125}$ I]LTT-SRIF<sub>28</sub> and assayed for receptor binding activity. The figure shows specific ( $\bullet$ ) and non-specific binding ( $\blacksquare$ ) expressed as amount of radioligand bound versus free radioligand concentration. Data represent the mean of triplicate determinations. Note low level of non-specific binding.

The motif NXFTS in the third transmembrane domain is found in all sst receptor subtypes, including *Apteronotus sst*<sub>3</sub>, but not in other members of the G-protein-coupled receptor superfamily. Similarly, the putative phosphorylation site RXXSE in the third intracellular loop and the motif YANSCAN in the seventh transmembrane domain are specifically conserved in sst receptors. The presence of such motifs in vertebrate groups as diverse as fish and man should help to design mutant receptors. Such constructs could then be employed to elucidate the role of certain segments and amino acids of the receptor protein in the process of ligand binding and signal transduction.

Although it appears likely that several of the conserved sites in the *Apteronotus sst*<sub>3</sub> receptor exert similar functions as they do in the corresponding mammalian receptors, their exact role remains to be elucidated. For example, three consensus sites for serine phosphorylation could be identified in the first and third intracellular loops of the *Apteronotus sst*<sub>3</sub> receptor. The corresponding sites Ser<sup>341</sup>, Ser<sup>346</sup>, and Ser<sup>351</sup> (in addition to Thr<sup>357</sup>) of the rat sst<sub>3</sub> receptor expressed in HEK293 cells have been shown to be phosphorylated; phosphorylation at these sites is essential for agonist-dependent internalization (Roth et al., 1997). The kinases by which sst receptors are phosphorylated have, however, not yet been identified.

**Table 1:** Comparison of potencies of SRIF receptor agonists for binding of [<sup>125</sup>I]LTT-SRIF<sub>28</sub> to *Apteronotus* sst<sub>3</sub> receptor gene expressed in CCL39 cells

ligand	pK <sub>d</sub>
SRIF <sub>14</sub>	8.73 ± 0.25
SRIF <sub>28</sub>	8.70 ± 0.20
BIM 23052	7.84 ± 0.06
octreotide	7.33 ± 0.10
BIM 23056	6.41 ± 0.05

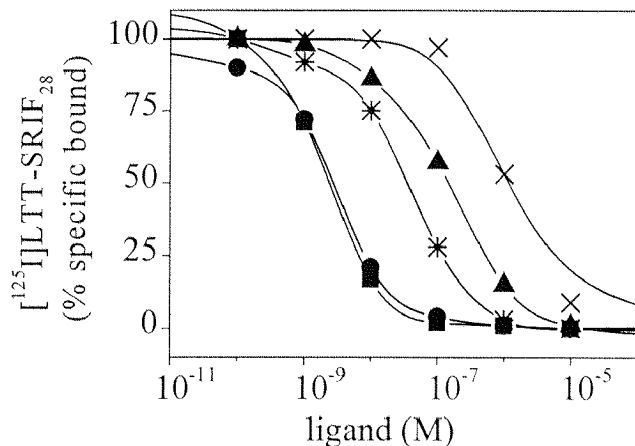
The data represent the mean of pK<sub>d</sub>-values (-log M) ± standard error of six determinations.

In another study, rat sst<sub>2A</sub> receptors were phosphorylated, primarily at serine residues, following stimulation of protein kinase C (Hipkin et al., 1997). However, protein kinase C may activate another kinase, rather than directly mediating receptor phosphorylation.

#### Pharmacological properties of the cloned fish sst<sub>3</sub> receptor

In addition to the sequence similarity, the pharmacological properties support the notion that the gene cloned in the present investigation codes for an *Apteronotus* homologue of a mammalian sst receptor. The saturation data indicate that the *Apteronotus* sst<sub>3</sub> receptor stably expressed in CCL39 cells recognizes [<sup>125</sup>I]LTT-SRIF<sub>28</sub> with high affinity (pK<sub>d</sub> = 10.5), thus being comparable to the pK<sub>d</sub>-values observed with mammalian sst<sub>2</sub>, sst<sub>3</sub>, and sst<sub>5</sub> receptors expressed recombinantly in various cell lines (Brunns et al., 1994, 1995; Siehler et al., 1998b).

**Figure 6:** Competitive radioligand binding assays on membranes prepared from CCL39 cells expressing *Apteronotus sst<sub>3</sub>* receptors.



Crude membrane preparations (4 µg/ assay) of CCL39 cells were incubated with 50 µl [<sup>125</sup>I]LTT-SRIF<sub>28</sub> (2175 Ci/mmol) and the indicated concentrations of SRIF<sub>14</sub> (■), SRIF<sub>28</sub> (●), BIM 23052 (\*), octreotide (▲), and BIM 23056 (×). The data are expressed as percentage of specific binding. They are the mean of triplicate determinations.

To further characterize the *Apteronotus sst<sub>3</sub>* receptor expressed in CCL39 cells, three other radioligands have been employed in a concurrent study (Siehler et al., 1999). This investigation has shown that, in addition to [<sup>125</sup>I]LTT-SRIF<sub>28</sub>, [<sup>125</sup>I]Tyr<sup>10</sup>-cortistatin<sub>14</sub> (the native peptide is a recently discovered putative member of the SRIF family; see De Lecea et al., 1996), as well as the short cyclic radioactively labelled SRIF analogues [<sup>125</sup>I]CGP 23996 and [<sup>125</sup>I]Tyr<sup>3</sup>-octreotide display high affinity. This result is surprising, since the human *sst<sub>3</sub>* receptor shows rather low affinity for octreotide (Siehler et al., 1998a, 1998b). Thus, the *Apteronotus sst<sub>3</sub>* receptor, pharmacologically, appears to be more closely related to the human *sst<sub>5</sub>* receptor than to the human *sst<sub>3</sub>* receptor.

Apparently, the rather minor differences in the amino acid sequence can result in pronounced differences in the pharmacological profile. A similar effect has been found in serotonin (= 5-hydroxytryptamin, 5-HT) receptors. Despite their marked sequence similarity, the rat and human 5-HT<sub>1B</sub> receptors express different pharmacological profiles. This is in contrast to the human 5-HT<sub>1B</sub> and 5-HT<sub>1D</sub> receptors which, although structurally different, exhibit overlapping pharmacological profiles (Hoyer et al., 1994a).

A second surprising finding made in the detailed analysis of the pharmacological properties of the cloned fish *sst<sub>3</sub>* receptor was that the affinities for ligands depend on the type of radioligand used (Siehler et al., 1999).

Especially, the profile of [<sup>125</sup>I]Tyr<sup>3</sup>-octreotide does not correlate well with those of [<sup>125</sup>I]LTT-SRIF, [<sup>125</sup>I]Tyr<sup>10</sup>-cortistatin<sub>14</sub>, and [<sup>125</sup>I]CGP 23996. This could be explained by assuming that [<sup>125</sup>I]Tyr<sup>3</sup>-octreotide might induce or recognize a distinct receptor conformation which is different from the receptor-ligand conformation present when employing the other three radioligands.

Similarly as reported for the mammalian sst<sub>1,5</sub> receptor subtypes (Patel et al., 1994), both SRIF<sub>14</sub> and SRIF<sub>28</sub> inhibit forskolin-stimulated adenylate cyclase activity with high potency and efficacy in CCL39 cells expressing the cloned *Apteronotus* sst<sub>3</sub> receptor (Siehler et al., 1999). The inhibition of forskolin-stimulated adenylate cyclase activity by SRIF<sub>14</sub>, as measured by cAMP accumulation in intact CCL39 cells, is totally blocked by pertussis toxin. This suggests that the inhibitory effect is mediated by G<sub>i</sub> and/or G<sub>o</sub>, thus resembling the effect of pertussis toxin on the five cloned mammalian SRIF receptors (Law et al., 1994; Murthy et al., 1996; Tallent and Reisine, 1992). The SRIF-induced second messenger pathway, therefore, appears to be conserved within the vertebrate phylum.

#### Somatostatin receptors in fish brain

The presence of the *Apteronotus* sst<sub>3</sub> receptor in the brain, as suggested by the initial cloning data obtained after reverse transcription of mRNA from brain tissue, was confirmed by preparation of poly(A)<sup>+</sup>-RNA from brain, followed by high amplification through RT-PCR and subsequent Southern Blot hybridization. On the other hand, the missing signals in Northern Blot analysis using poly(A)<sup>+</sup>-RNA suggest a very low level of expression of the *Apteronotus* sst<sub>3</sub> receptor mRNA *in vivo*. Although the very low level of expression was somewhat unexpected, similar difficulties have been encountered in other cases. When RDC4 (= 5-HT<sub>1D</sub> receptor) was cloned from dog, the authors were unable to find any transcript in the brain (Libert et al., 1989). Yet, as we know now, this receptor is expressed in the brain, but at very low levels and with a very limited distribution (cf. Hartig et al., 1996). Moreover, the low expression level of the *Apteronotus* sst<sub>3</sub> receptor in the brain may not necessarily correspond to a low level of receptor protein, since for this parameter the stability of the transcript is also of crucial importance.

As attempts to map the expression of the *Apteronotus* sst<sub>3</sub> receptor in the brain using *in situ* hybridization have failed so far, probably due to the very low level of expression, no comparison is possible between the distribution of the corresponding mRNA and that of SRIF binding sites. Such sites have been mapped in detail in the brain of *Apteronotus leptorhynchus* (Zupanc et al., 1994). *In situ*-hybridization studies have suggested a wide distribution of the sst<sub>3</sub> receptor mRNA in the rat (Perez and Hoyer, 1995) and the human (Thoss et al., 1996) brain. However, these data are currently unconfirmed at the protein level, since no selective radioligand is yet available to label sst<sub>3</sub> receptors. A preliminary report points to a wide distribution of sst<sub>3</sub> receptor immunoreactivity in the brain of rats and mice (Schulz et al., 1998b). Interestingly, sst<sub>3</sub>-like immunoreactivity was localized to the plasma membrane of neuronal cilia rather than to 'classical' pre- and postsynaptic sites (Händel et al., 1999).

#### Perspectives

It has been hypothesized that SRIF and its receptors are, in the gymnotiform brain, involved in neuronal control of behaviour (for review, see Zupanc and Maler, 1997) and in regulation of postembryonic neurogenesis (for review, see Zupanc, 1999). Future investigations in this field will greatly benefit from the wealth of molecular data obtained through the cloning, sequencing, and pharmacological characterization of the *Apteronotus* sst<sub>3</sub> receptor. These data, together with the availability of *A. albifrons*-specific probes, now enable researchers to explore the cellular mechanisms underlying the action of SRIF in the teleostean brain in much greater detail than was possible previously.



### 10.1. Abstract

The first cloned non-mammalian somatostatin (somatostatin release-inhibiting factor = SRIF) receptor previously obtained from the teleost fish *Apteronotus albifrons* and generically named somatostatin receptor 3 (fsst<sub>3</sub>), was stably expressed and characterised in Chinese hamster lung fibroblast (CCL39) cells. Radioligand binding studies were performed with four radioligands selective for SRIF receptors in CCL39 cells expressing fsst<sub>3</sub> receptors: [<sup>125</sup>I]LTT-SRIF<sub>28</sub> ([Leu<sup>8</sup>, D-Trp<sup>22</sup>, <sup>125</sup>I-Tyr<sup>25</sup>]-SRIF<sub>28</sub>), [<sup>125</sup>I]Tyr<sup>10</sup>-cortistatin, [<sup>125</sup>I]CGP 23996, and [<sup>125</sup>I]Tyr<sup>3</sup>-octreotide labelled fsst<sub>3</sub> receptor with high affinity (pK<sub>d</sub>-values: 10.47, 10.87, 9.59 and 9.57) and in a saturable manner but defined different B<sub>max</sub>-values: 4500, 4000, 3400 and 1500 fmol/ mg, respectively. The affinities of SRIF peptides and analogues determined for fsst<sub>3</sub> receptors displayed the following rank order of potency: seglitide = SRIF<sub>25</sub> > SRIF<sub>14</sub> = SRIF<sub>28</sub> > cortistatin 14 > BIM 23014 > RC160 = L361,301 = octreotide ≥ BIM 23052 ≥ L362,855 > CGP23996 > BIM 23056 > BIM 23030 = cycloantagonist > SRIF<sub>22</sub>. The pharmacological profiles determined with [<sup>125</sup>I]LTT-SRIF<sub>28</sub>, [<sup>125</sup>I]CGP 23996 and [<sup>125</sup>I]Tyr<sup>10</sup>-cortistatin correlated highly significantly (r = 0.96- 0.99), whereas [<sup>125</sup>I]Tyr<sup>3</sup>-octreotide binding was rather divergent (r = 0.78- 0.81). Further, [<sup>125</sup>I]Tyr<sup>3</sup>-octreotide- and [<sup>125</sup>I]CGP 23996-labelled sites showed higher affinity for the various peptides than [<sup>125</sup>I]LTT-SRIF<sub>28</sub> and [<sup>125</sup>I]Tyr<sup>10</sup>-cortistatin-labelled sites, although there were exceptions. [<sup>125</sup>I]LTT-SRIF<sub>28</sub>-binding to fsst<sub>3</sub> receptors and human sst<sub>1,5</sub> receptors was compared; the fsst<sub>3</sub> binding profile correlated better with the hsst<sub>5</sub>- than with the hsst<sub>3</sub> receptor profile. SRIF inhibited potently forskolin-stimulated adenylate cyclase activity in fsst<sub>3</sub> transfected CCL39 cells; this effect was blocked by pertussis toxin, suggesting coupling of the fsst<sub>3</sub> receptor to G<sub>iα</sub> and/ or G<sub>oα</sub>. [<sup>125</sup>I]LTT-SRIF<sub>28</sub> binding was detected in fish brain, liver, heart, spleen, and stomach, but not in gut. The pharmacological profile of [<sup>125</sup>I]LTT-SRIF<sub>28</sub>-labelled sites in brain, but not in liver, correlated significantly with the recombinant fsst<sub>3</sub> receptor, in agreement with expression of fsst<sub>3</sub> receptor gene found by RT-PCR in brain. However, biphasic binding curves obtained with two SRIF-analogues in brain, as well as the distinct pharmacological profile of the liver SRIF receptor, suggest the existence of several yet to be defined SRIF receptor subtypes in fish.

The present data demonstrate that the recombinantly expressed  $fsst_3$  receptor has a pharmacological profile compatible with that of a  $SRIF_1$  receptor, although the rank order of affinity of  $fsst_3$  is closer to that of  $hsst_3$  than  $hsst_3$  receptors, as may be found when comparing very distantly related species. The  $fsst_3$  receptor expressed in CCL39 cells, is negatively coupled to adenylate cyclase activity via pertussis toxin-sensitive G-proteins, like mammalian  $sst_3$  receptors. Radioligand binding performed with fish tissue suggests the presence of a native  $sst_3$  receptor in brain as well as other yet to be defined SRIF receptor subtypes.

## 10.2. Results

Radioligand binding in CCL39 cells expressing  $fsst_3$  receptors

$[^{125}I]LTT-SRIF_{28}$ ,  $[^{125}I]CGP\ 23996$ ,  $[^{125}I]Tyr^{10}-CST$  and  $[^{125}I]Tyr^3$ -octreotide labelled the cloned  $fsst_3$  receptor stably expressed in CCL39 cells with high affinity; the levels of non-specific binding were low for all four radioligands.  $[^{125}I]LTT-SRIF_{28}$  and  $[^{125}I]Tyr^{10}-CST$  ( $pK_d = 10.47 \pm 0.12$  and  $10.87 \pm 0.34$ , respectively) displayed somewhat higher affinity than  $[^{125}I]CGP\ 23996$  and  $[^{125}I]Tyr^3$ -octreotide ( $pK_d = 9.59 \pm 0.04$  and  $9.57 \pm 0.04$ ) (table 1). All saturation curves were monophasic and compatible with the labelling of a single population of receptor sites (figure 1). However, whereas  $[^{125}I]LTT\ SRIF_{28}$ ,  $[^{125}I]Tyr^{10}-CST$  and  $[^{125}I]CGP\ 23996$  labelled similar densities of receptor sites (between 3000 and 4400 fmol/ mg),  $[^{125}I]Tyr^3$ -octreotide - surprisingly - labelled only about 1500 fmol/ mg (see discussion). No specific binding was detected with any of the four radioligands in non-transfected CCL39 cells (data not shown).

The pharmacological profiles of  $[^{125}I]LTT-SRIF_{28}$ ,  $[^{125}I]Tyr^{10}\ CST$ ,  $[^{125}I]CGP\ 23996$  and  $[^{125}I]Tyr^3$ -octreotide-labelled sites were established in membranes of CCL39 cells expressing  $fsst_3$  receptors using a number of analogues of somatostatin including the native peptides  $SRIF_{14}$ ,  $SRIF_{22}$ ,  $SRIF_{25}$ ,  $SRIF_{28}$  and  $CST$ . The peptides tested showed very high affinity (in the range 30 pM to 100 nM). There were, however, disparities as listed in table 2.

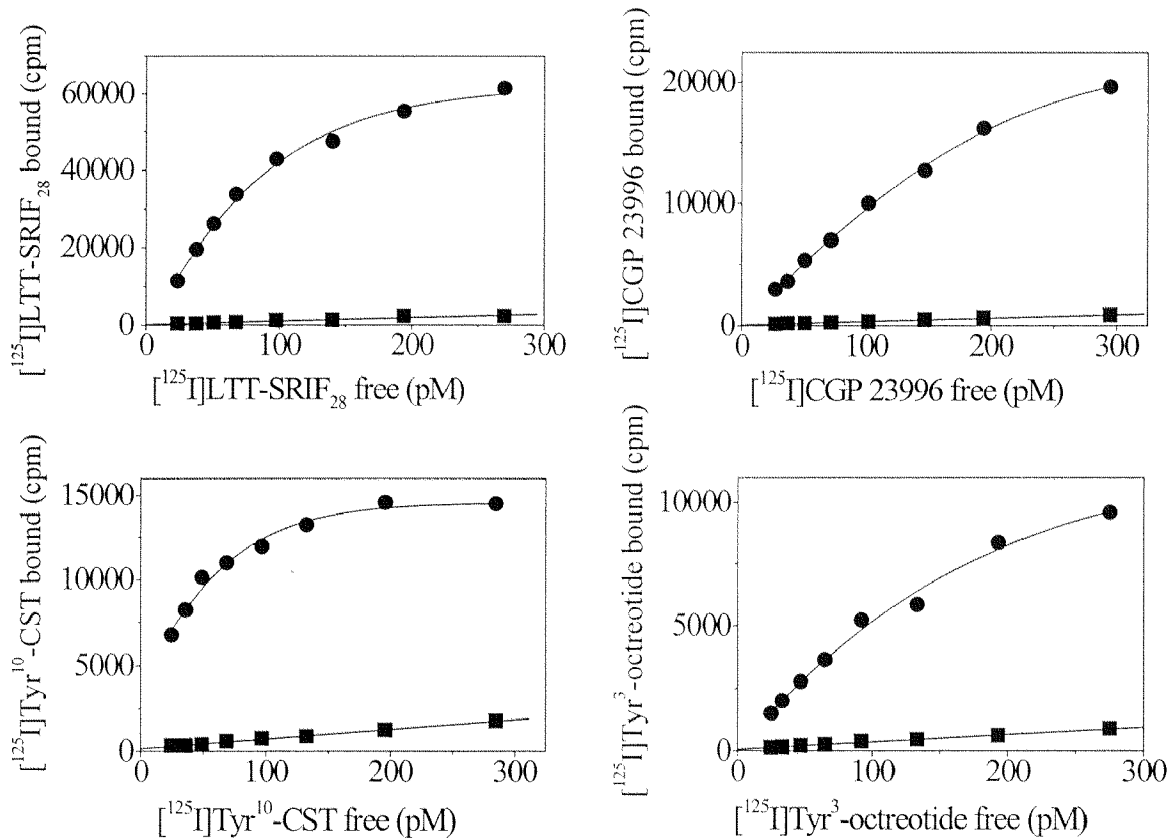
In general, the peptides showed somewhat higher affinity for sites labelled with [<sup>125</sup>I]Tyr<sup>3</sup>-octreotide when compared to [<sup>125</sup>I]CGP 23996, whereas sites labelled with [<sup>125</sup>I]LTT-SRIF<sub>28</sub> or [<sup>125</sup>I]Tyr<sup>10</sup>-CST displayed significantly lower affinity. Thus, the differences between [<sup>125</sup>I]Tyr<sup>10</sup>-CST and [<sup>125</sup>I]Tyr<sup>3</sup>-octreotide ranged from 13 to 160 fold, with two exceptions; there was no difference for BIM 23056, whereas that for BIM 23056 was 8900 fold. The differences tended to be larger for the synthetic analogues, about 40-160 fold (except BIM 23052 and BIM 23056), whereas the “natural” peptides showed only 13-51 times higher affinity for [<sup>125</sup>I]Tyr<sup>3</sup>-octreotide binding (figure 2). Nevertheless, the overall pharmacological profiles were similar, especially when the sites were labelled with [<sup>125</sup>I]LTT-SRIF<sub>28</sub>, [<sup>125</sup>I]Tyr<sup>10</sup>-CST, or [<sup>125</sup>I]CGP 23996 ( $r = 0.96- 0.99$ ,  $P < 0.0001$ , see figure 3). By contrast, the profile defined with [<sup>125</sup>I]Tyr<sup>3</sup>-octreotide was rather dissimilar from that determined with each of the three other radioligands ( $r = 0.75- 0.81$ ).

**Table 1:** Results of saturation experiments performed with different radioligands at fish  $sst_3$  receptors expressed in CCL39 cells

	pK <sub>d</sub>	B <sub>max</sub> [fmol/mg]
[ <sup>125</sup> I]LTT-SRIF <sub>28</sub>	10.47 ± 0.12	4470 ± 240
[ <sup>125</sup> I]CGP 23996	9.59 ± 0.04	3420 ± 190
[ <sup>125</sup> I]Tyr <sup>10</sup> -CST	10.87 ± 0.34	4030 ± 210
[ <sup>125</sup> I]Tyr <sup>3</sup> -octreotide	9.57 ± 0.04	1520 ± 60

The data are expressed as B<sub>max</sub> (fmol/ mg) and pK<sub>d</sub>-values (-log mol/ l) ± SEM of 3 different experiments. Dunnett’s multiple comparison test indicates that the B<sub>max</sub>-values defined by [<sup>125</sup>I]LTT-SRIF<sub>28</sub> and [<sup>125</sup>I]Tyr<sup>10</sup>-CST are not different ( $P > 0.05$ ), whereas [<sup>125</sup>I]CGP 23996 ( $P < 0.05$ ) and [<sup>125</sup>I]Tyr<sup>3</sup>-octreotide ( $P < 0.01$ ) labelled significantly less sites.

**Figure 1:** Saturation isotherms of binding of [ $^{125}$ I]LTT-SRIF<sub>28</sub>, [ $^{125}$ I]CGP 23996, [ $^{125}$ I]Tyr<sup>10</sup>-CST, and [ $^{125}$ I]Tyr<sup>3</sup>-octreotide to membranes prepared from CCL39 cells stably expressing fsst<sub>3</sub> receptors.



Crude membrane preparations from fsst<sub>3</sub> receptor expressing cells were incubated with increasing concentrations of each radioligand and assayed for receptor binding activity. The plots depict specific (●) and non-specific binding (■) expressed as bound (cpm/ assay) versus free radioligand concentration (pM). The data points represent one representative example of 3 different experiments.

#### Inhibition of forskolin-stimulated cAMP production

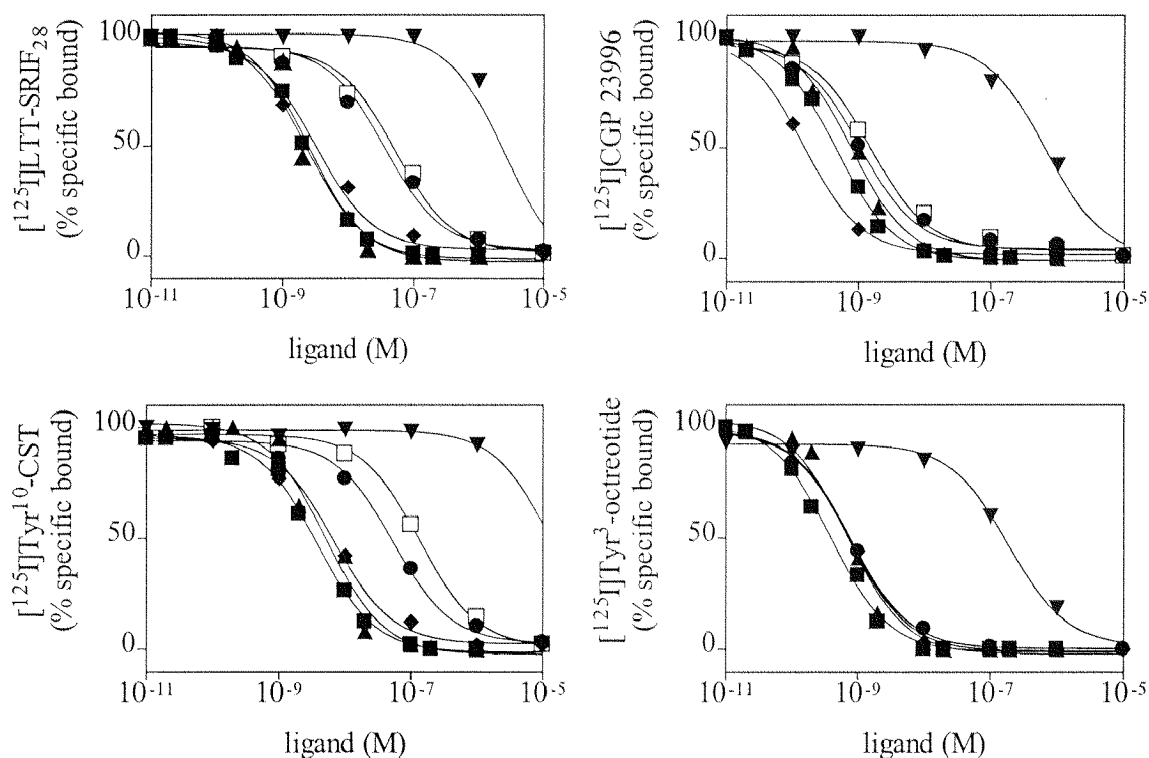
Since the mammalian sst<sub>1,5</sub> receptor subtypes have been reported to couple negatively to adenylate cyclase, we examined whether the fish sst<sub>3</sub> receptor modulates adenylate activity. Both SRIF<sub>14</sub> and SRIF<sub>28</sub> inhibited forskolin-stimulated adenylate cyclase activity (figure 4) with high potency and efficacy, as measured by cAMP accumulation in intact CCL39 cells.

**Table 2:** Comparison of affinities of SRIF, various SRIF-analogues and cortistatin for fish sst<sub>3</sub> receptors labelled with different radioligands

	[ <sup>125</sup> I]LTT-SRIF <sub>28</sub>	[ <sup>125</sup> I]Tyr <sup>10</sup> -CST	[ <sup>125</sup> I]CGP 23996	[ <sup>125</sup> I]Tyr <sup>3</sup> -octreotide
seglitide	9.15 ± 0.08	8.55 ± 0.11 <sup>ns</sup>	9.83 ± 0.13*	10.53 ± 0.23**
SRIF <sub>25</sub>	9.00 ± 0.07	8.85 ± 0.04 <sup>ns</sup>	9.93 ± 0.17**	10.32 ± 0.04**
SRIF <sub>14</sub>	8.93 ± 0.19	8.87 ± 0.07 <sup>ns</sup>	9.53 ± 0.28*	9.99 ± 0.12**
SRIF <sub>28</sub>	8.84 ± 0.15	8.61 ± 0.03 <sup>ns</sup>	9.64 ± 0.19*	10.21 ± 0.39**
cortistatin 14	8.82 ± 0.10	8.51 ± 0.16 <sup>ns</sup>	9.63 ± 0.01**	9.85 ± 0.05**
Tyr <sup>10</sup> -cortistatin	8.54 ± 0.08	8.32 ± 0.17 <sup>ns</sup>	9.37 ± 0.31 <sup>ns</sup>	9.98 ± 0.24**
BIM 23014	8.06 ± 0.08	7.69 ± 0.08*	9.37 ± 0.08**	9.63 ± 0.02**
RC160	7.67 ± 0.05	7.21 ± 0.06**	8.86 ± 0.08**	9.29 ± 0.02**
L361,301	7.73 ± 0.26	7.01 ± 0.15*	8.91 ± 0.08**	9.22 ± 0.02**
octreotide	7.45 ± 0.10	7.28 ± 0.18 <sup>ns</sup>	8.72 ± 0.10**	9.29 ± 0.02**
BIM 23052	7.92 ± 0.08	7.68 ± 0.08 <sup>ns</sup>	9.15 ± 0.12**	7.90 ± 0.16 <sup>ns</sup>
L362,855	7.54 ± 0.05	7.09 ± 0.13**	8.77 ± 0.02**	8.91 ± 0.06**
CGP23996	7.16 ± 0.28	6.78 ± 0.30 <sup>ns</sup>	8.24 ± 0.03*	8.94 ± 0.03**
BIM 23056	6.32 ± 0.07	5.88 ± 0.09**	6.97 ± 0.07**	9.83 ± 0.06**
BIM 23030	6.40 ± 0.05	6.04 ± 0.02**	7.46 ± 0.08**	7.62 ± 0.03**
cycloantagonist	6.25 ± 0.15	5.94 ± 0.18 <sup>ns</sup>	7.17 ± 0.07**	7.95 ± 0.12**
SRIF <sub>22</sub>	5.33 ± 0.08	5.17 ± 0.07 <sup>ns</sup>	6.19 ± 0.09**	6.88 ± 0.03**

The data represent the mean of pK<sub>d</sub>-values (-log mol/ l) ± SEM of at least 3 determinations. Dunnett's multiple comparison test indicates that the profiles defined by the four radioligands differ to various extents: whereas [<sup>125</sup>I]LTT-SRIF<sub>28</sub> and [<sup>125</sup>I]Tyr<sup>10</sup>-CST are not different (P > 0.05), the profiles defined by [<sup>125</sup>I]CGP 23996 (P < 0.05) and [<sup>125</sup>I]Tyr<sup>3</sup>-octreotide (P < 0.01) are different from that defined using [<sup>125</sup>I]LTT-SRIF<sub>28</sub>. In addition, individual pK<sub>d</sub>-values were compared to those obtained with [<sup>125</sup>I]LTT-SRIF<sub>28</sub> and significance of difference is indicated: ns = non significant, \* = P < 0.05, \*\* = P < 0.01.

**Figure 2:** Competitive radioligand binding assays on membranes prepared from CCL39 cells expressing *fsst*<sub>3</sub> receptors.



Crude membrane preparations from *fsst*<sub>3</sub> receptor-transfected cells were incubated with  $[^{125}\text{I}]\text{LTT-SRIF}_{28}$ ,  $[^{125}\text{I}]\text{CGP 23996}$ ,  $[^{125}\text{I}]\text{Tyr}^{10}\text{-CST}$  or  $[^{125}\text{I}]\text{Tyr}^3\text{-octreotide}$  respectively, and the indicated concentrations of SRIF<sub>14</sub> (■), SRIF<sub>28</sub> (▲), SRIF<sub>22</sub> (▼), seglitide (◆), octreotide (●), and RC160 (□). Data are expressed as percentage of specific binding. The data points represent one representative example of at least 3 different experiments.

The maximal inhibition induced by SRIF<sub>14</sub> and SRIF<sub>28</sub> was 87 % and 91 %, with  $\text{pEC}_{50}$ -values of  $9.52 \pm 0.01$  and  $9.19 \pm 0.01$  respectively (mean  $\pm$  SEM,  $n = 3$ ). The inhibition of forskolin-stimulated adenylate cyclase activity by SRIF<sub>14</sub> was totally blocked by pertussis toxin (figure 5). Therefore, the negative coupling of *fsst*<sub>3</sub> to adenylate cyclase is mediated by  $G_{i\alpha}$  and/or  $G_{0\alpha}$  in CCL39 cells.

## Radioligand binding in fish tissues

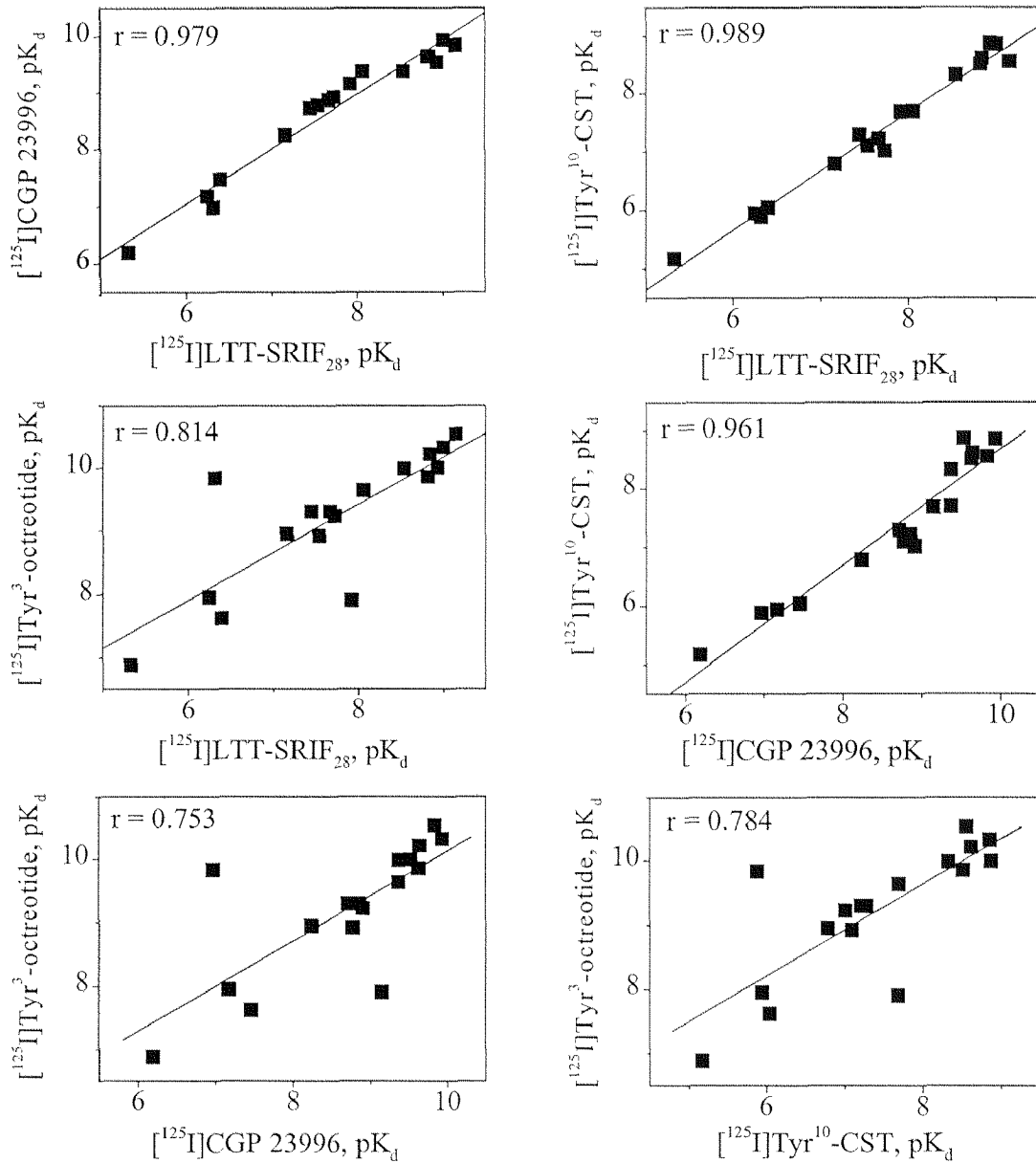
The presence and nature of somatostatin binding sites was studied in different tissues of *A. albifrons* with [<sup>125</sup>I]LTT-SRIF<sub>28</sub> (table 3). High levels of binding were observed in brain and liver, intermediate levels in heart and spleen, and a low level in stomach. No specific [<sup>125</sup>I]LTT-SRIF<sub>28</sub> binding was detectable in gut. Brain and liver were therefore used in competition experiments using [<sup>125</sup>I]LTT-SRIF<sub>28</sub> (table 4, figure 6), since binding was too low in stomach, whereas heart and spleen were not available in sufficient quantities. In brain, SRIF<sub>14</sub> and SRIF<sub>28</sub> displayed high affinity, as did the short cyclic SRIF-analogues seglitide and octreotide; however, both analogues produced biphasic competition curves suggesting the presence of two different populations of sites. In liver, SRIF<sub>28</sub> bound with somewhat higher affinity than SRIF<sub>14</sub>; other SRIF analogues displayed intermediate to high affinity except the cycloantagonist SA, which showed low affinity to both brain and liver.

The profile of the recombinant fsst<sub>3</sub> receptor was compared with that of fish brain and liver sites labelled with [<sup>125</sup>I]LTT-SRIF<sub>28</sub> (figure 7). Since two binding populations were defined by seglitide and octreotide in brain, only the high affinity values were considered. The brain and fsst<sub>3</sub> profiles correlated highly significantly ( $r = 0.942$ ,  $P < 0.001$ ), supporting the presence of fsst<sub>3</sub> receptor protein in fish brain as previously suggested by RT-PCR data (Zupanc et al., 1999). The correlation coefficient obtained with liver and fsst<sub>3</sub> sites was lower ( $r = 0.826$ ) suggesting the presence of either a mixture of sst<sub>3</sub> and some other site, or that of another SRIF receptor distantly related to fsst<sub>3</sub>.

## Comparison with human somatostatin receptors

Finally, the pharmacological profile of the fsst<sub>3</sub> receptor was compared with that of the five recombinant human somatostatin receptors; the data were obtained with [<sup>125</sup>I]LTT-SRIF<sub>28</sub> in CCL39 cells expressing hsst<sub>1,5</sub> receptors (Siehler et al., 1998a; 1998b). The fsst<sub>3</sub> profile did not correlate with those of hsst<sub>1</sub> and hsst<sub>4</sub> receptors, which belong to the SRIF<sub>2</sub> receptor family ( $r = 0.461$  and  $r = 0.357$ , respectively; data not shown).

**Figure 3:** Comparison of [ $^{125}$ I]LTT-SRIF<sub>28</sub>, [ $^{125}$ I]CGP 23996, [ $^{125}$ I]Tyr<sup>10</sup>-CST, and [ $^{125}$ I]Tyr<sup>3</sup>-octreotide defined pharmacological profiles of fish recombinant sst<sub>3</sub> receptor expressed in CCL39 cells.

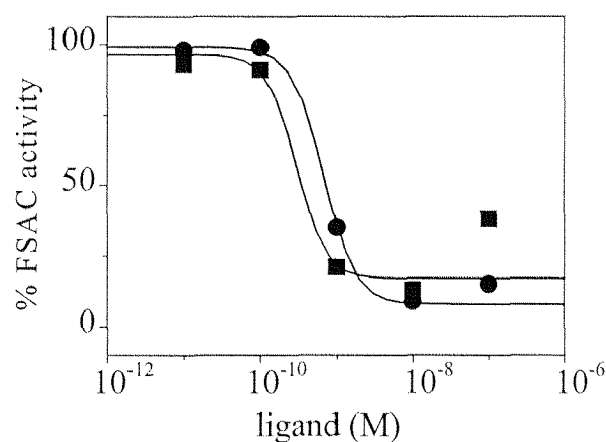


Data shown in table 2 are depicted as plots with pK<sub>d</sub>-values obtained by labelling of fish sst<sub>3</sub> receptor with distinct radioligands. Correlation coefficients (r) are indicated in all plots.



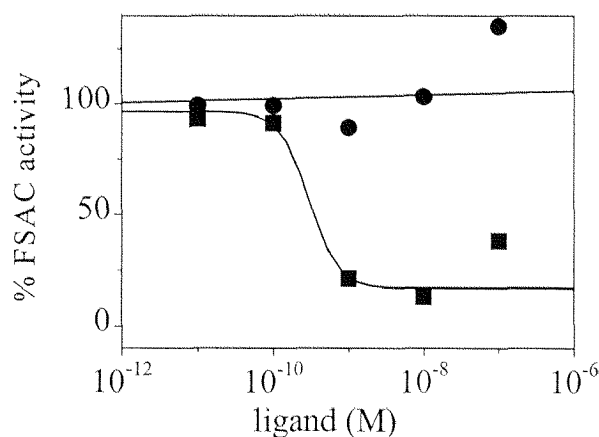
Therefore, only binding data of  $hsst_2$ ,  $hsst_3$ , and  $hsst_5$ , which belong to the  $SRIF_1$  family, are presented (table 5). The  $fsst_3$  profile correlated best with the  $hsst_5$  receptor ( $r = 0.920$ ,  $P < 0.001$ ), whereas lower correlation coefficients were observed with  $hsst_2$  ( $r = 0.832$ ) or  $hsst_3$  receptor ( $r = 0.689$ ) (figure 8).

**Figure 4:** Inhibition of forskolin-stimulated adenylate cyclase (FSAC) activity by  $SRIF_{14}$  and  $SRIF_{28}$  in CCL39 cells expressing  $fsst_3$  receptors.



Fish  $sst_3$  receptor transfected cells were incubated with 6  $\mu$ Ci [ $^3$ H]adenine, treated with forskolin (10  $\mu$ M) and the indicated concentrations of  $SRIF_{14}$  (■) or  $SRIF_{28}$  (●), and [ $^3$ H]cAMP isolated by sequential chromatography. Graphs represent the percentage of inhibition of forskolin-stimulated adenylate cyclase activity. The data points represent one representative example of 3 different experiments. The mean of the  $pEC_{50}$ -values  $\pm$  SEM of three determinations for  $SRIF_{14}$  is  $9.52 \pm 0.01$  and for  $SRIF_{28}$  is  $9.19 \pm 0.01$ .

**Figure 5:** Inhibition of forskolin-stimulated adenylate cyclase (FSAC) activity by  $SRIF_{14}$  in  $fsst_3$  receptor expressing CCL39 cells is inhibited by pertussis toxin.



$Fsst_3$  receptor transfected cells were treated for 24 hours with pertussis toxin (●) or not treated (■), incubated with 6  $\mu$ Ci [ $^3$ H]adenine, stimulated with forskolin (10  $\mu$ M) and the indicated concentrations of  $SRIF_{14}$ ; [ $^3$ H]cAMP was isolated by sequential chromatography. Graphs represent the percentage of inhibition of forskolin-stimulated adenylate cyclase activity. The data points represent one representative example of 3 different experiments.

### 10.3. Discussion

The present paper describes the pharmacological profile and receptor-effector coupling of the putative  $fsst_3$  receptor expressed recombinantly in hamster fibroblast CCL39 cells. In addition, the presence of the native  $sst_3$  receptor was investigated in various fish tissues.

The  $fsst_3$  receptor is a member of the  $SRIF_1$  receptor family

$[^{125}I]LTT-SRIF_{28}$ ,  $[^{125}I]CGP\ 23996$ ,  $[^{125}I]Tyr^{10}-CST$  and  $[^{125}I]Tyr^3$ -octreotide were used to label  $fsst_3$  receptors expressed in CCL39 cells.  $SRIF_{14}$  (which is found in all vertebrates),  $SRIF_{28}$ , and  $SRIF_{25}$  all displayed high affinity for  $fsst_3$  receptors. It may be surprising that  $SRIF_{22}$ , which has been identified in catfish, a teleostean order closely related to the gymnotiform fish, exhibited low affinity for  $fsst_3$ .

**Table 3:** Specific binding of  $[^{125}I]LTT-SRIF_{28}$  to tissue preparations of *Apteronotus albifrons*

	$[^{125}I]LTT-SRIF_{28}$
brain	80.0 % $\pm$ 0.7
liver	66.1 % $\pm$ 4.2
heart	51.8 % $\pm$ 0.5
spleen	45.8 % $\pm$ 2.4
stomach	29.9 % $\pm$ 2.4
gut	0.0 % $\pm$ 0.0

The data represent the percentage of specific binding (mean  $\pm$  SEM of 3 determinations) determined with a radioligand concentration of 30 pM.

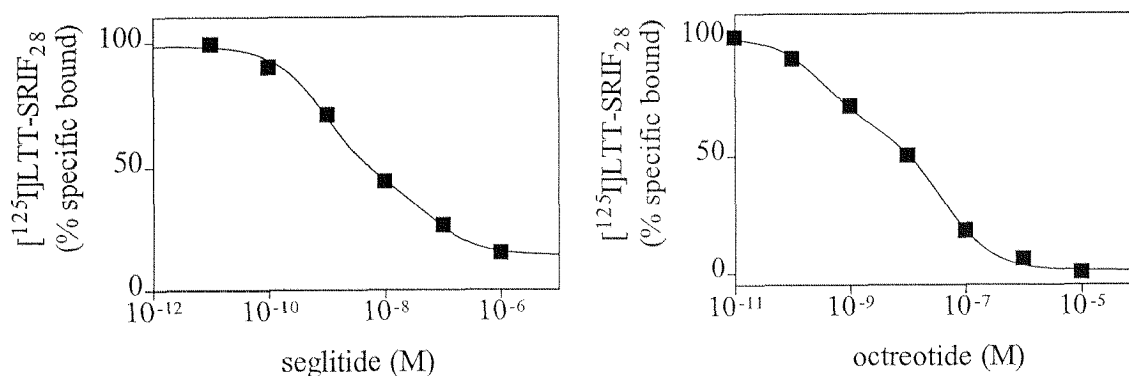
This suggests that SRIF<sub>22</sub> and its corresponding receptor are either not expressed at all in tissues of *Apteronotus albifrons*, or that at least one other receptor with higher affinity for SRIF<sub>22</sub> exists in fish. Cortistatin, of which the prepropeptide was cloned from rat, mouse, and human (De Lecea et al., 1996; De Lecea et al., 1997a; Fukusumi et al., 1997), displays similar high affinity for fsst<sub>3</sub> receptors as SRIF<sub>14</sub>, SRIF<sub>28</sub>, and SRIF<sub>25</sub>. CST also binds with high affinity for the hsst<sub>1,5</sub> receptors (Fukusumi et al., 1997; Siehler et al., 1998b). Since CST<sub>14</sub> is highly similar to SRIF<sub>14</sub> (11 out of 14 amino acids are identical), these findings provide additional support for the peptide to be considered a member of the SRIF family.

**Table 4:** Affinities of SRIF and various SRIF-analogues for brain and liver membranes of *Apteronotus albifrons* labelled with [<sup>125</sup>I]LTT-SRIF<sub>28</sub>

	brain	liver
SRIF <sub>14</sub>	9.42 ± 0.22	8.94 ± 0.15
SRIF <sub>28</sub>	9.58 ± 0.03	9.58 ± 0.06
seglitide	8.85 ± 0.05 / 6.34 ± 0.05	8.47 ± 0.06
octreotide	9.52 ± 0.01 / 7.55 ± 0.02	8.52 ± 0.14
L362,855	7.52 ± 0.06	8.22 ± 0.12
RC160	8.33 ± 0.03	8.44 ± 0.33
BIM 23014	8.09 ± 0.06	8.39 ± 0.24
cycloantagonist SA	6.38 ± 0.29	6.40 ± 0.03

The data represent the mean of pK<sub>d</sub>-values (-log mol/l) ± SEM of 3 different experiments. The competition curves were biphasic for seglitide and octreotide in brain membranes as evaluated by the high and low affinity values.

**Figure 6:** Competitive radioligand binding assays on membranes prepared from brain of the fish *Apteronotus albifrons*.



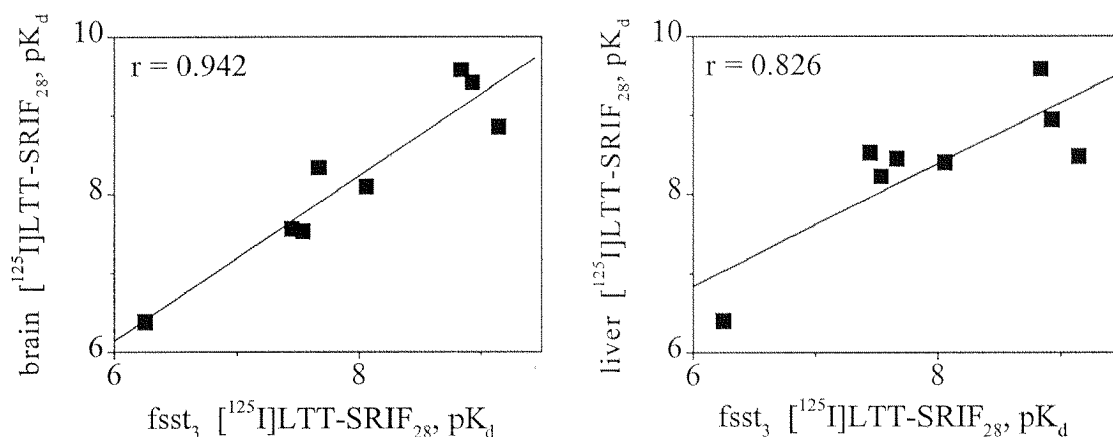
Crude membrane preparations from fish brain were incubated with [<sup>125</sup>I]LTT-SRIF<sub>28</sub> and the indicated concentrations of seglitide (■) or octreotide (●). Data are expressed as percentage of specific binding. The data points represent one representative example of at least 3 different experiments.

The short cyclic SRIF-analogues seglitide, octreotide, RC160, and BIM 23014 display high affinity for the *fst*<sub>3</sub> receptor, as is typical of the SRIF<sub>1</sub> receptor family (Hoyer et al., 1994b, 1995b), although these compounds tend to show higher affinity for the *fst*<sub>3</sub> compared to the human receptors. These findings are in line with the classification of SRIF receptors (Hoyer et al., 1995a), which considers *sst*<sub>2</sub>, *sst*<sub>3</sub> and *sst*<sub>5</sub> receptors to form the SRIF<sub>1</sub> receptor family.

#### Atypical pharmacological features

We have compared the binding characteristics of [<sup>125</sup>I]LTT-SRIF<sub>28</sub>, [<sup>125</sup>I]Tyr<sup>10</sup>-CST, [<sup>125</sup>I]CGP 23996, and [<sup>125</sup>I]Tyr<sup>3</sup>-octreotide: all four radioligands showed high affinity, including [<sup>125</sup>I]Tyr<sup>10</sup>-CST and, unexpectedly, also [<sup>125</sup>I]Tyr<sup>3</sup>-octreotide (since the mammalian *sst*<sub>3</sub> receptor shows rather low affinity for octreotide). The pharmacological profiles determined with [<sup>125</sup>I]LTT-SRIF<sub>28</sub>, [<sup>125</sup>I]CGP 23996, [<sup>125</sup>I]Tyr<sup>10</sup>-CST and [<sup>125</sup>I]Tyr<sup>3</sup>-octreotide were apparently radioligand-dependent.

**Figure 7:** Correlation analyses between binding affinities of SRIF and various analogues for recombinant  $fsst_3$  receptor expressed in CCL39 cells, and for fish brain and fish liver labelled with  $[^{125}I]LTT-SRIF_{28}$ .



$pK_d$ -values of SRIF and SRIF-analogues shown in both tables 2 and 4 are depicted as plots. Correlation coefficients ( $r$ ) are indicated in the plots. With seglitide and octreotide two binding sites in brain were detected; the high affinity value was used for correlation analysis.

With  $[^{125}I]LTT-SRIF_{28}$  and  $[^{125}I]Tyr^{10}-CST$ , affinity values were up to 160-fold lower than with  $[^{125}I]CGP\ 23996$  and  $[^{125}I]Tyr^3$ -octreotide. In extreme cases, the apparent affinity varied up to 250-300 (even 8900 fold) for a single peptide. However, these differences were not systematic and were more limited for the native peptides compared to synthetic ones. The pharmacological profiles obtained with  $[^{125}I]LTT-SRIF_{28}$ ,  $[^{125}I]CGP\ 23996$ , and  $[^{125}I]Tyr^{10}-CST$  were similar, whereas the profile obtained with  $[^{125}I]Tyr^3$ -octreotide was somewhat different from the others (correlation coefficient  $r \leq 0.81$ ). Differences in profiles have been reported for species variants of the same receptor; for example, the  $hsst_3$  receptor shows a 160-fold lower affinity for octreotide than the rat  $sst_3$  receptor (O'Carroll et al., 1994). Such differences in affinity may relate to changes in the amino acid sequence and/or protein folding, or to cell type-specific post-transcriptional and post-translational modifications, e.g. phosphorylation and glycosylation, or even cell-specific expression of G-protein subsets (Lefkowitz et al., 1993).

**Table 5:** Comparison of affinities of SRIF and various SRIF-analogues for fish  $ssst_3$  receptors and the human somatostatin receptor subtypes of the SRIF<sub>1</sub> receptor family, labelled with [<sup>125</sup>I]LTT-SRIF<sub>28</sub>

	fsst <sub>3</sub>	hsst <sub>3</sub>	hsst <sub>2</sub>	hsst <sub>3</sub>
SRIF <sub>14</sub>	8.93 ± 0.19	9.53 ± 0.13	10.00 ± 0.01	9.54 ± 0.05
SRIF <sub>28</sub>	8.84 ± 0.15	9.39 ± 0.22	9.92 ± 0.03	9.65 ± 0.04
seglitide	9.15 ± 0.08	8.70 ± 0.26	9.96 ± 0.02	6.88 ± 0.08
CGP23996	7.16 ± 0.28	6.59 ± 0.41	8.58 ± 0.07	8.82 ± 0.05
octreotide	7.45 ± 0.10	7.17 ± 0.30	9.19 ± 0.03	7.88 ± 0.04
L362,855	7.54 ± 0.05	7.17 ± 0.30	8.36 ± 0.05	7.62 ± 0.23
L361,301	7.73 ± 0.26	7.69 ± 0.13	8.39 ± 0.11	6.34 ± 0.06
RC160	7.67 ± 0.05	7.51 ± 0.06	9.35 ± 0.09	7.37 ± 0.15
BIM 23030	6.40 ± 0.05	6.02 ± 0.09	7.77 ± 0.07	7.17 ± 0.08
BIM 23014	8.06 ± 0.08	7.76 ± 0.13	9.27 ± 0.06	7.86 ± 0.41
BIM 23056	6.32 ± 0.07	7.17 ± 0.05	6.33 ± 0.10	6.90 ± 0.04
BIM 23052	7.92 ± 0.08	7.92 ± 0.19	8.30 ± 0.14	8.42 ± 0.12
cycloantagonist	6.25 ± 0.15	6.38 ± 0.23	5.40 ± 0.06	6.23 ± 0.03
Tyr <sup>10</sup> -cortistatin	8.54 ± 0.08	8.67 ± 0.24	8.77 ± 0.09	8.70 ± 0.18
cortistatin 14	8.82 ± 0.10	8.71 ± 0.02	8.75 ± 0.20	9.06 ± 0.12

The data represent the mean of pK<sub>d</sub>-values (-log mol/ l) ± SEM of at least 3 determinations. [<sup>125</sup>I]LTT-SRIF<sub>28</sub> labelled a single population of binding sites in hsst<sub>2</sub>, hsst<sub>3</sub>, and hsst<sub>5</sub> expressing CCL39 cells (pK<sub>d</sub> = 9.89 ± 0.04 / B<sub>max</sub> [fmol/ mg] = 370 ± 60, pK<sub>d</sub> = 10.28 ± 0.06 / B<sub>max</sub> = 560 ± 60, pK<sub>d</sub> = 10.48 ± 0.04 / B<sub>max</sub> = 6950 ± 220, respectively).

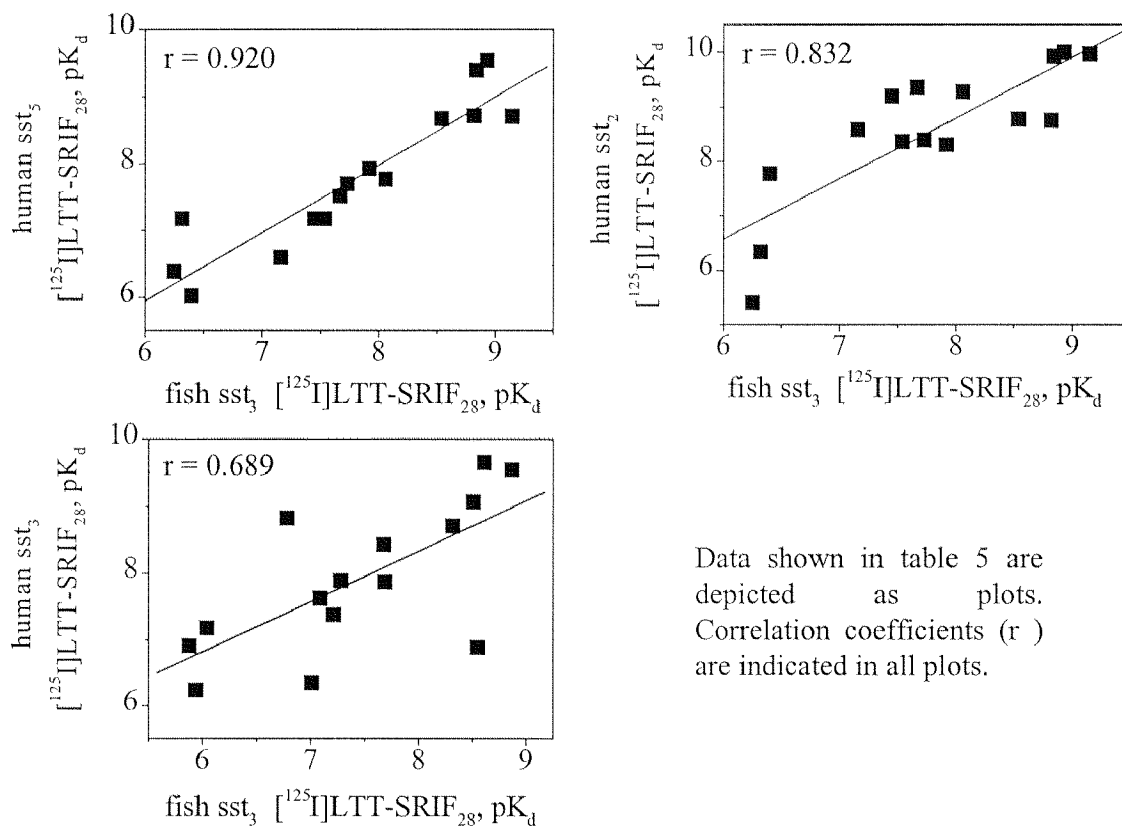
However, in the present study, the fsst<sub>3</sub> receptor was studied throughout in CCL39 cells, and, nevertheless, affinities for ligands appeared to be radioligand-dependent; this could be explained by varying receptor-ligand conformations. Since the profile of [<sup>125</sup>I]Tyr<sup>3</sup>-octreotide did not correlate well with those of the other radioligands, [<sup>125</sup>I]Tyr<sup>3</sup>-octreotide might induce/ recognise a distinct receptor conformation.

By inhibition of radioligand binding at the  $hsst_5$  receptor with the GTP-analogue GppNHp (guanylylimidodiphosphate) it could be shown that [ $^{125}$ I]Tyr<sup>3</sup>-octreotide labels almost exclusively G-protein-coupled receptors, while [ $^{125}$ I]LTT-SRIF<sub>28</sub> and [ $^{125}$ I]CGP 23996 labelled coupled and uncoupled receptors, although all radioligands behave as full agonists in functional assays (Siehler et al., 1998a). This might also be the case with the  $fsst_3$  receptor and could explain the different  $B_{max}$ -values obtained with these radioligands.

[ $^{125}$ I]LTT-SRIF<sub>28</sub> and [ $^{125}$ I]Tyr<sup>10</sup>-CST labelled more receptor sites (4470 and 4030 fmol/mg, respectively) compared to [ $^{125}$ I]CGP 23996 (3420 fmol/mg) and especially [ $^{125}$ I]Tyr<sup>3</sup>-octreotide (1520 fmol/mg). The data are surprising in that, although experiments were performed largely in parallel using the same batches of membranes, the four radioligands appear to recognise different populations of receptors. Such data have been reported previously when comparing agonist and antagonist binding, as in the case of 5-HT<sub>2</sub> receptors (Teitler et al., 1990); however, this may not apply here, since the equivalent non-radioactive somatostatin analogues have always been described as agonists at SRIF receptors. This cannot be tested formally, because the corresponding cold ligands (i.e. ligands labelled with  $^{127}$ I) are not available.

Nevertheless, assuming that the radioligands are agonists in nature, this would suggest that the ligand-receptor complexes defined by each radioligand are conformationally different. This may seem surprising, but appears to be supported by the competition data (see above). The conformation of the ligand-receptor complex may vary markedly depending on the radioligand used; in other words, higher concentrations of octreotide or seglitide are needed to displace [ $^{125}$ I]LTT-SRIF<sub>28</sub> or [ $^{125}$ I]Tyr<sup>10</sup>-CST compared to [ $^{125}$ I]Tyr<sup>3</sup>-octreotide or [ $^{125}$ I]CGP 23996 binding. Based on the affinity values determined by the former two ligands, it could hardly be anticipated that the iodinated forms of CGP 23996 or octreotide ( $pK_d$ -values 35- 166 nM) may be used to label the  $fsst_3$  receptor at concentrations as low as 30 pM (those used to perform competition experiments). Thus, depending on the radioligand used, the affinity of a given compound may be underestimated rather dramatically. Similar discrepancies in both affinity and  $B_{max}$ -values have been reported at the  $hsst_5$  receptor when comparing profiles obtained with [ $^{125}$ I]LTT-SRIF<sub>28</sub>, [ $^{125}$ I]CGP 23996, and [ $^{125}$ I]Tyr<sup>3</sup>-octreotide (Siehler et al., 1998a).

**Figure 8:** Correlation analyses of affinities of SRIF and various SRIF-analogues for  $fsst_3$  receptor expressed in CCL39 cells and human SRIF<sub>1</sub> receptor subtypes expressed in CCL39 cells labelled with [<sup>125</sup>I]LTT-SRIF<sub>28</sub>.



### Species variations

Pharmacologically, the  $fsst_3$  receptor is more closely related to the  $hsst_5$  than to the  $hsst_3$  receptor. Indeed, profiles established with [<sup>125</sup>I]LTT-SRIF<sub>28</sub> revealed a very high correlation between  $fsst_3$  and  $hsst_5$  receptors ( $r = 0.920$ ,  $P < 0.001$ ) and a lower correlation with  $hsst_3$  receptors; this observation cannot be explained by different cell systems, because all receptors were expressed in CCL39 cells and are, therefore, species related. This, however is not unusual, as it is well known that minor changes in the amino acid sequence of a receptor, as observed e.g. between rat and human 5-HT<sub>1B</sub> receptors, can result in rather marked differences in pharmacological profile.



For instance, the rat 5-HT<sub>1D</sub> receptor is pharmacologically closer to the human 5-HT<sub>1B</sub> receptor than the rat 5-HT<sub>1B</sub> receptor is to its own species variant, i.e. the human 5-HT<sub>1B</sub> receptor (Hoyer et al., 1994a).

#### Presence of sst<sub>3</sub> receptors in fish brain

The fsst<sub>3</sub> receptor is apparently expressed at a very low level in fish brain based on mRNA levels (Zupanc et al., 1999). High correlation of fsst<sub>3</sub> receptor binding data with the fish brain binding data suggested significant fsst<sub>3</sub> receptor protein levels in fish brain; the difference in mRNA and protein levels might be explained by high stability of the fsst<sub>3</sub> receptor transcript. The competition curves of seglitide and octreotide for fish brain labelled sites were biphasic, which is compatible with the presence of at least one additional SRIF subtype in fish. In liver, in contrast to brain, binding profiles obtained with [<sup>125</sup>I]LTT-SRIF<sub>28</sub> correlated much less with those obtained in the brain or with recombinant fsst<sub>3</sub>. Thus, the fsst<sub>3</sub> receptor is either not expressed in liver, or the SRIF binding represents a combination of different sites which may or may not include fsst<sub>3</sub>.

Fish liver recognition sites have preferential affinity for SRIF<sub>28</sub> compared to SRIF<sub>14</sub>, reminiscent of the sst<sub>5</sub> subtype (O'Carroll et al., 1992; Patel and Srikant, 1994; Raynor et al., 1993b). In addition, the intermediate to high affinity of the SRIF analogues seglitide, octreotide, RC160, BIM 23014, and L362,855 suggests that the liver SRIF receptor belongs to the SRIF<sub>1</sub> family which is characterised by this kind of affinity profile (Hoyer et al., 1994b).

Finally, the presence of specific [<sup>125</sup>I]LTT-SRIF<sub>28</sub> binding in fish spleen, heart, and stomach, in addition to brain and liver, agrees with SRIF receptors being widely distributed in fish as already suggested by the wide distribution of the SRIF peptide (Fletcher et al., 1983; Sas and Maler, 1991; Zupanc et al., 1991) and SRIF binding sites (Zupanc et al., 1994). In mammals, sst<sub>3</sub> receptor mRNA is expressed in specific areas of brain, e.g. in cerebellum, but also in stomach, liver, spleen, pancreas, and muscle (Kaupmann et al., 1993; Raulf et al., 1994; Piwko et al., 1997). However, the localisation of the native protein remains elusive.

## Second messenger coupling

Inhibition of forskolin-stimulated adenylate cyclase activity has been reported for all five known mammalian SRIF receptors (Patel et al., 1994). Similarly, negative coupling of  $fsst_3$  to adenylate cyclase is produced by SRIF<sub>14</sub> and SRIF<sub>28</sub> in CCL39 cells; the effect on cAMP production was potent and efficient for both peptides (around 90 % inhibition with EC<sub>50</sub> values in the subnanomolar range). The inhibition of forskolin-stimulated adenylate cyclase activity by SRIF<sub>14</sub> is completely blocked by pre-treatment of the cells with pertussis toxin, which is in line with a G<sub>i</sub> and/or G<sub>o</sub> mediated effect, similarly to the five cloned mammalian SRIF receptors (Law et al., 1994; Murthy et al., 1996; Tallent and Reisine, 1992). It seems that both somatostatins at concentrations above 0.1 micromolar produce less inhibition, either because at higher concentrations inhibition is taking place, or that G<sub>s</sub> is being activated directly or indirectly. This has not been investigated further but is not uncommon. It has been reported in COS cells, that the C-terminus of G<sub>i</sub>α1 and G<sub>i</sub>α2 (but not G<sub>o</sub>α) is recognised by the  $hsst_3$  receptor (Komatsuzaki et al., 1997). Thus, SRIF-induced cellular signalling pathways might be conserved within the vertebrate phylum.

In conclusion, the present manuscript describes the pharmacological profile of the putative  $fsst_3$  receptor recombinantly expressed in CCL39 cells. The overall pharmacological profile suggests that, indeed, the  $fsst_3$  receptor belongs to the SRIF<sub>1</sub> receptor family characterised by high affinity for small peptide analogues such as octreotide or seglitide. The native receptor can be found in fish brain as suggested from binding studies. The competition curves of seglitide and octreotide in brain are sufficiently shallow to allow delineation into two sites, which is compatible with the existence of multiple SRIF receptors in brain; one of these receptors shows a profile very similar to that of the recombinant  $fsst_3$  receptor. Binding was also found in liver, although the pharmacological profile is somewhat different from the recombinant  $fsst_3$  receptor; nevertheless, the high affinity of small SRIF analogues suggests, again, the presence of an additional member of the SRIF<sub>1</sub> family in liver.

The  $fsst_3$  receptor is apparently functional and couples well to the inhibition of forskolin-stimulated adenylate cyclase activity, similarly to human  $SRIF_1$  receptors (see Hoyer et al., 1995b). However, further work is needed to determine whether a 'true' pharmacological profile if at all, can be established for the  $fsst_3$  receptor.

## Chapter 11

---

**Fish somatostatin sst<sub>3</sub> receptor: comparison of radioligand and GTP $\gamma$ S binding, adenylate cyclase and phospholipase C activities reveals agonist-dependent pharmacological differences**

---

Sandra Siehler, Günther K. H. Zupanc, Klaus Seuwen and Daniel Hoyer,  
Neuropharmacology, submitted

### 11.1. Abstract

The  $fsst_3$  receptor is the only somatostatin (SRIF) receptor cloned from a non-mammalian species so far. Here we investigated the guanine nucleotide sensitivity of agonist radioligand binding, agonist-stimulated GTP $\gamma$ S binding, inhibition of forskolin-stimulated adenylate cyclase (FSAC) and stimulation of phospholipase C (PLC) activities, induced by somatostatin (SRIF)- and cortistatin (CST)-analogues, at fish somatostatin receptor 3 ( $fsst_3$ ) recombinantly expressed in CCL39 (Chinese hamster lung fibroblast) cells.

The GTP-analogue guanylylimidodiphosphate (GppNHp) inhibited binding of [ $^{125}$ I]CGP 23996 and [ $^{125}$ I][Tyr $^3$ ]octreotide by 72 % and 83 % suggesting preferential labelling of G-protein-coupled  $fsst_3$  receptors; by contrast, binding of the ligands [ $^{125}$ I]LTT-SRIF $_{28}$  and [ $^{125}$ I][Tyr $^{10}$ ]CST $_{14}$  was rather GppNHp-insensitive ( $E_{max} = 42$  % and 35 %) suggesting labelling of both coupled and non-coupled receptor states. These results might explain the apparent higher receptor densities determined in saturation experiments with the latter two radioligands compared to [ $^{125}$ I]CGP 23996 and [ $^{125}$ I][Tyr $^3$ ]octreotide.

SRIF $_{14}$  (10  $\mu$ M) stimulated specific [ $^{35}$ S]GTP $\gamma$ S binding by 314 %; SRIF $_{28}$  and octreotide displayed full agonism, whereas most other ligands reached 63- 81 % intrinsic activity compared to SRIF $_{14}$ . SRIF $_{14}$  and SRIF $_{28}$  inhibited forskolin-stimulated AC (FSAC) activity by 58 and 61 %; all tested ligands except of BIM 23056 inhibited FSAC with comparable high intrinsic activities. 10  $\mu$ M SRIF $_{14}$  induced stimulation of PLC activity via  $fsst_3$  receptors determined by measuring total [ $^3$ H]-IP $_x$  accumulation more than 8-fold ( $E_{max} = 831$  %); this response was rather insensitive to 100 ng/ml pertussis toxin (PTX) (21 % inhibition), which suggests the G $_q$ -family proteins couple to PLC activity. SRIF $_{14}$ , SRIF $_{28}$  and [Tyr $^{10}$ ]CST $_{14}$  showed full agonism at PLC, whereas all other ligands behaved as partial agonists (17- 72 % intrinsic activity). BIM 23056, which was a weak agonist in all 3 functional assays, antagonised SRIF $_{14}$ -induced total [ $^3$ H] IP $_x$  production ( $pK_B = 6.83$ ), but neither agonist-stimulated [ $^{35}$ S]GTP $\gamma$ S binding nor FSAC inhibition.

Comparison of the pharmacological profiles of  $fsst_3$  receptors established in GTP $\gamma$ S binding, FSAC inhibition and PLC stimulation resulted in low correlation coefficients ( $r = 0.410- 0.594$ ). Higher, although variable correlations were obtained comparing GTP $\gamma$ S binding and inhibition of AC activity with previously reported affinity profiles of [ $^{125}$ I]LTT-SRIF $_{28}$ , [ $^{125}$ I][Tyr $^{10}$ ]CST $_{14}$ , [ $^{125}$ I]CGP 23996, [ $^{125}$ I][Tyr $^3$ ]octreotide (Siehler et al., 1999) ( $r = 0.749- 0.829$ ;  $0.681- 0.888$ ). The PLC stimulation profile did not correlate with the affinity profiles.

Comparison of the functional data (GTP $\gamma$ S binding, FSAC inhibition, PLC stimulation) of  $fsst_3$  receptors with those of human  $sst_2$ ,  $sst_3$ ,  $sst_5$  ( $hsst_{2,3,5}$ ) receptors expressed in CCL39 cells (Siehler and Hoyer, submitted (b), (c), (d)) resulted in highest correlation with the  $hsst_5$  receptor ( $r = 0.936, 0.972, 0.489$ ) >  $hsst_2$  (0.800, 0.502, n.d.) >  $hsst_3$  (0.250, 0.190, 0.167).

In summary,  $fsst_3$  receptors expressed in CCL39 cells are involved in signalling cascades, which are also modulated by mammalian SRIF receptors, and therefore might be highly conserved in evolution. Binding and functional data showed highest similarity of  $fsst_3$  receptors with the mammalian  $sst_5$  receptor subtype (at least with  $hsst_5$ ). Different affinities, receptor densities and GppHNp-sensitivities determined with the four radioligands (agonists) are assumed to result from ligand-specific states of the  $fsst_3$ -ligand complex. The differences between the radioligand binding profiles and the various signalling cascades, may be explained by agonist-induced receptor trafficking.

## 11.2. Results

### Effect of GppNHp on radioligand binding

As previously described, [ $^{125}$ I]LTT-SRIF<sub>28</sub>, [ $^{125}$ I][Tyr<sup>10</sup>]CST<sub>14</sub>, [ $^{125}$ I]CGP 23996 and [ $^{125}$ I][Tyr<sup>3</sup>]octreotide labelled fsst<sub>3</sub> receptors stably expressed in CCL39 cells with high affinity, in a saturable manner, and with low levels of non-specific binding: pK<sub>d</sub> = 10.47, 10.87, 9.59, and 9.57; B<sub>max</sub> = 4470, 4030, 3420, and 1520 fmol/mg (Siehler et al., 1999; table 1(A)). [ $^{125}$ I][Tyr<sup>3</sup>]octreotide labelled significantly less receptor sites (2- 3 fold) compared to the other radioligands.

To study, whether these apparent differences in receptor densities may be due to labelling of different receptor affinity states, saturation binding experiments were performed in the presence of 10 μM GppNHp (table 1(B); figure 1). The affinities of [ $^{125}$ I]LTT-SRIF<sub>28</sub>, [ $^{125}$ I][Tyr<sup>10</sup>]CST<sub>14</sub>, [ $^{125}$ I]CGP 23996 and [ $^{125}$ I][Tyr<sup>3</sup>]octreotide were comparable to those measured in the absence of GppNHp (pK<sub>d</sub> = 10.37 ± 0.03, 10.23 ± 0.07, 9.71 ± 0.04, 9.81 ± 0.02). However, the B<sub>max</sub>-values determined with the 4 radioligands were differently affected by GppNHp (B<sub>max</sub> = 2910 ± 40, 4480 ± 290, 930 ± 70 and 190 ± 20 fmol/mg, respectively). The binding of [ $^{125}$ I][Tyr<sup>10</sup>]CST<sub>14</sub> was not modified by GppNHp, that of [ $^{125}$ I]LTT-SRIF<sub>28</sub> was only slightly affected, whereas both [ $^{125}$ I]CGP 23996 and [ $^{125}$ I][Tyr<sup>3</sup>]octreotide were drastically inhibited, almost 4-fold and 8-fold, respectively (figure 1); i.e. in the presence of GppNHp, [ $^{125}$ I][Tyr<sup>3</sup>]octreotide labelled about 24-fold less receptor sites compared to e.g. [ $^{125}$ I][Tyr<sup>10</sup>]CST<sub>14</sub>.

In another experimental set up, increasing concentrations of GppNHp (up to 100 μM) were used to inhibit binding of the different radioligands to fsst<sub>3</sub> receptors (table 2; figure 2). Again, [ $^{125}$ I]LTT-SRIF<sub>28</sub> and [ $^{125}$ I][Tyr<sup>10</sup>]CST<sub>14</sub> binding were only moderately affected (E<sub>max</sub> = 42 ± 1 % and 35 ± 2 %, pIC<sub>50</sub> = 6.10 ± 0.11 and 6.22 ± 0.25, respectively), whereas [ $^{125}$ I]CGP 23996 and [ $^{125}$ I][Tyr<sup>3</sup>]octreotide were almost entirely inhibited at high GppNHp concentrations (E<sub>max</sub> = 72 ± 1 % and 83 ± 5 %, pIC<sub>50</sub> = 6.87 ± 0.14 and 7.70 ± 0.29, respectively).

**Table 1:** Saturation data obtained with [ $^{125}$ I]LTT-SRIF<sub>28</sub>, [ $^{125}$ I][Tyr<sup>10</sup>]CST<sub>14</sub>, [ $^{125}$ I]CGP 23996 and [ $^{125}$ I][Tyr<sup>3</sup>]octreotide at fish sst<sub>3</sub> receptors expressed in CCL39 cells

**Table 1(A)**

	pK <sub>d</sub>	B <sub>max</sub>
[ $^{125}$ I]LTT-SRIF <sub>28</sub>	10.47 ± 0.12	4470 ± 240
[ $^{125}$ I][Tyr <sup>10</sup> ]CST <sub>14</sub>	10.87 ± 0.34	4030 ± 210
[ $^{125}$ I]CGP 23996	9.59 ± 0.04	3420 ± 190
[ $^{125}$ I][Tyr <sup>3</sup> ]octreotide	9.57 ± 0.04	1520 ± 60

**Table 1(B)**

+GppNHp	pK <sub>d</sub>	B <sub>max</sub>
[ $^{125}$ I]LTT-SRIF <sub>28</sub>	10.37 ± 0.03	2910 ± 40
[ $^{125}$ I][Tyr <sup>10</sup> ]CST <sub>14</sub>	10.23 ± 0.07	4480 ± 290
[ $^{125}$ I]CGP 23996	9.71 ± 0.04	930 ± 70
[ $^{125}$ I][Tyr <sup>3</sup> ]octreotide	9.81 ± 0.02	190 ± 20

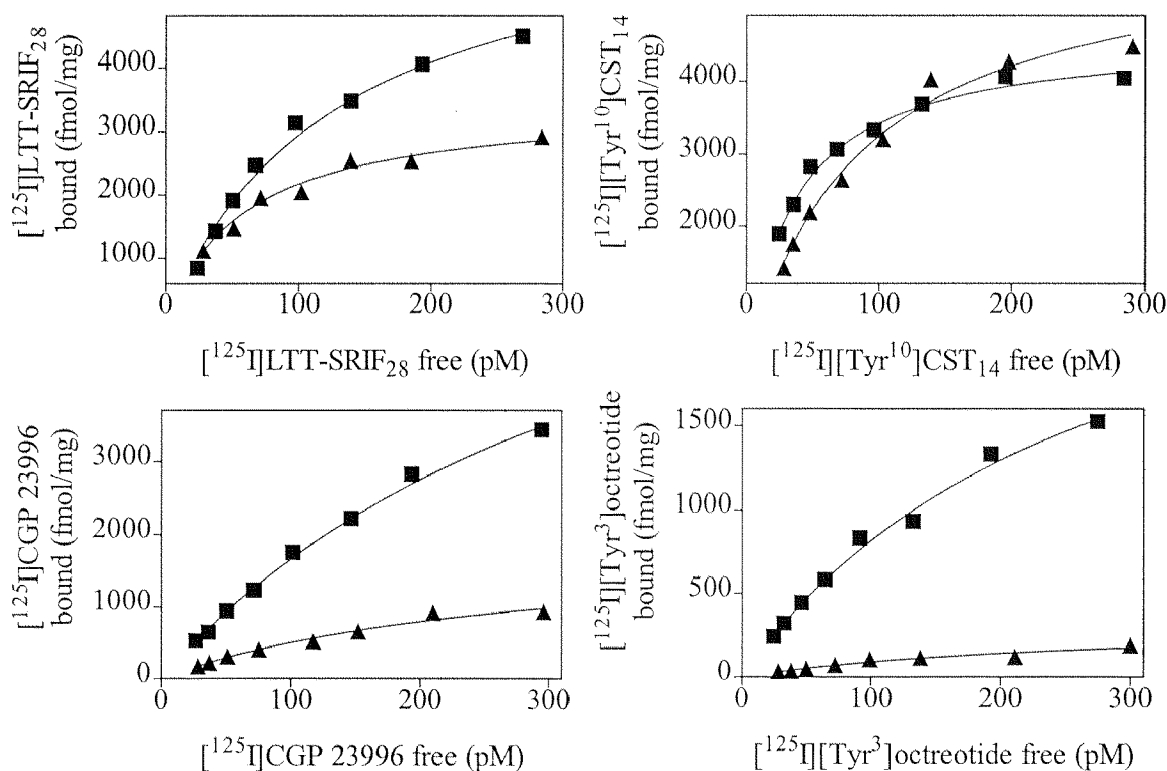
The data are expressed as means of B<sub>max</sub>-values (fmol/ mg) and pK<sub>d</sub>-values (-log M) ± SEM of 3 different experiments; in contrast to table (A), table (B) shows data from saturation experiments performed in the presence of GppNHp (10<sup>-5</sup> M). Paired t-test analysis for individual values indicates that B<sub>max</sub>-values defined in the absence (table (A)) or the presence (table (B)) of GppNHp are not different (P > 0.05) using [ $^{125}$ I][Tyr<sup>10</sup>]CST<sub>14</sub>, but significantly differ with [ $^{125}$ I]LTT-SRIF<sub>28</sub>, [ $^{125}$ I]CGP 23996, and [ $^{125}$ I][Tyr<sup>3</sup>]octreotide (P < 0.01).

#### Induction of specific [ $^{35}$ S]GTPγS binding by SRIF analogues

Experimental conditions have been established previously at human sst<sub>5</sub> receptors expressed in CCL39 cells (Siehler and Hoyer, submitted (b)). SRIF<sub>14</sub> stimulated [ $^{35}$ S]GTPγS binding by 314 ± 3 %. E<sub>max</sub>-values of all studied peptides were 234- 324 %, and thereby close to full agonism, with the exception of BIM 23056, which was almost devoid of agonist activity (table 3; figure 3).



**Figure 1:** Saturation isotherms using [ $^{125}$ I]LTT-SRIF<sub>28</sub>, [ $^{125}$ I][Tyr<sup>10</sup>]CST<sub>14</sub>, [ $^{125}$ I]CGP 23996 or [ $^{125}$ I][Tyr<sup>3</sup>]octreotide to membranes prepared from CCL39 cells stably expressing fsst<sub>3</sub> receptors.



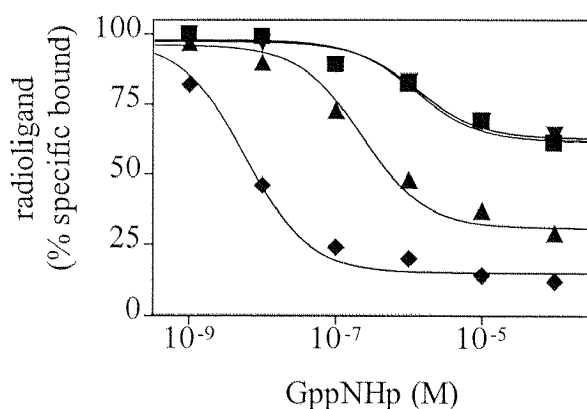
Crude membrane preparations (2  $\mu$ g per assay) were incubated with increasing concentrations of the radioligand in the absence (■) or presence (▲) of GppNHp (10<sup>-5</sup> M; final concentration), and assayed for receptor binding. The plots represent specific binding expressed as radioligand bound (fmol/mg) versus free radioligand concentration (pM). The figures show one representative example of 3 different experiments.

However, BIM 23056 failed to antagonise SRIF<sub>14</sub>-stimulated [ $^{35}$ S]GTP $\gamma$ S binding (table 7; figure 7). SRIF<sub>14</sub>, seglitide and SRIF<sub>28</sub> induced [ $^{35}$ S]GTP $\gamma$ S binding with comparable high potency (pEC<sub>50</sub> = 8.19, 8.29 and 7.55, respectively). The rank order of potencies in [ $^{35}$ S]GTP $\gamma$ S binding was: seglitide  $\geq$  SRIF<sub>14</sub> > [Tyr<sup>10</sup>]CST<sub>14</sub>  $\geq$  SRIF<sub>28</sub> = LTT-SRIF<sub>28</sub> > SRIF<sub>25</sub> > octreotide > BIM 23052  $\geq$  CGP 23996  $\approx$  [Tyr<sup>3</sup>]octreotide > L362,855.

**Table 2:** Binding inhibition of [ $^{125}$ I]LTT-SRIF<sub>28</sub>, [ $^{125}$ I][Tyr<sup>10</sup>]CST<sub>14</sub>, [ $^{125}$ I]CGP 23996 and [ $^{125}$ I][Tyr<sup>3</sup>]octreotide at fish sst<sub>3</sub> receptors by increasing concentrations of GppNHp (max. 10<sup>-4</sup> M): comparison of pIC<sub>50</sub>-values (-log M) or E<sub>max</sub>-values [% inhibition] ± SEM of three experiments

	E <sub>max</sub>	pEC <sub>50</sub>
[ $^{125}$ I]LTT-SRIF <sub>28</sub>	42 ± 1	6.10 ± 0.11
[ $^{125}$ I][Tyr <sup>10</sup> ]CST <sub>14</sub>	35 ± 2	6.22 ± 0.25
[ $^{125}$ I]CGP 23996	72 ± 1	6.87 ± 0.14
[ $^{125}$ I][Tyr <sup>3</sup> ]octreotide	83 ± 5	7.70 ± 0.29

**Figure 2:** Inhibition of radioligand binding at fsst<sub>3</sub> receptors by different GppNHp-concentrations (max. 10<sup>-4</sup> M).



Crude membrane preparations from fsst<sub>3</sub> receptor transfected cells were incubated with [ $^{125}$ I]LTT-SRIF<sub>28</sub> (■), [ $^{125}$ I][Tyr<sup>10</sup>]CST<sub>14</sub> (▼), [ $^{125}$ I]CGP 23996 (▲) or [ $^{125}$ I][Tyr<sup>3</sup>]octreotide (◆) and the indicated concentrations of GppNHp. Data are expressed as percentage of specific binding. The data points show one representative example of at least three independent experiments.

#### Inhibition of forskolin-stimulated adenylate cyclase (FSAC) activity

Forskolin-stimulated cytosolic cyclic adenosine monophosphate (cAMP) was inhibited by SRIF analogues via fsst<sub>3</sub> receptors as indirectly measured using a radioimmunoassay (table 4; figure 4).

**Table 3:** Stimulation of [<sup>35</sup>S]GTPγS binding by SRIF analogues at recombinantly expressed fish sst<sub>3</sub> receptors: comparison of pEC<sub>50</sub> values (-log M) and E<sub>max</sub>-values [% stimulation] ± SEM of 3 independent determinations.

	E <sub>max</sub>	pEC <sub>50</sub>
SRIF <sub>14</sub>	314 ± 3	8.19 ± 0.01
SRIF <sub>28</sub>	320 ± 14	7.55 ± 0.14
LTT-SRIF <sub>28</sub>	272 ± 5	7.55 ± 0.12
SRIF <sub>25</sub>	274 ± 23	7.25 ± 0.07
[Tyr <sup>10</sup> ]CST <sub>14</sub>	267 ± 2	7.64 ± 0.03
seglitide	264 ± 31	8.29 ± 0.06
CGP 23996	255 ± 30	6.68 ± 0.04
octreotide	324 ± 29	7.12 ± 0.09
[Tyr <sup>3</sup> ]octreotide	259 ± 6	6.64 ± 0.13
L362,855	234 ± 39	6.29 ± 0.05
BIM 23056	64 ± 1	(-)
BIM 23052	269 ± 6	6.77 ± 0.01

In direct cAMP determinations using a column assay, SRIF<sub>14</sub> and SRIF<sub>28</sub> inhibited FSAC activity via fsst<sub>3</sub> receptors expressed in CCL39 cells by 87 and 91 %, with pEC<sub>50</sub>-values of 9.52 and 9.19, respectively, and in a pertussis toxin-sensitive manner (Siehler et al., 1999). In the radioimmunoassay, SRIF<sub>14</sub> and SRIF<sub>28</sub> inhibited the cAMP production by 58 ± 2 % and 61 ± 3 %, and with pEC<sub>50</sub>'s of 7.71 and 8.24, respectively. Seglitide was the most potent to inhibit FSAC activity (pEC<sub>50</sub> = 8.83). All tested compounds behaved as full agonists, except BIM 23056, which showed weak partial agonism (E<sub>max</sub> = 24 ± 1 %), but failed to antagonise SRIF<sub>14</sub>-induced inhibition of FSAC activity (table 6; figure 7). The rank order of potencies was: seglitide > SRIF<sub>25</sub> ≈ SRIF<sub>28</sub> > LTT-SRIF<sub>28</sub> ≈ SRIF<sub>14</sub> > [Tyr<sup>10</sup>]CST<sub>14</sub> > octreotide > BIM 23052 > [Tyr<sup>3</sup>]octreotide > CGP 23996 ≈ L362,855 ≈ BIM 23056.

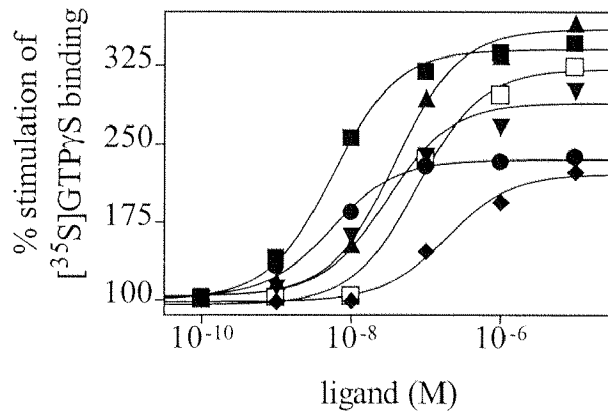
**Table 4:** Inhibition of forskolin-stimulated adenylate cyclase activity by fish  $ssst_3$  receptors expressed in CCL39 cells: comparison of  $pEC_{50}$  values (-log M) and  $E_{max}$ -values [% inhibition]  $\pm$  SEM of three experiments

	$E_{max}$	$pEC_{50}$
SRIF <sub>14</sub>	58 $\pm$ 2	7.71 $\pm$ 0.06
SRIF <sub>28</sub>	61 $\pm$ 3	8.24 $\pm$ 0.18
LTT-SRIF <sub>28</sub>	59 $\pm$ 1	7.75 $\pm$ 0.03
SRIF <sub>25</sub>	54 $\pm$ 2	8.29 $\pm$ 0.10
[Tyr <sup>10</sup> ]CST <sub>14</sub>	56 $\pm$ 3	7.59 $\pm$ 0.02
seglitide	63 $\pm$ 2	8.83 $\pm$ 0.11
CGP 23996	62 $\pm$ 1	6.58 $\pm$ 0.07
octreotide	66 $\pm$ 2	7.37 $\pm$ 0.10
[Tyr <sup>3</sup> ]octreotide	67 $\pm$ 3	6.85 $\pm$ 0.12
L362,855	65 $\pm$ 1	6.56 $\pm$ 0.15
BIM 23056	24 $\pm$ 1	6.51 $\pm$ 0.04
BIM 23052	66 $\pm$ 1	7.24 $\pm$ 0.10

#### Induction of total [<sup>3</sup>H]-IP<sub>x</sub> accumulation via $fsst_3$ receptors

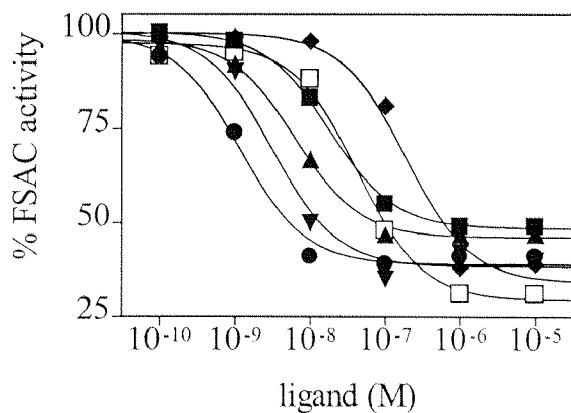
Fs $st_3$  receptor-stimulated phospholipase C (PLC) activity was studied by measuring total [<sup>3</sup>H]-IP<sub>x</sub> levels in an anion exchange column assay. The maximal [<sup>3</sup>H]-IP<sub>x</sub> levels were measured after 50 min incubation of the cells with SRIF ligands. 10  $\mu$ M SRIF<sub>14</sub> induced a 8-fold stimulation of PLC activity:  $E_{max} = 831 \pm 165$  %, and addition of pertussis toxin (PTX) blocked this effect only by 21 %:  $E_{max} = 669 \pm 218$  % (figure 5). The  $E_{max}$ -value of control cells in the absence of lithium ions (90  $\pm$  5 %) was below the basal level of 100 %, and therefore suggests some basal activity of the fish  $ssst_3$  receptor on induction of PLC enzymes in CCL39 cells.

**Figure 3:** Stimulation of specific [ $^{35}$ S]GTP $\gamma$ S binding to microsome preparations from CCL39 cells expressing fish sst $_3$  receptors by SRIF analogues:



Microsomes of fsst $_3$  transfected cells (2  $\mu$ g protein) were incubated with [ $^{35}$ S]GTP $\gamma$ S (0.2 nM), the indicated concentrations of SRIF $_{14}$  (■), SRIF $_{25}$  (▲), SRIF $_{28}$  (▼), CGP 23996 (◆), seglitide (●), or octreotide (□) in the presence of 5 mM MgCl $_2$ , 1  $\mu$ M GDP, and 100 mM NaCl. Graphs represent the percentage of stimulated specific [ $^{35}$ S]GTP $\gamma$ S binding. The data points depict one representative example of 3 different experiments performed in triplicates.

**Figure 4:** Inhibition of forskolin-stimulated adenylate cyclase (FSAC) activity by SRIF peptides in CCL39 cells expressing fsst $_3$  receptors.

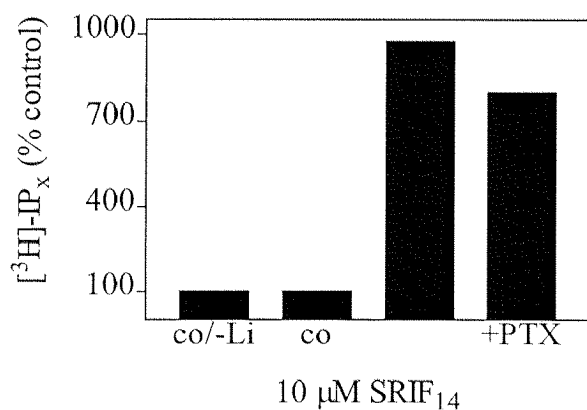


Transfected cells were treated with forskolin (10  $\mu$ M) and the indicated concentrations of SRIF $_{14}$  (■), SRIF $_{25}$  (▲), SRIF $_{28}$  (▼), CGP 23996 (◆), seglitide (●) or octreotide (□), and cAMP levels determined by radioimmunoassay using [ $^{125}$ I]cAMP. Graphs represent the percentage of inhibition of FSAC activity. The data points represent one example of 3 different experiments. The mean of pEC $_{50}$ -values  $\pm$  SEM of 3 determinations are shown in table 4.

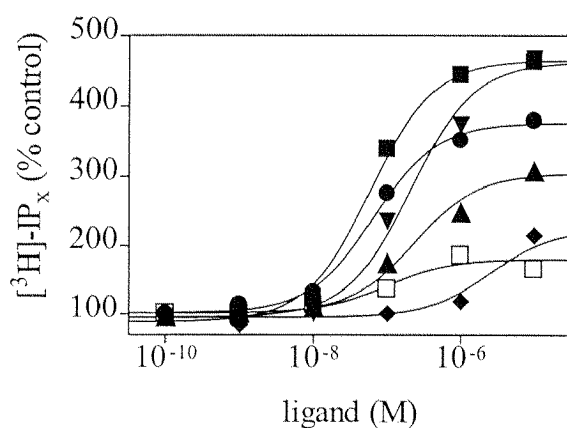
**Table 5:** Activation of total [ $^3\text{H}$ ]-IP $_x$  accumulation by SRIF peptides and analogues by fsst $_3$  receptors: comparison of pEC $_{50}$ -values (-log M) and E $_{\text{max}}$ -values [% stimulation]  $\pm$  SEM of 3 different determinations.

	E $_{\text{max}}$	pEC $_{50}$
SRIF $_{14}$	463 $\pm$ 59	7.21 $\pm$ 0.05
SRIF $_{28}$	463 $\pm$ 45	6.59 $\pm$ 0.09
LTT-SRIF $_{28}$	289 $\pm$ 15	6.16 $\pm$ 0.17
SRIF $_{25}$	361 $\pm$ 69	6.88 $\pm$ 0.13
[Tyr $^{10}$ ]CST $_{14}$	578 $\pm$ 127	6.17 $\pm$ 0.10
seglitide	324 $\pm$ 40	7.26 $\pm$ 0.18
CGP 23996	246 $\pm$ 20	5.73 $\pm$ 0.08
octreotide	186 $\pm$ 36	6.82 $\pm$ 0.22
[Tyr $^3$ ]octreotide	161 $\pm$ 20	7.43 $\pm$ 0.15
L362,855	168 $\pm$ 10	6.46 $\pm$ 0.21
BIM 23056	194 $\pm$ 3	6.02 $\pm$ 0.07
BIM 23052	182 $\pm$ 23	7.03 $\pm$ 0.16

The pharmacological profile of fsst $_3$  receptor-mediated stimulation of PLC activity was established with a number of SRIF analogues (table 5; figure 6). The intrinsic activity of the ligands varied over a broad range: from 578 % ([Tyr $^{10}$ ]CST $_{14}$ ), 463 % (SRIF $_{14}$ , SRIF $_{28}$ ), 324 % (seglitide), 246 % (CGP 23996), to 161 % ([Tyr $^3$ ]octreotide); i.e. most of the tested compounds revealed partial agonism. [Tyr $^3$ ]octreotide, seglitide and SRIF $_{14}$  were the most potent ligands in this functional assay (pEC $_{50}$  = 7.43, 7.26, and 7.21, respectively). The rank order was: [Tyr $^3$ ]octreotide > seglitide  $\approx$  SRIF $_{14}$  > BIM 23052 > SRIF $_{25}$   $\approx$  octreotide > SRIF $_{28}$  > L362,855 > [Tyr $^{10}$ ]CST $_{14}$   $\approx$  LTT-SRIF $_{28}$  > BIM 23056 > CGP 23996. BIM 23056 behaved as a competitive antagonist on SRIF $_{14}$ -induced [ $^3\text{H}$ ]-IP $_x$  accumulation (table 6; figure 7).

**Figure 5:** Stimulation of total [ $^3\text{H}$ ]-IP $_x$  accumulation at fsst $_3$  receptors.

Fsst $_3$  expressing cells were incubated in HBS buffer (control) either with or without 20 mM LiCl, or stimulated with 10  $\mu\text{M}$  SRIF $_{14}$  (in HBS/ Li $^+$ ) either in the absence or presence of PTX (100 ng/ ml). Bars represent  $E_{\text{max}}$ -values  $\pm$  SEM as percentage of stimulation over the basal level (HBS/ Li $^+$  = 100 %) of at least 3 experiments.

**Figure 6:** Induction of total [ $^3\text{H}$ ]-IP $_x$  accumulation by SRIF ligands.

Cells were incubated with 2  $\mu\text{Ci}$  myo-[2- $^3\text{H}$ (N)]-inositol, treated with the indicated concentrations of SRIF $_{14}$  (■), SRIF $_{25}$  (▲), SRIF $_{28}$  (▼), CGP 23996 (◆), seglitide (●), or octreotide (□), and total [ $^3\text{H}$ ]-IP $_x$  levels were determined by anion exchange chromatography. Graphs represent the percentage of stimulation over the basal level, and one example of at least 3 separate experiments; the mean of pEC $_{50}$ -values  $\pm$  are given in table 5.

Comparison of radioligand binding, [ $^{35}\text{S}$ ]GTP $\gamma$ S binding, inhibition of FSAC activity, and stimulation of PLC activity

Data obtained in fsst $_3$ -induced GTP $\gamma$ S binding, inhibition of cAMP production, and stimulation of PLC activity were compared to the pharmacological profiles of radioligand binding determined using [ $^{125}\text{I}$ ]LTT-SRIF $_{28}$ , [ $^{125}\text{I}$ ][Tyr $^{10}$ ]CST $_{14}$ , [ $^{125}\text{I}$ ]CGP 23996 and [ $^{125}\text{I}$ ][Tyr $^3$ ]octreotide (tables 7 and 8; figures 7- 9; Siehler et al., 1999).

**Table 6:** Antagonist activity of BIM 23056 ( $10^{-6}$  M final concentration) on SRIF<sub>14</sub>-stimulated [<sup>35</sup>S]GTPγS binding, SRIF<sub>14</sub>-inhibited adenylate cyclase (AC) activity, and SRIF<sub>14</sub>-stimulated total [<sup>3</sup>H]-IP<sub>x</sub> accumulation at fish sst<sub>3</sub> receptors

	SRIF <sub>14</sub>		SRIF <sub>14</sub> +BIM 23056		
	E <sub>max</sub>	pEC <sub>50</sub>	E <sub>max</sub>	pEC <sub>50</sub>	pK <sub>B</sub>
[ <sup>35</sup> S]GTPγS binding	100 ± 1	8.19 ± 0.01	37 ± 0	8.58 ± 0.05	-
AC activity	100 ± 3	7.71 ± 0.06	65 ± 5	8.64 ± 0.17	-
total [ <sup>3</sup> H]-IP <sub>x</sub>	100 ± 16	7.21 ± 0.05	94 ± 27	6.38 ± 0.06	6.83 ± 0.06

Comparison of pEC<sub>50</sub>-values (-log M), E<sub>max</sub>-values [% stimulation/ inhibition; normalised to the E<sub>max</sub> of SRIF<sub>14</sub> = 100 %], and pK<sub>B</sub>-value ± SEM of 3 independent determinations.

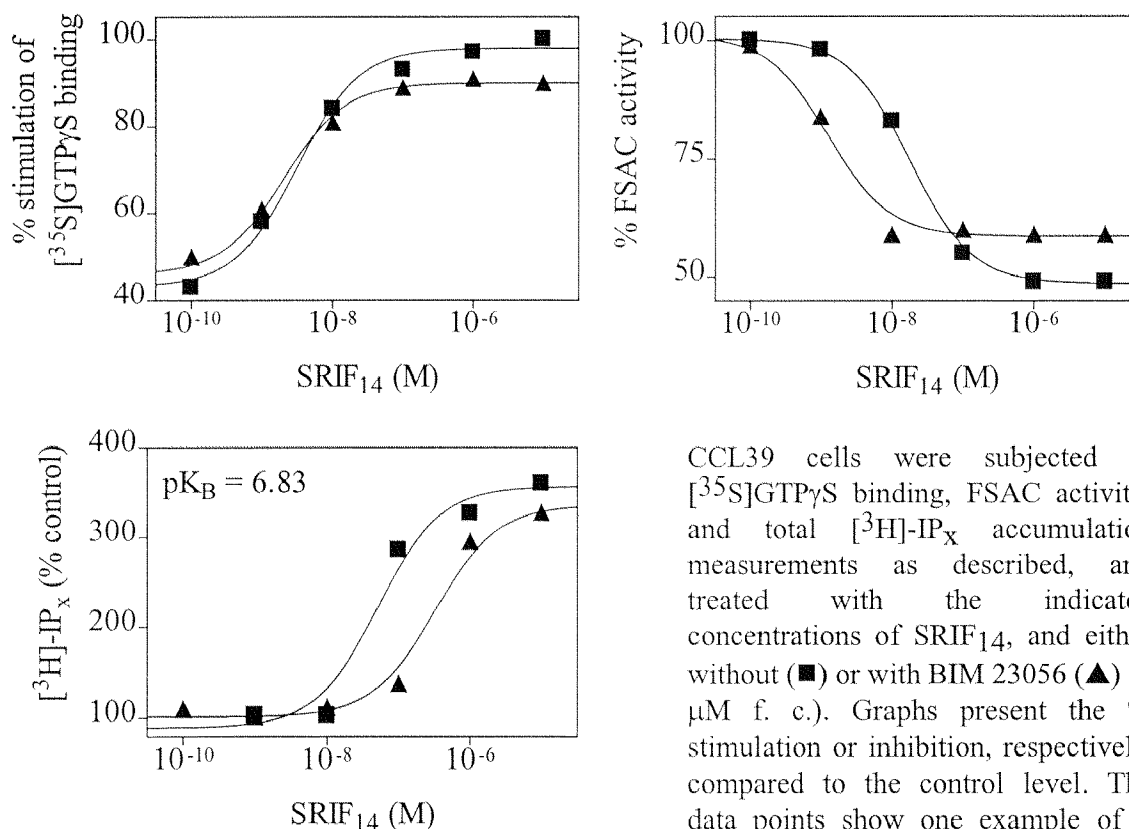
Linear regression analyses revealed intermediate correlation of the [<sup>35</sup>S]GTPγS binding profile with the different affinity profiles ( $r = 0.749$ -  $0.829$ ). Similarly, [<sup>35</sup>S]GTPγS binding correlated very moderately with FSAC inhibition and PLC activation ( $r = 0.594$  and  $0.410$ , respectively). The pharmacological profile of fsst<sub>3</sub>-mediated inhibition of cAMP production correlated significantly with the affinity profiles of [<sup>125</sup>I]LTT-SRIF<sub>28</sub>, [<sup>125</sup>I][Tyr<sup>10</sup>]CST<sub>14</sub>, [<sup>125</sup>I]CGP 23996 ( $r = 0.842$ -  $0.888$ ), but less significantly with radioligand binding data obtained with [<sup>125</sup>I][Tyr<sup>3</sup>]octreotide ( $r = 0.681$ ) as well as with PLC stimulation ( $r = 0.424$ ). Interestingly, induction of total [<sup>3</sup>H]-IP<sub>x</sub> accumulation showed very low correlation coefficients with the 4 radioligand binding profiles ( $r = 0.056$ -  $0.403$ ).

Comparison of functional assay data of fish sst<sub>3</sub> receptor and of human SRIF<sub>1</sub> receptors

Data from fsst<sub>3</sub> receptor-mediated [<sup>35</sup>S]GTPγS binding, FSAC inhibition, and PLC activation were compared to data obtained using CCL39 cells stably transfected with either human sst<sub>2</sub>, sst<sub>3</sub>, or sst<sub>5</sub> receptors (tables 9 and 10; figure 11; Siehler and Hoyer, submitted (b), (c), (d)).



**Figure 7:** Antagonism of BIM 23056 on SRIF<sub>14</sub>-induced [<sup>35</sup>S]GTP<sub>γ</sub>S binding, inhibition of FSAC activity, and total [<sup>3</sup>H]-IP<sub>x</sub> accumulation at fsst<sub>3</sub> receptors.



CCL39 cells were subjected to [<sup>35</sup>S]GTP<sub>γ</sub>S binding, FSAC activity, and total [<sup>3</sup>H]-IP<sub>x</sub> accumulation measurements as described, and treated with the indicated concentrations of SRIF<sub>14</sub>, and either without (■) or with BIM 23056 (▲) (1 μM f. c.). Graphs present the % stimulation or inhibition, respectively, compared to the control level. The data points show one example of 3 different experiments. The pK<sub>B</sub>-value ± SEM is shown in the graph presenting [<sup>3</sup>H]-IP<sub>x</sub> data.

In all 3 functional assays studied, fsst<sub>3</sub> receptors were more similar to hsst<sub>2</sub> and hsst<sub>5</sub>, than to hsst<sub>3</sub> receptors: e.g. seglitide revealed in these experiments relatively high potencies at fsst<sub>3</sub> receptors, which are typical for hsst<sub>2</sub> and hsst<sub>5</sub> receptors, whereas hsst<sub>3</sub> receptors showed only low potencies for seglitide. The [<sup>35</sup>S]GTP<sub>γ</sub>S binding and FSAC inhibition profiles of fsst<sub>3</sub> receptors correlated significantly with those of hsst<sub>5</sub> receptors ( $r = 0.936$  and  $0.972$ ), moderately with those of hsst<sub>2</sub> receptors ( $r = 0.800$  and  $0.502$ ), and very little with those of hsst<sub>3</sub> receptors ( $r = 0.250$  and  $0.190$ ). The PLC stimulation profile of fsst<sub>3</sub> and hsst<sub>5</sub> receptors correlated with  $r = 0.489$ , and of fsst<sub>3</sub> and hsst<sub>3</sub> very low ( $r = 0.167$ ); hsst<sub>2</sub> receptors induced PLC activity only weakly, and therefore no profile could be established (Siehler and Hoyer, submitted (d)).

**Table 7:** Fish sst<sub>3</sub> receptors: comparison of ligand potencies (pEC<sub>50</sub>'s) to activate total [<sup>3</sup>H]-IP<sub>x</sub> accumulation (table 6) (a) with affinities (pK<sub>d</sub>'s) of the receptors labelled with [<sup>125</sup>I]LTT-SRIF<sub>28</sub>, [<sup>125</sup>I][Tyr<sup>10</sup>]CST<sub>14</sub>, [<sup>125</sup>I]CGP 23996 or [<sup>125</sup>I][Tyr<sup>3</sup>]octreotide, (b) with potencies (pEC<sub>50</sub>'s) to stimulate [<sup>35</sup>S]GTPγS specific binding (table 3), and (c) potencies to inhibit forskolin-stimulated adenylate cyclase (FSAC) activity (table 4)

	[ <sup>125</sup> I] LTT- SRIF <sub>28</sub>	[ <sup>125</sup> I] [Tyr <sup>10</sup> ] CST <sub>14</sub>	[ <sup>125</sup> I] CGP 23996	[ <sup>125</sup> I] [Tyr <sup>3</sup> ] octreo tide	[ <sup>35</sup> S]GTPγS		FSAC activity		total [ <sup>3</sup> H]IP <sub>x</sub>	
	pK <sub>d</sub>	pK <sub>d</sub>	pK <sub>d</sub>	pK <sub>d</sub>	E <sub>max</sub>	pEC <sub>50</sub>	E <sub>max</sub>	pEC <sub>50</sub>	E <sub>max</sub>	pEC <sub>50</sub>
SRIF <sub>14</sub>	8.93	8.87	9.53	9.99	100	8.19	100	7.71	100	7.21
SRIF <sub>28</sub>	8.84	8.61	9.64	10.21	103	7.55	105	8.24	100	6.59
LTT-SRIF <sub>28</sub>	8.94 ± 0.08	8.71 ± 0.06	9.56 ± 0.06	9.55 ± 0.16	80	7.55	102	7.75	52	6.16
SRIF <sub>25</sub>	9.00	8.85	9.93	10.32	81	7.25	93	8.29	72	6.88
[Tyr <sup>10</sup> ]CST <sub>14</sub>	8.54	8.32	9.37	9.98	78	7.64	96	7.59	132	6.17
seglitide	9.15	8.55	9.83	10.53	77	8.29	108	8.83	62	7.26
CGP 23996	7.16	6.78	8.24	8.94	72	6.68	107	6.58	40	5.73
octreotide	7.45	7.28	8.72	9.29	105	7.12	113	7.37	24	6.82
[Tyr <sup>3</sup> ] octreotide	6.91 ± 0.02	6.31 ± 0.10	8.36 ± 0.17	8.42 ± 0.03	74	6.64	115	6.85	17	7.43
L362,855	7.54	7.09	8.77	8.91	63	6.29	112	6.56	19	6.46
BIM 23056	6.32	5.88	6.97	9.83	-17	(-)	41	6.51	26	6.02
BIM 23052	7.92	7.68	9.15	7.90	79	6.77	113	7.24	23	7.03

The data are expressed as pK<sub>d</sub>'s or pEC<sub>50</sub>'s (-log M), or E<sub>max</sub>-values [% stimulation or inhibition, respectively] of 3 different experiments; E<sub>max</sub>-values were normalised to the stimulation/ inhibition reached by SRIF<sub>14</sub> (= 100 %).

**Table 8:** Fish  $sst_3$  receptors expressed in CCL39 cells: correlation coefficients (r) of linear regression analyses between (a) the affinity profiles of [ $^{125}$ I]LTT-SRIF<sub>28</sub>, [ $^{125}$ I][Tyr<sup>10</sup>]CST<sub>14</sub>, [ $^{125}$ I]CGP 23996 and [ $^{125}$ I][Tyr<sup>3</sup>]octreotide, (b) the pharmacological profile of stimulation of [ $^{35}$ S]GTP $\gamma$ S binding, (c) the pharmacological profile of inhibition of forskolin-stimulated adenylate cyclase (FSAC) activity, and (d) the pharmacological profile of stimulation of total [ $^3$ H]-IP<sub>x</sub> accumulation

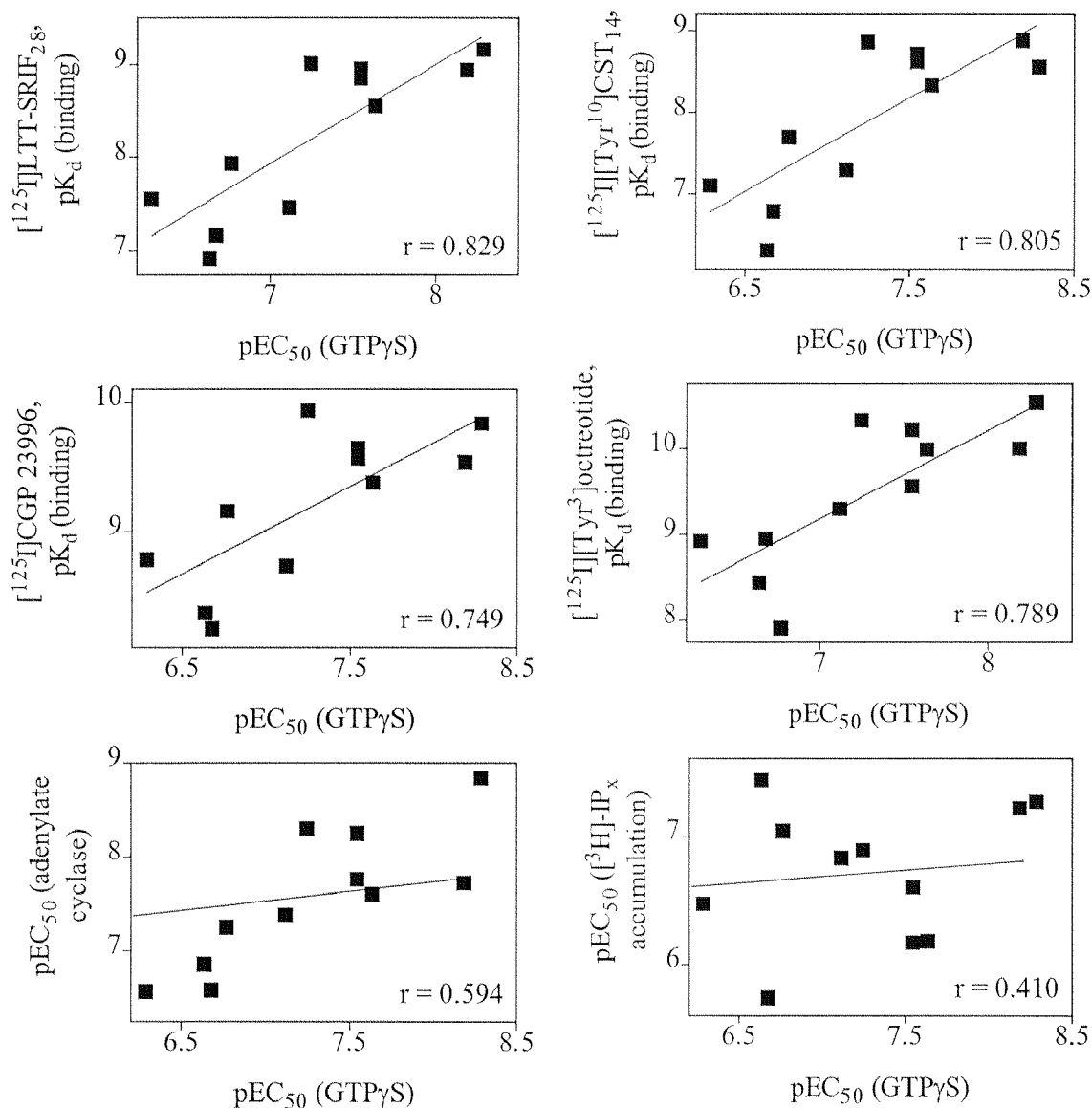
	[ $^{35}$ S]GTP $\gamma$ S binding		inhibition of FSAC activity		[ $^3$ H]-IP <sub>x</sub> accumulation	
	r	P	r	P	r	P
[ $^{125}$ I]LTT-SRIF <sub>28</sub>	0.829	0.0016	0.888	0.0001	0.281	0.3763
[ $^{125}$ I][Tyr <sup>10</sup> ]CST <sub>14</sub>	0.805	0.0028	0.853	0.0004	0.243	0.4470
[ $^{125}$ I]CGP 23996	0.749	0.0079	0.842	0.0006	0.403	0.1935
[ $^{125}$ I][Tyr <sup>3</sup> ]octreotide	0.789	0.0039	0.681	0.0148	0.056	0.8625
inhibition of FSAC activity	0.594	0.0417	-	-	-	-
[ $^3$ H]-IP <sub>x</sub> accumulation	0.410	0.1857	0.424	0.1692	-	-

Data used for correlation analyses are presented in table 8.

### 11.3. Discussion

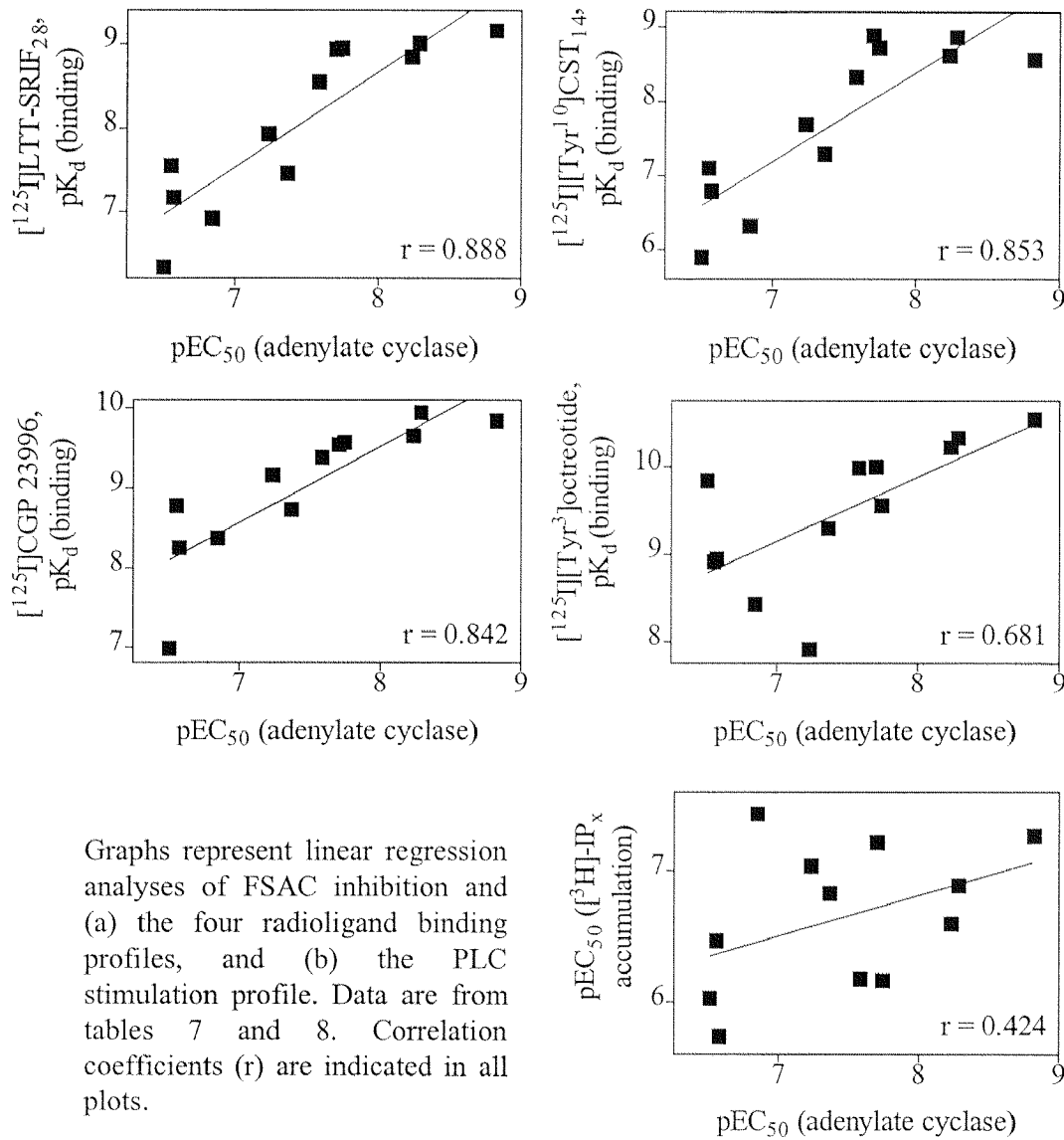
#### GppNHp-inhibited binding of radiolabelled ligands

In saturation binding experiments, the presence of the GTP-analogue GppNHp reduced the apparent receptor density determined with [ $^{125}$ I]CGP 23996 and [ $^{125}$ I][Tyr<sup>3</sup>]octreotide by 4-fold and 8-fold, but did not affect [ $^{125}$ I]LTT-SRIF<sub>28</sub> or [ $^{125}$ I][Tyr<sup>10</sup>]CST<sub>14</sub> binding, although the affinities of all 4 iodinated ligands were not significantly altered by GppNHp.

**Figure 8:** Fish  $sst_3$  receptors expressed in CCL39 cells: correlation analyses.

Data of [ $^{35}S$ ]GTP $\gamma$ S binding experiments were correlated to (a) the affinity profiles of [ $^{125}I$ ]LTT-SRIF $_{28}$ , [ $^{125}I$ ][Tyr $^{10}$ ]CST $_{14}$ , [ $^{125}I$ ]CGP 23996 or [ $^{125}I$ ][Tyr $^3$ ]octreotide, (b) the FSAC inhibition profile, as well as (c) the [ $^3H$ ]-IP $_x$  accumulation profile. Data are from tables 7 and 8. Correlation coefficients (r) are indicated in all plots.

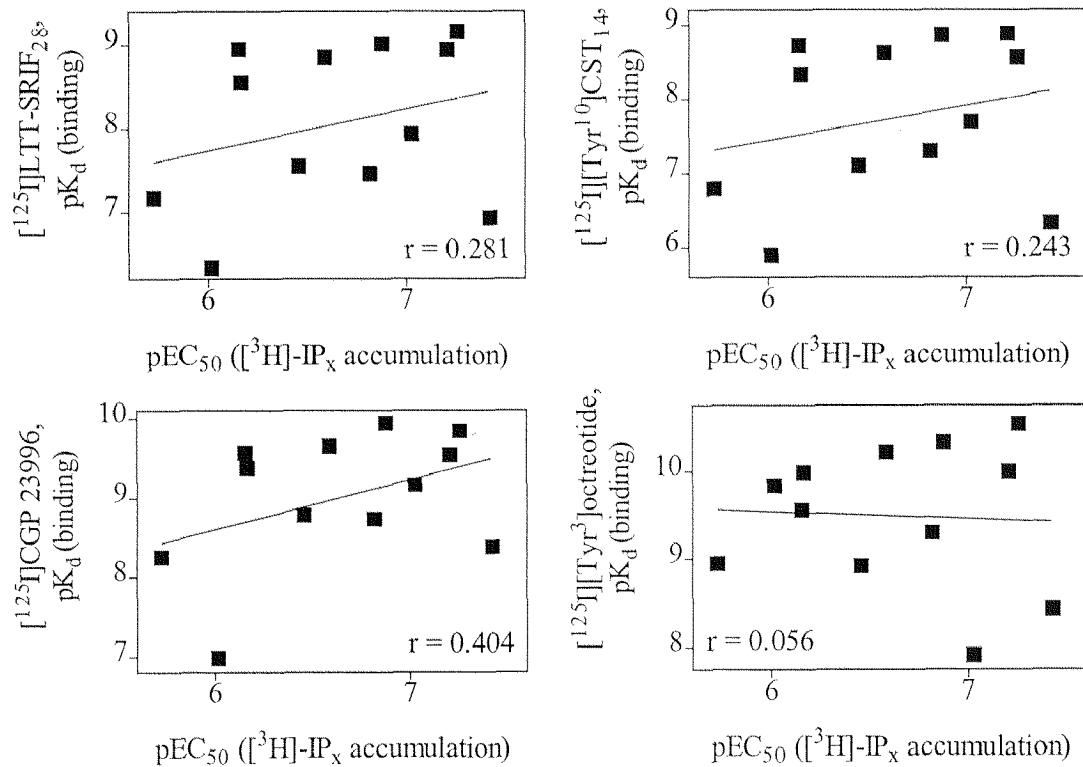
This might explain the different receptor densities determined when using various radioligands at the same receptor subtype: e.g. [ $^{125}I$ ]LTT-SRIF $_{28}$  labelled about 3-times more receptor sites than [ $^{125}I$ ][Tyr $^3$ ]octreotide (4470 and 1520 fmol/ mg, respectively) (Siehler et al., 1999).

**Figure 9:** Fsst<sub>3</sub> receptors: correlation of pharmacological profiles.

Graphs represent linear regression analyses of FSAC inhibition and (a) the four radioligand binding profiles, and (b) the PLC stimulation profile. Data are from tables 7 and 8. Correlation coefficients (r) are indicated in all plots.

However, binding of [<sup>125</sup>I][Tyr<sup>11</sup>]SRIF<sub>14</sub> to rat sst<sub>2</sub> receptors was also found to not be fully sensitive to a GTP-analogue (Gu et al., 1995). Differential GppNHp-sensitivity was observed for the two endogenous ligands – pancreatic polypeptide and peptide YY – of rat Y<sub>4</sub> receptors (Walker et al., 1997). We already reported radioligand-dependent receptor densities observed at human sst<sub>3</sub> receptors; similarly, binding of radioligands to this receptor subtype was differently GppNHp-sensitive (Siehler et al., 1998b).

**Figure 10:** Fsst<sub>3</sub> receptors: correlation of affinity profiles with the PLC activation profile.



Affinity profiles obtained with the 4 different radioligands were correlated to the total [<sup>3</sup>H]-IP<sub>x</sub> accumulation profile. Data are from tables 7 and 8; correlation coefficients (r) are shown all 4 graphs.

Saturation data were confirmed by using increasing concentrations of GppNHp: the binding of [<sup>125</sup>I]CGP 23996 and [<sup>125</sup>I][Tyr<sup>3</sup>]octreotide was drastically inhibited, but not that of the other two radioligands studied. GTP-analogue induced ligand dissociation from the receptor indicates that the receptor is coupled to G-proteins (Brown and Schonbrunn, 1993). Thereby, our data suggest [<sup>125</sup>I]CGP 23996 and [<sup>125</sup>I][Tyr<sup>3</sup>]octreotide to preferentially bind to G-protein-coupled fsst<sub>3</sub> receptors, whereas [<sup>125</sup>I]LTT-SRIF<sub>28</sub> and [<sup>125</sup>I][Tyr<sup>10</sup>]CST<sub>14</sub> seem to label fsst<sub>3</sub> receptors in both states, but surprisingly for an agonist, with a high proportion in an uncoupled state.

**Table 9:** Fish  $ssst_3$  receptors and human  $SRIF_1$  receptor subtypes expressed in CCL39 cells: comparison of ligand potencies obtained by measurement of stimulation of [ $^{35}S$ ]GTP $\gamma$ S binding, inhibition of FSAC activity, and stimulation of [ $^3H$ ]-IP $_x$  accumulation

**Table 9(A)** Stimulation of [ $^{35}S$ ]GTP $\gamma$ S binding

	fsst <sub>3</sub>		hsst <sub>5</sub>		hsst <sub>2</sub>		hsst <sub>3</sub>	
	E <sub>max</sub>	pEC <sub>50</sub>	E <sub>max</sub>	pEC <sub>50</sub>	E <sub>max</sub>	pEC <sub>50</sub>	E <sub>max</sub>	pEC <sub>50</sub>
SRIF <sub>14</sub>	100	8.19	100	8.39	100	6.95	100	7.32
SRIF <sub>28</sub>	103	7.55	101	7.65	116	6.14	104	6.96
LTT-SRIF <sub>28</sub>	80	7.55	107	7.63	110	6.78	119	7.44
[Tyr <sup>10</sup> ]CST <sub>14</sub>	78	7.64	69	7.43	39	6.28	43	6.83
seglitide	77	8.29	84	7.89	137	7.39	49	5.78
CGP 23996	72	6.68	67	7.12	95	6.06	81	7.14
octreotide	105	7.12	107	6.89	94	6.52	42	6.70
[Tyr <sup>3</sup> ]octreotide	74	6.64	72	6.56	131	6.57	47	5.76
L362,855	63	6.29	79	6.29	52	5.65	23	6.27
BIM 23056	-17	(-)	0	(-)	-35	(-)	-10	(-)
BIM 23052	79	6.77	100	6.80	53	5.91	93	6.29

These data are not explained by the “ternary complex model”, which predicts agonists to bind only G-protein-coupled receptors with high affinity and to uncoupled receptors with low affinity (De Lean et al., 1980; Lefkowitz et al., 1993; Samama et al., 1993); the radioligands used behaved at fsst<sub>3</sub> receptors as full agonists in [ $^{35}S$ ]GTP $\gamma$ S binding and AC activity inhibition experiments.

**Table 9(B)** Inhibition of FSAC activity

	fsst <sub>3</sub>		hsst <sub>5</sub>		hsst <sub>2</sub>		hsst <sub>3</sub>	
	E <sub>max</sub>	pEC <sub>50</sub>	E <sub>max</sub>	pEC <sub>50</sub>	E <sub>max</sub>	pEC <sub>50</sub>	E <sub>max</sub>	pEC <sub>50</sub>
SRIF <sub>14</sub>	100	7.71	100	8.13	100	8.15	100	7.76
SRIF <sub>28</sub>	105	8.24	109	8.38	111	8.72	94	8.19
LTT-SRIF <sub>28</sub>	102	7.75	106	7.84	111	8.33	97	8.40
[Tyr <sup>10</sup> ]CST <sub>14</sub>	96	7.59	109	7.69	107	6.80	84	6.80
seglitide	108	8.83	119	9.33	107	10.03	89	6.68
CGP 23996	107	6.58	112	7.07	100	7.79	89	7.84
octreotide	113	7.37	123	7.68	104	8.44	97	7.01
[Tyr <sup>3</sup> ]octreotide	115	6.85	118	7.30	115	9.70	81	6.31
L362,855	112	6.56	143	6.81	137	6.87	58	6.70
BIM 23056	41	6.51	47	6.60	22	(-)	26	(-)
BIM 23052	113	7.24	125	7.40	122	6.74	104	7.43

**Table 9(C)** Stimulation of [<sup>3</sup>H]IP<sub>x</sub> accumulation

	fsst <sub>3</sub>		hsst <sub>5</sub>		hsst <sub>3</sub>	
	E <sub>max</sub>	pEC <sub>50</sub>	E <sub>max</sub>	pEC <sub>50</sub>	E <sub>max</sub>	pEC <sub>50</sub>
SRIF <sub>14</sub>	100	7.21	100	7.22	100	7.71
SRIF <sub>28</sub>	100	6.59	66	6.90	98	7.36
LTT-SRIF <sub>28</sub>	52	6.16	21	6.45	87	7.90
[Tyr <sup>10</sup> ]CST <sub>14</sub>	132	6.17	46	6.31	78	7.05
seglitide	62	7.26	73	7.27	77	6.01
CGP 23996	40	5.73	16	5.53	87	7.05
octreotide	24	6.82	18	6.00	71	6.27
[Tyr <sup>3</sup> ]octreotide	17	7.43	11	5.76	47	5.79
L362,855	19	6.46	3	6.78	31	6.61
BIM 23056	26	6.02	2	5.81	21	5.62
BIM 23052	23	7.03	9	6.80	81	7.44

The data are expressed as means of pEC<sub>50</sub>-values (-log M) or of E<sub>max</sub>-values [% stimulation or inhibition, respectively] of 3 independent experiments; E<sub>max</sub>-values were normalised to the stimulation/ inhibition reached by SRIF<sub>14</sub> (= 100 %).



**Table 10:** Comparison of fish  $ss\tau_3$  receptors with human  $ss\tau_2$ ,  $ss\tau_3$ , and  $ss\tau_5$  receptors expressed in CCL39 cells: correlation coefficients (r) of correlation analyses between pharmacological profiles obtained by measuring stimulation of [ $^{35}$ S]GTP $\gamma$ S binding, inhibition of FSAC activity, and stimulation of total [ $^3$ H]-IP $_x$  accumulation

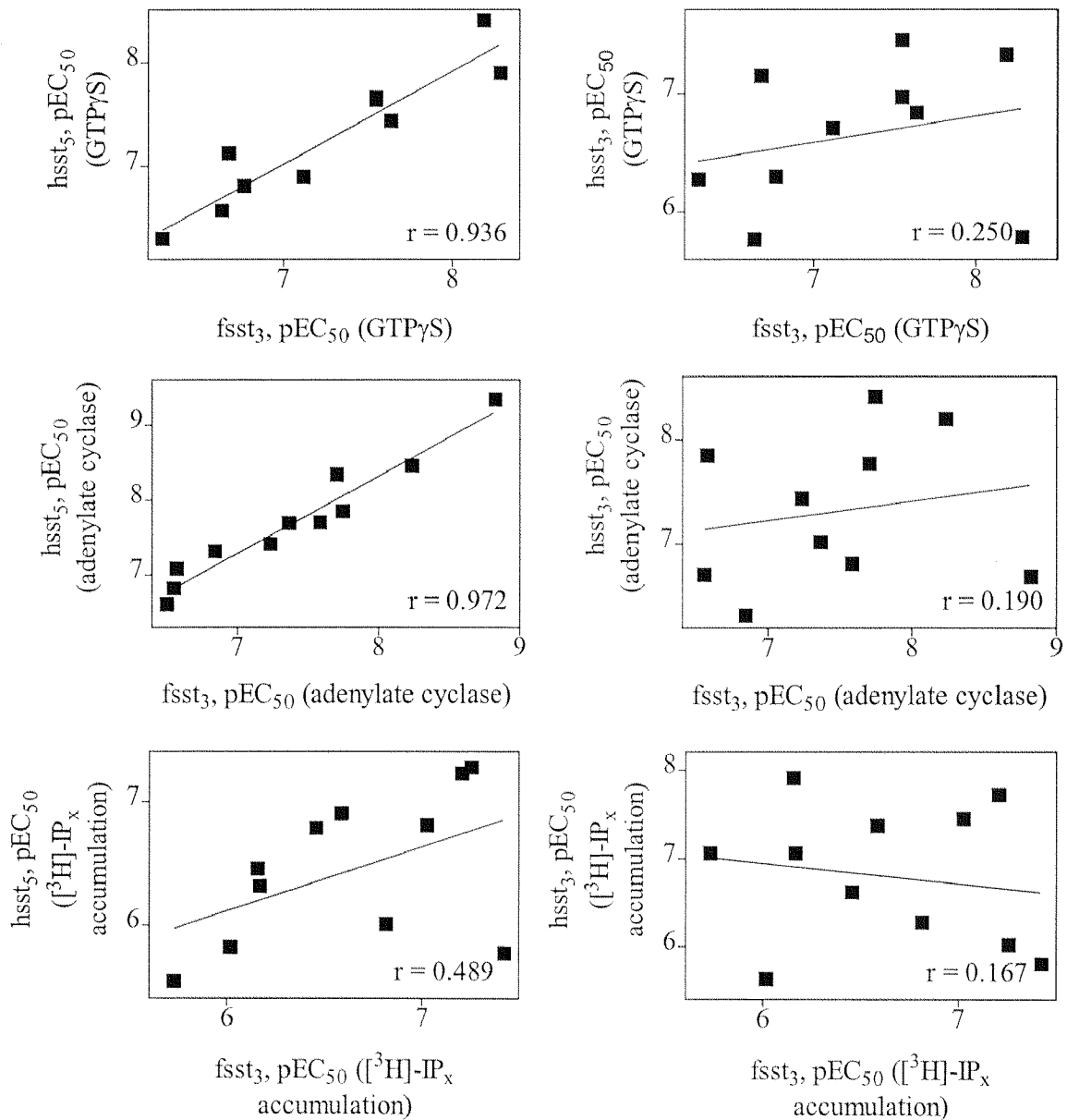
	hsst <sub>5</sub>		hsst <sub>2</sub>		hsst <sub>3</sub>	
	r	P	r	P	r	P
[ $^{35}$ S]GTP $\gamma$ S binding	0.936	< 0.0001	0.800	0.0055	0.250	0.0623
inhibition of FSAC activity	0.972	< 0.0001	0.502	0.1392	0.190	0.5987
[ $^3$ H]-IP $_x$ accumulation	0.489	0.1273	-	-	0.167	0.6227

Data used for linear regression analyses are presented in tables 10(A)-(C).

Functional studies: GTP $\gamma$ S binding, FSAC inhibition, and PLC stimulation

In [ $^{35}$ S]GTP $\gamma$ S binding and PLC stimulation, the potency of SRIF<sub>14</sub> was higher compared to that of SRIF<sub>28</sub> (pEC<sub>50</sub> = 8.19 and 7.55; 7.21 and 6.59, respectively), whereas it was the opposite when studying inhibition of AC activity (pEC<sub>50</sub> = 7.71 and 8.24). In contrast, affinities of both SRIF peptides were similar as determined in radioligand binding studies (Siehler et al., 1999). Rank orders of potency were different from one assay to the other. Seglitide was very potent in all 3 functional assays: GTP $\gamma$ S binding (8.29), FSAC inhibition (8.83), PLC stimulation (7.26). In AC activity determinations, all tested compounds revealed full agonism, with the exception of BIM 23056, which showed weak agonist activity also in the other assays. Only SRIF<sub>14</sub>, SRIF<sub>28</sub> and octreotide were full agonists to stimulate [ $^{35}$ S]GTP $\gamma$ S binding at  $ss\tau_3$  receptors; other ligands reached 63- 81 % efficacy compared to SRIF<sub>14</sub>. Most ligands revealed even lower partial agonism in total [ $^3$ H]-IP $_x$  accumulation measurements: full agonism could be seen with SRIF<sub>14</sub>, SRIF<sub>28</sub> and [Tyr<sup>10</sup>]CST<sub>14</sub>, but the efficacies of other ligands were in the range of 17- 72 % of the E<sub>max</sub>-value of SRIF<sub>14</sub>.

**Figure 11:** Fsst<sub>3</sub> receptors: correlation of GTPγS binding, AC inhibition, and PLC stimulation data with those of human SRIF<sub>1</sub> receptors expressed in CCL39 cells.



Pharmacological profiles of [<sup>35</sup>S]GTPγS binding, FSAC activity inhibition, and total [<sup>3</sup>H]-IP<sub>x</sub> accumulation of fsst<sub>3</sub> receptors were correlated to those of human sst<sub>3</sub> and sst<sub>5</sub> receptors. pEC<sub>50</sub>-values are from table 10. Correlation coefficients (r) are indicated in all graphs.

BIM 23056, which displayed weak agonism at fsst<sub>3</sub> receptors in all 3 functional assays, antagonised SRIF<sub>14</sub>-induced phosphoinositide turnover with an pK<sub>B</sub> of 6.83, but neither SRIF<sub>14</sub>-induced [<sup>35</sup>S]GTPγS binding nor FSAC inhibition.

In contrast, at human  $sst_3$  receptors, BIM 23056 antagonised SRIF<sub>14</sub>-induced GTP $\gamma$ S binding, AC inhibition, and PLC activation with  $pK_B$ -values of 6.33, 6.33, and 5.85, respectively (Siehler and Hoyer, submitted (b), (c), (d)).

The pharmacological profiles of GTP $\gamma$ S binding, FSAC inhibition, and PLC stimulation correlated rather poorly with each other:  $r = 0.410$ -  $0.594$ . More significant, although varying correlations were seen comparing the GTP $\gamma$ S binding and FSAC inhibition profiles with the 4 radioligand binding profiles:  $r = 0.749$ -  $0.829$  and  $r = 0.681$ -  $0.888$ ; the [<sup>125</sup>I][Tyr<sup>3</sup>]octreotide affinity profile ( $r = 0.681$ ) was markedly less significantly correlated with FSAC inhibition compared to the other radioligands. Total [<sup>3</sup>H]-IP<sub>x</sub> accumulation correlated little with the four binding profiles, suggesting other pathways to be more important than the PLC/IP<sub>3</sub> pathway in  $fsst_3$  mediated signalling.

The expression of AC and PLC $\beta$  isoenzymes has not been established in CCL39 cells. The inhibition of FSAC activity by  $fsst_3$  receptors in this cell line was shown to involve the PTX-sensitive G<sub>i</sub>/G<sub>o</sub> proteins (Siehler et al., 1999). G<sub>i</sub>/G<sub>o</sub> proteins inhibit AC type I, V and VI. In CCL39 lung fibroblast cells only type V and VI might be expressed and inhibited by recombinantly expressed  $fsst_3$  receptors, since AC type I expression is neuron-specific (for review, Birnbaumer and Birnbaumer, 1995; Taussig et al., 1993; 1994). Stimulation of PLC activity by SRIF<sub>14</sub> at  $fsst_3$  receptors was only partially affected by PTX (21 %); thus, other G-protein isoforms are suggested to be responsible for mediating this effect; possibly G<sub>q</sub> $\alpha$  and G<sub>11</sub> $\alpha$ , which activate PLC $\beta_{1-4}$ , whereas G<sub>v</sub> $\alpha$  couple to PLC $\beta_{2+3}$  activation (Berridge, 1993; for review: Exton, 1996). In fish, AC and PLC isoenzymes are not characterised yet, but different isotypes may also exist as known in mammals.

Fish  $sst_3$  receptor: comparison with human  $sst_2$ ,  $sst_3$ , and  $sst_5$  receptors expressed in CCL39 cells

Mammalian SRIF receptor-modulated signalling cascades such as the cAMP/protein kinase A- and the PLC/IP<sub>3</sub> pathways (for review: Meyerhof, 1998) seem to be highly conserved among the vertebrate class, since the  $fsst_3$  receptor is able to interact with these different second messengers when expressed in a mammalian cell line.

In all functional assays ( $[^{35}\text{S}]\text{GTP}\gamma\text{S}$  binding, FSAC inhibition, and PLC activation) highest correlation coefficients were observed comparing pharmacological data of  $\text{fsst}_3$  and  $\text{hsst}_5$  receptors:  $r = 0.936$  and  $0.972$  comparing  $\text{GTP}\gamma\text{S}$  binding and AC inhibition. In contrast, the functional data obtained with  $\text{fsst}_3$  and  $\text{hsst}_3$  receptors did not correlate ( $r = 0.167$ -  $0.250$ ). This finding may not be surprising, since previous comparison of affinity profiles of human  $\text{SRIF}_1$  receptors with the  $\text{fsst}_3$  receptor revealed higher similarity with  $\text{hsst}_5$  receptors than with  $\text{hsst}_3$  receptors, although the  $\text{fsst}_3$  protein sequence is more similar to the mammalian  $\text{sst}_3$  receptor subtype (Zupanc et al., 1999; Siehler et al., 1999).

In summary, the differential GppNHp sensitivity of the four agonists  $[^{125}\text{I}]\text{LTT-SRIF}_{28}$ ,  $[^{125}\text{I}][\text{Tyr}^{10}]\text{CST}_{14}$ ,  $[^{125}\text{I}]\text{CGP 23996}$  and  $[^{125}\text{I}][\text{Tyr}^3]\text{octreotide}$  binding suggests labelling of various agonist-specific  $\text{fsst}_3$  receptor states, which are predominantly coupled to G-proteins in the case of  $[^{125}\text{I}]\text{CGP 23996}$  and  $[^{125}\text{I}][\text{Tyr}^3]\text{octreotide}$ , but rather uncoupled in the case of the other two radioligands. Modulation of signalling pathways by somatostatin receptors (stimulation of  $\text{GTP}\gamma\text{S}$  binding, inhibition of AC activity, induction of PLC activity) are conserved, even when comparing such distantly related species as fish and man/ rodents.

The apparent differences in receptor profile observed in radioligand binding and the various second messenger cascades studied, suggest that agonist-specific receptor-trafficking is taking place. In other words, an agonist may favour a ligand-receptor complex, which then preferentially activates one pathway preferentially to another. This has already been suggested by previous work carried out with  $\text{hsst}_5$  receptors and elegantly demonstrated for the human  $5\text{-HT}_{2c}$  receptors (Berg et al., 1998a, 1998b, 1998c) in agreement with a three-state receptor model suggested by Scaramellini and collaborators (Leff et al, 1997, 1998; Scaramellini et al., 1998).

## Conclusions

The aims of this thesis were multiple:

1) We wanted to compare the pharmacological and transductional features of the five cloned human SRIF receptors: to this end, all five receptor subtypes were recombinantly expressed in a cell line known to tolerate well G-protein-coupled receptors negatively linked to adenylate cyclase, a common feature that has been documented for all 5 cloned SRIF receptors, although not always in a consistent manner. Therefore, the CCL39 hamster lung fibroblast cell line was chosen.

2) A second aim was to define the binding features of a number of somatostatin analogues at the five human SRIF receptors, and subsequently to compare the pharmacological profiles defined at a same receptor subtype by several different radioligands: to this end, radioligand binding studies were performed with two analogues of the natural peptides, [ $^{125}\text{I}$ ]LTT-SRIF<sub>28</sub> and [ $^{125}\text{I}$ ][Tyr<sup>10</sup>]CST<sub>14</sub>, and two synthetic analogues, i.e. [ $^{125}\text{I}$ ][Tyr<sup>3</sup>]octreotide and [ $^{125}\text{I}$ ]CGP 23996.

3) A third goal was to use the five human SRIF receptors expressed in the same cellular environment to perform not only radioligand binding studies, but also to measure receptor-G-protein interactions (effects of GppNHp and agonist-stimulated GTP $\gamma$ S binding), and to characterise transductional features of the receptors by studying cAMP, PLC and Ca<sup>2+</sup> accumulation, i.e. the protein kinase A and PLC cascades.

4) A fourth aim was to characterise in a similar manner and in the same cellular environment the first cloned non-mammalian somatostatin receptor, namely the fish sst<sub>3</sub> receptor: thus we established in stably transfected CCL39 cells the binding features of the fsst<sub>3</sub> receptor using the four radioligands [ $^{125}\text{I}$ ]LTT-SRIF<sub>28</sub>, [ $^{125}\text{I}$ ][Tyr<sup>10</sup>]CST<sub>14</sub>, [ $^{125}\text{I}$ ]CGP 23996 and [ $^{125}\text{I}$ ][Tyr<sup>3</sup>]octreotide, studied the effects on receptor-G-protein interactions, and the transductional cascades, as previously done for the human SRIF receptors.

In addition, we compared the pharmacological profile of the *fsst*<sub>3</sub> receptor with that of human SRIF receptors to establish possible species differences, and finally, we also compared the profile of the recombinant *fsst*<sub>3</sub> receptor with that of endogenously expressed receptor binding sites present in various tissues, specially brain and liver.

5) The ultimate goal was to compare all the data in order to provide support or to reject the hypothesis, that some SRIF receptors may display different pharmacological profiles depending on the nature of the ligand-receptor interaction considered: radioligand binding, G-protein activation, second messenger studies. Indeed, a survey of the literature shows, that various groups working on the same recombinant receptor, report very different affinity and potency values for a number of compounds depending on the cell line, binding test or second messenger system studied. In addition, it becomes evident that at least for some receptors (e.g. 5-HT<sub>2a</sub>, 5-HT<sub>2c</sub>, PACAP receptors), the possibility of receptor trafficking may exist, although final proof has not yet been provided.

[<sup>125</sup>I][Tyr<sup>10</sup>]CST<sub>14</sub>, an iodinated analogue of the recently cloned cortistatin (CST) (De Lecea et al., 1996, 1997a; Fukusumi et al., 1997), bound with similar high affinity to [<sup>125</sup>I]LTT-SRIF<sub>28</sub> to all five human somatostatin receptors recombinantly expressed in CCL39 cells, as well as the non-iodinated analogues [Tyr<sup>10</sup>]CST<sub>14</sub> and CST<sub>17</sub>; binding of CST to the SRIF receptors suggests CST to belong functionally to the somatostatin peptide family. In addition, the affinity profiles established with [<sup>125</sup>I][Tyr<sup>10</sup>]CST<sub>14</sub> and [<sup>125</sup>I]LTT-SRIF<sub>28</sub> were comparable. The CNS-specific expression of the CST-prepropeptide (De Lecea et al., 1996, 1997a; Fukusumi et al., 1997) suggests CST-specific functions solely in the brain compared to SRIF, which possesses multiple functions in the brain and periphery. It remains to be seen whether there exist receptors selective for SRIF or CST.

Ocreotide has antiproliferative properties *in vitro* and *in vivo* in hormone-secreting tumours, and is used in the treatment of acromegaly, neuroendocrine and gastroenteropancreatic tumours, and AIDS-related diarrhoea. These effects are assumed to be mediated by SRIF<sub>1</sub> receptors, primarily the sst<sub>2</sub> type. In CCL39 cells, the analogue [<sup>125</sup>I][Tyr<sup>3</sup>]octreotide labelled not only human sst<sub>2</sub> receptors as previously reported (Hoyer et al., 1994b; Piwko et al., 1997; Schoeffter et al., 1995), but also human sst<sub>5</sub> receptors. Therefore, results of autoradiographic/ binding studies using [<sup>125</sup>I][Tyr<sup>3</sup>]octreotide possibly document the presence of sst<sub>2</sub> and sst<sub>5</sub> receptors, when both subtypes are expressed in the tissue studied; similarly, the antiproliferative effect of octreotide on tumour growth might be mediated by both, human sst<sub>2</sub> and sst<sub>5</sub> receptors. It should however be realised that sst<sub>5</sub> receptors show overall very low expression levels.

At human sst<sub>5</sub> receptors, apparent receptor densities (920- 6950 fmol/mg) and binding affinities (up to 1000-fold variation) were dependent on the radioligand used ([<sup>125</sup>I]LTT-SRIF<sub>28</sub>, [<sup>125</sup>I][Tyr<sup>10</sup>]CST<sub>14</sub>, [<sup>125</sup>I]CGP 23996, [<sup>125</sup>I][Tyr<sup>3</sup>]octreotide = full agonists); e.g. [<sup>125</sup>I][Tyr<sup>3</sup>]octreotide recognised the lowest receptor number, and affinities of competing peptides were higher compared to other radioligands. However, this radioligand-dependency of binding data was not observed to that extent at human sst<sub>1-4</sub> receptors (whereas at fsst<sub>3</sub> similar findings were made).

Binding of the four radioligands to human sst<sub>5</sub> receptors was, to a various extent, sensitive to the presence of the GTP-analogue GppNHp, explaining the different B<sub>max</sub>-values: the binding of e.g. [<sup>125</sup>I][Tyr<sup>3</sup>]octreotide was highly inhibited, which suggests [<sup>125</sup>I][Tyr<sup>3</sup>]octreotide to label almost exclusively G-protein-coupled sst<sub>5</sub> receptors, and therefore only low receptor densities; in contrast, the binding of [<sup>125</sup>I]LTT-SRIF<sub>28</sub> and [<sup>125</sup>I][Tyr<sup>10</sup>]CST<sub>14</sub> was rather GppNHp-insensitive, which suggests labelling of predominantly G-protein- uncoupled sst<sub>5</sub> receptors, and hence of higher receptor density. Distinct GppNHp sensitivity was also found for the two endogenous peptides of NPY<sub>4</sub> receptors (Walker et al., 1997). Binding of the radioligands to human sst<sub>2</sub> or sst<sub>3</sub> receptors was highly guanine nucleotide sensitive, and rather insensitive at sst<sub>1</sub> or sst<sub>4</sub> receptors, although all ligands used display agonism all five SRIF receptor.

This suggests at least that all agonists do not favour an “active” receptor state, some may even favour the “inactive”, assuming that the two species can be distinguished by GppNHp sensitivity or absence of it. One may even suggest more than two states for G-protein-coupled receptors in the SRIF family. Indeed, the findings at human *sst*<sub>5</sub> receptors cannot be explained by the ternary complex model (De Lean et al., 1980; Lefkowitz et al., 1993; Samama et al., 1993), since the cold peptides of all radioligands used behave as full agonists in functional assays (De Lecea et al., 1996; Hoyer et al., 1994b), but rather by proposing multiple receptor conformations induced by different agonists, which has been already suggested by functional data for  $\beta_2$ -adrenergic receptors (Krumins et al., 1997).

On the other hand, the binding of analogues of the endogenous peptides SRIF<sub>28</sub> and CST to G-protein-uncoupled SRIF receptors may suggest coupling to G-protein-independent signalling pathways, like that inhibiting Na<sup>+</sup>/H<sup>+</sup> exchange activity and discovered for  $\beta_2$ -adrenergic receptors (Hall et al., 1998); SRIF receptors are known to mediate PTX-insensitive inhibition of Na<sup>+</sup>/H<sup>+</sup> exchange activity (Barber et al., 1989; Hou et al., 1994).

The [<sup>35</sup>S]GTP $\gamma$ S binding profile established at *sst*<sub>2-5</sub> correlated significantly, although to various degrees with the different radioligand binding profiles at human *sst*<sub>4</sub>/*sst*<sub>5</sub> receptors, and modestly at *sst*<sub>2</sub>/*sst*<sub>3</sub> receptors. Similarly, affinity profiles of *sst*<sub>3-5</sub> receptors correlated well, but differentially with inhibition of forskolin-stimulated adenylate cyclase (FSAC) activity, although modestly at *sst*<sub>1</sub>/*sst*<sub>2</sub> receptors. In CCL39 cells, human *sst*<sub>3</sub> and *sst*<sub>5</sub> receptors, but not the other SRIF receptors, couple significantly to stimulation of PLC activity (IP<sub>x</sub> accumulation) and intracellular Ca<sup>2+</sup> increase. PLC stimulation was partially PTX-sensitive suggesting other G-proteins in addition to G<sub>i/o</sub>, to be primarily involved. IP<sub>x</sub> accumulation correlated for both receptor subtypes well with the radioligand binding profiles, although to a various degree, but rather poorly with forskolin-stimulated adenylate cyclase activity.



The rank orders of affinities/ potencies was specific for each receptor subtype and for the second messenger system considered (radioligand binding, [<sup>35</sup>S]GTP $\gamma$ S binding, AC inhibition, PLC induction). The results of the two studied signalling pathways (AC/ protein kinase A, PLC/ IP<sub>3</sub>) may suggest human sst<sub>1</sub>/ sst<sub>2</sub> receptors to preferentially couple to the Ras/ Raf/ MAPK pathway, which has been reported to be modulated by SRIF receptors.

Recently, the first non-mammalian somatostatin receptor (fish sst<sub>3</sub>) was cloned from the fish *Apteronotus albifrons* (Zupanc et al., 1999); weak expression in brain was shown by RT-PCR. The [<sup>125</sup>I]LTT-SRIF<sub>28</sub> profile of fsst<sub>3</sub> receptors recombinantly expressed in CCL39 cells correlated highly with that of *Apteronotus* brain, but not of liver. In addition, biphasic competition curves obtained with brain tissue binding, as well the different profile observed in liver preparation suggests the existence of at least one further SRIF receptor subtype in fish.

Like the mammalian receptors, fish sst<sub>3</sub> receptors in CCL39 cells, couple negatively to adenylate cyclase via PTX-sensitive G-proteins (G<sub>i</sub>/G<sub>o</sub>), and to PLC stimulation in a partially PTX-sensitive manner. Similarly to human sst<sub>5</sub> receptor, affinities and receptor densities defined with [<sup>125</sup>I]LTT-SRIF<sub>28</sub>, [<sup>125</sup>I][Tyr<sup>10</sup>]CST<sub>14</sub>, [<sup>125</sup>I]CGP 23996, [<sup>125</sup>I][Tyr<sup>3</sup>]octreotide were radioligand-dependent, and radioligand binding was differentially inhibited by GppNHp. In contrast to PLC activation, [<sup>35</sup>S]GTP $\gamma$ S binding and AC correlated significantly, although to different extents with the affinity profiles. Thus, the comments made about multiple receptor states and receptor effector coupling made for some mammalian SRIF receptors also apply to the fish species. The binding and functional data of fish sst<sub>3</sub> receptors display highest similarity with those of human sst<sub>5</sub> receptor, although the amino acid sequence matches better with mammalian sst<sub>3</sub> receptors. The results indicate that the signal transduction cascades modulated by SRIF receptors were highly conserved during evolution of the vertebrate class.

Taken together, the results suggest (1) that multiple agonist-specific receptor conformations can be achieved at recombinant SRIF receptor subtypes, which are G-protein coupled and/ or G-protein uncoupled, (2) that the nature of agonist-modulated receptor/ G-protein/ effector interactions might be more complex than initially suggested by the ternary complex model, and (3) different rank orders of apparent potency can be observed at SRIF receptors depending on the nature of the ligand/ receptor interaction studied (radioligand binding, [<sup>35</sup>S]GTP $\gamma$ S binding, AC activity, PLC activity); this suggests that receptor-effector trafficking can take place, as proposed for the human 5-HT<sub>2c</sub> receptor (Berg et al. 1998a, 1998b, 1998c; Leff et al., 1997, 1998; Scaramellini et al., 1998), i.e. that each agonist-specific receptor conformation triggers specifically the modulated signalling pathways.

## References

- Aguila MC, Dess WL, Haensly WE, McCann SM (1991). Evidence that somatostatin is localized and synthesized in lymphoid organs. *Proc. Natl. Acad. Sci. USA* 88: 11485-11489.
- Akbar M, Okajima F, Tomura H, Majid MA, Yamada Y, Seino S, Kondo Y (1994). Phospholipase C activation and Ca<sup>2+</sup> mobilization by the cloned human somatostatin receptor subtypes 1-5, transfected in COS-7 cells. *FEBS Lett.* 348: 192- 196.
- Andrews PC, Dixon JE (1981). Isolation and structure of a peptide hormone predicted from a mRNA sequence. *J. Biol. Chem.* 256: 8267- 8270.
- Andrews PC, Pollock HG, Elliott WM, Youson JH, Plisetskaya EM (1988). Isolation and characterization of a variant somatostatin-14 and two related somatostatins of 34 and 37 residues from lamprey (*Petromyzon marinus*). *J. Biol. Chem.* 263: 15809- 15814.
- Andrews, PC, Pubols MH, Hermodson MA, Sheares BT, Dixon JE (1984). Structure of the 22-residue somatostatin from catfish. *J. Biol. Chem.* 259: 13267- 13272.
- Aronin N, Cooper PE, Lorenz LJ, Bird ED, Sagar SM, Leeman SE, Martin JB (1983). Somatostatin is increased in the basal ganglia in Huntington disease. *Ann. Neurol.* 13: 519-526.
- Avigan J, Murtagh JJ, Stevens LA, Angus CW, Moss J, Vaughan M (1992). Pertussis toxin-catalyzed ADP-ribosylation of G<sub>o</sub> alpha with mutation at the carboxy terminus. *Biochemistry* 31: 7736- 7740.
- Barber DL, McGuire ME, Ganz MB (1989).  $\beta$ -Adrenergic and somatostatin receptors regulate Na<sup>+</sup>-H<sup>+</sup>exchange independent of cAMP. *J. Biol. Chem.* 264: 21038- 21042.
- Bauer W, Briner U, Doepfner W, Haller R, Huguenin R, Marbach P, Petcher TJ, Pless J (1982). SMS 201-995: A very potent and selective octapeptide analogue of somatostatin with prolonged action. *Life Sci.* 31: 1133- 1140.
- Beal MF, Mazurek MF, Black PL, Martin JB (1985). Human cerebrospinal fluid somatostatin in neurological disease. *J. Neurol. Sci.* 71: 91- 104.
- Bell GI, Reisine T (1993). Molecular biology of somatostatin receptors. *Trends Neurosci.* 16: 34- 38.
- Bell GI, Yasuda K, Kong H, Law SF, Raynor K, Reisine T (1995). Molecular biology of somatostatin receptors. *Ciba Found. Symp.* 190: 65- 79.
- Berg KA, Maayani S, Clarke WP (1998a). Interactions between effectors linked to serotonin receptors. *Ann. N. Y. Acad. Sci.* 861 (Advances in Serotonin Receptor Research): 111-120.
- Berg KA, Maayani S, Goldfarb J, Clarke WP (1998b). Pleiotropic behavior of 5-HT<sub>2A</sub> and 5-HT<sub>2C</sub> receptor agonists. *Ann. N. Y. Acad. Sci.* 861(Advances in Serotonin Receptor Research): 104- 110.
- Berg KA, Maayani S, Goldfarb J, Scaramellini C, Leff P, Clarke WP (1998c). Effector pathway-dependent relative efficacy at serotonin type 2A and 2C receptors: evidence for agonist-directed trafficking of receptor stimulus. *Mol. Pharmacol.* 54: 94- 104.

- Berridge MJ (1993). Inositol triphosphate and calcium signalling. *Nature* 361: 315- 325.
- Birnbaumer L, Birnbaumer M (1995). Signal transduction by G proteins: 1994 edition. *J. Rec. & Signal Transduction Res.* 15: 213- 252.
- Bito H, Mori M, Sakanaka C, Takano T, Honda Z, Gotoh Y, Nishida E, Shimizu T (1994). *J. Biol. Chem.* 269: 1272- 12730.
- Bradford MM (1976). A rapid and sensitive method for the quantitation of microgram quantities of protein utilizing the principle of protein-dye binding. *Anal. Biochem.* 72: 248- 254.
- Brazeau P, Vale W, Burgus R, Ling N, Rivier J, Guillemin R (1972). Hypothalamic polypeptide that inhibits the secretion of the immunoreactive pituitary growth hormone. *Science* 129: 77- 79.
- Breder CD, Yamada Y, Yasuda K, Seino S, Saper CB, Bell GI (1992). Differential expression of somatostatin receptor subtypes in brain. *J. Neurosci.* 12: 3920- 3934.
- Brown M, Rivier J, Vale W (1977). SRIF analogs with selected biological activities. *Science* 196: 1476- 1468.
- Brown PJ, Schonbrunn A (1993). Affinity purification of a somatostatin receptor-G protein complex demonstrates specificity in receptor-G protein coupling. *J. Biol. Chem.* 268: 6668- 6676.
- Bruno JF, Xu Y, Song J, Berelowitz M (1992). Molecular cloning and functional expression of a brain-specific somatostatin receptor. *Proc. Natl. Acad. Sci. USA* 89: 11151- 11155.
- Bruno JF, Xu Y, Song J, Berelowitz M (1993). Tissue distribution of somatostatin receptor subtype messenger ribonucleic acid in the rat. *Endocrinology* 133: 2561- 2567.
- Bruns C, Weckbecker G, Raulf F, Kaupmann K, Hoyer D, Lübbert H (1994). Molecular Pharmacology of Somatostatin receptor subtypes. *Ann. N. Y. Acad. Sci.* 733: 138- 146.
- Bruns C, Weckbecker G, Raulf F, Kaupmann K, Schoeffter P, Lübbert H, Hoyer D (1995). Characterization of somatostatin receptor subtypes. In: Somatostatin and its receptors. *Ciba Found. Symp.* 190: 89- 110.
- Buscail L, Esteve JP, Prats H, Bayard F, Bell GI, Vaysse N, Susini C (1993). Human somatostatin receptor hSSTR-2 may mediate the antiproliferative effect of octreotide. *Gastroenterol.* 104: 816- 819.
- Buscail L, Esteve JP, Saint-Laurent N, Bertrand V, Reisine T, O'Carroll AM, Bell GI, Schally AV, Vaysse N, Susini C (1994). Inhibition of cell proliferation by the somatostatin analogue RC-160 is mediated by somatostatin receptor subtypes SSTR2 and SSTR5 through different mechanisms. *Proc. Natl. Acad. Sci. USA* 92: 1580- 1584.
- Carruthers AM, Warner A, Michel AD, Feniuk W, Humphrey PPA (1999). Activation of adenylate cyclase by human recombinant sst<sub>5</sub> receptors expressed in CHO-K1 cells and involvement of G $\alpha$ s proteins. *Br. J. Pharmacol.* 126: 1221- 1229.
- Cello JP, Grendell JH, Basuk P, Simon D, Weiss L, Wittner M, Rood RP, Wilcox CM, Forsmark CE, Read AE (1991). Effect of octreotide on refractory AIDS-associated diarrhoea. *Ann. Intern. Med.* 115: 705- 710.

- Chadwick DJ, Cardew G, editors (1995). Somatostatin and its receptors. *Ciba Found. Symp.* 190, 247 pp.
- Chen L, Fitzpatrick VD, Vandlen RL, Tashjian AH (1997). Both overlapping and distinct signaling pathways for somatostatin receptor subtypes SSTR1 and SSTR2 in pituitary cells. *J. Biol. Chem.* 272: 18666- 18672.
- Chesselet MF, Reisine TD (1983). Somatostatin regulates dopamine release in rat striatal slices and cat caudate nuclei. *J. Neurosci.* 3: 232- 236.
- Cheung NW, Boyages SC (1995). Somatostatin-14 and its analog octreotide exert a cytostatic effect on GH<sub>3</sub> rat pituitary tumour cell proliferation via a transient G<sub>0</sub>/G<sub>1</sub> cell cycle block. *Endocrinology* 136: 4174- 4181.
- Chneiweiss H, Glowinski J, Premont J (1984). Vasoactive intestinal polypeptide receptors linked to an adenylate cyclase, and their relationship with biogenic amine- and somatostatin-sensitive adenylate cyclases on central neuronal and glial cells in primary cultures. *J. Neurochem.* 44: 779- 786.
- Clapham DE (1995). Calcium signaling. *Cell* 80: 259- 268.
- Clarke WP, Bond RA (1998). The elusive nature of intrinsic efficacy. *Trends Pharmacol. Sci.* 19: 270- 276.
- Connor M, Ingram SL, Christie MJ (1997). Cortistatin increase of a potassium conductance in rat locus coeruleus in vitro. *Br. J. Pharmacol.* 122: 1567- 1572.
- Colas B, Valencia AM, Prieto JC, Arilla E (1992). Somatostatin binding and modulation of adenylate cyclase in ovine retina membranes. *Mol. Cell. Endocrinol.* 88: 111- 117.
- Conlon JM (1990). [Ser<sup>5</sup>]-somatostatin-14: isolation from the pancreas of a holocephalan fish, the Pacific ratfish (*Hydrolagus colliciei*). *Gen. Comp. Endocrinol.* 80: 314- 320.
- Conlon JM, Agoston DV, Thim L (1985). An elasmobranchian somatostatin: primary structure and tissue distribution in *Torpedo marmorata*. *Gen. Comp. Endocrinol.* 60: 406- 413.
- Conlon JM, Askensten U, Falkmer S, Thim L (1988a). Primary structures of somatostatins from the islet organ of the hagfish suggest an anomalous pathway of posttranslational processing of prosomatostatin-1. *Endocrinology* 122: 1855- 1859.
- Conlon JM, Bondareva V, Rusakov Y, Plisetskaya EM, Mynarcik DC, Whittaker J (1995). Characterization of insulin, glucagon, and somatostatin from the river lamprey, *Lampetra fluviatilis*. *Gen. Comp. Endocrinol.* 100: 96- 105.
- Conlon JM, Deacon CF, Hazon N, Henderson IW, Thim L (1988b). Somatostatin-related and glucagon-related peptides with unusual structural features from the European eel (*Anguilla anguilla*). *Gen. Comp. Endocrinol.* 72: 181- 189.
- Conlon JM, Hicks JW (1990). Isolation and structural characterization of insulin, glucagon and somatostatin from the turtle, *Pseudemys scripta*. *Peptides* 11: 461- 466.
- Corness JD, Demchyshyn LL, Seeman P, Van Tol HH, Srikant CB, Kent G, Patel YC, Niznik HB (1993). A human somatostatin receptor (SSTR3), located on chromosome 22, displays preferential affinity for somatostatin-14-like peptides. *FEBS Lett.* 321: 279- 284.

- Costa T, Lang J, Gless C, Herz A (1990). Spontaneous association between opioid receptors and GTP-binding regulatory proteins in native membranes: specific regulation by antagonists and sodium ions. *Mol. Pharmacol.* 37: 383- 394.
- Cotecchia S, Kobilka BK, Daniel KW, Nolan RD, Lapetina EY, Caron MG, Lefkowitz RJ, Regan J (1990). Multiple second messenger pathways of  $\alpha$ -adrenergic receptor subtypes expressed in eukaryotic cells. *J. Biol. Chem.* 265: 63- 69.
- Coy DH, Taylor JE (1996). Receptor specific somatostatin analogs: correlation with biological activity. *Metabolism* 34: 21- 23.
- Coy DH, Taylor JE, Rossowski WJ (1998). Biological properties of old and new human and rat receptor specific somatostatin analogs. *Yale J. Biol. Med.* 8: 21- 26.
- Czernik AJ, Petrack B (1983). Somatostatin receptor binding in rat cerebral cortex. *J. Biol. Chem.* 258: 5525 -5530.
- Daaka Y, Luttrell LM, Lefkowitz RJ (1997). Switching of the coupling of the  $\beta_2$ -adrenergic receptor to different G proteins by protein kinase A. *Nature* 390: 88- 91.
- Da Cunha A, Rausch DM, Eiden LE (1993). An early increase in somatostatin mRNA expression in the frontal cortex of rhesus monkeys infected with simian immunodeficiency virus. *Proc. Natl. Acad. Sci. USA* 92: 1371- 1375.
- Davies P, Katzman R, Terry RD (1980). Reduced somatostatin-like immunoreactivity in cerebral cortex from cases of Alzheimer disease and Alzheimer senile dementia. *Nature* 288: 279- 280.
- De Lean A (1979). SCTFIT: A Computer Program for Simultaneous Analysis of Saturation and Competition Curves, Howard Hughes Medical Institute, Duke University Medical Center, Durham, North Carolina.
- De Lean A, Stadel JM, Lefkowitz RJ (1980). A ternary complex model explains the agonist-specific binding properties of the adenylate cyclase-coupled  $\beta$ -adrenergic receptor. *J. Biol. Chem.* 255: 7108- 7117.
- De Lecea L, Criado JR, Prospero-Garcia O, Gautvik KM, Schweitzer P, Danielson PE, Dunlop CL, Siggins GR, Henriksen SJ, Sutcliffe JG (1996). A cortical neuropeptide with neuronal depressant and sleep-modulating properties. *Nature* 381: 242- 245.
- De Lecea L, Del Rio JA, Criado JR, Alcantara S, Morales M, Danielson PE, Henriksen SJ, Soriano E, Sutcliffe JG (1997a). Cortistatin is expressed in a distinct subset of cortical interneurons. *J. Neurosci.* 17: 5868- 5880.
- De Lecea L, Ruiz-Lozano P, Danielson PE, Peelle-Kirley J, Foye PE, Frankel WN, Sutcliffe JG (1997b). Cloning, mRNA expression, and chromosomal mapping of mouse and human preprocortistatin. *Genomics* 42: 499- 506.
- Demchyshyn LL, Srikant CB, Sunahara RK, Kent G, Seeman P, Van Tol HH, Panetta R, Patel YC, Niznik HB (1993). Cloning and expression of a human somatostatin-14-selective receptor variant (somatostatin receptor 4) located on chromosome 20. *Mol. Pharmacol.* 43: 894- 901.
- Dohlman HG, Thorner J, Caron MC, Lefkowitz RJ (1991). Model systems for the study of seven-transmembrane-segment receptors. *Annu. Rev. Biochem.* 60: 653- 688.

- Dournaud P, Gu YZ, Schonbrunn A, Mazella J, Tannenbaum GS, Beaudet A (1996). Localization of the somatostatin receptor SST2A in rat brain using a specific antipeptide antibody. *J. Neurosci.* 16: 4468- 4478.
- Edwards CA, Cann PA, Read NW, Holdsworth CD (1986). The effect of somatostatin analogue SMS 201-995 on fluid and electrolyte transport in a patient with secretory diarrhoe. *Scand. J. Gastroent.* 21: 259- 261.
- Efendic S, Mattson O (1978). Effect of somatostatin on intestinal motility. *Acta Radiol.* 19: 348- 352.
- Eilertson CD, Sheridan MA (1993). Differential effects of somatostatin-14 and somatostatin-25 on carbohydrate and lipid metabolism in rainbow trout *Oncorhynchus mykiss*. *Gen. Comp. Endocrinol.* 92: 62- 70.
- Epelbaum J (1986). Somatostatin in the central nervous system: physiology and pathological modifications. *Prog. Neurobiol.* 27: 63- 100.
- Epelbaum J, Dournaud P, Fodor M, Viollet C (1994). The neurobiology of somatostatin. *Crit. Rev. Neurobiol.* 8: 25- 44.
- Epelbaum J, Dussailant M, Enjalbart A, Kordon C, Rostene W (1985). Autoradiographic localization of a non-reducible somatostatin analog <sup>125</sup>I-CGP-23996, binding sites in the rat brain: Comparison with membrane binding. *Peptides* 6: 713- 719.
- Epelbaum J, Enjalbert A, Krantic S, Musset F, Bertrand P, Rasolonjanahary R, Shu C, Kordon C (1987). Somatostatin receptors on pituitary somatotrophs, thyrotrophs, and lactotrophs: pharmacological evidence for loose coupling to adenylate cyclase. *Endocrinology* 121: 2177- 2185.
- Exton JH (1996). Regulation of phosphoinositide phospholipases by hormones, neurotransmitters and other agonists linked to G proteins. *Ann. Rev. Pharmacol. Toxicol.* 36: 481- 510.
- Fabbri E, Brighenti L, Ottolenghi C, Puviani AC, Capuzzo A (1992). Beta-adrenergic receptors in catfish liver membranes: characterization and coupling to adenylate cyclase. *Gen. Comp. Endocrinol.* 85: 254- 260.
- Feniuk W, Dimech J, Humphrey PPA (1993). Characterization of somatostatin receptors in guinea-pig isolated ileum, vas deferens and right atrium. *Br. J. Pharmacol.* 110: 154- 157.
- Feniuk W, Dimech J, Jarvie EM, Humphrey PPA (1995). Further evidence from functional studies for somatostatin receptor heterogeneity in guinea pig isolated ileum, vas deferens and right atrium. *Br. J. Pharmacol.* 115: 975- 980.
- Findlay J, Eliopoulos E (1990). Three-dimensional modelling of G protein-linked receptors. *Trends Pharmacol. Sci.* 11: 492- 499.
- Finley JC, Maderdrut JL, Roger LJ, Pertrusz P (1981). The immunocytochemical localization of somatostatin-containing neurons in the rat central nervous system. *Neuroscience* 6: 2173- 2192.
- Fitzpatrick V, Vandlen R (1994). Agonist selectivity determinants in SRIF receptor subtypes I and II. *J. Biol. Chem.* 269: 24621- 24626.

- Fletcher DJ, Trent DF, Weir GC (1983). Catfish somatostatin is unique to piscine tissues. *Regulatory Peptides* 5: 181- 187.
- Flood JF, Uezu K, Morley JE (1997). The cortical neuropeptide, cortistatin-14, impairs post-training memory processing. *Brain Res.* 775: 250- 252.
- Florio T, Rim C, Hershberger RE, Loda M, Stork PJ (1994). The somatostatin receptor SSTR1 is coupled to phosphotyrosine phosphatase activity in CHO-K1 cells. *Mol. Endocrinol.* 8: 1289- 1297.
- Florio T, Thellung S, Schettini G (1996). Intracellular transducing mechanisms coupled to brain somatostatin receptors. *Pharmacol. Res.* 33: 297- 305.
- Florio T, Yao H, Carey KD, Dillon TJ, Stork PJS (1999). Somatostatin activation of mitogen-activated protein kinase via somatostatin receptor 1 (SSTR1). *Mol. Endocrinol.* 13: 24- 37.
- Freidinger RM, Perlow DS, Randall WC, Saperstein R, Arison BH, Veber DF (1984). Conformational modifications of cyclic hexapeptide somatostatin analogs. *Int. J. Peptide Protein Res.* 23: 142- 150.
- Fujii Y, Gonoi T, Yamada Y, Chihara K, Inagaki N, Seino S (1994). Somatostatin receptor subtype SSTR2 mediates the inhibition of high-voltage-activated calcium channels by somatostatin and its analogue SMS 201-995. *FEBS Lett.* 355: 117- 120.
- Fukusumi S, Kitada C, Takekawa S, Kizawa H, Sakamoto J, Miyamoto M, Hinuma S, Kitano K, Fujino M (1997). Identification and characterization of a novel human cortistatin-like peptide. *Biochem. Biophys. Res. Comm.* 232: 157 -163.
- Gilman AG (1987). G-proteins: transducers of receptor-generated signals. *Annu. Rev. Biochem.* 56: 615- 649.
- Goodman R, Jacobs J, Chin W, Lund P, Dee P, Habener J (1980). Nucleotide sequence of a cloned structural gene coding for a precursor of pancreatic somatostatin. *Proc. Natl. Acad. Sci. USA* 77: 5869- 5873.
- Grimaldi M, Florio T, Schettini G (1997). Somatostatin inhibits interleukin 6 release from rat cortical type I astrocytes via the inhibition of adenylyl cyclase. *Biochem. Biophys. Res. Commun.* 235: 242- 248.
- Gu YZ, Brown PJ, Loose-Mitchell DS, Stork PJS, Schonbrunn A (1995). Development and use of a receptor antibody to characterise the interaction between somatostatin receptor subtype 1 and G proteins. *Mol. Pharmacol.* 48: 1004- 1014.
- Guibbolini ME, Lahlou B (1992). G<sub>i</sub> protein mediates adenylyl cyclase inhibition by neurohypophyseal hormones in fish gill. *Peptides* 13: 865- 871.
- Gutkind JS (1998). The pathways connecting G protein-coupled receptors to the nucleus through divergent mitogen-activated protein kinase cascades. *J. Biol. Chem.* 273: 1839- 1842.



- Hall RA, Premont RT, Chow CW, Blitzer JT, Pitcher JA, Claing A, Stoffel RH, Barak LS, Shenolikar S, Weinman E, Grinstein S, Lefkowitz RJ (1998). The  $\beta_2$ -adrenergic receptor interacts with the  $\text{Na}^+/\text{H}^+$ -exchanger regulatory factor to control  $\text{Na}^+/\text{H}^+$  exchange. *Nature* 392: 626- 630.
- Hamm HE (1998). The many faces of G protein signaling. *J. Biol. Chem.* 273: 669- 672.
- Händel M, Schulz S, Stanarius A, Schreff M, Erdtmann-Vourliotis M, Schmidt H, Wolf G, Höllt V (1999). Selective targeting of somatostatin receptor sst<sub>3</sub> to neuronal cilia. *Neuroscience* 89: 909- 926.
- Hartig PR, Hoyer D, Humphrey PPA, Martin GR (1996). Alignment of receptor nomenclature with the human genome: effects on classification of 5-HT<sub>1B</sub> and 5-HT<sub>1D</sub> receptor subtypes. *Trends Pharmacol. Sci.* 17: 103- 105.
- Hartmann D, Fehr S, Meyerhof W, Richter D (1995). Distribution of somatostatin receptor subtype 1 mRNA in the developing cerebral hemispheres of the rat. *Dev. Neurosci.* 17: 246- 255.
- Hastrup H, Schwartz TW (1996). Septide and neurokinin A are high-affinity ligands on the NK-1 receptor evidence from homologous versus heterologous binding analysis. *FEBS Lett.* 399: 264- 266.
- Hebert TE, Moffett S, Morello JP, Loisel TP, Bichet DG, Barret C, Bouvier M (1996). A peptide derived from a  $\beta_2$ -adrenergic receptor transmembrane domain inhibits both receptor dimerization and activation. *J. Biol. Chem.* 271: 16384- 16392.
- Helboe L, Stidsen CE, Moller M (1998). Immunohistochemical and cytochemical localization of the somatostatin receptor subtype sst<sub>1</sub> in the somatostatinergic parvocellular neuronal system of the rat hypothalamus. *J. Neurosci.* 18: 4938- 4945.
- Helms LM, Grau EG, Borski RJ (1991). Effects of osmotic pressure and somatostatin on the cAMP messenger system of the osmosensitive prolactin cell of a teleost fish, the tilapia (*Oreochromis mossambicus*). *Gen. Comp. Endocrinol.* 83: 111- 117.
- Hervieu G, Emson PC (1998). The localization of somatostatin receptor 1 (sst<sub>1</sub>) immunoreactivity in the rat brain using an N-terminal specific antibody. *Neuroscience* 85: 1263- 1284.
- Heximer SP, Watson N, Linder ME, Blumer KJ, Hepler JR (1997). RGS2/G0S8 is a selective inhibitor of G<sub>q</sub> $\alpha$  function. *Proc. Natl. Acad. Sci. USA* 94: 14389- 14393.
- Higuchi R (1990). Recombinant PCR. In "PCR Protocols: A Guide to Methods and Applications" (M. A. Innis, D. H. Gelfand, J. J. Sninsky and T. J. White, Eds.), Academic Press, San Diego., pp. 177-183.
- Hipkin RW, Friedman J, Clark RB, Eppler CM, Schonbrunn A (1997). Agonist-induced desensitization, internalization, and phosphorylation of the sst<sub>2A</sub> somatostatin receptor. *J. Biol. Chem.* 272: 13869- 13876.

- Hjorth SA, Thirstrup K, Schwartz TW (1996). Radioligand-dependent discrepancy in agonist affinities enhanced by mutations in the  $\kappa$ -opioid receptor. *Mol. Pharmacol.* 50: 977-984.
- Hobart P, Crawford R, Shen LP, Pictet R, Rutter W (1980). Cloning and sequence analysis of cDNAs encoding two distinct somatostatin precursors found in the endocrine pancreas of anglerfish. *Nature* 288: 137-141.
- Horstman D, Brandon S, Wilson A, Guyer C, Cragoe E, Limbird L (1990). An aspartate conserved among G-protein receptors confers allosteric regulation of  $\alpha_2$ -adrenergic receptors by sodium. *J. Biol. Chem.* 265: 21590-21595.
- Hou C, Gilbert RL, Barber DL (1994). Subtype-specific signalling mechanisms of somatostatin receptors SSTR1 and SSTR2. *J. Biol. Chem.* 269: 10357-10362.
- Hoyer D, Bell GI, Berelowitz M, Epelbaum J, Feniuk W, Humphrey PPA, O'Carroll AM, Patel YC, Schonbrunn A, Taylor JE, Reisine T (1995a). Classification and nomenclature of somatostatin receptors. *Trends Pharmacol. Sci.* 16: 86-88.
- Hoyer D, Clarke DE, Fozard JR, Hartig PR, Martin GR, Mylecharane EJ, Saxena PR, Humphrey PPA (1994a). International Union of Pharmacology classification of receptors for 5-hydroxytryptamine (Serotonin). *Pharmacological Reviews* 46: 157-204.
- Hoyer D, Lübbert H, Bruns C (1994b). Molecular pharmacology of somatostatin receptors. *Naunyn Schmiedeberg's Arch. Pharmacol.* 350: 441-453.
- Hoyer D, Perez J, Schoeffter P, Langenegger D, Schüpbach E, Kaupmann K, Lübbert H, Bruns C, Reubi JC (1995b). Pharmacological identity between somatostatin SS-2 binding sites and SSTR-1 receptors. *Eur. J. Pharmacol.* 289: 151-161.
- Hunyady B, Hipkin RW, Schonbrunn A, Mezey E (1997). Immunohistochemical localization of somatostatin receptor SST2A in the rat pancreas. *Endocrinology* 138: 2632-2635.
- Ikeda S, Schonfield G (1989). Somatostatin blocks  $Ca^{++}$  current in rat sympathetic ganglion neurons. *J. Physiol.* 409: 221-240.
- Innis MA, Gelfand DH, Sninsky JJ, White TJ, Eds. (1990). "PCR Protocols: A Guide to Methods and Applications." Academic Press, San Diego.
- Jakobs K, Aktories K, Schultz G (1983). A nucleotide regulatory site for somatostatin inhibition of adenylyl cyclase in S49 lymphoma cells. *Nature* 303: 177-178.
- Johansson O, Hökfelt T, Elde RP (1984). Immunohistochemical distribution of somatostatin-like immunoreactivity in the central nervous system of the adult rat. *Neuroscience* 13: 265-339.
- Jones TL, Simonds WF, Merendino JJ, Brann MR, Spiegel AM (1990). Myristoylation of an inhibitory GTP-binding protein alpha subunit is essential for its membrane attachment. *Proc. Natl. Acad. Sci. USA* 87: 568-572.

- Kagimoto S, Yamada Y, Kubota A, Someya Y, Ihara Y, Yasuda K, Kozasa T, Imura H, Seino S, Seino Y (1994). Human somatostatin receptor, SSTR2, is coupled to adenylyl cyclase in the presence of G<sub>i</sub> alpha 1 protein. *Biochem. Biophys. Res. Commun.* 202: 1188-1195.
- Kaupmann K, Bruns C, Hoyer D, Seuwen K, Lübbert H (1993). Distribution and second messenger coupling of four somatostatin receptor subtypes expressed in brain. *FEBS Lett.* 331: 53- 59.
- Kaupmann K, Bruns C, Raulf F, Weber HP, Mattes H, Lübbert H (1995). Two amino acids, located in transmembrane domains VI and VII, determine the selectivity of the peptide agonist SMS 201-995 for the SSTR2 somatostatin receptor. *EMBO J.* 14: 727- 735.
- Kaupmann K, Malitschek B, Schuler V, Heid J, Froestl W, Beck P, Mosbacher J, Bischoff S, Kulik A, Shigemoto R, Karschin A, Bettler B (1998). GABA<sub>B</sub>-receptor subtypes assemble into functional heteromeric complexes. *Nature* 396: 683- 687.
- Kemp BE, Pearson RB (1990). Protein kinase recognition sequence motifs. *Trends Biochem. Sci.* 15: 342- 346.
- Kennelly PJ, Krebs EG (1991). Consensus sequences as substrate specificity determinants for protein kinases and protein phosphatases. *J. Biol. Chem.* 266: 15555- 15558.
- Kleuss C, Hescheler J, Ewel C, Rosenthal W, Schultz G, Wittig B (1991). Assignment of G-protein subtypes to specific receptors inducing inhibition of calcium currents. *Nature* 353: 43- 48.
- Kluxen FW, Bruns C, Luebbert H (1992). Expression cloning of a rat brain somatostatin receptor cDNA. *Proc. Natl. Acad. Sci. USA* 89: 4618- 4622.
- Kobilka BK, Kobilka TS, Daniel K, Regan JW, Caron MG, Lefkowitz RJ (1988). Chimeric  $\alpha_2$ - $\beta_2$ -adrenergic receptors: delineation of domains involved in effector coupling and ligand binding specificity. *Science* 240: 1310- 1316.
- Koch B, Schonbrunn A (1984). The somatostatin receptor is directly coupled to adenylyl cyclase in GH<sub>4</sub>C<sub>1</sub> pituitary cell membranes. *Endocrinology* 114: 1784- 1790.
- Komatsuzaki K, Murayama Y, Giambarella U, Ogata E, Seino S, Nishimoto I (1997). A novel system that reports the G-proteins linked to a given receptor: a study of type 3 somatostatin receptor. *FEBS Lett.* 406: 165- 170.
- Kong H, Raynor K, Yasuda K, Bell GI, Reisine T (1993). Mutation of aspartate residue 79 in the SRIF receptor subtype SSTR2 prevents Na<sup>+</sup> regulation of agonist binding, but does not affect apparent receptor/ G-protein association. *Mol. Pharmacol.* 44: 380- 384.
- Kornfeld R, Kornfeld S (1985). Assembly of asparagine-linked oligosaccharides. *Annu. Rev. Biochem.* 54: 631- 664.
- Kraenzlin ME, Wood SM, Nenfeld M, Adrian TE, Bloom SR (1985). Effect of long-acting somatostatin analogue SMS 201-995, on gut hormone secretion in normal subjects. *Experientia* 41: 738- 740.

- Krenning EP, Kooij PPM, Bakker WH, Breeman WAP, Postema PTE, Kwekkeboom DJ, Oei HY, De Jong M, Visser TJ, Reijs AEM, Lamberts SWJ (1994). Radiotherapy with a radiolabelled somatostatin analogue, [ $^{111}\text{In}$ -DPTA-D-Phe1]-octreotide. *Ann. New York Acad. Sci.* 733: 496- 506.
- Krenning EP, Kwekkeboom DJ, Pauwels S, Kvols LK, Reubi JC (1995). Somatostatin receptor scintigraphy, in: *Nucl. Med. Ann.* (L.M. Freeman ed.), pp. 1-50. Raven Press, New York.
- Krulich L, Dhariwal APS, McCann SM (1968). Stimulatory and inhibitory effects of purified hypothalamic extracts on growth hormone release from rat pituitary in vitro. *Endocrinology* 83: 787- 790.
- Krumins AM, Barber R (1997). The stability of the agonist  $\beta_2$ -adrenergic receptor- $G_s$  complex: evidence for agonist-specific states. *Mol. Pharmacol.* 52: 144- 154.
- Kubota A, Yamada Y, Kagimoto S, Shimatsu A, Imamura M, Tsuda K, Imura H, Seino S, Seino Y (1994a). Identification of somatostatin receptor subtypes and an implication for the efficacy of somatostatin analogue SMS 201-955 in treatment of human endocrine tumours. *J. Clin. Invest.* 93: 1321- 1325.
- Kubota A, Yamada Y, Kagimoto S, Yasuda K, Someya Y, Ihara Y, Okamoto Y, Kozasa T, Seino S, Seino Y (1994b). Multiple effector coupling of somatostatin receptor subtype SSTR1. *Biochem. Biophys. Res. Commun.* 204: 176- 186.
- Lamberts SW, De Herder WW, Van Koetsveld PM, Koper JW, Van der Lely AJ, Visser-Wisselaar HA, Hofland LJ (1995). Somatostatin receptors: clinical implications for endocrinology and oncology. *Ciba Found. Symp.* 190: 222- 236.
- Lamberts SW, Koper JW, Reubi JC (1987). Potential role of somatostatin analogues in the treatment of cancer. *Eur. J. Clin. Invest.* 17: 281- 287.
- Lamberts SW, Krenning EP, Reubi JC (1991). The role of somatostatin and its analogs in the diagnosis and treatment of tumors. *Endocrine Rev.* 12: 450- 482.
- Lancranjan I, Bruns C, Grass P, Jaquet P, Jevell J, Kendall-Taylor P, Lamberts SWJ, Marbach P, Orskov H, Pagani G, Sheppard M, Simionescu L (1996). Sandostatin LAR: A promising therapeutic tool in the management of acromegalic patients. *Metabolism* 45: 67-71.
- Lanneau C, Bluet-Pajot MT, Zizzari P, Hoyer D, Kordon C, Pellegrini E, Tannenbaum GS, Epelbaum J, Gardette R (1999). Involvement of the sst $_1$  somatostatin receptor subtype in the intrahypothalamic neuronal network regulating growth hormone secretion: an in vitro and in vivo antisense study. *Cell. Mol. Neurosci.*, in press.
- Lauder H, Sellers LA, Fan TPD, Feniuk W, Humphrey PPA (1997). Somatostatin sst $_5$  inhibition of receptor mediated regeneration of rat aortic vascular smooth muscle cells. *Br. J. Pharmacol.* 122: 663- 670.
- Law SF, Manning D, Reisine T (1991). Identification of the subunits of GTP-binding proteins coupled to somatostatin receptors. *J. Biol. Chem.* 266: 17885- 17897.

- Law SF, Yasuda K, Bell GI, Reisine T (1993). G<sub>i</sub> alpha 3 and G(o) alpha selectively associate with the cloned somatostatin receptor subtype SSTR2. *J. Biol. Chem.* 268: 1021- 10727.
- Law SF, Zaina S, Sweet R, Yasuda K, Bell GI, Stadel J, Reisine T (1994). G<sub>i</sub> alpha 1 selectively couples somatostatin receptor subtype 3 to adenylyl cyclase: identification of the functional domains of this alpha subunit necessary for mediating the inhibition by somatostatin of cAMP formation. *Mol. Pharmacol.* 45: 587- 590.
- Leff P, Scaramellini C, (1998). Promiscuity, pre-coupling and instability. *Trends Pharmacol. Sci.* 19: 13.
- Leff P, Scaramellini C, Law C, McKechnie K (1997). A three-state receptor model of agonist action. *Trends Pharmacol. Sci.* 18: 355- 362.
- Lefkowitz RJ, Cotecchia S, Samana P, Costa T (1993). Constitutive activity of receptors coupled to guanine nucleotide regulatory proteins. *Trends Pharmacol. Sci.* 14: 303- 307.
- Le Romancer M, Cherifi Y, Levasseur S, Laigneau JP, Peranzi G, Jais P, Lewin MJ, Reyl DF (1996). Messenger RNA expression of somatostatin receptor subtypes in human and rat gastric mucosae. *Life Sci.* 58: 1091-1098.
- Li XJ, Forte M, North RA, Ross CA, Snyder SH (1992). Cloning and expression of a rat somatostatin receptor enriched in brain. *J. Biol. Chem.* 267: 21307- 21312.
- Liapakis G, Fitzpatrick D, Hoeger C, Rivier J, Vandlen R, Reisine T (1996). Identification of ligand binding determinants in the somatostatin receptor subtypes 1 and 2. *J. Biol. Chem.* 271: 20331-20339.
- Libert F, Parmentier M, Lefort A, Dinsart C, Van Sande J, Maenhaut C, Simons MJ, Dumont J E, Vassart G (1989). Selective amplification and cloning of four new members of the G protein-coupled receptor family. *Science* 244: 569- 572.
- Liu YF, Jakobs KH, Rasenick MM, Albert PR (1994). G protein specificity in receptor-effector coupling. Analysis of the roles of G<sub>O</sub> and G<sub>i2</sub> in GH4C1 pituitary cells. *J. Biol. Chem.* 269: 13880- 13886.
- Lopez F, Esteve JP, Buscail L, Delesque N, Saint-Laurent N, Theveniau M, Nahmias C, Vaysse N, Susini C (1997). The tyrosine phosphatase SHP-1 associates with the sst<sub>2</sub> somatostatin receptor and is an essential component of sst<sub>2</sub>-mediated inhibitory growth signaling. *J. Biol. Chem.* 272: 24448- 24454.
- Lorenzen A, Fuss M, Vogt H, Schwabe U (1993). Measurement of guanine nucleotide-binding protein activation by A<sub>1</sub> adenosine receptor agonists in bovine brain membranes: stimulation of guanosine-5'-O-(3-[<sup>35</sup>S]thio)triphosphate binding. *Mol. Pharmacol.* 44: 115- 123.
- Lublin AL, Diehl NL, Hochgeschwender U (1997). Isolation and characterization of the gene encoding the type 5 mouse (*Mus musculus*) somatostatin receptor (msst<sub>5</sub>). *Gene* 195: 63-66.

- Magazin M, Minth CD, Funckes CL, Deschenes R, Tavianini MA, Dixon JE (1982). Sequence of a cDNA encoding pancreatic preprosomatostatin-22. *Proc. Natl. Acad. Sci. USA* 79: 5152- 5156.
- Mandarino L, Stenner D, Blanchard W, Nissen S, Gerich J, Ling N, Brazeau P, Bulhem P, Esch F, Guillemin R (1981). Selective effects of somatostatin-14, -25 and -28 on in vitro insulin and glucagon secretion. *Nature* 291: 76- 77.
- Martin JL, Chesselet MF, Raynor K, Gonzales C, Reisine T (1991). Differential distribution of somatostatin receptor subtypes in rat brain revealed by newly developed somatostatin analogs. *Neuroscience* 41: 581- 593.
- Martinez V, Curi AP, Torkian B, Schaeffer JM, Wilkinson HA, Walsh JH, Tache Y (1998). High basal gastric acid secretion in somatostatin receptor subtype 2 knockout mice. *Gastroenterology* 114: 1125- 1132.
- Matsumoto K, Yokogoshi Y, Fujinaka Y, Zhang C, Saito S (1994). Molecular cloning and sequencing of porcine somatostatin receptor 2. *Biochem. Biophys. Res. Commun.* 199: 298- 305.
- McLatchie LM, Fraser NJ, Main MJ, Wise A, Brown J, Thompson N, Solari R, Lee MG, Foord SM (1998). RAMPs regulate the transport and ligand-specificity of the calcitonin-receptor-like-receptor. *Nature* 393: 333- 339.
- Meriney SD, Gray DB, Pilar R (1994). Somatostatin-induced inhibition of neuronal  $Ca^{2+}$  current modulated by cGMP-dependent protein kinase. *Nature* 369: 336- 339.
- Meyer zu Heringdorf D, Lass H, Alemany R, Laser KT, Neumann E, Zhang C, Schmidt M, Rauen U, Jakobs KH, Van Koppen CJ (1998). Sphingosine kinase-mediated  $Ca^{2+}$  signalling by G-protein-coupled receptors. *EMBO J.* 17: 2830- 2837.
- Meyerhof W (1998). The elucidation of somatostatin receptor functions: a current view. *Rev. Physiol. Biochem. Pharmacol.* 133: 55- 108.
- Meyerhof W, Wulfsen I, Schoenrock C, Fehr S, Richter D (1992). Molecular cloning of a somatostatin-28 receptor and comparison of its expression pattern with that of a somatostatin-14 receptor in rat brain. *Proc. Natl. Acad. Sci. USA* 89: 10267- 10271.
- Mikoshiha K (1997). The  $InsP_3$  receptor and intracellular  $Ca^{2+}$  signalling. *Curr. Opin. Neurobiol.* 7: 339- 345.
- Monté M, Fanning M, Sutherland L, Broadhead M, Harris A (1989). A pilot study of Sandostatin (SMS 201-995) in the treatment of immunodeficiency-related diarrhoea. Int. Symposium on Somatostatin, Montreal, August 1989, Abstract NV.
- Mumby SM, Heukeroth RO, Gordon JI, Gilman AG (1990). G-protein alpha-subunit expression, myristoylation, and membrane association in COS cells. *Proc. Natl. Acad. Sci. USA* 87: 728- 732.
- Murthy KS, Coy DH, Makhlof GM (1996). Somatostatin receptor-mediated signalling in smooth muscle. Activation of phospholipase C-beta3 by G beta gamma and inhibition of adenylyl cyclase by G alpha<sub>11</sub> and G alpha<sub>o</sub>. *J. Biol. Chem.* 271: 23458- 23463.

- Nehring RB, Meyerhof W, Richter D (1995). Aspartic acid residue 124 in the third transmembrane domain of the somatostatin receptor subtype 3 is essential for somatostatin-14 binding. *DNA Cell. Biol.* 14: 939- 944.
- Nemeroff CB, Youngblood WW, Manberg PJ, Prange AJ, Kizer JS (1983). Regional brain concentration of neuropeptides in Huntington's chorea and schizophrenia. *Science* 221: 972- 975.
- Nishi M, Movérus B, Bukovskaya OS, Takahashi A, Kawauchi H (1995). Isolation and characterization of [pro<sup>2</sup>]somatostatin-14 and melanotropins from Russian sturgeon, *Acipenser gueldenstaedti* Brandt. *Gen. Comp. Endocrinol.* 99: 6- 12.
- Noe BD, Spiess J, Rivier JE, Vale W (1979). Isolation and characterization of somatostatin from anglerfish pancreatic islet. *Endocrinology* 105: 1410- 1415.
- O'Carroll AM, Lolait SJ, Koenig M, Mahan LC (1992). Molecular cloning and expression of a pituitary somatostatin receptor with preferential affinity for somatostatin-28. *Mol. Pharmacol.* 42: 939- 946.
- O'Carroll AM, Raynor K, Lolait SJ, Reisine T (1994). Characterization of cloned human somatostatin receptor SSTR5. *Mol. Pharmacol.* 63: 127- 133.
- Ochman H, Gerber AS, Hartl DL (1988). Genetic applications of an inverse polymerase chain reaction. *Genetics* 120: 621- 623.
- Ochman H, Medhora MM, Garza D, Hartl DL (1990). Amplification of flanking sequences by inverse PCR. In "PCR Protocols: A Guide to Methods and Applications" (M. A. Innis, D. H. Gelfand, J. J. Sninsky and T. J. White, Eds.), pp. 219- 227. Academic Press, San Diego.
- Okamoto T, Nishimoto I (1992). Detection of G protein-activator regions in M<sub>4</sub> subtype muscarinic, cholinergic, and  $\beta_2$ -adrenergic receptors based upon characteristics in primary structure. *J. Biol. Chem.* 267: 8342- 8346.
- Ozenberger BA, Hadcock JR (1995). A single amino acid substitution in somatostatin receptor subtype 5 increases affinity for somatostatin-14. *Mol. Pharmacol.* 47: 822- 827.
- Panetta R, Greenwood MT, Warszynska A, Demchyshyn LL, Day R, Niznik HB, Srikant CB, Patel YC (1994). Molecular cloning, functional characterization and chromosomal localization of a human somatostatin receptor (somatostatin receptor type 5) with preferential affinity for somatostatin 28. *Mol. Pharmacol.* 45: 417- 427.
- Patel YC (1997). Molecular pharmacology of somatostatin receptor subtypes. *J. Endocrinol. Invest.* 20: 348- 367.
- Patel YC, Greenwood MT, Panetta R, Demchyshyn L, Niznik H, Srikant CB (1995). The somatostatin receptor family. *Life Sci.* 57: 1249- 1265.
- Patel YC, Greenwood M, Panetta R, Hukovic N, Grigorakis S, Robertson LA, Srikant CB (1996). Molecular biology of somatostatin receptor subtypes. *Metabolism* 45: 31- 38.

- Patel YC, Greenwood MT, Warszynska A, Panetta R, Srikant CB (1994). All five cloned human somatostatin receptors (hSSTR1-5) are functionally coupled to adenylyl cyclase. *Biochem. Biophys. Res. Comm.* 198: 605- 612.
- Patel YC, Srikant CB (1994). Subtype selectivity of peptide analogues for all five cloned human somatostatin receptors (hsstr 1-5). *Endocrinology* 135: 2814- 2817.
- Patel YC, Wheatley T, Ning C (1981). Multiple forms of immunoreactive somatostatin: comparison of distribution in neural and non-neural tissues and portal plasma of the rat. *Endocrinology* 109: 1943- 1949.
- Patel YC, Zingg HH, Srikant CB (1985). Somatostatin 14 like immunoreactive forms in the rat: characterization, distribution and biosynthesis. In: Patel, Y.C., Tannenbaum, G.S. (eds) *Advances in experimental biology and medicine*, vol 188: *Somatostatin*, New York, pp. 71- 87.
- Pérez J, Hoyer D (1995). Co-expression of somatostatin SSTR-3 and SSTR-4 receptor messenger RNAs in the rat brain. *Neuroscience* 64: 241- 253.
- Piwko C, Thoss VS, Probst A, Hoyer D (1997). Somatostatin receptors in the human brain: radioligand binding. *Naunyn Schmiedeberg's Arch. Pharmacol.* 355: 161- 167.
- Plisetskaya EM, Pollock HG, Rouse JB, Hamilton JW, Kimmel JR, Andrews PC, Gorbman A (1986). Characterization of coho salmon (*Oncorhynchus kisutch*) islet somatostatins. *Gen. Comp. Endocrinol.* 63: 252- 263.
- Pradayrol L, Jornvall H, Mutt V, Ribet A (1980). N-terminally extended somatostatin 28. *FEBS Lett.* 109: 55- 58.
- Prinz C, Sachs G, Walsh JH, Coy DH, Wu SV (1994). The somatostatin receptor subtype on rat enterochromaffin-like cells. *Gastroenterology* 107: 1067- 1074.
- Probst WC, Snyder LA, Schuster DI, Brosius J, Sealton SC (1992). Sequence alignment of the G-protein coupled receptor superfamily. *DNA Cell Biol.* 11: 1- 20.
- Raulf F, Pérez J, Hoyer D, Bruns C (1994). Differential expression of five somatostatin receptor subtypes, SSTR1-5, in the CNS and peripheral tissue. *Digestion* 55: 46- 53.
- Raynor K, Coy DC, Reisine T (1992). Analogues of somatostatin bind selectively to brain somatostatin receptor subtypes. *J. Neurochem.* 59: 1241- 1250.
- Raynor K, Murphy WA, Coy DH, Taylor JE, Moreau JP, Yasuda K, Bell GI, Reisine T (1993a). Cloned Somatostatin Receptors: Identification of subtype-selective peptides and demonstration of high affinity binding of linear peptides. *Mol. Pharmacol.* 43: 838- 844.
- Raynor K, O'Carroll AM, Kong H, Yasuda K, Mahan LC, Bell GI, Reisine T (1993b). Characterization of cloned somatostatin receptors SSTR4 and SSTR5. *Mol. Pharmacol.* 44: 385- 392.
- Raynor K, Reisine T (1989). Analogs of somatostatin selectively label distinct subtypes of somatostatin receptors in rat brain. *J. Pharmacol. Exp. Ther.* 251: 510- 517.



- Raynor K, Reisine T (1992). Differential coupling of somatostatin1 receptors to adenylyl cyclase in the rat striatum vs. the pituitary and other regions of the rat brain. *J. Pharmacol. Exp. Ther.* 260: 841- 848.
- Reardon DB, Dent P, Wood SL, Kong T, Sturgill TW (1997). Activation in vitro of somatostatin receptor subtypes 2, 3, or 4 stimulates protein tyrosine phosphatase activity in membranes from transfected Ras-transformed NIH 3T3 cells: coexpression with catalytically inactive SHP-2 blocks responsiveness. *Mol. Endocrinol.* 11: 1062-1069.
- Reardon DB, Wood SL, Brautigam DL, Bell GI, Dent P, Sturgill TW (1996). Activation of a protein tyrosine phosphatase and inactivation of Raf-1 by somatostatin. *Biochem. J.* 314: 401- 404.
- Rebois RV, Warner DR, Basi NS (1997). Does subunit dissociation necessarily accompany the activation of all heterotrimeric G proteins? *Cell. Signal.* 9: 141- 151.
- Reichlin S (1983). Somatostatin. *N. Engl. J. Med.* 309: 1495- 1505, 1556- 1563.
- Reisine T, Bell GI (1995). Molecular properties of somatostatin receptors. *Neuroscience* 67: 777- 790.
- Reisine T, Heerding J, Raynor K (1994). The third intracellular loop of the delta receptor is necessary for coupling to adenylyl cyclase and receptor desensitization. *Regul. Pept.* 54: 241- 242.
- Reisine T, Woulfe D, Raynor K, Kong H, Heerding J, Hines J, Tallent M, Law S (1995). Interaction of somatostatin receptors with G proteins and cellular effector systems. In: Somatostatin and its receptors. *Ciba Found. Symp.* 190: 160- 170.
- Reisine T, Zhang YL, Sekura R (1985). Pertussis toxin treatment blocks the inhibition of somatostatin and increases the stimulation by forskolin of cyclic AMP accumulation and adrenocorticotropin secretion from mouse anterior pituitary tumour cells. *J. Pharmacol. Exp. Ther.* 232: 275- 282.
- Remmers AE, Neubig RR (1996). Partial G protein activation by fluorescent guanine nucleotide analogues. Evidence for a triphosphate-bound but inactive state. *J. Biol. Chem.* 271: 4791- 4797.
- Rens-Domiano S, Reisine T (1991). Structural analysis and functional role of the carbohydrate component of somatostatin receptors. *J. Biol. Chem.* 266: 20094- 20102.
- Rens-Dominano S, Reisine T (1992). Biochemical and functional properties of somatostatin receptors. *J. Neurochem.* 58: 1987- 1996.
- Reubi JC, Kappeler A, Waser B, Laissue J, Hipkin RW, Schonbrunn A (1998). Immunohistochemical localization of somatostatin receptors sst<sub>2A</sub> in human tumors. *Am. J. Pathol.* 153: 233- 245.
- Reubi JC (1985). New specific radioligand for one subpopulation of brain somatostatin receptors. *Life Sci.* 36: 1829- 1836.
- Reubi JC (1984). Evidence for two somatostatin-14 receptor types in rat brain cortex. *Neurosci. Lett.* 49: 259- 263.

- Reubi JC, Kvols L, Krenning EP, Lamberts SWJ (1990a). Distribution of somatostatin receptors in normal and tumor tissue. *Metabolism* 39: 78- 81.
- Reubi JC, Kvols L, Waser B, Nagorney DM, Heitz PU, Charborneau JW, Reading CC, Moertel C (1990b). Detection of somatostatin receptors in surgical and percutaneous needle biopsy samples of carcinoids and islets cell carcinomas. *Cancer Res.* 50: 5969- 5977.
- Reubi JC, Laissue JA, Waser B, Steffen DL, Hipkin RW, Schonbrunn A (1999). Immunohistochemical detection of somatostatin sst<sub>2A</sub> receptors in the lymphatic, smooth muscular and peripheral nervous systems of the human gastrointestinal tract: facts and artefacts. *J. Clin. Endocrinol. Metab.*, in press.
- Reubi JC, Landolt AM (1984). High density of somatostatin receptors in pituitary tumours from acromegalic patients. *J. Clin. Endocrinol. Metab.* 59: 1148- 1153.
- Reubi JC, Lang W, Maurer R, Koper JW, Lamberts SWJ (1987). Distribution and biochemical characterization of somatostatin receptors in tumours of the human central nervous system. *Cancer Res.* 47: 5758- 5765.
- Reubi JC, Maurer R (1986). Different ionic requirements for somatostatin receptor subpopulations in the brain. *Reg. Peptides* 14: 301- 311.
- Riekkinen PJ, Pitkänen A (1990). Somatostatin and epilepsy. *Metabolism* 39: 112- 115.
- Robbins RJ, Reichlin S (1983). Somatostatin biosynthesis by cerebral cortical cells in monolayer culture. *Endocrinology* 113: 574- 581.
- Rodriguez ME, Alvaro AI, Bodega G, Arilla E (1997). The somatostatin receptor-adenylate cyclase system in rat pancreatic acinar membranes after temporary pancreaticobiliary duct ligation. *Life Sci.* 61: 2255- 2269.
- Rohrer L, Raulf F, Bruns C, Buettner R, Hofstaedter F, Schuele R (1993). Cloning and characterization of a fourth somatostatin receptor. *Proc. Natl. Acad. Sci. USA* 90: 4196- 4200.
- Romano C, Yang WL, O'Malley KL (1996). Metabotropic glutamate receptor 5 is a disulfide-linked dimer. *J. Biol. Chem.* 271: 28612- 28616.
- Roth A, Kreienkamp HJ, Meyerhof W, Richter D (1997). Phosphorylation of four amino acid residues in the carboxyl terminus of the rat somatostatin receptor subtype 3 is crucial for its desensitization and internalization. *J. Biol. Chem.* 272: 23769- 23774.
- Rosenthal W, Hescheler J, Hinsch KD, Spicher K, Trautwein W, Schultz G (1988). Cyclic AMP-independent, dual regulation of voltage-dependent Ca<sup>++</sup> currents by LHRH and somatostatin in a pituitary cell line. *EMBO J.* 7: 1627- 1633.
- Rossowski WJ, Coy DH (1994). Specific inhibition of rat pancreatic insulin or glucagon release by receptor-selective somatostatin analogues. *Biochem. Biophys. Res. Commun.* 206: 341- 346.
- Roush W (1996). Regulating G protein signalling. *Science* 271: 1056- 1058.

- Roy C (1984). Inhibition by somatostatin of the vasopressin-stimulated adenylate cyclase in a kidney-derived line of cells grown in defined medium. *FEBS Lett.* 169: 133- 137.
- Saiki RK, Scharf S, Faloona F, Mullis KB, Horn GT, Erlich HA, Arnheim N (1985). Enzymatic amplification of  $\beta$ -globin genomic sequences and restriction site analysis for diagnosis of sickle cell anemia. *Science* 230: 1350- 1354.
- Samama P, Cotecchia S, Costa T, Lefkowitz RJ (1993). A mutation induced an activated state of the  $\beta_2$ -adrenergic receptor. Extending the ternary complex model. *J. Biol. Chem.* 268: 4625- 4636.
- Sambrook J, Fritsch EF, Maniatis T (1989). "Molecular Cloning: A Laboratory Manual", Cold Spring Harbor Laboratory, Cold Spring Harbor, N.Y.
- Sarret P, Beaudet A, Vincent JP, Mazella J (1998). Regional and cellular distribution of low affinity neurotensin receptor mRNA in adult and developing mouse brain. *J. Comp. Neurol.* 394: 344- 356.
- Sas E, Maler L (1991). Somatostatin-like immunoreactivity in the brain of an electric fish (*Apteronotis leptorhynchus*) identified with monoclonal antibodies. *J. Chem. Neuroanat.* 4: 155- 186.
- Scaramellini, C, Leff, P (1998). A three-state receptor model: predictions of multiple agonist pharmacology for the same receptor type. *Ann. N. Y. Acad. Sci.* 861(Advances in Serotonin Receptor Research): 97- 103.
- Schally AV (1988). Oncological applications of somatostatin analogues. *Cancer Res.* 48: 6977- 6985.
- Schindler M, Holloway S, Humphrey PPA, Waldvogel H, Faull RL, Berger W, Emson PC (1998a). Localization of somatostatin sst2(A) receptor in human cerebral cortex, hippocampus and cerebellum. *Neuroreport* 16: 521- 525.
- Schindler M, Humphrey PPA, Emson PC (1996). Somatostatin receptors in the central nervous system. *Progr. Neurobiol.* 50: 39-47.
- Schindler M, Kidd EJ, Carruthers AM, Wyatt MA, Jarvie EM, Sellers LA, Feniuk W, Humphrey PPA (1998b). Molecular cloning and functional characterization of a rat somatostatin sst2(B) receptor splice variant. *Br. J. Pharmacol.* 125: 209- 217.
- Schindler M, Sellers LA, Humphrey PPA (1997). Immunohistochemical localization of the somatostatin SST2(A) receptor in the rat brain and spinal cord. *Neuroscience* 76: 225- 240.
- Schloos J, Raulf F, Hoyer D, Bruns C (1997). Identification and characterization of somatostatin receptors in rat lung. *Br. J. Pharmacol.* 121: 963- 971.

- Schoeffter P, Perez J, Langenegger D, Schüpbach E, Lübbert H, Bruns C, Hoyer D (1995). Characterization and distribution of somatostatin SS-1 and SRIF-1 binding sites in rat brain: identity with SSTR-2 receptors. *Eur. J. Pharmacol.* 289: 163- 173.
- Schulz S, Schreff M, Schmidt H, Handel M, Przewlocki R, Hoell V (1998a). Immunocytochemical localization of somatostatin receptor sst2A in the rat spinal cord and dorsal root ganglia. *Eur. J. Neurosci.* 10: 3700- 3708.
- Schulz S, Schulz S, Schmitt j, Wiborny D, Schmidt H, Olbricht S, Weise W, Roessner A, Gramsch C, Hoell V (1998b). Immunocytochemical detection of somatostatin receptors sst<sub>1</sub>, sst<sub>2A</sub>, sst<sub>2B</sub>, and sst<sub>3</sub> in paraffin-embedded breast cancer tissue using subtype-specific antibodies. *Clin. Cancer Res.* 4: 2047- 2052.
- Schwartz TW, Rosenkilde MM (1996). Is there a 'lock for all agonist 'keys' in 7TM receptors?. *Trends Pharmacol. Sci.* 17: 213- 216.
- Schweitzer R, Madamba S, Siggins GR (1990). Arachidonic acid and metabolites as mediators of somatostatin-induced increase of neuronal M-current. *Nature* 346: 464- 466.
- Seamon KB, Daly JW (1986). Forskolin: its biological and chemical properties. *Adv. Cyclic Nucleotide Res.* 20: 1- 150.
- Senogles SE (1994). The D<sub>2</sub> dopamine receptor isoforms signal through distinct G<sub>i</sub>α proteins to inhibit adenylyl cyclase: a study with site-directed mutant G<sub>i</sub>α proteins. *J. Biol. Chem.* 269: 23210- 23127.
- Sharma K, Patel YC, Srikant CB (1996). Subtype-selective induction of wild-type p53 and apoptosis, but not cell cycle arrest, by human somatostatin receptor 3. *Mol. Endocrinol.* 10: 1688- 1696.
- Shen LP, Pictet RL, Rutter WJ (1982). Human somatostatin I: sequence of the cDNA. *Proc. Natl. Acad. Sci. USA* 79: 4575- 4579.
- Shimizu T, Mori M, Bito H, Sakanaka C, Tabuchi S, Aihara M, Kume K (1996). Platelet-activating factor and somatostatin activated mitogen-activated protein kinase (MAP kinase) and arachidonate release. *J. Lipid. Mediat. Cell. Signal.* 14: 103- 108.
- Siehler S, Seuwen K, Hoyer D (1998a). [<sup>125</sup>I]Tyr<sup>10</sup>-cortistatin<sub>14</sub> labels all five somatostatin receptors. *Naunyn Schmiedeberg's Arch. Pharmacol.* 357: 483-489.
- Siehler S, Seuwen K, Hoyer D (1998b). [<sup>125</sup>I][Tyr<sup>3</sup>]octreotide labels human somatostatin sst<sub>2</sub> and sst<sub>5</sub> receptors. *Eur. J. Pharmacol.* 348: 311- 320.
- Siehler S, Zupanc GKH, Seuwen K, Hoyer D (1999). Characterisation of the fish sst<sub>3</sub> receptor, a member of the SRIF<sub>1</sub> receptor family: atypical pharmacological features. *Neuropharmacology* 38: 449- 462.
- Siehler S, Seuwen K, Hoyer D. Characterisation of human recombinant somatostatin receptors: 1) radioligand binding studies. *Naunyn Schmiedeberg's Arch. Pharmacol.*, submitted (a)
- Siehler S, Hoyer D. Characterisation of human recombinant somatostatin receptors: 2) modulation of GTPγS binding. *Naunyn Schmiedeberg's Arch. Pharmacol.*, submitted (b)

- Siehl S, Hoyer D. Characterisation of human recombinant somatostatin receptors: 3) modulation of adenylate cyclase activity. *Naunyn Schmiedeberg's Arch. Pharmacol.*, submitted (c)
- Siehl S, Hoyer D. Characterisation of human recombinant somatostatin receptors: 4) modulation of phospholipase C activity. *Naunyn Schmiedeberg's Arch. Pharmacol.*, submitted (d)
- Siehl S, Zupanc GKH, Hoyer D. Fish somatostatin sst3 receptor: comparison of radioligand and GTP $\gamma$ S binding, adenylate cyclase and phospholipase C activities reveals agonist-dependent pharmacological differences. *Neuropharmacol.*, submitted
- Simon MI, Strathmann MP, Gautam M (1991). Diversity of G-proteins in signal transduction. *Science* 252: 802- 808.
- Spiess J, Rivier JE, Rodkey JA, Bennett CD, Vale W (1979). Isolation and characterization of somatostatin from pigeon pancreas. *Proc. Natl. Acad. Sci. USA* 76: 2974- 2978.
- Srikant CB (1995). Cell cycle dependent induction of apoptosis by somatostatin analog SMS 201-995 in AtT-20 mouse pituitary cells. *Biochem. Biophys. Res. Comm.* 209: 400- 406.
- Srikant CB, Shen SH (1996). Octapeptide somatostatin analog SMS 201-995 induces translocation of intracellular PTP1C to membranes in MCF-7 human breast adenocarcinoma cells. *Endocrinology* 137: 3461- 3468.
- Srivastava RK, Van der Kraak G (1994). Effects of activators of different intracellular signaling pathways on steroid production by goldfish vitellogenic ovarian follicles. *Gen. Comp. Endocrinol.* 93: 181- 191.
- Sternweiss PC, Smrcka AV (1992). Regulation of phospholipase C by G proteins. *Trends Biochem. Sci.* 17, 502- 506.
- Stroh T, Kreienkamp HJ, Beaudet A (1998). Immunohistochemical distribution of sst5 in the adult rat brain. *Society of Neuroscience Abstract* No. 817.12, Vol. 24, p. 2044 (Meeting Abstract of the 28th annual meeting, Los Angeles, USA).
- Stroh T, Zupanc GKH (1993). Identification and localization of somatostatin-like immunoreactivity in the cerebellum of gymnotiform fish, *Apteronotus leptorhynchus*. *Neurosci. Lett.* 160: 145- 148.
- Stroh T, Zupanc GKH (1995). Somatostatin in the prepacemaker nucleus of weakly electric fish, *Apteronotus leptorhynchus*: evidence for a nonsynaptic function. *Brain Res.* 674: 1- 14.
- Stroh T, Zupanc GKH (1996). The postembryonic development of somatostatin immunoreactivity in the central posterior/prepacemaker nucleus of weakly electric fish, *Apteronotus leptorhynchus*: a double-labelling study. *Dev. Brain Res.* 93: 76- 87.
- Strosberg AD (1991). Structure/function relationship of proteins belonging to the family of receptors coupled to GTP-binding proteins. *Eur. J. Biochem.* 196: 1- 10.
- Sunahara RK, Dessauer CW, Gilman AG (1996). Complexity and diversity of mammalian adenylyl cyclases. *Annu. Rev. Pharmacol. Toxicol.* 36: 461- 480.

- Tallent M, Reisine T (1992). G<sub>i</sub> alpha 1 selectively couples somatostatin receptors to adenylyl cyclases in pituitary-derived AtT-20 cells. *Mol. Pharmacol.* 41: 452- 455.
- Taussig R, Iniguez LJA, Gilman AG (1993). Inhibition of adenylyl cyclase by G<sub>i</sub> alpha. *Science* 261: 218- 221.
- Taussig R, Tang WJ, Hepler JR, Gilman AG (1994). Distinct patterns of bidirectional regulation of mammalian adenylyl cyclases. *J. Biol. Chem.* 269: 6093- 6100.
- Taylor JE (1995). Somatostatin (SSTR2) receptors mediate phospholipase C-independent Ca<sup>2+</sup> mobilization in rat AR42J pancreas cells. *Biochem. Biophys. Res. Commun.* 214: 81- 85.
- Taylor WL, Collier KJ, Deschenes RJ, Weith HL, Dixon JE (1981). Sequence analysis of a cDNA coding for a pancreatic precursor to somatostatin. *Proc. Natl. Acad. Sci. USA* 78: 6694- 6698.
- Teitler M, Leonhardt S, Weisberg E, and Hoffman BJ (1990). 4-[<sup>125</sup>I]iodo-(2, 5-dimethoxy)-phenyliopropylamine and [<sup>3</sup>H]ketanserin labeling of 5-hydroxytryptamine<sub>2</sub> (5-HT<sub>2</sub>) receptors in mammalian cells transfected with a rat 5-HT<sub>2</sub> cDNA: evidence for multiple states and not multiple 5-HT<sub>2</sub> receptor subtypes. *Mol. Pharmacol.* 38: 594- 598.
- Tentler JJ, Hadcock JR, Gutierrez-Hartmann A (1997). Somatostatin acts by inhibiting the cyclic 3', 5'-adenosine monophosphate (cAMP)/ protein kinase A pathway, cAMP response element-binding protein (CREB) phosphorylation, and CREB transcription potency. *Mol. Endocrinol.* 11: 859- 866.
- Thoss VS, Pérez J, Duc D, Hoyer D (1995). Embryonic and postnatal mRNA distribution of the five somatostatin receptor subtypes in the rat brain. *Neuropharmacology* 34: 1673- 1688.
- Thoss VS, Pérez J, Probst A, Hoyer D (1996). Expression of five somatostatin receptor mRNAs in the human brain and pituitary. *Naunyn-Schmiedeberg's Arch. Pharmacol.* 354: 411- 419.
- Thoss VS, Piwko C, Probst A, Hoyer D (1997). Somatostatin receptors in the human brain and pituitary: an autoradiographic study. *Naunyn Schmiedeberg's Arch. Pharmacol.* 355: 168- 176.
- Todisco A, Seva C, Takeuchi Y, Dickinson CJ, Yamada T (1995). Somatostatin inhibits AP-1 function via multiple protein phosphatases. *Am. J. Physiol.* 269: G160- G166.
- Todisco A, Takeuchi Y, Yamada J, Sadoshima JI, Yamada T (1997). Molecular mechanisms for somatostatin inhibition of c-fos gene expression. *Am. J. Physiol.* 272: G721- G726.
- Tomura H, Okajima F, Akbar M, Majid MA, Sho K, Kondo Y (1994). Transfected human somatostatin receptor type 2, SSTR2, not only inhibits adenylyl cyclase but also stimulates phospholipase C and Ca<sup>2+</sup> mobilization. *Biochem. Biophys. Res. Commun.* 200: 986- 992.

- Tran V, Beal F, Martin J (1985). Two types of somatostatin receptors differentiated by cyclic somatostatin analogs. *Science* 228: 492- 495.
- Uesaka T, Yano K, Yamasaki M, Ando M (1995). Somatostatin-, vasoactive intestinal peptide-, and granulin-like peptides isolated from intestinal extracts of goldfish, *Carassius auratus*. *Gen. Comp. Endocrinol.* 99: 298- 306.
- Vanetti M, Kouba M, Wang X, Vogt G, Hoell V (1992). Cloning and expression of a novel mouse somatostatin receptor (SSTR2B). *FEBS Lett.* 311: 290- 294.
- Vanetti M, Vogt G, Hoell V (1993). The two isoforms of the mouse somatostatin receptor (mSSTR2A and mSSTR2B) differ in coupling efficiency to adenylate cyclase and in agonist-induced receptor desensitization. *FEBS Lett.* 331: 260- 266.
- Vaudry H, Chartrel N, Conlon JM (1992). Isolation of [pro<sup>2</sup>,met<sup>13</sup>]somatostatin-14 and somatostatin-14 from the frog brain reveals the existence of a somatostatin gene family in a tetrapod. *Biochem. Biophys. Res. Commun.* 188, 477- 482.
- Veber DF, Freidinger RM, Perlow DS, Paleveda WJ, Holly FW, Strachan RG, Nutt RF, Arison BH, Homnick C, Randall WC, Glitzer MS, Saperstein R, Hirschmann R (1981). A potent cyclic hexapeptide analogue of somatostatin. *Nature* 292: 55- 58.
- Viguerie N, Tahiri-Jouti N, Esteve JP, Clerc P, Logsdon C, Svoboda M, Susini C, Vaysse N, Riberet A (1988). Functional somatostatin receptors on a rat pancreatic acinar cell line. *Am. J. Physiol.* 255: G113- G120.
- Vikić-Topić S, Reisch KP, Kvěls LK, Vuk-Pavlović S (1995). Expression of somatostatin receptor subtypes in breast carcinoma, carcinoid tumor, and renal cell carcinoma. *J. Clin. Endocrinol. Metab.* 80: 2974- 2979.
- Vincent SR, McIntosh CHS, Buchan AMJ, Brown JC (1985). Central somatostatin systems revealed with monoclonal antibodies. *J. Comp. Neurol.* 238, 169- 186.
- Vornanen M (1998). L-type Ca<sup>2+</sup> current in fish cardiac myocytes: effects on the thermal acclimation and beta-adrenergic stimulation. *J. Exp. Biol.* 201: 533- 547.
- Walker MW, Smith KE, Bard J, Vaysse PJJ, Gerald C, Daouti S, Weinshank RL, Branchek TA (1997). A structure-activity analysis of the cloned rat and human Y4 receptors for pancreatic polypeptide. *Peptides* 18: 609- 612.
- Wang H, Bogen C, Reisine T, Dichter M (1989). Somatostatin-14 and somatostatin-28 induce opposite effects on potassium currents in rat neocortical neurons. *Proc. Natl. Acad. Sci USA* 86: 9616- 9620.
- Wang Y, Conlon JM (1993). Neuroendocrine peptides (NPY, GRP, VIP, somatostatin) from the brain and stomach of the alligator. *Peptides* 14: 573- 579.
- Wang H, Reisine T, Dichter M (1990). Somatostatin-14 and somatostatin-28 inhibit calcium currents in rat neocortical neurons. *Neuroscience* 38: 335- 342.

- Warhurst G, Higgs NB, Fakhoury H, Warhurst AC, Garde J, Coy DH (1996). Somatostatin receptor subtype 2 mediates somatostatin inhibition of ion secretion in rat distal colon. *Gastroenterology* 111: 325- 333.
- Weckbecker G, Raulf F, Stolz B, Bruns C (1993). Somatostatin analogs for diagnosis and treatment of cancer. *Pharmacol. Ther.* 60: 245- 264.
- West R, Moss J, Vaughan M, Liu T (1985). Pertussis toxin-catalyzed ADP-ribosylation of transducin. Cysteine 347 is the ADP ribose acceptor site. *J. Bio. Chem.* 260: 14428-14430.
- Whitford C, Candy JM, Bloxham CA, Oakley AE, Snell CR (1985). Human cerebellar cortex possesses high affinity binding sites for [<sup>3</sup>H]somatostatin. *Eur. J. Pharmacol.* 113: 129-132.
- Whitford CA, Bloxham CA, Snell CR, Candy JM, Hirst BH (1986). Regional distribution of high affinity [<sup>3</sup>H]somatostatin binding sites in the human brain. *Brain Res.* 398: 141-147.
- Whitford CA, Candy JM, Snell CR, Hirst BH, Oakley AE, Johnson M, Thompson JE (1987). Autoradiographic visualization of binding sites for [<sup>3</sup>H]somatostatin in the rat brain. *Eur. J. Pharmacol.* 138: 327- 333.
- Wilkinson GF, Feniuk W, Humphrey PPA (1997). Characterization of human recombinant somatostatin sst5 receptors mediating activation of phosphoinositide metabolism. *Br. J. Pharmacol.* 121: 91- 96.
- Wilkinson GF, Thurlow RJ, Sellers RJ, Coote LA, Feniuk W, Humphrey PPA (1996). Potent antagonism by BIM-23056 at the human recombinant somatostatin sst5 receptor. *Br. J. Pharmacol.* 118: 445- 447.
- Williams AJ, Michel AD, Feniuk W, Humphrey PPA (1997). Somatostatin<sub>5</sub> receptor-mediated [<sup>35</sup>S]guanosine-5'-O-(3-thio)triphosphate binding: agonist potencies and the influence of sodium chloride on intrinsic activity. *Mol. Pharmacol.* 51: 1060- 1069.
- Wulfsen I, Meyerhof W, Fehr S, Richter D (1993). Expression patterns of rat somatostatin receptor genes in pre- and postnatal brain and pituitary. *J. Neurochem.* 61: 1549- 1552.
- Xin WW, Wong ML, Rimland J, Nestler EJ, Duman RS (1992). Characterization and functional expression of a somatostatin receptor isolated from locus coeruleus. Gen Bank, accession no. L06613.
- Xu Y, Song J, Bruno JF, Berelowitz M (1993). Molecular cloning and sequencing of a human somatostatin receptor, hSSTR4. *Biochem. Biophys. Res. Commun.* 193: 648- 652.
- Yajima Y, Akita Y, Katada T, Saito T (1993). Somatostatin induces release of the alpha subunits of pertussis toxin-sensitive G proteins in native membranes and in intact GH<sub>4</sub>C<sub>1</sub> rat pituitary cells. *Mol. Cell. Endocrinol.* 92: 143- 152.



- Yamada Y, Kagimoto S, Kubota A, Yasuda K, Masuda K, Someya Y, Ihara Y, Li Q, Imura H, Seino S, Seino Y (1993). Cloning, functional expression and pharmacological characterization of a fourth (hSSTR4) and a fifth (hSSTR5) human somatostatin receptor subtype. *Biochem. Biophys. Res. Comm.* 195: 844- 852.
- Yamada Y, Post SR, Wang K, Tager HS, Bell GI, Seino S (1992a). Cloning and functional characterization of a family of human and mouse somatostatin receptors expressed in brain, gastrointestinal tract, and kidney. *Proc. Natl. Acad. Sci. USA* 89: 251- 255.
- Yamada Y, Reisine T, Law SF, Ihara Y, Kubota A, Kagimoto S, Seino M, Seino Y, Bell GI, Seino S (1992b). Somatostatin receptors, an expanding gene family: cloning and functional characterization of human SSTR3, a protein coupled to adenylyl cyclase. *Mol. Endocrinol.* 6: 2136- 2142.
- Yasuda K, Rens-Domiano S, Breder CD, Law SF, Saper CB, Reisine T, Bell GI (1992). Cloning of a novel somatostatin receptor, SSTR3, coupled to adenylylcyclase. *J. Biol. Chem.* 267: 20422- 20428.
- Yatani A, Codina J, Sekura R, Birnbaumer L, Brown A (1987). Reconstitution of somatostatin and muscarinic receptor mediated stimulation of K<sup>+</sup> channels by G<sub>k</sub> protein in clonal rat anterior pituitary cell membrane. *Mol. Endocrinol.* 1: 283- 293.
- Zaki M, Harrington L, McCuen R, Coy DH, Arimura A, Schubert ML (1996). Somatostatin receptor subtype 2 mediates inhibition of gastrin and histamine secretion from human, dog, and rat antrum. *Gastroenterology* 111: 919- 924.
- Zheng H, Bailey A, Jiang MH, Hona K, Chen HY, Trumbauer ME, Van der Ploeg LH, Schaeffer JM, Leng G, Smith RG (1997). Somatostatin receptor subtype 2 knockout mice are refractory to growth hormone-negative feedback on arcuate neurons. *Mol. Endocrinol.* 11: 1709- 1717.
- Zingg HH, Patel YC (1982). Biosynthesis of immunoreactive somatostatin by hypothalamic neurons in culture. *J. Clin. Invest.* 70: 1101- 1109.
- Zupanc GKH (1996). Peptidergic transmission: from morphological correlates to functional implications. *Micron* 27: 35- 91.
- Zupanc GKH (1999). Neurogenesis, cell death, and neuronal regeneration in the brain of adult gymnotiform fish. *J. Exp. Biol.*, in press.
- Zupanc GKH, Cecyre D, Maler L, Zupanc MM, Quirion R (1994). The distribution of somatostatin binding sites in the brain of gymnotiform fish, *Apteronotus leptorhynchus*. *J. Chem. Neuroanat.* 7: 49- 63.
- Zupanc GKH, Horschke I, Stroh T (1997). Expression of somatostatin in neurons of the central posterior/ prepacemaker nucleus projecting to the preglomerular nucleus: immunohistochemical evidence for a non-synaptic function. *Neurosci. Lett.* 224: 123- 126.

- Zupanc GKH, Maler L (1997). Neuronal control of behavioral plasticity: the prepacemaker nucleus of weakly electric gymnotiform fish. *J. Comp. Physiol.* 180: 99- 111.
- Zupanc GKH, Okawara Y, Zupanc MM, Fryer JN, Maler L (1991). In situ hybridization of putative somatostatin mRNA in the brain of electric gymnotiform fish. *Neuroreport* 2: 707- 710.
- Zupanc GKH, Siehler S, Jones EMC, Seuwen K, Furuta H, Hoyer D, Yano H (1999). Molecular cloning and pharmacological characterization of a fish-specific somatostatin receptor subtype. *Gen. Comp. Endocrinol.*, in press.

## Curriculum vitae

### Personal data:

Sandra Siehler  
Hegenheimerstrasse 85  
CH-4055 Basel  
Switzerland  
PH 41 61 382 2671

January 4, 1971	born in Geislingen (Steige)/ Germany
nationality	German
marital status	single

### Education:

1977-1981	Primary School in Salach/ Germany
1981-1990	Erich Kästner-Grammar-School in Eislingen (Fils)/ Germany
1990-1995	Study of Biology at the University of Karlsruhe (TH), in particular Genetics, Zoology, Chemistry and Biochemistry
6/1995-6/1996	Diploma Thesis at the Institute of Genetics, Forschungszentrum Karlsruhe/ Germany “Valproic Acid-induced Differentiation of Mouse F9 Teratocarcinoma Cells”
since 8/1996	Ph.D. Thesis in the laboratory of Daniel Hoyer, Novartis Pharma Inc., Basel/ Switzerland, Ph.D. Student of the ETH Zurich/ Switzerland, promotor: Prof. Dr. Gerd Folkers, ETH Zurich, copromotor: Prof. Dr. Vladimir Pliska, ETH Zurich, “Ligand binding and signal transduction of vertebrate somatostatin receptors recombinantly expressed in CCL39 cells”
9/1998	EMBO course on signal transduction at the Weizmann Institute of Science, Rehovot/ Israel
6/1999	Defense of the Ph.D. Thesis at the ETH Zurich

## List of publications

- (1) Siehler S, Seuwen K, Hoyer D (1998) [<sup>125</sup>I][Tyr<sup>3</sup>]octreotide labels human sst<sub>2</sub> and sst<sub>5</sub> receptors. *European Journal of Pharmacology*, 348: 311-320.
- (2) Siehler S, Seuwen K, Hoyer D (1998) [<sup>125</sup>I]Tyr<sup>10</sup>-cortistatin<sub>14</sub> labels all five somatostatin receptors. *Naunyn-Schmiedeberg's Archives of Pharmacology*, 357: 483-489.
- (3) Siehler S, Zupanc GKH, Seuwen K, Hoyer D (1999) Characterization of the fish sst<sub>3</sub> receptor, a member of the SRIF<sub>1</sub> receptor family: atypical pharmacological features. *Neuropharmacology*, 38: 449-462.
- (4) Zupanc GKH, Siehler S, Jones EMC, Seuwen K, Hoyer D, Yano H (1999) Molecular cloning and pharmacological characterization of a fish-specific somatostatin receptor subtype. *General and Comparative Endocrinology*, in press.
- (5) Criado JR, Li H, Jiang X, Spina M, Huitron-Resendiz S, Liapakis g, Calbet M, Siehler S, Garcia C, Prospero-Garcia O, Igarashi J, Henriksen SJ, Koob GF, Reisine T, Hoyer D, Sutcliffe G, Goodman M, de Lecea L (1999) Structural and compositional determinants of cortistatin activity. *Journal of Neuroscience Research*, in press.
- (6) Siehler S, Seuwen K, Hoyer D. Characterization of human recombinant somatostatin receptors: 1) radioligand binding studies. *Naunyn-Schmiedeberg's Archives of Pharmacology*, submitted.
- (7) Siehler S, Hoyer D. Characterization of human recombinant somatostatin receptors: 2) modulation of GTPγS binding. *Naunyn-Schmiedeberg's Archives of Pharmacology*, submitted.
- (8) Siehler S, Hoyer D. Characterization of human recombinant somatostatin receptors: 3) modulation of adenylate cyclase activity. *Naunyn-Schmiedeberg's Archives of Pharmacology*, submitted.
- (9) Siehler S, Hoyer D. Characterization of human recombinant somatostatin receptors: 4) modulation of phospholipase C activity. *Naunyn-Schmiedeberg's Archives of Pharmacology*, submitted.
- (10) Siehler S, Zupanc GKH, Hoyer D. Fish somatostatin sst<sub>3</sub> receptor: comparison of radioligand and GTPγS binding, adenylate cyclase and phospholipase C activities reveals agonist-dependent pharmacological differences. *Neuropharmacology*, submitted.

## Meeting abstracts

- (1) Siehler S, Seuwen K, Hoyer D (1998) [<sup>125</sup>I]Tyr<sup>3</sup> octreotide labels human sst<sub>2</sub> and sst<sub>5</sub> receptors expressed in CCL39 cells. Naunyn-Schmiedeberg's Archives of Pharmacology 357: R35 (Meeting Abstract of the 39th Spring Meeting, Mainz, Germany).
- (2) Siehler S, Zupanc, GKH, Seuwen K, Hoyer D (1998) Pharmacological characterization and expression of the cloned fish somatostatin sst<sub>3</sub> receptor, a member of the SRIF<sub>1</sub> family. Society of Neuroscience Abstract No. 234.15, Vol. 24, 591 (Meeting Abstract of the 28th Annual Meeting, Los Angeles, USA).
- (3) Siehler S, Zupanc, GKH, Seuwen K, Hoyer D (1999) Characterisation of the cloned fish somatostatin receptor sst<sub>3</sub>, a member of the SRIF<sub>1</sub>-receptor family: atypical pharmacological features. British Journal of Pharmacology 126: 25P (Meeting Abstract, Brighton, England).
- (4) Siehler S, Seuwen K, Hoyer D (1999) System- and agonist-dependent ligand-receptor interactions at human somatostatin hsst<sub>5</sub> receptors: radioligand and [<sup>35</sup>S]GTPγS binding and adenylate cyclase inhibition studies. British Journal of Pharmacology 126: 26P (Meeting Abstract, Brighton, England).
- (5) Siehler S, Seuwen K, Hoyer D (1999) System- and agonist-dependent ligand-receptor interactions at human somatostatin hsst<sub>5</sub> receptors. Naunyn-Schmiedeberg's Archives of Pharmacology 359: R17 (Meeting Abstract of the 40th Spring Meeting, Mainz, Germany).
- (6) Zupanc GKH, Siehler S, Jones EMC, Seuwen K, Furuta H, Hoyer D, Yano H (1999) Molecular cloning and pharmacological characterization of a fish-specific somatostatin receptor subtype. Göttingen Neurobiology Report Vol II: 822 (Meeting Abstract of the 27th Neurobiology Conference, Göttingen, Germany).
- (7) Zupanc GKH, Siehler S, Jones EMC, Seuwen K, Furuta H, Hoyer D, Yano H (1999) Molecular cloning and pharmacological characterization of a somatostatin receptor subtype in a teleost fish. Biological Chemistry, submitted (Meeting Abstract of the Society of Biochemistry and Molecular Biology, Hamburg, Germany).
- (8) Zupanc GKH, Siehler S, Jones EMC, Seuwen K, Furuta H, Hoyer D, Yano H (1999) Molecular cloning and pharmacological characterization of a somatostatin receptor subtype in the gymnotiform fish *Apteronotus albifrons*. Society of Neuroscience Abstract, submitted (Meeting Abstract of the 29th Annual Meeting, Miami, USA).